Electronic Thesis and Dissertation Repository

10-30-2020 10:15 AM

# Elucidating the consequence and cause of microRNA dysregulation in amyotrophic lateral sclerosis (ALS)

Zachary C. E. Hawley, *The University of Western Ontario*

Follow this and additional works at: https://ir.lib.uwo.ca/etd

Part of the Molecular and Cellular Neuroscience Commons

**Abstract**

   Amyotrophic Lateral Sclerosis (ALS) is a progressive motor neurodegenerative disorder with an average life expectancy of 2-5 years post-diagnosis. Common pathological features associated with ALS are the formation of cytoplasmic inclusions of intermediate filaments and RNA-binding proteins within motor neurons. The formation of intermediate filament cytoplasmic inclusions is believed to be driven by a loss of stochiometric expression between five neuronal intermediate filament proteins—NFL, NFM, NFH, INA and PRPH—where there is a selective suppression of the steady-state levels of *NEFL*, *INA* and *PRPH* mRNA. Further, three RNA-binding proteins—TDP-43, FUS and RGNEF—have been shown to co-aggregate with each other in ALS motor neurons indicating a possible common mechanism that leads to their dysregulation.

   In the last decade, microRNAs (miRNAs)—small RNA molecules generally responsible for post-transcriptional regulation of gene expression—were observed to be massively dysregulated in the spinal cord tissue of ALS patients, providing a possible explanation for the changes observed in intermediate filament steady-state mRNA levels and RNA-binding protein dysregulation in ALS. Further, TDP-43 and FUS regulate miRNA biogenesis, indicating there may be a regulatory network between RNA-binding proteins and miRNAs that is disrupted in ALS. I hypothesize that a regulatory network between specific RNA-binding proteins and miRNAs is disrupted in ALS leading to changes in miRNA processing which contributes to intermediate filament and RNA-binding protein pathology.

   In this dissertation, I have examined: 1) whether ALS-linked miRNA(s) contribute to the selective suppression of *NEFL*, *PRPH*, and *INA*; 2) whether ALS-linked miRNAs regulate the expression of *NEFM* and *NEFH*; 3) whether ALS-linked miRNAs regulate the expression of

ii

RNA-binding proteins whose metabolism is dysregulated in ALS (TDP-43, FUS, and RGNEF); and, 4) whether TDP-43 and FUS are in a regulatory network with ALS-linked miRNAs. Overall, 12 ALS-linked miRNAs were identified to regulate either intermediate filament or RNA-binding protein expression, and further, a novel negative feedback loop between TDP-43 and two miRNAs (miR-27b-3p and miR-181c-5p) was identified. This dissertation highlights that changes to miRNA levels, as seen in ALS, would contribute to overall ALS pathology, making them viable avenues for potential therapeutics.

**Keywords:** MicroRNA, ALS, RNA-binding proteins, TDP-43, intermediate filaments, neurofilaments, RNA, neurodegeneration, regulatory networks

## Lay Abstract

Amyotrophic Lateral Sclerosis (ALS) is a neurodegenerative disorder defined by the progressive loss of motor function such as walking, reaching grabbing, standing, etc., eventually confining individuals to a wheelchair. ALS is generally fatal within 2-5 years of diagnosis. This disease results from the dramatic loss of a specific cell-type within the brain and spinal cord tissue called motor neurons. Decades of research has tried to understand what causes the loss of motor neurons in ALS, and while much progress has been made, there remains a considerable amount that is not understood regarding the underlying cause(s) of ALS. Recent research has shown that small molecules known as microRNAs (miRNAs) are reduced in ALS motor neurons. MiRNAs regulate the levels of gene expression within our cells which is critical for cells to efficiently respond to environmental cues (i.e. stress) and maintain overall cell health. Lack of these small molecules, as seen in ALS motor neurons, has been shown to cause motor neuron death in mice, indicating the importance of miRNAs to motor neuron function. In this dissertation, I explored the potential consequence of reduced miRNA levels, as seen in ALS, and how this may relate to what we already know about ALS pathology. Further, I explored potential molecular pathways that may explain why miRNA reduction occurs in ALS. I have found that the loss of a specific pool of miRNAs in ALS may contribute to overall ALS pathogenesis. In addition, I have identified a novel molecular network between miRNAs and TDP-43—a protein that is dysregulated in 97% of all ALS cases—which may explain the loss of miRNAs seen in ALS motor neurons. Overall, this thesis implicates miRNAs as major contributors to ALS pathogenesis and identifies a disrupted molecular network between miRNAs and TDP-43, providing new avenues to explore potential therapeutics for ALS.

**Co-authorship Statement**

**Chapter 1:** Manuscript entitled "MotomiRs: miRNAs in motor neuron function and disease." Published in Frontiers of Molecular Neuroscience. Zachary C. E. Hawley*, Danae Campos-Melo*, Cristian A. Droppelmann, Michael J. Strong. (*shared first author).

1. Zachary C. E. Hawley – conceived the idea for the manuscript and wrote 50% of the content.

2. Danae Campos-Melo – assisted with the development of the manuscript and wrote 50% of the content.

3. Cristian A. Droppelmann – assisted with the design and production of the figures.

4. Michael J. Strong – assisted with the conception and writing of the manuscript. Supervised the work.

**Chapter 2:** Manuscript entitled "MiR-105 and miR-9 regulate the mRNA stability of neuronal intermediate filaments. Implications for the pathogenesis of amyotrophic lateral sclerosis (ALS)." Published in Brain Research. Zachary C. E. Hawley, Danae Campos-Melo, Michael J. Strong.

1. Zachary C. E. Hawley – designed and performed all experiments and statistical analyses. Wrote the manuscript.

2. Danae Campos-Melo – assisted with the experimental design and writing of the manuscript.

3. Michael J. Strong – assisted in the writing of the manuscript. Supervised the project.

**Chapter 3:** Manuscript entitled "Dysregulation of human *NEFM* and *NEFH* mRNA stability by ALS-linked miRNAs." Published in Molecular Brain. Danae Campos-Melo*, Zachary C. E. Hawley*, Michael J. Strong. (*shared first author).

1. Danae Campos-Melo – conceived the idea and designed the experiments. Performed 50% of the experiments and writing.

2. Zachary C. E. Hawley – assisted in the design of the experiments. Performed 50% of the experiments and writing.

3. Michael J. Strong – assisted in the writing of the manuscript. Supervised the project.


**Chapter 4:** Manuscript entitled "Novel miR-b2122 regulates several ALS-related RNA-binding proteins." Published in Molecular Brain. Zachary C. E. Hawley, Danae Campos-Melo, Michael J. Strong.

1. Zachary C. E. Hawley – designed and performed all experiments and statistical analyses. Wrote the manuscript.

2. Danae Campos-Melo – assisted with the experimental design and writing of the manuscript.

3. Michael J. Strong – assisted in the writing of the manuscript. Supervised the project.


**Chapter 5:** Manuscript entitled "Evidence of a negative feedback network between TDP-43 and miRNAs dependent on TDP-43 nuclear localization." Accepted in Journal of Molecular Biology. Zachary C. E. Hawley, Danae Campos-Melo, Michael J. Strong.

1. Zachary C. E. Hawley – designed and performed all experiments and statistical analyses. Wrote the manuscript.

2. Danae Campos-Melo – assisted with the experimental design and writing of the manuscript.

3. Michael J. Strong – assisted in the writing of the manuscript. Supervised the project.

**Appendix B:** Manuscript entitled "miR-129-5p: A novel therapeutic target for ALS?" Published in Non-Coding RNA Investigation. Zachary C. E. Hawley, Danae Campos-Melo, Michael J. Strong.

1. Zachary C. E. Hawley – Wrote the editorial and designed the figure.

2. Danae Campos-Melo – Assisted in the writing of the editorial.

3. Michael J. Strong – Assisted in the writing of the editorial. Supervised the work.

**Epigraph**

*In the long history of humankind those who learned to collaborate and improvise most effectively*

*have prevailed.*

- Charles Darwin

**Dedication**

   To the individuals and families who have had to endure the extreme challenges of ALS. It is your continued bravery and relentless fight that inspires the research community to find a cure without surrender.

**Acknowledgements**

First, I would like to acknowledge my supervisor Michael Strong. His patience and guidance throughout the entire process is deeply appreciated. Thank you for all your support both inside and outside the lab. The lessons that I have learned from him I will carry throughout my life.

Another great mentor to me was Danae Campos-Melo. She took the time to foster my skills as a scientist. She always asked the hard questions forcing me to critically think before I got ahead of myself. It was truly a pleasure working with Danae.

Alex Moszczynski, I could not imagine my PhD experience without you there. You were a great mentor and friend who was always willing to offer advice whenever I needed it. I will always remember our great chats about science, politics and life while performing surgeries or over pints at the grad club.

To all past and present graduate students during my time in the Strong Lab, Sali Farhan, Michael Tavolieri, Ben Withers, Hind Amzil, Matt Hintermayer, Neil Donison and Asieh Alikhah. It was amazing to get to know all of you and I will cherish the experience we all had together. I look forward to our paths crossing in the future.

Kathy Volkening, Cristian Droppelmann, Cheryl Leystra-Lantz and Crystal McLellan - all of you have supported me in my research by offering me advice or helping me in the lab. I am truly grateful for all your contributions to my success as a graduate student.

Madeline Harvey and Kassandra Hebert, I am truly grateful for your assistance with the animal work. I had lived in your shoes for 6-months during the time where Madeline was gone and Kassandra had not quite started… mildly putting it, it was not easy. In that 6-months, I truly got to appreciate all the work you put into animal care which allow us graduate students to

perform our research. Thanks to both of you. I really appreciated your hard work and our time together.

Thanks to all my PhD advisors, Robert Hammond, Subrata Chakrabarti, Shawn Whitehead, Arthur Brown and Macro Prado for your guidance and always meaningful advice on my projects and progression through my graduate degree. Also, I would like to thank Michael J. Rieder for reviewing my thesis and providing his thoughtful comments.

Thanks to all the students and faculty in the Neuroscience Program and at Robarts Research Institute. Whether it be student seminars, data clubs, assisting in developing the Robarts Associates for Trainees, the neuroscience research blog (The Dorsal Column), Neurobeers, Robarts Refreshers, etc., it was truly a blast working and getting to know each and every one of you.

Thank you to my mother, Suzanne Herron. She has always been supportive in whatever my pursuits and willing to offer advice when I needed it. Thank you for all that you have done for me throughout my life. You are the inspiration to my success. Also, thank you to my brother Justin Patriquin a person I have looked up to my whole life and who was always willing to put up with my shenanigans.

Finally, thanks to Jacqueline Dron. The success that I have achieved throughout my graduate studies could not have been done without you. You have made me a better person, always wanting to challenge myself and thrive in my current pursuits which you have always been supportive. We are a scientific power couple, watch out world.

**Table of Contents**

**List of Tables**

## List of Figures

**List of Appendices**

**List of Abbreviations**

| | |
|---|---|
| ΔΔCT | Delta Delta Cycle Threshold |
| 18S | 18S Ribosomal RNA |
| 3'RACE PCR | 3 Prime Rapid Amplification of cDNA Ends PCR |
| 3'UTR | 3 Prime Untranslated Region |
| 5'UTR | 5 Prime Untranslated Region |
| ADAR | Adenosine Deaminase 1 |
| AGO1-4 | Argonaute 1-4 |
| ALDOA | Aldolase A |
| ALDOC | Aldolase C |
| ALS | Amyotrophic Lateral Sclerosis |
| ALS2 | Alsin Rho Guanine Nucleotide Exchange Factor ALS2 |
| ALS7 | Amyotrophic Lateral Sclerosis 7 |
| ANOVA | Analysis of Variance |
| ARE | Adenylyl Repeat Elements |
| ARHGEF28 | Rho Guanine Nucleotide Exchange Factor 28 – gene name of RGNEF |
| ATP | Adenosine Triphosphate |
| ATXN2 | Ataxin 2 |
| BDNF | Brain-Derived Neurotrophic Factor |
| C6 | Complement Component 6 |
| C9ORF72 | Chromosome 9 Open Reading Frame 72 |
| CCNB1 | Cyclin B1 |
| CCR4 | C-C Motif Chemokine Receptor 4 |

| | |
|---|---|
| cDNA | Complementary DNA |
| cel | *Caenorhabditis Elegans* |
| ceRNAs | Competitive Endogenous RNA |
| ChIP | Chromatin Immunoprecipitation |
| CLASH | Cross Linking, Ligation and Sequencing Hybrids |
| CNS | Central Nervous System |
| CSF | Cerebrospinal Fluid |
| CT | Cycle Threshold |
| DCGR8 | DiGeorge Syndrome Critical Region 8 |
| DICER | Dicer, Ribonuclease III |
| DIG | Digoxigenin |
| DIS3L2 | DIS3 Like 3'-5' Exoribonuclease 2 |
| DMEM | Dulbecco's Modified Eagle Media |
| DNA | Deoxyribonucleic Acid |
| DNAJC7 | DnaJ Heat Shock Protein Family (Hsp40) member C7 |
| DPE | Downstream Promoter Elements |
| DROSHA | Drosha, Ribonuclease III |
| dsRNA | Double Stranded RNA |
| eIF2A | Elongation Translation Initiation Factor 2A |
| eIF4A | Elongation Translation Initiation Factor 4A |
| eIF4F | Elongation Translation Initiation Factor 4F |
| EMEM | Essential Modified Eagle Media |
| ER | Endoplasmic Reticulum |

| | |
|---|---|
| EWSR1 | Ewing Sarcoma and Demoplastic Small Cell Round Tumor 1 |
| fALS | Familial Amyotrophic Lateral Sclerosis |
| FBS | Fetal Bovine Serum |
| FET | FUS, EWRS1 & TAF15 |
| FFPE | Formalin Fixed Paraffin Embedded |
| FGF-2 | Fibroblast Growth Factor 2 |
| FGFR-1 | Fibroblast Growth Factor Receptor 1 |
| FISH | Fluorescent *In Situ* Hybridization |
| FMRP | Fragile X Mental Retardation Protein 1 |
| FOXP1 | Forkhead Box P1 |
| FTD | Frontotemporal Dementia |
| FUS | Fused in Sarcoma |
| G3BP1 | GTPase Activating Protein (SH3 Domain) Binding Protein |
| GAPDH | Glyceraldehyde 3-phosphate Dehydrogenase |
| GLD-2 | Germ Line Development 2 |
| GRSF1 | G-Rich RNA Sequence Binding Factor 1 |
| GTP | Guanosine Triphosphate |
| GW182 | Glycine-Tryptophan Protein of 182 kilodaltons |
| H3K4me3 | Tri-methylation of Histone H3 Lysine 4 |
| HCV | Hepatitis C Virus |
| HDAC | Histone Deacetylase |
| HEK293T | Human Embryonic Kidney 293 T-antigen |
| hnRNPA1 | Heterogeneous Nuclear Ribonucleoprotein A1 |

| | |
|---|---|
| hnRNPA1B | Heterogeneous Nuclear Ribonucleoprotein A1 isoform B |
| hnRNPA2B1 | Heterogeneous Nuclear Ribonucleoprotein A2 B1 |
| hnRNPE1/E2 | Heterogeneous Nuclear Ribonucleoprotein E1/E2 |
| hnRNPK | Heterogeneous Nuclear Ribonucleoprotein K |
| HRP | Horse Radish Peroxide |
| HuB | Hu Antigen B (protein of ELAVL2 gene) |
| IL-10 | Interleukin 10 |
| IMR-32 | Institute for Medical Research-32 |
| INA | Alpha-Internexin |
| Inr | Initiator Element |
| IPO8 | Importin-8 |
| iPSC | Induced Pluripotent Stem Cells |
| KHSRP | KH-Type Splicing Regulator Protein |
| KIF5A | Kinesin Family Member 5A |
| Lamin A/C | Lamin Type A and C |
| LCD | Low-Complexity Domain |
| LIN28 | Lin-28 Homolog A |
| LMN | Lower Motor Neuron |
| LNA | Locked Nucleic Acid |
| lncRNA | Long Non-coding RNA |
| m6A | N6-methyladenosine |
| MAP1B | Microtubule Associated Protein 1B |
| MATR3 | Matrin 3 |

| | |
|---|---|
| MCPIP1 | Monocyte Chemotactic Protein-1-induced Protein-1 |
| miRNA | MicroRNA |
| MRE | MiRNA Recognition Element |
| mRNA | Messenger RNA |
| MTE | Motif Ten Element |
| mtSOD1 | Mutant SOD1 |
| MYC | MYC Proto-Oncogene |
| NAD+ | Nicotinamide Adenine Dinucleotide |
| NADH | Nicotinamide Adenine Dinucleotide, Reduced |
| NCI | Neuronal Cytoplasmic Inclusions |
| ncRNA | Non-coding RNA |
| NEAT1_2 | Nuclear Enriched Abundant Transcript 1 and 2 |
| NEFH | Neurofilament Heavy (transcript) |
| NEFL | Neurofilament Light (transcript) |
| NEFM | Neurofilament Medium (transcript) |
| NEK1 | NIMA Related Kinase 1 |
| NF | Neurofilament |
| NFH | Neurofilament Heavy (protein) |
| NF-kB | Nuclear Factor Kappa-light-chain-enhancer Activated B cells |
| NFL | Neurofilament Light (protein) |
| NFM | Neurofilament Medium (protein) |
| NLS | Nuclear Localization Signal |
| NOT | Negative Regulator of Transcription Subunit 1 Homolog |

NP40            Nonyl Phenooxypolyethoxylethanol 40

NS              Not Significant

OC1             Onecut 1

OPTN            Optineurin

p190RhoGEF      190 Kilodalton Guanine Nucleotide Exchange Factor

p53             Tumor Protein p53

pA1             Polyadenylation Site 1

PABP            Poly(A) Binding Protein

PACT            Protein Activator of the Interferon-Induced Protein Kinase

PAN2            Poly(A)-Nuclease Deadenylation Complex Subunit 2

PAN3            Poly(A)-Nuclease Deadenylation Complex Subunit 3

PARIS           Protein and RNA Isolation System

PARN            Poly(A)-specific ribonuclease

pC32            Plasmid C32

pcDNA 3.1       Plasmid Cloning DNA

PCR             Polymerase Chain Reaction

PFA             Paraformaldehyde

PFN1            Profilin 1

PLS             Primary Lateral Sclerosis

PNS             Peripheral Nervous System

pre-miRNA       Precursor MicroRNA

pri-miRNA       Primary MicroRNA

PRPH            Peripherin

| | |
|---|---|
| RAN-GTP | Ras-related Nuclear Protein Guanine Triphosphate |
| RBM45 | RNA-binding Motif Protein 45 |
| RGNEF | Rho Guanine Nucleotide Exchange Factor |
| RGNEF-L | RGNEF Long |
| RGNEF-S | RGNEF Short |
| RhoA | RAS Homolog Family Member A |
| RISC | RNA-induced silencing complex |
| RNA | Ribonucleic Acid |
| RNA Pol. | RNA Polymerase |
| RNAa | RNA Activation |
| RNP | Ribonucleoprotein |
| rRNA | Ribosomal RNA |
| RT-qPCR | Reverse Transcriptase Quantitative PCR |
| S1-3 | Site 1-3 |
| sALS | Sporadic Amyotrophic Lateral Sclerosis |
| SCR | Scramble |
| SDS | Sodium Dodecyl Sulfate |
| SEM | Standard Error of the Mean |
| SEXT | Synataxin |
| SFPQ | Splicing Factor Proline and Glutamine Rich |
| SH-SY5Y | Thriced sub-cloned cell derived from SK-N-SH neuroblastoma cell line |
| siFUS | siRNA Targeting FUS mRNA |
| siRES | siRNA Resistant Plasmid |

| | |
|---|---|
| siRNA | Small Interfering RNA |
| siTDP | siRNA Targeting TARDBP mRNA |
| SMA | Spinal Muscular Atrophy |
| SMN1 | Survival Motor Neuron 1 |
| snoRNA | Small Nucleolar RNA |
| SNP | Single Nucleotide Polymorphism |
| SOD1 | Superoxide Dismutase 1 |
| SPG11 | Spastic Paraplegia 11 |
| SQSTM1 | Sequestosome 1 |
| STMN2 | Stathmin-2 |
| TAF15 | TATA-box Binding Protein Associated Factor 15 |
| TARDBP | Transactive Response DNA-binding Protein – gene name of TDP-43 |
| TBK1 | TANK Binding Kinase 1 |
| TDP-43 | Transactive Response DNA-binding Protein of 43 kilodaltons |
| TERT | Telomerase Reverse Transcriptase |
| TFIIB | Transcription Factor II B |
| TIA-1 | TIA1 Cytotoxic Granule Associated RNA-binding protein |
| TRBP | Trans-Activation Response RNA-binding Protein |
| trkB | Tropomyosin receptor kinase B |
| tRNA | Transfer RNA |
| TSA | Tyramide Signal Amplification |
| TTP | Tristetraprolin |
| TUT2 | Terminal Uridylyl Transferase 2 |

| | |
|---|---|
| TUT4 | Terminal Uridylyl Transferase 4 |
| TUT7 | Terminal Uridylyl Transferase 7 |
| UBQLN2 | Ubiquilin 2 |
| UMN | Upper Motor Neuron |
| UV | Ultraviolet |
| VAPB | VAMP Associated Protein B and C |
| VCP | Vasolin-containing Protein |
| VEGF | Vascular Endothelial Growth Factor |
| WT | Wild-Type |
| XPO1 | Exportin-1 |
| XPO5 | Exportin-5 |
| ZEB1 | Zinc Finger E-box Binding Homeobox 1 |
| ZEB2 | Zinc Finger E-box Binding Homeobox 2 |

# Chapter 1

## Introduction

Materials from the following text can be found in the following manuscript with the appropriate modifications:

Hawely, ZCE*., Campos-Melo, D*., Droppelmann CA. & Strong, MJ. MotomiRs: miRNAs in motor neuron function and disease. *Front. Mol. Neurosci*. (2017). PMID: 28522960. *shared first authorship.

Amyotrophic lateral sclerosis (ALS) is generally a late-onset neurodegenerative disease that results in motor neuron loss causing death within 2-5 years after diagnosis. Several genetic and pathological features of ALS have given us insights into the etiology of the disease (Strong, 2017). However, despite these efforts, very few therapeutics have been successful in treating ALS. Therefore, we need to continue to explore the biological mechanisms underpinning ALS if we are to find novel drug targets that may slow or halt the progression. Recent work has shown that microRNAs (miRNAs) may be a major contributor to the disease pathogenesis.

MicroRNAs (miRNAs) are endogenous small non-coding RNAs that regulate gene expression via formation of a ribonucleoprotein complex with Argonaute (AGO) proteins and complementary base pairing with their target mRNAs (Lee et al., 1993; Slack et al., 2000). Despite the apparent simplicity of miRNA function, their expression and mRNA targets are highly dependent on the stage of development, environmental cues, aging and cellular type. This highly dynamic process allows for the fine-tuning of gene expression depending not only on the global needs of the cell, but also somatotopically-specific needs such as the maintenance of the synaptic junction or the response to neuronal injury (van Rooij et al., 2007; Wilczynska and Bushell, 2015).  In this introduction, we will discuss motor neurons, ALS pathology, miRNA biology and their role in motor neuron disease, and finally, potential mechanisms that may contribute to the dysregulation of miRNAs seen in ALS.

### 1.1 Motor Neurons

Motor neurons are classified as either somatic or visceral. Visceral motor neurons are responsible for innervating smooth and cardiac muscle allowing for involuntary contractions. In contrast, somatic motor neurons innervate skeletal muscle to perform voluntary movement

(Goulding, 1998; Guthrie, 2007). This dissertation will focus on somatic motor neurons (henceforth referred to as "motor neurons").

In general, motor neurons can be further grouped into those whose projections remain within the central nervous system (CNS) and those that do not. Upper motor neurons (UMNs) are a group of descending supraspinal neurons, the majority of which arise from the primary motor cortex, premotor cortex and the supplementary motor area (Dum and Strick, 2005; Nachev et al., 2008). UMNs arising in these cortical regions course through the corticospinal tracts with the majority (75-90%) crossing at the level of the medulla to ultimately innervate contralateral spinal motor neurons. The remaining 10-25% innervate ipsilateral spinal motor neurons. UMNs send excitatory chemical signals via glutamate to activate spinal motor neurons (**Fig. 1.1A**). Spinal motor neurons belong to the category of lower motor neurons (LMNs) that, in concert with the muscle fibers that they innervate through their axonal terminals, constitute the motor unit (Lemon, 2008; Welniarz et al., 2016). The interaction between the axon terminals and skeletal muscle occurs at the neuromuscular junction (NMJ) where acetylcholine release across the synapse induces muscle contractions which allow us to perform basic motor functions such as standing, walking, reaching, grabbing, etc. (**Fig 1.1B**).

### 1.1.1 Axonal Transport

Axonal transport is necessary for motor neurons to send signals to other cells within the body. An individual motor neuron axon can extend for upwards of a meter, giving rise to a unique set of metabolic demands. Mitochondria, ribonucleoprotein (RNP) granules, and vesicles must be positioned at specific sites along the length of the axon depending on somatotopic needs and thus requiring a high degree of regulation (**Fig. 1.1C**) (Lin and Sheng, 2015; Vuppalanchi et al., 2009). Critical to the integrity of the axonal projection are key cytoskeletal proteins,

A. Glutamatergic synapse

Upper motor neuron

Ca++

Ca++
Na+

Na+

Astrocyte

Lower motor neuron

B. Neuromuscular junction

Presynaptic neuron

Ca++

Ca++

K+          K+

Na+          Na+          Na+          Na+

Muscle fiber

C. Axonal transport

AMPA receptor

Glutamate receptor

Glutamate reuptake transporter

Calcium channel

NMDA Receptor

Mitochondria

Synaptic vesicle with glutamate

Synaptic vesicle with acetylcholine

Sodium/Potassium exchange channel

Sodium voltage-gated channel

Microtubule

Neurofilament

Kinesin (arrow indicates anterograde transport)

Dynein (arrow indicates retrograde transport)

RNP granule

Vesicle

**Figure 1.1. Motor neuron transmission.** (A) The glutamatergic synaptic connection between lower motor neurons (LMNs) and upper motor neurons (UMNs). This synapse drives excitation of the LMN through a process that is dependent on the influx of $Ca^{++}$ into the presynaptic terminus which in turn triggers release of glutamate into the synaptic cleft. There, glutamate stimulates the influx of $Na^+$ and $Ca^{++}$ into the post-synaptic LMN, which leads to its depolarization. (B) Transport across the long axon of motor neurons. Neurons must be constantly transferring mitochondria, vesicles and RNPs granules to localized spots in the axon depending on the need of the cell. Transport is bidirectional along the axon where the molecular motor kinesin drives anterograde transport, whereas dynein provides retrograde transport. This is crucial for the proper distribution of proteins, transcripts and organelles. (C) Neuromuscular junction. When the action potential has reached the neuromuscular junction, there is an influx of $Ca^{++}$ into the axonal presynaptic bouton resulting in the synaptic release of acetylcholine. This causes the efflux of $K^+$ and the influx of $Na^+$ leading to the depolarization of the muscle fiber. The influx of $Na^+$ causes the opening of sodium voltage-gated channels along the muscle fiber, allowing for the action potential to propagate through the muscle fiber (indicated by the golden arrows), generating the muscle contraction.

including microtubules which provide the highway that guides axonal transport, and neurofilaments which are key to maintaining the cytoskeletal architecture of the axon and thus indirectly, the degree of myelination (Hirokawa et al., 2010; Szaro and Strong, 2010). Further, axons and synapses are highly dynamic structures that are constantly changing in an activity-dependent manner, and thus, there is a constant redistribution of mitochondria depending on localized energy demands (Miller and Sheetz, 2004). This is especially true for motor neurons as their axonal length requires precise movement of mitochondria to meet their high energy demands (Hinckelmann et al., 2013).

Beyond mitochondrial trafficking, the transport of mRNA along the axon allows for somatotopically-specific protein synthesis. To accommodate this, mRNAs and translational machinery are incorporated into RNP granules and transported to distal regions along the axon for localized translation (Sutton and Schuman, 2006; Vuppalanchi et al., 2009). It is widely accepted that during RNP transport that the mRNA within the granule is translationally silent, a state that is suggested to be largely mediated by various RNA-binding proteins (Bramham and Wells, 2007). However, it has also been shown that proteins essential for miRNA processing are found within these RNP transport granules (Barbee et al., 2006), suggesting that the post-transcriptional regulation of mRNA within RNPs is likely an interaction between RNA-binding proteins and regulatory RNA molecules, allowing for localized protein synthesis and even mRNA degradation.

### 1.1.2 Regeneration

One of the fundamental differences between mature UMNs and LMNs is the ability for LMNs to regenerate. In general, the peripheral nervous system (PNS) in which LMNs reside

provides an environment where neurons can survive and regenerate subsequent to axonal damage. This is not the case in the CNS (Fitch and Silver, 1997; Fu and Gordon, 1997). This phenomenon has been attributed to the lack of neurotrophic factors and an abundance of inhibitory proteins present after a nerve injury in the CNS (Schwab, 1996). For example, the increased expression of neurotrophic factors brain-derived neurotrophic factor (BDNF) and fibroblast growth factor 2 (FGF-2) and their receptors – trkB and FGFR-1, respectively – promotes LMN regeneration in response to a nerve injury. However, within the CNS, the expression of these receptors and ligands are reduced after nerve injury, creating a less permissive environment for regeneration (Funakoshi et al., 1993; Kobayashi et al., 1996; Lewin and Barde, 1996). Interestingly, ectopic expression of BDNF within the CNS after a neuronal injury enhances the regenerative capacity of the neurons, suggesting it is an essential protein for nerve recovery (Giehl and Tetzlaff, 1996; Kobayashi et al., 1997).

Further, the upregulation of cytoskeleton proteins including actin, tubulin and peripherin also assist with the regeneration of LMNs by restructuring the axon as it recovers (Bisby and Tetzlaff, 1992; Chadan et al., 1994; Jiang et al., 1994). However, there is a downregulation in neurofilament expression after a nerve injury, which has been shown to allow for efficient transport of actin, tubulin and peripherin to distal regions of the injured axon (Tetzlaff et al., 1996; Zhu et al., 1998). This change in cytoskeleton proteins after an axonal injury is far less robust within the CNS, and thus, could be another reason why regeneration is not able to occur within UMNs (Kost and Oblinger, 1993; Tetzlaff et al., 1991). This tightly coordinated change in the expression of cytoskeleton genes within the PNS allows for efficient axonal repair, and thus, a transient network of regulatory elements, such as miRNAs, must play an essential role in this

regenerative process. Disruption of molecular pathways that are critical to motor neuron function like axonal transport and regeneration have been shown to be disrupted in patients with ALS.

## 1.2 ALS

ALS is a neurodegenerative disease which is defined by the loss of both upper and lower motor neurons within the brain and spinal cord tissue, respectively (Strong et al., 2005). This debilitating disease ultimately leads to a person being confined to a wheelchair with the inability to perform basic motor tasks including and not limited to reaching, grabbing, standing, walking, speech, swallowing and breathing (Strong et al., 2017). Currently, there are limited treatments for this disease which has an expected survival time of 2-5 years post-diagnosis.

### 1.2.1  Demographics of ALS

Generally, ALS is a late onset disease with an average age of diagnosis between 40-70 years of age with an incidence rate of two out of 100,000 people (Zarei et al., 2015). Ninety percent of ALS cases have no familial history (sporadic ALS [sALS]), and within those cases, only about 12-13% carry a known genetic mutation to explain the etiology of their disease. The remaining 10% of ALS cases are familial (fALS), and in those cases, about two-thirds have a known genetic defect (Mathis et al., 2019; Taylor et al., 2016). By far, in both sporadic and familial ALS cases, the most common genetic alteration is a hexanucleotide (GGGGCC) repeat expansion in *C9ORF72* making up about 25-40% of familial and 10% of sporadic genetic cases. This is followed by mutations in SOD1, TDP-43 and FUS, respectively, which total to about 30% within familial cases and 2-3% within sporadic cases (Majounie et al., 2012; Taylor et al., 2016). There have been several other genes that contain disease causative mutations which accumulate to ~12% of familial and <1% of sporadic ALS cases (**Table 1.1**). While it is clear that genetic alterations play a critical role within the disease etiology for some patients, the vast

**Table 1.1.** Known genes that carry disease causative variants of familial and sporadic ALS

| Gene ID | Chromosome Location | Mode of inheritance* | Protein Function | % of fALS cases** | % of sALS cases** | Reference |
|---|---|---|---|---|---|---|
| *C9ORF72* | 9p21.2 | AD | Nucleocytoplasmic transport | 25-40% | 10% | (DeJesus-Hernandez et al., 2011; Renton et al., 2011) |
| *SOD1* | 2q22.11 | AD, AR | Superoxide dimutase | 20% | 2% | (Rosen et al., 1993) |
| *TARDBP* | 1p36.22 | AD | DNA/RNA-binding protein | 5% | <1% | (Sreedharan et al., 2008) |
| *FUS* | 16p11.2 | AD | DNA/RNA-binding protein | 5% | <1% | (Belzil et al., 2009; Vance et al., 2009) |
| *OPTN* | 10p13 | AD, AR | Autophagy | 4% | <1% | (Maruyama et al., 2010) |
| *NEK1* | 4q33 | Not determined | Kinase and DNA repair | 2-3% | <1% | (Kenna et al., 2016) |
| *VCP* | 9q13.3 | AD | Autophagy | 2% | <1% | (Johnson et al., 2010) |
| *TIA-1* | 2p13.3 | AD | DNA/RNA-binding protein, stress granule formation | 2% | <1% | (Mackenzie et al., 2017) |
| *hnRNPA1* | 7p15.2 | AD | RNA-binding protein | <1% | <1% | (Kim et al., 2013) |
| *hnRNPA2B1* | 12q13.3 | AD | RNA-binding protein | <1% | <1% | (Kim et al., 2013) |
| *UBQLN2* | Xp11.21 | X-linked | Autophagy | <1% | <1% | (Deng et al., 2011) |
| *KIF5A* | 12q13.3 | AD | Anterograde transport of organelles and RNP granules | <1% | <1% | (Brenner et al., 2018; Nicolas et al., 2018) |
| *TBK1* | 12q154.2 | AD | Autophagy and inflammation | <1% | <1% | (Freischmidt et al., 2015b) |
| *PFN1* | 17p13.2 | AD | Actin polymerization | <1% | <1% | (Wu et al., 2012) |
| *DNAJC7* | 17q21.2 | Not determined | Heat Shock 40 protein | <1% | <1% | (Farhan et al., 2019) |
| *SQSTM1* | 5q35.3 | AD | Autophagy | <1% | - | (Fecto et al., 2011; Le Ber et al., 2013) |
| *VAPB* | 20q13.33 | AD | Axonal transport | <1% | - | (Nishimura et al., 2004) |
| *SEXT* | 9q34.13 | AD | DNA/RNA helicase | ? | ? | (Chen et al., 2004) |
| *ALS2* | 2p33.2 | AR | Rho nucleotide exchange factor | ? | ? | (Hadano et al., 2001; Yang et al., 2001) |
| *SPG11* | 15q21.1 | AR | Transmembrane protein | ? | ? | (Hentati et al., 1998; Orlacchio et al., 2010) |
| *ALS7* | 20p13 | AD | Unknown | ? | - | (Sapp et al., 2003) |

*Autosomal Dominate (AD); Autosomal Recessive (AR)

**Percentages represent approximate values. May vary in different ALS cohorts studied.

majority of cases have no known genetic cause, suggesting that environmental factors may also play a critical role in ALS. Thus, we must further explore changes to both RNA and protein if we are to understand the progression of the disease at the molecular level.

### 1.2.2    ALS Pathology

The formation of neuronal cytoplasmic inclusions (NCIs), consisting of aberrantly aggregated proteins, is a common pathological phenomenon is several neurodegenerative diseases, including ALS. The most common protein groups found to be aberrantly aggregated in ALS are intermediate filaments and RNA-binding proteins (Strong, 2017). The formation of intermediate filament inclusions is believed to be driven by changes to stochiometric expression between cytoskeleton proteins (Szaro and Strong, 2010), whereas RNA-binding protein inclusions are believed to be driven by changes to their low-complexity domain (LCD; i.e. post-translational modifications, or mutations) that make the protein more prone to aggregate (Franzmann and Alberti, 2019; Molliex et al., 2015; Murakami et al., 2015; Murray et al., 2017; Patel et al., 2015). The formation of RNA-binding protein cytoplasmic aggregates is the most common pathology seen in ALS, indicating that RNA dysregulation may be a major driver of ALS (Keller et al., 2012; Strong, 2017).

In 1981, Davidson et al. demonstrated using tinctorial stains that there was an 31% and 42% reduction in total RNA content within ALS lumbar and cervical motor neurons, respectively, providing the first evidence of RNA dysregulation in ALS (Davidson and Hartmann, 1981; Davidson et al., 1981). It was subsequently demonstrated that an overall reduction in polyadenylated RNA in ALS motor neurons bearing neurofilament NCIs was present when assessed using *in situ* hybridization (Bergeron et al., 1994), suggesting a dysregulation of coding RNA. These works would kick-off decades of research that would later

show issues in mRNA expression, splicing, polyadenylation, transport, stability, and further, dysregulation of non-coding RNAs in ALS motor neurons. In this section, we will discuss the various RNA-binding protein pathologies followed by what we currently understand about RNA dysregulation in ALS as these two phenomena are highly connected.

### 1.2.2.1 RNA-binding Protein Pathology

### 1.2.2.1.1  TDP-43

TAR DNA-binding protein 43 kDa (TDP-43) is a ubiquitously expressed nuclear protein that has a diverse set of functions which include: mRNA transcription, mRNA splicing, RNA export, mRNA translation, miRNA biogenesis, long non-coding RNA (lncRNA) processing, and stress granule formation (Ratti and Buratti, 2016). Re-localization of TDP-43 from the nucleus to the cytoplasm and the subsequent formation of NCIs in motor neurons is the most common pathological feature of ALS, being observed in 97% of all cases (Ling et al., 2013).

Several of the ALS-linked mutations and phosphorylation sites associated with TDP-43 pathology are harbored in the LCD (Buratti, 2015). LCD's are intrinsically disordered domains which can form either alpha-helical or pleated beta-sheet structures regulating the solubility of the protein (Franzmann and Alberti, 2019). Both aberrant mutations and phosphorylation within the LCD of TDP-43 promotes beta-sheet structures which lead to the eventual accumulation and formation of insoluble protein aggregates (Barmada et al., 2010; Choksi et al., 2014; Liachko et al., 2010). The primary phosphorylation sites of TDP-43 associated with pathological aggregates in motor neurons of ALS patients are serine 409/410, amino acids that are found in the LCD (Neumann et al., 2009a; Neumann et al., 2006). This suggests that conformational changes within the LCD of TDP-43 contributes to its pathogenic role in ALS; however, the exact mechanism(s) that lead to these changes are still unclear.

Mixed results have been seen in whether or not overexpression of wild-type TDP-43 in mouse models can actually lead to the formation of pathological aggregates in motor neurons (Mitchell et al., 2015; Xu et al., 2010). However, in sporadic ALS cases with no known genetic background, increased expression of TDP-43 protein and mRNA levels within the spinal cord and motor neurons has been observed, and further, the overexpression of other proteins with LCD's similar to TDP-43 have been shown to form insoluble aggregates in both *in vitro* and *in vivo* models (Koyama et al., 2016; Mitchell et al., 2013; Patel et al., 2015; Swarup et al., 2011; Xu et al., 2010).TDP-43 has been shown to co-aggregate with several other LCD-containing proteins including FUS, TIA-1 and MATR3 in ALS motor neurons (Keller et al., 2012; Liu-Yesucevitz et al., 2010; Tada et al., 2018; Volkening et al., 2009). These observations suggest that the simple accumulation of TDP-43 alone may not sufficient to drive this protein into insoluble aggregates and that the presence of other LCD-containing proteins may be needed. Further investigation is needed.

### 1.2.2.1.2   FUS, EWSR1 and TAF15 (FET) Proteins

Fused in liposarcoma (FUS), Ewing sarcoma (EWSR1), and TATA-binding associated factor 15 (TAF15) make up the family of FET proteins that are mainly responsible for genomic maintenance, RNA transcription, mRNA splicing, mRNA metabolism and miRNA production. FET proteins are a highly conserved set of proteins that are primarily nuclear and expressed in every cell (Andersson et al., 2008; Ballarino et al., 2013; Morlando et al., 2012; Svetoni et al., 2016).

In ALS, all three of these proteins have been shown to re-localize from the nucleus to the cytoplasm and produce cytoplasmic aggregates, or contain mutations associated with the disease (Belzil et al., 2009; Couthouis et al., 2012; Couthouis et al., 2011; Kwiatkowski et al., 2009;

Neumann et al., 2009b; Ticozzi et al., 2011; Vance et al., 2009). Out of the three FET proteins,

FUS immunoreactive NCIs are the most often observed in ALS, being present in about 1% of all

ALS cases. EWSR1 and TAF15 inclusions have been seen in only a small number of ALS cases

(>0.1%) (Ling et al., 2013). Similar to TDP-43, FET proteins contain an LCD that is believed to

be the major driver of pathological aggregate formation in ALS.

Causative FUS mutations for ALS tend to be concentrated within the nuclear localization

sequence (NLS) and also in the LCD (Taylor et al., 2016). This suggests that the loss of nuclear

localization of FUS is critical to the pathogenesis of ALS. Further, the accumulation of wild-type

FUS leads to phase separation and insoluble protein aggregates in a process that can be

accelerated by mutations in the LCD of FUS (Mitchell et al., 2013; Patel et al., 2015). Several

rodent and *in vitro* models have shown that the overexpression of FUS is sufficient to drive

cytoplasmic aggregation and that this aggregation is dependent on its' LCD (Kato et al., 2012;

Mitchell et al., 2013; Murakami et al., 2015). Increased levels of FUS protein have also been

observed in sALS spinal cord with no known genetic history (Hawley et al., 2017). Thus, the

pathological formation of aggregates by FUS may be concentration dependent, where mutations

accelerate phase separation and the formation of cytoplasmic aggregates by promoting the

accumulation of FUS through the LCD.

### 1.2.2.1.3   HnRNPA1 and HnRNPA2B1

Heterogeneous nuclear Ribonucleoprotein A1 and A2B1 (hnRNPA1 and hnRNPA2B1,

respectively) are primarily nuclear proteins that are involved in mRNA splicing, stability,

transport and miRNA processing (Zhao et al., 2018). Both these proteins contain mutations

within their LCD in less than 1% of ALS cases (Kim et al., 2013; Molliex et al., 2015).

Interestingly, muscle biopsies from ALS patients revealed that hnRNPA1 and hnRNPA2B1

mutations can lead to cytoplasmic aggregates within muscle tissue, although no aggregates were observed in motor neurons (Kim et al., 2013). While neither protein specifically has been shown to aggregate in motor neurons, loss of TDP-43 nuclear localization results in aberrant splicing of hnRNPA1, promoting an alternative isoform called hnRNPA1B that has an extended LCD. Interestingly, hnRNPA1B does form cytoplasmic aggregates in ALS motor neurons where there are also pathological aggregates of TDP-43 (Deshaies et al., 2018). These findings suggest that hnRNP's may play multiple roles in the pathogenesis of ALS affecting both muscle and motor neuron cell populations.

### 1.2.2.1.4 RGNEF

Rho Guanine Nucleotide Exchange Factor (RGNEF) is both a guanine exchange factor involved in the RhoA signaling pathway and an RNA-binding protein. The mouse homologue, p190RhoGEF, was first described in murine tissues and was shown to activate RhoA and interact with microtubules (van Horck et al., 2001). Further, work showed that p190RhoGEF interacted with and destabilized mouse *Nefl* mRNA preventing neurofilament aggregation—a common feature seen in ALS (Lin et al., 2004). This provided the first clue that RGNEF may be involved in the pathogenesis of ALS.

Several guanine exchange factors and RNA-binding proteins are associated with neurodegenerative diseases, but RGNEF is the only protein that shares these two functions and is also associated with neurodegeneration (Droppelmann et al., 2014). Still, little is known about RGNEF's role in RNA regulation although it has been shown to negatively regulate the mRNA stability of *NEFL* through interactions with the 3'UTR (Droppelmann et al., 2013a). Further, RGNEF has been shown to interact with *NEFL* mRNA only in ALS, but not control, spinal cord

homogenates (Volkening et al., 2010), and therefore, may play a major role in intermediate filament pathogenesis associated with ALS.

In terms of pathology, RGNEF has been observed in ubiquitin-positive aggregates and to co-localize with TDP-43 and FUS cytoplasmic aggregates (Keller et al., 2012). Further, several mutations in *ARHGEF28* (gene name of RGNEF) have been associated with ALS (Droppelmann et al., 2013b; Farhan et al., 2017; Ma et al., 2014; Song et al., 2020; Zhang et al., 2016). However, while there is a definite association between RGNEF and ALS, it is still unclear whether these mutations alone are causative of the disease.

### 1.2.2.1.5 ATXN2

Ataxin 2 (ATXN2) is an RNA-binding protein that is primarily expressed within the cytoplasm where it regulates mRNA stability, RNA polyadenylation and mRNA translation. In ~5% of all ALS cases, *ATXN2* contains a polyglutamine (polyQ) repeat element (CAG) that is greater than 37 repeats, while healthy individuals tend to have ~15-22 repeats (Ostrowski et al., 2017; Zhao et al., 2018). Expanded repeats of this gene has been associated with other neurodegenerative diseases including Spinal Cerebellar Ataxia (SCA), frontotemporal dementia and Parkinson's disease (Houlden and Singleton, 2012; Majounie et al., 2007; Rubino et al., 2019). The exact role that these repeat expansions play in disease is relatively unclear. However, the repeat expansion of ATXN2 in ALS appears to enhance TDP-43 and FUS toxicity, while the suppression of ATXN2 expression using antisense oligos (ASOs) reduces TDP-43 toxicity in fly and rodent ALS models overexpressing TDP-43, making it a possible therapeutic target of ALS (Elden et al., 2010; Farg et al., 2013).

### 1.2.2.1.6 MATR3

Matrin 3 (MATR3) is an DNA/RNA-binding protein that is involved with mRNA transcription, export and stability, and primarily found within the nuclear matrix. In less than 1% of ALS cases, there is a missense or splicing mutation in the *MATR3* gene (Leblond et al., 2016; Taylor et al., 2016). Mutations in *MATR3* still result in it being primarily nuclear within ALS motor neurons; however, some have reported either MATR3 diffusely localized to the cytoplasm, or in cytoplasmic inclusions with TDP-43 (Johnson et al., 2014; Tada et al., 2018). Transgenic mice overexpressing ALS-mutant *MATR3* F115C showed muscle atrophy, but no effect on spinal motor neurons, indicating that *MATR3* mutations may have a greater impact on muscle than motor neurons (Moloney et al., 2018). Others have observed in primary rat neuronal cell culture models that *MATR3* mutations enhance neuronal death, where neurotoxicity is dependent on its nuclear localization, not cytosolic localization, as we have seen with other ALS-associated RNA-binding proteins (Malik et al., 2018). Overall, a lot still needs to be understood about *MATR3* mutations and its relation to the pathogenicity of ALS.

### 1.2.2.1.7  TIA-1

TIA1 cytotoxic granule associated RNA-binding protein (TIA-1) is a primarily nuclear protein involved in RNA processing and translation (Del Gatto-Konczak et al., 2000; Dixon et al., 2003; Forch et al., 2000; Piecyk et al., 2000). However, TIA-1 is better known for its role in stress granule assembly (Gilks et al., 2004; Kedersha et al., 2000; Kedersha et al., 1999). During periods of cellular stress, TIA-1 leaves the nucleus and enters the cytoplasm where it nucleates and initiates the formation of stress granules, which contain several ALS-related RNA-binding proteins including TDP-43, FUS, hnRNPA1, hnRNPA2B1, ATXN2 and MATR3 (Gilks et al., 2004; Kedersha et al., 2000; Zhao et al., 2018). Stress has been suggested to be a seed to cytoplasmic aggregation of proteins associated with ALS as TIA-1 has been shown to form

pathological aggregates in ALS motor neurons that co-localize with TDP-43 (Liu-Yesucevitz et al., 2010; Volkening et al., 2009). More recently, several ALS-associated mutations have been observed within the LCD of TIA-1 (Mackenzie et al., 2017; Yuan et al., 2018; Zhang et al., 2018b). While patients with these mutations did show TDP-43 cytoplasmic aggregates in motor neurons, no TIA-1 was observed in cytoplasmic aggregates. Despite this finding, mutations within the LCD of TIA-1 still promoted the phase separation of TDP-43 into insoluble aggregates in *in vitro* motor neuron models, indicating that *TIA-1* mutations and its LCD likely contribute to TDP-43 pathology (Mackenzie et al., 2017).

## 1.2.2.2 Other Major Protein Pathologies in ALS

Several other proteins have been observed in ALS motor neurons to form cytoplasmic aggregates that are not categorized as RNA-binding proteins. However, here I will discuss two other major protein pathologies—SOD1 and C9ORF72—that have been also shown to contribute to RNA dysregulation in ALS.

### 1.2.2.2.1  SOD1

Cu/Zn-superoxide dimutase 1 (SOD1) cytoplasmic protein aggregation is seen in 2% of all ALS cases. Mutations in SOD1 (mtSOD1) leads to misfolding of the protein causing reduced activity and increased accumulation of free radicals that are toxic to cells (Kaur et al., 2016). Interestingly, mutant, but not wild-type, SOD1 binds to the 3' untranslated region (UTR) of *NEFL* and *VEGF* mRNA, destabilizing these mRNA molecules and reducing their steady-state levels (Li et al., 2009; Lin et al., 2004; Lu et al., 2007; Menzies et al., 2002). Therefore, while not classically an RNA-binding protein, mtSOD1 appears to acquire a gain-of-function where it negatively regulates the levels of *NEFL* and *VEGF* through direct interactions with their 3'UTRs.

*VEGF* is a critical trophic factor known to promote motor neuron survival, while *NEFL* is critical

for cytoskeleton formation (Oosthuyse et al., 2001; Szaro and Strong, 2010). This highlights that

mtSOD1 toxicity not only disrupts cytoskeleton formation, which is critical for motor neuron

structure and function, but as well reducing the expression of trophic factors critical for motor

neuron survival. MtSOD1, due to protein misfolding, appears to have a high affinity for

adenylate- and uridylate-rich elements (ARE's) located in the 3'UTRs of *NEFL* and *VEGF*, and

thus, while these are currently the only two RNA molecules known to be affected by mtSOD1,

there could be other RNA molecules with ARE regions that mtSOD1 could target (Li et al.,

2009).

**1.2.2.2.2   C9ORF72**

*Chromosome 9 open reading frame 72* (*C9ORF72*) GGGGCC intronic repeat expansions

are the most common genetic variant associated with ALS where less than 24 repeats is

considered a normal state, between 24-100 repeats represents an intermediate state (between

normal and pathological), and over 100 repeats represents a pathological state (DeJesus-

Hernandez et al., 2011; Mathis et al., 2019; Renton et al., 2011). This expansion leads to aberrant

translation—non-ATG or RAN-translation—of *C9ORF72* creating dipeptide repeats (poly-GA,

poly-GP, poly-GR, poly-PA and poly-PR dipeptides) that are known to form cytoplasmic

aggregates that are linked to neurotoxicity (Mori et al., 2013a; Mori et al., 2013b; Wen et al.,

2014). Through a gain-of-function mechanism via the dipeptide repeats several RNA processing

pathways are affected including RNA transcription, splicing and translation (Kwon et al., 2014;

Suzuki et al., 2018; Zhang et al., 2018c). Further, in several *in vitro* and *in vivo* models, the

dipeptide repeats have been shown to bind to multiple nucleoporin proteins which blocks nuclear

export of RNA molecules (Freibaum et al., 2015; Shi et al., 2017; Zhang et al., 2015).

Overall, several proteins associated with ALS are in involved in the regulation of coding and non-coding RNA pathways making it clear that RNA dysfunction is likely a major contributor in the disease pathogenesis.

**1.2.2.3 RNA Dysregulation in ALS**

**1.2.2.3.1   Cytoskeleton Pathology and RNA Dysregulation in ALS**

Intermediate filaments are a critical component that provide cellular structure, and in particular, provide axonal structure to neurons which allow for axonal transport and signaling which are necessary for neuronal survival (Szaro and Strong, 2010). In mature neurons, there are three intermediate filaments, generally called neurofilaments, that are critical for axonal structure; neurofilament light (NFL), medium (NFM) and heavy (NFH). Together they form a triplet protein structure where NFL either forms homopolymers or heteropolymers with NFM and NFH. Neither NFM or NFH alone can form homopolymers and are therefore dependent on NFL to form the cytoskeleton structure of an axon (Carpenter and Ip, 1996). Further, peripherin (PRPH) and α-internexin (INA) are two intermediate filaments responsible for forming the early cytoskeleton structure in developing neurons, but also interact with the neurofilament triplet protein structure in mature neurons (Athlan and Mushynski, 1997; Kaplan et al., 1990; Yuan et al., 2006; Yuan et al., 2012). These five intermediate filaments are under tight spatiotemporal control to maintain axonal structure and integrity (Szaro and Strong, 2010).

In ALS, several of these intermediate filaments have been shown to form pathological aggregates within motor neurons, including NFH, NFM and PRPH (He and Hays, 2004; Keller et al., 2012; Mendonca et al., 2005; Migheli et al., 1993; Mizuno et al., 2011; Munoz et al., 1988; Strong et al., 2005). It is believed that loss of spatiotemporal control leads to an alteration in the stoichiometry between the intermediate filaments causing intermediate filament aggregation

(Szaro and Strong, 2010). This is because in several ALS mouse models where intermediate filaments have either been knocked-out, or knocked-in, intermediate filament aggregation was observed that was representative of what was seen in the disease, and in most cases, led to motor neuron death (Beaulieu and Julien, 2003; Beaulieu et al., 1999; Cote et al., 1993; Kriz et al., 2000; Lee et al., 1994; Robertson et al., 2002; Zhu et al., 1997). Further, in motor neurons of patients with sALS with no known genetic background, there is reduced expression of *NEFL*, *PRPH* and *INA* mRNA levels with no change to *NEFM* or *NEFH* levels (Wong et al., 2000). These changes in mRNA levels between intermediates filaments causes a change in stoichiometry that could result in intermediate filament aggregation.

While intermediate filament mRNA dysregulation is a well-known phenomenon in ALS, it is unclear what causes this RNA dysregulation. Two ALS-related RNA-binding proteins— TDP-43 and RGNEF—have been shown to interact with the 3'UTR and regulate *NEFL* mRNA by either increasing or reducing the mRNA levels, respectively (Droppelmann et al., 2013a; Volkening et al., 2009). Interestingly, *NEFL* mRNA in spinal cord homogenates was only bound to RGNEF when homogenates were derived from ALS patients and not from controls (Volkening et al., 2010). This suggests that dysregulation of TDP-43 and RGNEF, as seen in ALS motor neurons, may alter *NEFL* mRNA steady-state levels, contributing to changes in intermediate filament stoichiometry.

Further, our group has shown several ALS-linked miRNAs interact with the *NEFL* 3'UTR to regulate mRNA stability including: miR-146a*, miR-524-5p, miR-582-3p miR-b1336, and miR-b2403. Expression levels of miR-524-5p, miR-582-3p, miR-b1336 and miR-b2403 have all been shown to be reduced in ALS spinal cord but increase mRNA stability when interacting with the *NEFL* 3'UTR. In contrast, miR-146a* has been shown to be increased in

ALS spinal cord but decreases mRNA stability when interacting with the *NEFL* 3'UTR

(Campos-Melo et al., 2013; Ishtiaq et al., 2014). These observations suggest that miRNA

dysregulation may be a major contributor to reduced *NEFL* mRNA levels in ALS motor neurons,

and to overall changes in intermediate filament stoichiometry. However, research still needs to

be done to understand why there is a selective suppression of *NEFL*, *PRPH* and *INA* in ALS

motor neurons while sparing the remaining intermediate filaments.

### 1.2.2.3.2  Splicing Dysregulation in ALS

Several ALS-related RNA-binding proteins are known to be involved in mRNA splicing

including: TDP-43, FUS, TAF15, EWSR1, valosin-containing protein (VCP), hnRNPA1 and

hnRNPA2B1 (Perrone et al., 2020). Thus, it is not surprising that mis-splicing of mRNA in

motor neurons and spinal cord is a common phenomenon found in patients with ALS.

TDP-43 dysregulation has been heavily associated with mis-splicing of several genes

including, but not limited to *CFTR*, *MAPT*, *SMN2*, *hnRNPA1* and *STMN2* (Bose et al., 2008;

Buratti and Baralle, 2001; Deshaies et al., 2018; Gu et al., 2017; Klim et al., 2019). In particular,

mutations in the C-terminal end of TDP-43 have been associated with a gain-of-function where

TDP-43 creates an alternative splicing event which skips exons that would normally be included

(Fratta et al., 2018). These are known as "skiptic exons". Further, loss of TDP-43 nuclear

localization has been associated with loss-of-function splicing by which exons that would not

normally be a part of the final transcript are placed in the transcript due to the absence of TDP-43

(Fratta et al., 2018). These are known as "cryptic exons." Both skiptic and cryptic exons have an

increased prevalence in mouse models that contain gain or loss-of-function of TDP-43,

respectively (Fratta et al., 2018). More recently, reduced TDP-43 levels within iPSC-derived

motor neurons resulted in the production of a cryptic exon in the gene *stathmin-2* (*STMN2*)—a

protein necessary for axonal regeneration—which leads to early termination of translation and loss of protein production. Further, this cryptic exon in *STMN2* showed increased prevalence in ALS motor neurons where reduced STMN2 protein was also observed (Klim et al., 2019).

TDP-43 also functions in the splicing of *hnRNPA1*. However, loss of TDP-43 nuclear localization promotes the production of the *hnRNPA1B* transcript, an alternative splice isoform which produces a protein that has an extended LCD and promotes the formation of hnRNPA1B cytoplasmic aggregates in ALS motor neurons (Deshaies et al., 2018).

ALS-associated mutations in VCP have been shown to result in mis-splicing of *Splicing Factor Proline and Glutamine rich* (*SFPQ*) transcript causing the retention of intron 9 as shown in iPSC-derived motor neuron models (Luisier et al., 2018). The retention of this intron leads to increased binding of the SFPQ protein on the *SFPQ* transcript resulting in the protein exiting the nucleus and forming cytoplasmic aggregates. Clearance of SFPQ from the nucleus can be seen in motor neurons of mtVCP, mtSOD1, and sporadic ALS cases (Luisier et al., 2018). This provides an interesting mechanism by which mis-splicing, or intron retention, may directly contribute to the cytoplasmic aggregation of nuclear proteins as seen in ALS.

Finally, FUS and other FET proteins (TAF15 and EWSR1) are known to interact with the spliceosome and regulate the splicing of several transcripts in the central nervous system (Kapeli et al., 2016; Orozco and Edbauer, 2013; Rogelj et al., 2012; Svetoni et al., 2016; Yu and Reed, 2015; Zhou et al., 2002). FUS splicing events have been shown to be critical for neuronal function and survival (Lagier-Tourenne et al., 2012). Loss of FUS nuclear localization due to ALS-associated mutations has been known to cause massive changes in splicing within brain tissue of rodent models and *in vitro* neuronal models (Dormann et al., 2010; Kapeli et al., 2016;

Lagier-Tourenne et al., 2012; Reber et al., 2016; Zhou et al., 2013b). Overall, mis-splicing of transcripts appears to be a major contributor to the disease pathogenesis.

### 1.2.2.3.3 Altered Polyadenylation in ALS

Recent research has shown that altered poly(A) may be a contributing factor to the disease pathogenesis as a consequence of the loss of TDP-43 nuclear localization. In particular, TDP-43 regulates the poly(A) of *STMN2* as shown in iPSC-derived motor neuron models, but loss of TDP-43 regulation promotes an early poly(A) termination site during transcription of *STMN2* (Melamed et al., 2019). This leads to loss of STMN2 protein which, as mentioned previously, is a protein considered necessary for axonal regeneration (Klim et al., 2019). This early poly(A) termination of *STMN2* has been observed in patients with ALS, indicating altered polyadenylation could be a factor contributing to motor neuron degeneration (Melamed et al., 2019). While *STMN2* is one example of altered polyadenylation in ALS, it would be worth exploring the extent of poly(A) dysregulation due to loss of TDP-43 nuclear function to understand the scope of this alteration across the transcriptome.

### 1.2.2.3.4 Dysregulation of RNA Export in ALS

Disruption in nucleocytoplasmic transport is a major phenomenon that occurs in ALS due to dysregulation of nuclear pore complexes (Chou et al., 2018; Freibaum et al., 2015; Taylor et al., 2016; Zhang et al., 2018a; Zhang et al., 2015). Nuclear pore complexes have been shown to interact with insoluble TDP-43. Mouse models and iPSC-derived motor neuron models containing disease-related mutations in TDP-43 showed impaired poly(A)-containing RNA export causing it to accumulate in the nucleus (Chou et al., 2018). Further, ALS-related mutations in *MATR3* and *C9ORF72* have also been shown to cause nuclear mRNA export

defects (Boehringer et al., 2017; Zhang et al., 2015). However, whether this is a global effect or if specific mRNA molecules are being retained is still in question.

**1.2.2.3.5    Non-coding RNA Dysregulation in ALS**

Non-coding RNA molecules that have been associated with the pathogenesis of ALS include miRNAs, long non-coding RNA's (lncRNA's) and small nucleolar RNA's (snoRNA's) (Campos-Melo et al., 2013; Chen and Chen, 2020; De Felice et al., 2014; Emde et al., 2015; Figueroa-Romero et al., 2016; Nishimoto et al., 2013; Riva et al., 2016). Although several snoRNA's have been shown to be upregulated in ALS motor neurons, the significance of this finding and how it contributes to the pathogenesis of ALS is still unclear (Riva et al., 2016).

LncRNA *NEAT1_2* has been observed to be increased in the motor neurons of sALS patients (Nishimoto et al., 2013). *NEAT1_2* is an essential component for nuclear paraspeckle formation—RNP granules that regulate gene expression via nuclear retention of mRNA (Fox and Lamond, 2010). Increased *NEAT1_2* levels coincide with an increase number of paraspeckles in sALS motor neurons where *NEAT1_2* has been shown to interact with TDP-43 and FUS proteins (Nishimoto et al., 2013). Interestingly, ALS-linked mutations in FUS have been shown to cause paraspeckle dysfunction, but also lead to greater *NEAT1_2* levels, indicating that FUS may be needed to form paraspeckles, and the loss of these structures could contribute to the pathology of the disease (An et al., 2019).

As previously discussed, miRNAs have been the most extensively studied non-coding RNA molecules in ALS. The majority of miRNAs, but not all, have been shown to be reduced in the spinal cord and motor neurons of ALS patients (Campos-Melo et al., 2013; De Felice et al., 2014; Emde et al., 2015; Figueroa-Romero et al., 2016; Reichenstein et al., 2019). It is tempting to hypothesize that this may be because several RNA-binding proteins that are dysregulated in

ALS are also involved in miRNA biogenesis. These include TDP-43, FUS, TAF15, EWSR1, hnRNPA1, and hnRNPA2B1 (Alarcon et al., 2015; Ballarino et al., 2013; Guil and Caceres, 2007; Kawahara and Mieda-Sato, 2012; Kim et al., 2014; Morlando et al., 2012). However, very little is known about how miRNAs become dysregulated in the first place and whether this change in miRNA expression really has an impact on the disease pathogenesis. In this dissertation, my goal is to try and understand possible mechanisms for why miRNAs are reduced in ALS motor neurons and whether if any of the miRNAs affected result in altered expression of genes associated ALS. For example, does reduced miRNA expression alter intermediate filament stoichiometry, or lead to increased expression of LCD-containing proteins which may promote their aggregation? To understand miRNA dysregulation, we must first understand miRNA regulation. In the next section, I will discuss miRNA biogenesis, regulation and function, and then briefly discuss our current understanding of the role of miRNAs in motor neuron function and disease.

**1.3 MiRNAs**

MiRNAs are evolutionary conserved non-coding RNAs (ncRNAs) of 18-22 nucleotides that post-transcriptionally regulate the expression of most mammalian genes. First discovered in *Caenorhabditis elegans* over 25 years ago, miRNAs are the dominant class of small RNAs in somatic cells (Ha and Kim, 2014; Lee et al., 1993). The human genome harbours more than 2,500 mature miRNAs that play major roles in a variety of biological pathways such as apoptosis, cell proliferation, development, differentiation and pathological processes (Bartel, 2018). Each miRNA contains a unique nomenclature used to identify them (**Table 1.2**).

**1.3.1   MiRNA Biogenesis**

**1.3.1.1 Canonical miRNA Biogenesis Pathway**

**Table 1.2.** MiRNA nomenclature.

| Examples of miRNAs | Symbol | Meaning |
|:---:|:---:|:---:|
| **miR-**218 | "miR-" | Abbreviation for "miRNA" |
| miR-**218** | "218" | Unique identifier for specific miRNA |
| **miR-1** | "miR-1" | Name listed without asterisks represent predominant miRNA product that originates from precursor miRNA |
| miR-1* | "*" | Asterisk refers to miRNA which is on the opposite arm from predominant product on the precursor miRNA |
| miR-124-**5p** or miR-124-**3p** | "-5p, -3p" | Suffixes determine whether the miRNA originated from the 5' end (-5p) or 3'end (-3p) of precursor miRNA molecule |
| miR-27**a**-3p or miR-27**b**-3p | "a, b" | Letters beside miRNAs with the same unique identifier refer to miRNAs that are a part of the same family. If miRNAs are in the same family, they contain the exact same seed sequence, but the full mature miRNA sequence is not the same |
| miR-9-**1**-5p, miR-9-**2**-5p or miR-9-**3**-5p | "-1, -2, -3" | Numbers, written as such beside the unique identifiers, refer to duplicate miRNAs. These miRNAs have the exact same mature miRNA sequence but originate from different areas of the genome |

In mammals, the majority of miRNAs are encoded within introns of either protein-coding or non-coding genes (Rodriguez et al., 2004). Several miRNA loci close in proximity are generally co-transcribed, thus constituting a miRNA cluster. Most miRNAs are transcribed by RNA polymerase II (Pol II); however RNA Pol III has been also shown to transcribe some viral and human miRNAs (Borchert et al., 2006; Pfeffer et al., 2005). MiRNA transcription is controlled by RNA Pol II-associated transcription factors such as MYC, ZEB1 and ZEB2 and epigenetic regulators (Cai et al., 2004; Davis-Dusenbery and Hata, 2010; Lee et al., 2004). Transcription products - primary miRNAs that are over 1 kb in length (pri-miRNAs) - contain a stem-loop structure in which mature miRNA sequences are embedded. Similar to mRNAs, pri-miRNA transcripts contain a 7-methyl guanylate cap at the 5' end and a poly(A) tail at the 3' end (Davis and Hata, 2009). The nuclear RNAse III-type endonuclease DROSHA, and its essential cofactor DiGeorge syndrome chromosomal region 8 (DGCR8), form the microprocessor complex to target and cleave pri-miRNAs at the stem-loop to release the ~65 nt length precursor miRNA (pre-miRNA) (Denli et al., 2004; Gregory et al., 2004; Han et al., 2004; Lee et al., 2003). The pre-miRNA is then exported to the cytoplasm by exportin-5 and Ras-related nuclear protein guanosine-5'-triphosphate (Ran-GTP) (Bohnsack et al., 2004; Lund et al., 2004; Yi et al., 2003). It has been reported that exportin-5 is necessary but not critical for miRNA maturation, suggesting that other mechanisms complement its function (Kim et al., 2016).

Pre-miRNA is cleaved by another RNAse III-type endonuclease called DICER, releasing the small miRNA duplex (Hutvagner et al., 2001; Ketting et al., 2001). DICER associates with the cofactors human immunodeficiency virus transactivating response RNA-binding protein (TRBP) and protein activator of the interferon-induced protein kinase (PACT), which do not seem to be essential for DICER-mediated pre-miRNA processing (Chendrimada et al., 2005;

Haase et al., 2005; Lee et al., 2013; Lee et al., 2006). However, it has been shown that TRBP is

an integral cofactor for DICER processing in RNA-crowded environments, acting as a

gatekeeper to preclude DICER from engaging with pre-miRNA-like substrates (Fareh et al.,

2016). After DICER processing, the miRNA duplex is loaded into AGO proteins (AGO 1-4 in

humans) to form the RNA-induced silencing complex (RISC). Subsequently, the miRNA is

unwound into two separate strands. The guide strand, which is determined during the AGO

loading step based on relative thermodynamic stability, is usually much more prevalent and more

biologically active than the passenger strand (miRNA*) (Ha and Kim, 2014; Kawamata and

Tomari, 2010).  After AGO-mature miRNA binding, AGO seeks target mRNAs that are

complementary to the miRNA seed sequence. Of note, miRNA silencing likely occurs by

submicroscopic complexes in the cytoplasm that are constantly exchanging with cytoplasmic

RNA granules called processing bodies (p-bodies) (Leung and Sharp, 2013). Finally, an

interesting observation is that most mature miRNAs are also present in the nucleus, indicating

that mature miRNAs can shuttle between the nucleus and cytoplasm. Exportin-1 (XPO1) and

importin-8 (IPO8) have been shown to mediate the translocation to the nucleus of not only

miRNAs, but also AGO proteins (Castanotto et al., 2009; Weinmann et al., 2009). Within the

nucleus, miRNAs can function in gene activation or in an unconventional manner regulating the

biogenesis and functions of miRNAs and long non-coding RNAs (lncRNAs) (Liang et al., 2013)

(**Fig. 1.2**).

### 1.3.1.2 Non-canonical miRNA Biogenesis Pathway

Several alternative mechanisms of miRNA biogenesis have been described besides the

canonical pathway, although only about 1% of conserved miRNAs are produced independently

of DICER or DROSHA in vertebrates (Ha and Kim, 2014). The most common non-canonical

pathway is used for mirtron production: miRNAs encoded in introns at the exon junction site.

Mirtron miRNAs bypass the DROSHA-DGCR8 complex. Pre-miRNAs are instead generated by

mRNA splicing, lariat debranching and trimming (Berezikov et al., 2007; Ruby et al., 2007).

DROSHA-mediated processing is also bypassed in the case of miRNAs derived from shRNAs,

tRNAs or tRNA-like precursors, small nucleolar RNAs (snoRNAs) or snoRNA-like viral RNAs

(Babiarz et al., 2008; Cazalla et al., 2011; Ender et al., 2008).

In some cases, such as miR-451, miRNAs can also be generated by DICER-independent

miRNA biogenesis. After DROSHA cleavage, pre-miR-451 is directly loaded and sliced by

AGO2 (Cifuentes et al., 2010). Then, a poly(A)-specific ribonuclease (PARN) trims down the 3′

end of pre-miR-451 to produce the mature miR-451 (Yoda et al., 2013).

Another class of miRNAs undergo DROSHA and DICER dependent biogenesis, but an

additional processing step is included in between the two RNases. Precursors of these miRNAs

carry a shorter (one-nucleotide long instead of two) 3′ overhang. Terminal uridylyl transferases

(TUT2, TUT4 and TUT7) target these pre-miRNAs and extend their 3'end by 1 nucleotide

through monouridylation for efficient DICER processing (Heo et al., 2012) (**Fig. 1.3**). Of

interest, TUTs can also trigger pre-miRNA degradation through oligouridylation of 3' trimmed

pre-miRNAs and pre-let-7 (see section "Regulation of miRNA expression") (Kim et al., 2015).

### 1.3.2   Regulation of miRNA Expression

MiRNA expression can be regulated at multiple levels. Transcription is the first control

point of the miRNA biogenesis. Of note, one-third of intronic miRNAs have transcription

initiation regions independent of their host promoters. RNA Pol II-transcribed miRNA promoters

are generally similar to mRNA promoters in terms of frequencies of CpG islands, TATA

elements, TFIIB recognition elements, initiator elements (Inr), motif ten elements (MTE) and
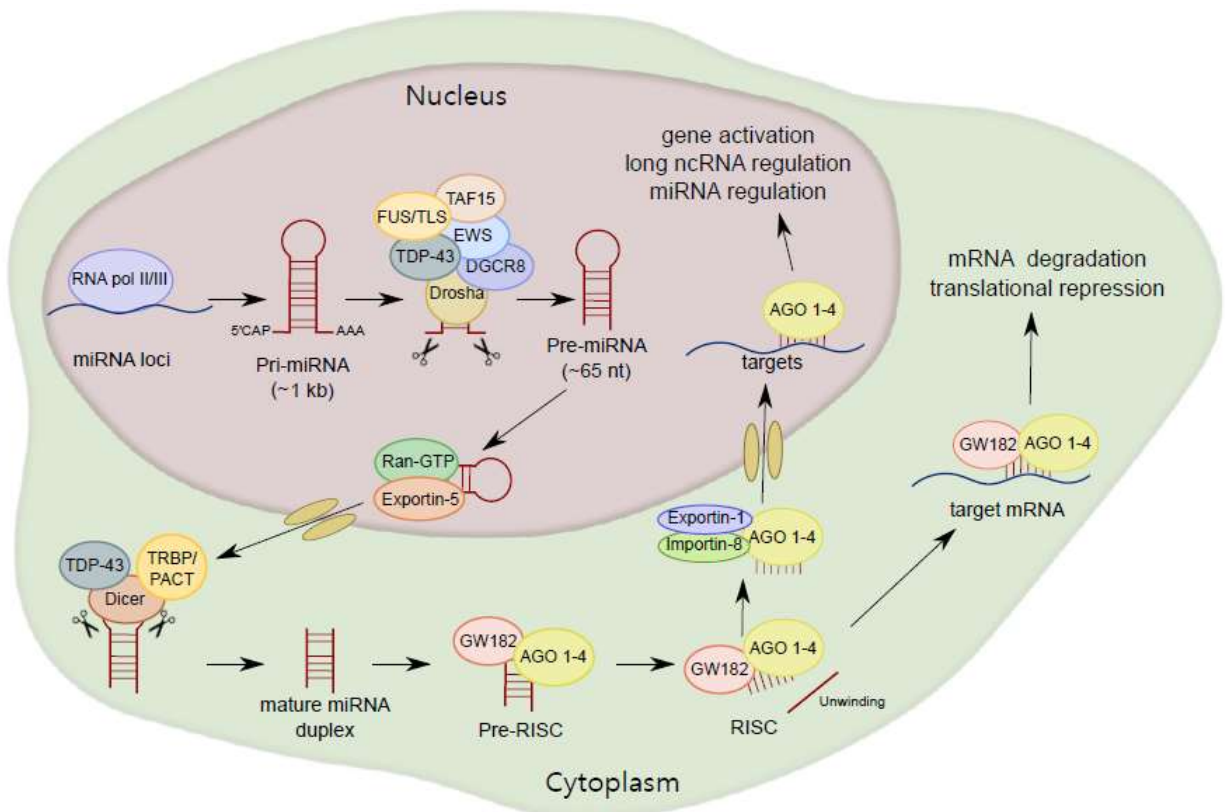
**Figure 1.2. MiRNA biogenesis of canonical miRNAs**. The first part of miRNA processing occurs in the nucleus. Pri-miRNA is transcribed by RNA polymerase II or III (RNA pol II/III) and then cleaved by DROSHA/DGCR8 to form pre-miRNA. Pre-miRNA is exported to the cytoplasm by exportin-5 and then cleaved by DICER. MiRNA duplex is loaded into argonaute proteins (AGO 1–4) and subsequently unwound into two separated strands. For most miRNA targets, AGO is recruited to a complex that contains GW182 proteins (RNA-induced silencing complex, RISC) that induces translational repression and degradation of the mRNA targets. TDP-43 and FET family, RNA-binding proteins linked to amyotrophic lateral sclerosis (ALS), interact with DROSHA and/or DICER, regulating miRNA processing at both primary and precursor levels.

**Drosha and DGCR8-independent**

Mirtron

Spliceosome → Splicing, lariat debranching and trimming → Exportin 5 → Dicer → AGO (mature RISC)

**Dicer-independent**

5'CAP — AAA → Drosha → Exportin 5 → AGO 2 → Splicing → PARN → Trimming → AGO (mature RISC)

**TUTase-dependent**

5'CAP — AAA → Drosha → Exportin 5 → TUT2, TUT4 and TUT7 / One-nucleotide long 3' overhang → Mono Uridylation → Two-nucleotide long 3' overhang → Dicer → AGO (mature RISC)
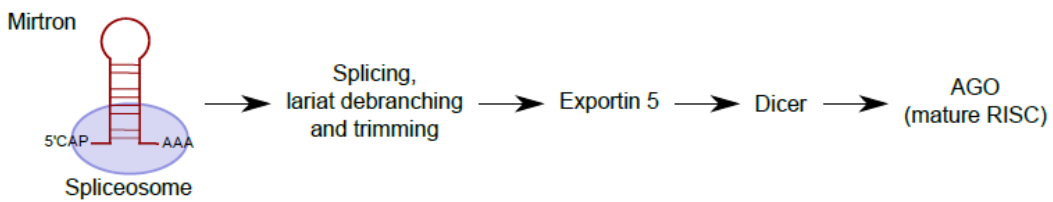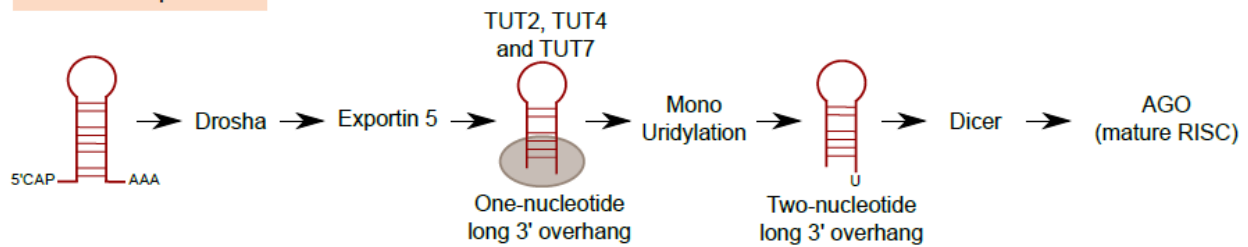
**Figure 1.3. Non-canonical pathways of miRNA processing.** For mirtron production, miRNAs encoded in introns at the exon junction site, miRNAs bypass DROSHA/DGCR8 and pre-miRNAs are instead generated by mRNA splicing, lariat debranching and trimming. In other cases, miRNAs can also be generated by DICER independent miRNA biogenesis. After DROSHA cleavage miRNA is directly loaded and sliced by AGO2. PARN then trims down the 3' end of the pre-miRNA to produce the mature miRNA. A third class of miRNAs undergo DROSHA and DICER dependent biogenesis, but an additional processing step is included in between the two RNAases. Precursors of these miRNAs carry a shorter 3' overhang. Terminal uridylyl transferases (TUT2, TUT4 and TUT7) target these pre-miRNAs and extend their 3' end by 1 nucleotide through monouridylation for efficient DICER processing.

downstream promoter elements (DPE). Also, some transcription factors that control mRNA production regulate the transcription of miRNAs encoded in introns of protein coding genes (Davis and Hata, 2009; Ozsolak et al., 2008).

Changes in the methylation of miRNA promoters or miRNA sequences can impact on the expression of miRNAs. The methylation status of some miRNA genes has been associated with cancer. For instance, hypermethylation of the CpG island upstream of the tumor suppressor miR-33b, is responsible for its downregulation in gastric cancer (Yin et al., 2016). Also, methylation of promoters of the miR-200b cluster is associated with metastasis in advanced breast cancer (Wee et al., 2012). Interestingly, methylation of the 5' monophosphate of pre-miR-23b and pre-miR-145 inhibits the processing of these miRNAs by DICER (Xhemalce et al., 2012). This is because the interaction between DICER and the 5' monophosphate is necessary for the efficient processing of pre-miRNAs (Park et al., 2011). MiRNA promoters are also regulated by histone modifications. Some miRNAs have been reported to be up- or down-regulated after the treatment with histone deacetylase (HDAC) inhibitors (Nasser et al., 2008; Saito and Jones, 2006; Scott et al., 2006). For instance, acetylation regulates the expression of miR-133a during chronic pressure overload-induced cardiac fibrosis (Renaud et al., 2015). Single nucleotide polymorphisms (SNPs) in miRNA genes can also affect miRNA biogenesis (Duan et al., 2007). For example, SNPs in miR-1206 and miR-612 genes within two cancer risk loci affect the expression of both mature miRNAs (Kim et al., 2012).

RNA editing (adenosine to inosine catalyzed by adenosine deaminase that acts on RNA; (ADARs)) also impacts on miRNA processing. Let-7 pri-miRNA editing impairs the biogenesis of this miRNA and drives leukemia stem cell self-renewal (Zipeto et al., 2016). Another type of regulation of miRNA biogenesis is by RNA-tailing (nucleotidyl addition to the 3´ end of RNA).

For example, LIN28 proteins recruit terminal uridylyl transferases TUT4 and TUT7 C6 to induce oligouridylation of pre-let-7 (Hagan et al., 2009; Heo et al., 2008; Heo et al., 2009). This oligo-U tail blocks DICER processing, and facilitates miRNA decay by 3'-5' exonuclease DIS3L2 (Chang et al., 2013; Ustianenko et al., 2013). Some miRNA transcripts, like most mRNAs, are methylated at N6-adenosine (m6A). This modification acts as a mark for pri-miRNA processing. RNA-binding protein hnRNPA2B1 binds to m6A, interacts with DGCR8, and promotes pri-miRNA cleavage to produce pre-miRNA (Alarcon et al., 2015).  Finally, levels of certain miRNAs are controlled by regulating miRNA stability. For instance, levels of miR-122 are stabilized by monoadenylation via the non-canonical cytoplasmic poly(A) polymerase GLD-2 (TUT2) in mammals (D'Ambrogio et al., 2012; Katoh et al., 2009). Moreover, a highly complementary mRNA target can induce miRNA degradation through 3' addition of a single non-templated uridine followed by 3' to 5' trimming of the miRNA with a 2′-O-methyl group added by Hen1 enzyme in *Drosophila* (Ameres et al., 2010; Baccarini et al., 2011).

Recently, another layer of complexity has been added into miRNA regulation. Levels of mature forms of miR-122 are post-transcriptionally regulated by modulating its processing in a target-dependent manner during recovery from starvation-related stress (Bose and Bhattacharyya, 2016).

### 1.3.3   Mechanisms of miRNA Function

MiRNAs are able to regulate gene expression by several mechanisms (**Fig. 1.4**). In RNA silencing, miRNAs function as a guide to recognize target mRNAs, whereas AGO proteins function as effectors by recruiting factors that induce translational repression and/or mRNA decay (Ha and Kim, 2014). The 5' region of the miRNA (seed, nucleotides 2 to 7) is crucial for target recognition through the complementary base pairing of miRNA recognition elements

A. RNA degradation
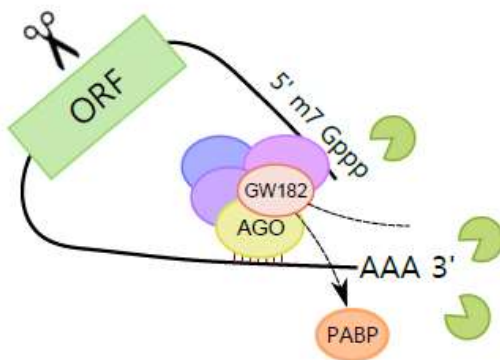
B. Translational inhibition
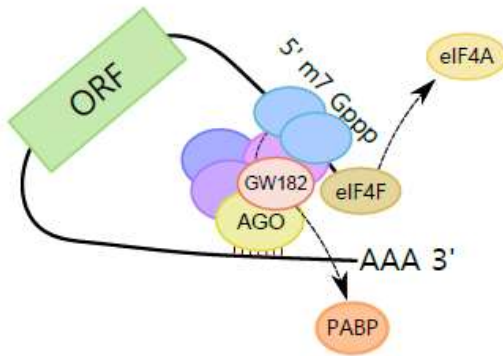
C. Gene activation by RNAa
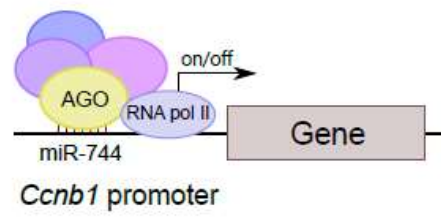
D. miRNA-mediated up-regulation through 3'UTR binding
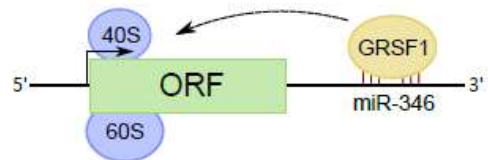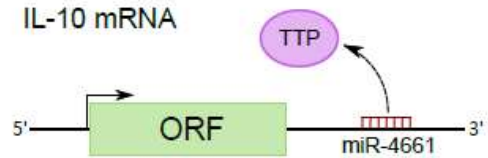
**Figure 1.4. Mechanisms of action of miRNAs.** (A) MiRNAs promote mRNA degradation by recruiting deadenylases on the target mRNA via GW182 and also through the dissociation of PABP, increasing the accessibility of the poly(A) tail to deadenylases. (B) MiRNAs inhibit translation at the initiation step, however the exact mechanism is still unclear. Three mechanisms have been proposed; (i) PABP displacement mediated by GW182; (ii) recruitment of the translational repressors through GW182; and (iii) dissociation of eukaryotic initiation factor-4A (eIF4A) from the cap-binding complex eIF4F. (C) MiRNAs also induce upregulation of their targets. MiRNAs have been implicated in gene activation triggered by promoter-targeted small RNAs, known as RNA activation (RNAa). (D) Upregulation of certain transcripts can also be mediated by miRNA binding to mRNA 3'untranslated regions (3'UTRs), resulting in either translation activation or RNA stability enhancement. MiR-346-dependent upregulation of telomerase reverse transcriptase (TERT) occurs through the binding to TERT mRNA 3'UTR and is mediated by G-rich RNA sequence binding factor 1 (GRSF1). MiR-346 facilitates the recruitment of TERT mRNA to ribosomes to promote translation. In another example, miR-4661 uses the binding sites of the tristetraprolin (TTP) in the IL-10 3'UTR preventing TTP-mediated IL-10 mRNA degradation in macrophages.

(MREs) that are mostly localized in the mRNA 3'untranslated region (UTR). Currently, MREs in 3'UTRs are determined using prediction algorithms and then validated with functional analysis. However, seedless 3'UTR MREs have been described, as well as MREs localized within 5'UTRs and coding regions (Forman et al., 2008; Lal et al., 2009; Moretti et al., 2010). To provide an alternative view of human miRNA targets, a protocol termed cross-linking, ligation and sequencing of hybrids (CLASH) was developed for high-throughput identification of miRNA-target RNA duplexes associated with AGO and is independent of bioinformatic predictors. Transcriptome-wide data set revealed that binding of most miRNAs to their targets includes the seed region, but around 60% of seed interactions are noncanonical. Of interest, seed interactions are generally accompanied by non-seed base pairing (Helwak et al., 2013). MiRNAs downregulate target mRNAs through translational repression and mRNA destabilization, with mRNA destabilization dominating most miRNA-mediated repression (Eichhorn et al., 2014; Guo et al., 2010; Hendrickson et al., 2009). Although miRNAs inhibit translation at the initiation step, the exact mechanism is still unclear. Three mechanisms have been proposed i) PABP displacement mediated by GW182 (Moretti et al., 2012; Zekri et al., 2013), ii) recruitment of the translational repressors through GW182 (Kamenska et al., 2014; Meijer et al., 2013; Waghray et al., 2015) and iii) dissociation of eukaryotic initiation factor-4A (eIF4A) from the cap-binding complex eIF4F (Fukao et al., 2014; Fukaya et al., 2014). At the same time, mRNA destabilization is a consequence of miRNA-mediated deadenylation of target mRNAs which causes these mRNAs to undergo decapping and 5' –3'decay (Behm-Ansmant et al., 2006; Rehwinkel et al., 2005; Wu et al., 2006). MiRNAs promote mRNA decay by recruiting the deadenylase complex CCR4–NOT or PAN2–PAN3 on the target mRNA via GW182 (Braun et al., 2011; Fabian et al., 2011). Also, miRNAs promote mRNA decay through

the dissociation of PABP, increasing the accessibility of the poly(A) tail to deadenylases (Moretti et al., 2012).

Beside well-known downregulatory functions, there is increasing evidence that miRNAs can also induce upregulation of their targets (Campos-Melo et al., 2014; Valinezhad Orang et al., 2014; Vasudevan et al., 2007). MiRNAs, similar to double stranded RNAs (dsRNAs), have been implicated in gene activation triggered by promoter-targeted small RNAs, known as RNA activation (RNAa). For instance, the expression of *cyclin B1* (*Ccnb1*) depends on RNAa by miRNAs and components of miRNA biogenesis in mouse cells. Chromatin immunoprecipitation (ChIP) analysis had shown that AGO1 is selectively associated to the *Ccnb1* promoter and miR-744, which induces *Ccnb1* expression, increases enrichment of RNA Pol II and trimethylation of histone 3 at lysine 4 (H3K4me3) at the *Ccnb1* transcription start site. At a functional level, short-term expression of miR-744 enhances cell proliferation, but prolonged overexpression causes tumor suppression (Huang et al., 2012).

Finally, the upregulation of certain mRNA transcripts can also be mediated by miRNA binding to mRNA 3'UTRs, resulting in either translation activation or RNA stability enhancement. For example, miR-346-dependent upregulation of telomerase reverse transcriptase (TERT) occurs through the binding of miR-346 to TERT mRNA 3'UTR. When miR-346 is bound to the TERT mRNA 3′UTR, its middle sequence motif forms a "bulge loop", facilitating the G-rich RNA sequence binding factor 1 (GRSF1)-mediated recruitment of TERT mRNA to polysomes to promote translation (Song et al., 2015). A similar mechanism of GRSF1 interaction with AGO2 in a miR-346-dependant manner, leading to upregulate the expression of AGO2, has been described for cervical cancer (Guo et al., 2015). It has also been reported that miR-4661 uses the binding sites of the RNA-binding protein tristetraprolin (TTP) in the *IL-10* 3'UTR AU-

rich elements, thus preventing TTP-mediated IL-10 mRNA degradation in macrophages (Ma et al., 2010).

## 1.4 MiRNAs in Motor Neuron Function

Transgenic mouse models containing loss of DICER function set the foundation for the importance of miRNA regulation within motor neurons. These experiments showed that in early development, loss of DICER function within motor neuron progenitor cells leads to aberrant motor neuron development in the lateral motor column, while in adult mice, loss of DICER expression in motor neurons resulted in progressive motor neurodegeneration (Chen and Wichterle, 2012; Haramati et al., 2010). With these two studies, it became apparent that the production of miRNAs is a critical factor to overall motor neuron function and survival. There is very little known about the miRNome (the full spectrum of miRNAs being expressed) of motor neurons. However, as we further discover miRNAs related to motor neuron development and degeneration, it becomes increasingly evident that there are specific miRNAs needed to regulate cytoskeleton integrity, neuronal development, signalling and function, synaptic plasticity, and overall survival of motor neurons which we have termed "MotomiR's" (**Table 1.3**).

### 1.4.1   MiRNAs in Motor Neuron Diseases

Given the several roles of miRNAs in regulating motor neuron differentiation, structure, activity and cytoskeletal integrity, it is not surprising that alterations in the expression of miRNAs have been increasingly linked to human motor neuron degenerative disorders. These alterations can be in the miRNAs and/or MREs such as changes in the expression, editing and methylation, mutations and SNPs, and also alterations in competing endogenous RNAs (ceRNAs) involved in the regulation of the interaction of miRNAs and their targets.

**Table 1.3.** List of current MotomiRs and their function*

| MotomiR | Genes shown to regulate | Role within motor neurons | Organism/Cell models used to describe function | References |
|---|---|---|---|---|
| miR-9 | *OC1, FoxP1, NEFH, MAP1B, MCPIP1* | Development, cytoskeleton maintenance, cell survival | Chick, mouse neuronal precursor cells, mouse | (Dajas-Bailador et al., 2012; Haramati et al., 2010; Luxenhofer et al., 2014; Otaegi et al., 2011; Xu et al., 2016) |
| miR-124 | *REST, Stat3, Kfl6* | Development, regeneration | Mouse | (Nagata et al., 2014; Visvanathan et al., 2007) |
| miR-146*, miR-524, miR-582, miR-b1336, & miR-b2403 | *NEFL* | Cytoskeleton maintenance | *In vitro* interactions done in HEK293T cells | (Campos-Melo et al., 2013; Ishtiaq et al., 2014) |
| miR-218 | *TEAD1, FOXP2, LHX1, SLC6A1, BCL11A, SLC1A1* | Development, membrane excitability, NMJ synaptic connections | Mouse | (Amin et al., 2015; Thiebes et al., 2015) |
| miR-8 | *FasIII, Nrg, wg, lar* | Synaptic plasticity | *Drosophila* | (Lu et al., 2014; Nesler et al., 2013) |
| miR-958 & miR-289 | *Lar* | Synaptic plasticity | *Drosophila* | (Nesler et al., 2013) |
| miR-375 | *PAX6, CCND2, p53* | Development, cell survival | Human neural progenitor cell cultures | (Bhinge et al., 2016) |
| miR-310-313 | *Khc-43* | Synaptic vesicle release | *Drosophila* | (Tsurudome et al., 2010) |
| miR-128 & miR-20a | *PDZ-RhoGEF* | Axonal growth, regeneration | Rat cortical neuron cultures | (Sun et al., 2013) |
| miR-153 | *SNAP-25* | Axonal growth, synaptic vesicle release | Zebrafish | (Wei et al., 2013) |
| miR-196 | *Hoxb8* | Development | *Drosophila* | (Asli and Kessel, 2010) |
| miR-183 | *mTOR* | Neurite growth | Rat primary spinal motor neuron cultures | (Kye et al., 2014) |
| miR-206 | *BDNF, HDAC4* | NMJ Regeneratoin | Mouse | (Miura et al., 2012; Williams et al., 2009) |

| miR-34 | *Nrx-IV, Hts* | NMJ synaptic connections | *Drosophila* | (McNeill et al., 2020) |
|---|---|---|---|---|
| miR-126 | *Sema3, NRP* | NMJ synaptic connections | *In vitro* motor neuronal models | (Maimon et al., 2018) |
| miR-137 | *Calpain-2* | Regeneration, survival | *In vivo* rat motor neurons | (Tang et al., 2018) |

*Table adapted from Hawley *et al*., 2017a

**1.4.1.1 MiRNA Dysregulation in Spinal Muscular Atrophy (SMA)**

SMA is an autosomal recessive disease characterized by progressive loss of lower motor neurons and atrophy of muscle (Burghes and Beattie, 2009). Proximal SMA has an incidence of ~1:10,000 newborns and is the most frequent SMA type (Wirth et al., 2006). SMA is caused by homozygous deletion or mutation of *survival motor neuron 1* (*SMN1*) (Lefebvre et al., 1995). SMN has been found to play roles in RNA metabolism, specifically in snRNP (small nuclear ribonucleoproteins) biogenesis, alternative splicing, trafficking of RNA-binding proteins and translation of target mRNAs in neurites. SMN also binds to fragile X mental retardation protein (FMRP), KH-type splicing regulatory protein (KSRP) and FUS, which are important for miRNA biogenesis and function (Akten et al., 2011; Fallini et al., 2014; Fallini et al., 2011; Gubitz et al., 2004; Hubers et al., 2011; Piazzon et al., 2008; Tadesse et al., 2008; Trabucchi et al., 2009; Yamazaki et al., 2012). In fact, several lines of evidence have involved miRNAs in SMA. It was reported that mice lacking the miRNA-processing enzyme DICER selectively in motor neurons display hallmarks of SMA (Haramati et al., 2010). Also, SMN protein has been shown to alter miRNA expression and distribution in neurons (Kye et al., 2014; Wang et al., 2014).

Specifically, miR-183 is increased in neurites of SMN-deficient neurons. Inhibition of miR-183 expression in the spinal cord of an SMA mouse model prolongs survival and improves motor function of *Smn*-mutant mice (Kye et al., 2014). SMN protein also downregulates the expression of miR-9a. Interestingly, miR-9a levels have shown a positive correlation with SMA severity (Wang et al., 2014). A more recent study has shown that miR-431, involved in motor neuron neurite length, also plays a role in the SMA motor neuron phenotype. By integrating miRNA:mRNA profiles, it was observed that miR-431 expression is highly increased in spinal motor neurons, and a number of its putative mRNA targets are significantly downregulated in motor neurons after SMN loss (Wertz et al., 2016). Another miRNA involved in SMA motor

neuron phenotype is miR-375. Besides its role in neurogenesis, miR-375 protects neurons from apoptosis in response to DNA damage. Motor neurons derived from a SMA patient have shown reduced levels of miR-375, elevated p53 protein levels, and higher susceptibility to DNA damage induced apoptosis (Bhinge et al., 2016).

Recently, the first vertebrate system allowing transgenic spatio-temporal control of the *smn1* gene was developed using stable miR-mediated knockdown technology in zebrafish. The expression of anti-*smn1* miRNAs in motor neurons reproduced most hallmarks observed previously in the ubiquitous knockdown model. In addition, *smn1* knockdown in zebrafish motor neurons is sufficient to induce late-onset motor neuron degeneration (Laird et al., 2016). Finally, the potential use of miR-9, miR-206 and miR-132 as biomarkers in SMA has been proposed. It was shown that there is differential expression of all three miRNAs in spinal cord, skeletal muscle and serum samples in SMA mouse models, while only miR-9 and miR-132 were differentially expressed in serum samples of SMA patients (Catapano et al., 2016).

### 1.4.1.2 MiRNA Dysregulation in ALS

Numerous studies in ALS models and patient samples have demonstrated a mass disruption of miRNA expression in ALS (Butovsky et al., 2012; Dobrowolny et al., 2015; Koval et al., 2013; Marcuzzo et al., 2014; Parisi et al., 2013; Toivonen et al., 2014; Williams et al., 2009; Zhou et al., 2013a). The most consistent observation from the mtSOD1 mice is the upregulation of miR-9 and miR-206 (Dobrowolny et al., 2015; Toivonen et al., 2014; Williams et al., 2009; Zhou et al., 2013a). Specifically, miR-9 expression is upregulated in mtSOD1 mouse spinal cord (Dobrowolny et al., 2015; Shi et al., 2004; Tan et al., 2012; Zhao et al., 2009; Zhou et al., 2013a), while miR-206 expression is upregulated in muscle in both mtSOD1 and SMA

mouse models (Valsecchi et al., 2015). Of note, mtSOD1 disease progression is accelerated with downregulation of miR-206 expression (Williams et al., 2009).

The first miRNA profile of human spinal cord tissue was obtained in 2013 and observed a massive downregulation of miRNAs in ALS (Campos-Melo et al., 2013). This disruption was subsequently shown to be specific to motor neurons (Emde et al., 2015). The reduction of miRNA levels has been previously indicated to be a consequence of the inhibition of DICER pre-miRNA processing activity (Emde et al., 2015). Of note, the downregulation of miRNAs has also been observed in other ALS-derived tissues such as in motor cortex, fibroblasts, serum /plasma, and CSF (Benigni et al., 2016; Freischmidt et al., 2015a; Raman et al., 2015; Takahashi et al., 2015; Wakabayashi et al., 2014). A consistent upregulation of miR-206 in muscle (de Andrade et al., 2016; Russell et al., 2013) and in serum samples of ALS patients has also been reported (de Andrade et al., 2016; Toivonen et al., 2014). The latter appears to correlate with the rate of clinical deterioration (de Andrade et al., 2016). Although studies in larger cohorts are necessary, these results suggest that miR-206 could be a potential biomarker for ALS.

While miRNAs have clearly been shown to be reduced within the spinal cord and motor neurons of ALS patients (Campos-Melo et al., 2013; Emde et al., 2015), the exact cause of this mechanism is still unclear. However, a major contributor to reduced miRNA levels in ALS motor neurons is that several ALS-associated RNA-binding proteins have been shown to be involved in miRNA biogenesis as discussed earlier, including: TDP-43, FUS, TAF15, EWSR1, hnRNPA1 and hnRNPA2B1 (Alarcon et al., 2015; Ballarino et al., 2013; Kawahara and Mieda-Sato, 2012; Kim et al., 2014; Kooshapur et al., 2018; Morlando et al., 2012). The common pathological feature among all these proteins in ALS is that they have been found to re-locate from the nucleus to the cytoplasm in motor neurons, and subsequently form cytoplasmic

aggregates. This indicates a loss of nuclear function of RNA-binding proteins in ALS may contribute to the changes in miRNA processing. Interestingly, cellular stress has been shown to transiently induce the re-localization of many ALS-related nuclear RNA-binding proteins to the cytoplasm providing a potential mechanism that could induce the pathology of these proteins in ALS and disrupt miRNA biogenesis.

**1.5 Stress Granules**

The compendium of genes that have been associated with ALS have shown a high enrichment for RNA-binding proteins, indicating that changes to RNA processing in motor neurons is a major factor to the disease progression (Andersen and Al-Chalabi, 2011; Chen et al., 2013; Therrien et al., 2016). Further, many of the ALS-associated RNA-binding proteins are responsible for the formation, assembly, and disassembly of stress granules—transient ribonucleoprotein (RNP) granules that form during periods of cellular stress and contain translationally silent mRNA (Anderson and Kedersha, 2008; Aulas and Vande Velde, 2015; Buchan, 2014). ALS-linked RNA-binding proteins associated with stress granules include: TDP-43, FUS, ATXN2, hnRNPA1, hnRNPA2B1, TAF15, EWSR1, RBM45, C9ORF72 and TIA1 (Andersson et al., 2008; Colombrita et al., 2009; Kim et al., 2013; Li et al., 2015; Mackenzie et al., 2017; Maharjan et al., 2017; Nonhoff et al., 2007). This list contains many of the ALS-related RNA-binding proteins that are involved in miRNA biogenesis mentioned in the previous section. Based on this information, it is widely believed that stress granules may be the seed to pathological aggregate formation of RNA-binding proteins ultimately leading to changes in miRNA processing in ALS.

**1.5.1   Stress Granule Assembly and Disassembly**

When cells face adverse conditions within their environment (e.g. oxidative, osmotic, or proteasomal stress), cells start to produce structures called stress granules (Gilks et al., 2004; Kedersha et al., 2000; Kedersha et al., 1999). The purpose of these granules is to act as a triage for mRNA, where mRNA can be either stored within the stress granule, transferred to processing bodies (p-bodies) for degradation, or go back into polysomes to be translated (Anderson and Kedersha, 2008; Aulas and Vande Velde, 2015).

Phosphorylation of eIF2α appears to be an early trigger that initiates stress granule assembly; however, there are cases of stress granule assembly that are independent of eIF2α phosphorylation (Kedersha et al., 2002; Kim et al., 2007; McEwen et al., 2005; Shenton et al., 2006). The phosphorylation of eIF2α results in reduced formation and activity of translational machinery (Shenton et al., 2006). This is followed by an accumulation of RNA-binding proteins and RNA molecules into granules that lack a membrane structure (Anderson and Kedersha, 2008; Baradaran-Heravi et al., 2020; Gilks et al., 2004). TIA-1 and G3BP1 are two RNA-binding proteins that early on were thought to be critical for proper stress granule formation. However, as we learn more about stress and stress granules, we are starting to understand how truly dynamic and diverse these structures are. Thus, while some proteins are critical for the formation of stress granules for certain stresses, they might not be critical for others (Aulas et al., 2015; Gilks et al., 2004; Kedersha et al., 2016; Markmiller et al., 2018). For example, G3BP1 is critical for the formation of stress granules during oxidative stress, but it is not needed for stress granule assembly during periods of osmotic stress (Kedersha et al., 2016; Solomon et al., 2007). Further, proteomics of stress granules has shown different stresses and different cell types result in different protein profiles (Markmiller et al., 2018). This suggests that stress granule formation and proteomic profile are highly dynamic and context dependent.

After cellular stress disappears, stress granules start disassembling as the cell goes back to its homeostatic state allowing translation of previously silent mRNA to begin again (Molliex et al., 2015). Several mechanisms have been implicated in stress granule disassembly, including: reduced stress results in the formation and increased activity of translational machinery destabilizing the granule structure; inhibition of RNA helicases that promote assembly and maintenance of stress granules; heat shock proteins disassemble RNP complexes; and, ubiquitination of proteins via VCP allowing for stress granules to be targeted by autophagy pathways (Buchan et al., 2013; Cherkasov et al., 2013; Jain et al., 2016; Kroschwald et al., 2015; Meyer and Weihl, 2014; Protter and Parker, 2016; Wheeler et al., 2016). All these pathways likely work together to allow for efficient disassembly of stress granules. It is also clear that stress granule disassembly is an active process that requires ATP hydrolysis (Jain et al., 2016; Meyer and Weihl, 2014; Protter and Parker, 2016).

In all of this, LCD-containing proteins appear to be critical for the formation of stress granules by allowing them to phase separate and form liquid droplets, which produces dynamic interactions with p-bodies, other stress granules and the cytosol of the cell (Aulas et al., 2015; Gilks et al., 2004; Kato et al., 2012; Mackenzie et al., 2017; Molliex et al., 2015; Murray et al., 2017; Patel et al., 2015). Structurally, this is because the LCD participates in β-pleated sheet formation and forms amyloid-like interactions similar to what is seen in prion disease (Molliex et al., 2015; Murakami et al., 2015; Patel et al., 2015). These interactions are critical for the formation of RNA granules which lack a membrane to contain its components (Baradaran-Heravi et al., 2020; Taylor et al., 2016). Therefore, phase transition into reversible liquid droplets is a critical mechanism for the formation of stress granules. While the LCD's are necessary for quick assembly of stress granules, it can also be a detriment to the cells if proteins are left to

accumulate, risking the formation of hydrogels (Kato et al., 2012; Li et al., 2013; Molliex et al., 2015).

### 1.5.2 Hydrogels

LCD-containing proteins in both cell-free and cell *in vitro* models have been shown to form hydrogels (Kato et al., 2012; Molliex et al., 2015; Murakami et al., 2015; Murray et al., 2017). Hydrogels are defined by the aggregation of proteins leading to phase transition into liquid droplets and eventually irreversible gelatin structures (Murakami et al., 2015). The formation of these hydrogel structures is primarily driven by the LCD. (Kato et al., 2012; Molliex et al., 2015; Murakami et al., 2015; Murray et al., 2017).

As discussed, several ALS-related proteins are LCD-containing proteins, including: TDP-43, FUS, hnRNPA1, hnRNPA2B1, TAF15, EWSR1, RBM45 and TIA-1 (Baradaran-Heravi et al., 2020). ALS-linked mutations within the LCD of TDP-43, FUS and hnRNPA1 have been shown to increase the rate at which these proteins phase separate and form hydrogel-like structures (Conicella et al., 2016; Kim et al., 2013; Molliex et al., 2015; Murakami et al., 2015). Since LCD-containing ALS-related proteins tend to form insoluble aggregates, several researchers have focused on therapeutics that prevent the accumulation of these proteins. However, little research has been done on the dysregulation of miRNAs in ALS, and potential changes to their regulation on the expression of ALS-related genes that could be a major contributor to the accumulation of these proteins.

### 1.6 Putting it all together: ALS, cell stress and miRNA dysfunction

Based on the number of ALS-linked genes associated with stress granules, improper stress granule formation has been suggested to be a key precursor to the pathogenesis of ALS

(Aulas and Vande Velde, 2015; Li et al., 2013; Taylor et al., 2016). Intriguingly, out of the 190 RNA-binding proteins identified by Treiber and colleagues to be involved in miRNA processing, 33.2% were associated with stress granules (Treiber et al., 2017). This high enrichment of stress granule associated RNA-binding proteins found with pre-miRNA molecules provides some insight into how miRNAs are able to dynamically change their expression under different physiological conditions (Wilczynska and Bushell, 2015). Interestingly, cellular stressors like endoplasmic reticulum (ER) or oxidative stress have been known to impair miRNA biogenesis reducing overall miRNA expression (Emde et al., 2015). Many RNA-binding proteins during cellular stress are re-localized to stress granules, including TDP-43, FUS, TAF15, EWSR1, hnRNPA1, hnRNPA2B1 and ATXN2, which could explain the reduction in miRNA processing during cellular stress, as many of these proteins are involved with miRNA biogenesis (Alarcon et al., 2015; Andersson et al., 2008; Ballarino et al., 2013; Colombrita et al., 2009; Guil and Caceres, 2007; Kawahara and Mieda-Sato, 2012; Kim et al., 2013; Kim et al., 2014; Li et al., 2015; Morlando et al., 2012; Nonhoff et al., 2007). Therefore, reduced miRNA levels, and by inference reduced activity, during periods of stress could result in accumulation of LCD-containing proteins due to reduced miRNA-mediated silencing, indicating a potential negative feedback loop between miRNAs and RNA-binding proteins that is lost in ALS. Further, during periods of chronic or repeated stress, excessive protein accumulation due to low miRNA levels could result in the formation of insoluble aggregates.

Further, prolonged stress that alters the levels of miRNAs that target intermediate filaments would likely alter the stoichiometry of intermediate filament expression in a fashion that would promote their aggregation. Overall, changes to altered miRNA levels, as seen in ALS,

likely alters the regulation of RNA-binding protein and intermediate filament expression, thus contributing to the resulting pathology of these two protein groups in ALS.

## 1.7 Hypothesis and Aims

Taken together, the downregulation of miRNAs in ALS could be due to altered function and localization of RNA-binding proteins that would normally promote miRNA production, which in turn, leads to loss of miRNA regulation of ALS-associated RNA-binding proteins and intermediate filaments contributing to their pathogenesis.

**Hypothesis:** A negative feedback loop between specific RNA-binding proteins and miRNAs is disrupted in ALS leading to changes in miRNA processing that contributes to RNA-binding protein and intermediate filament pathology.

**Aim 1:** Determine if ALS-linked miRNAs contribute to the selective suppression of *NEFL*, *PRPH*, and *INA* intermediate filaments as seen in ALS motor neurons – Chapter 2.

**Aim 2:** Determine if ALS-linked miRNAs regulate the expression of *NEFM* and *NEFH*, which may contribute to the loss of stoichiometry seen between intermediate filaments in ALS – Chapter 3.

**Aim 3:** Determine if ALS-linked miRNAs regulate the expression of RNA-binding proteins (*TARDBP*, *FUS*, and *RGNEF*) associated with ALS – Chapter 4.

**Aim 4:** Determine if TDP-43 and FUS are in a negative feedback network with ALS-linked miRNAs that is dependent on their nuclear localization – Chapter 5.

## 1.8 References

Akten, B., Kye, M.J., Hao le, T., Wertz, M.H., Singh, S., Nie, D., Huang, J., Merianda, T.T., Twiss, J.L., Beattie, C.E.*, et al.* (2011). Interaction of survival of motor neuron (SMN) and HuD proteins with mRNA cpg15 rescues motor neuron axonal deficits. Proc Natl Acad Sci U S A *108*, 10337-10342.

Alarcon, C.R., Goodarzi, H., Lee, H., Liu, X., Tavazoie, S., and Tavazoie, S.F. (2015). HNRNPA2B1 Is a Mediator of m(6)A-Dependent Nuclear RNA Processing Events. Cell *162*, 1299-1308.

Ameres, S.L., Horwich, M.D., Hung, J.H., Xu, J., Ghildiyal, M., Weng, Z., and Zamore, P.D. (2010). Target RNA-directed trimming and tailing of small silencing RNAs. Science *328*, 1534-1539.

Amin, N.D., Bai, G., Klug, J.R., Bonanomi, D., Pankratz, M.T., Gifford, W.D., Hinckley, C.A., Sternfeld, M.J., Driscoll, S.P., Dominguez, B.*, et al.* (2015). Loss of motoneuron-specific microRNA-218 causes systemic neuromuscular failure. Science *350*, 1525-1529.

An, H., Skelt, L., Notaro, A., Highley, J.R., Fox, A.H., La Bella, V., Buchman, V.L., and Shelkovnikova, T.A. (2019). ALS-linked FUS mutations confer loss and gain of function in the nucleus by promoting excessive formation of dysfunctional paraspeckles. Acta Neuropathol Commun *7*, 7.

Andersen, P.M., and Al-Chalabi, A. (2011). Clinical genetics of amyotrophic lateral sclerosis: what do we really know? Nat Rev Neurol *7*, 603-615.

Anderson, P., and Kedersha, N. (2008). Stress granules: the Tao of RNA triage. Trends Biochem Sci *33*, 141-150.

Andersson, M.K., Stahlberg, A., Arvidsson, Y., Olofsson, A., Semb, H., Stenman, G., Nilsson, O., and Aman, P. (2008). The multifunctional FUS, EWS and TAF15 proto-oncoproteins show cell type-specific expression patterns and involvement in cell spreading and stress response. BMC Cell Biol *9*, 37.

Asli, N.S., and Kessel, M. (2010). Spatiotemporally restricted regulation of generic motor neuron programs by miR-196-mediated repression of Hoxb8. Dev Biol *344*, 857-868.

Athlan, E.S., and Mushynski, W.E. (1997). Heterodimeric associations between neuronal intermediate filament proteins. J Biol Chem *272*, 31073-31078.

Aulas, A., Caron, G., Gkogkas, C.G., Mohamed, N.V., Destroismaisons, L., Sonenberg, N., Leclerc, N., Parker, J.A., and Vande Velde, C. (2015). G3BP1 promotes stress-induced RNA granule interactions to preserve polyadenylated mRNA. J Cell Biol *209*, 73-84.

Aulas, A., and Vande Velde, C. (2015). Alterations in stress granule dynamics driven by TDP-43 and FUS: a link to pathological inclusions in ALS? Front Cell Neurosci *9*, 423.

Babiarz, J.E., Ruby, J.G., Wang, Y., Bartel, D.P., and Blelloch, R. (2008). Mouse ES cells express endogenous shRNAs, siRNAs, and other Microprocessor-independent, Dicer-dependent small RNAs. Genes Dev *22*, 2773-2785.

Baccarini, A., Chauhan, H., Gardner, T.J., Jayaprakash, A.D., Sachidanandam, R., and Brown, B.D. (2011). Kinetic analysis reveals the fate of a microRNA following target regulation in mammalian cells. Curr Biol *21*, 369-376.

Ballarino, M., Jobert, L., Dembele, D., de la Grange, P., Auboeuf, D., and Tora, L. (2013). TAF15 is important for cellular proliferation and regulates the expression of a subset of cell cycle genes through miRNAs. Oncogene *32*, 4646-4655.

Baradaran-Heravi, Y., Van Broeckhoven, C., and van der Zee, J. (2020). Stress granule mediated protein aggregation and underlying gene defects in the FTD-ALS spectrum. Neurobiol Dis *134*, 104639.

Barbee, S.A., Estes, P.S., Cziko, A.M., Hillebrand, J., Luedeman, R.A., Coller, J.M., Johnson, N., Howlett, I.C., Geng, C., Ueda, R.*, et al.* (2006). Staufen- and FMRP-containing neuronal RNPs are structurally and functionally related to somatic P bodies. Neuron *52*, 997-1009.

Barmada, S.J., Skibinski, G., Korb, E., Rao, E.J., Wu, J.Y., and Finkbeiner, S. (2010). Cytoplasmic mislocalization of TDP-43 is toxic to neurons and enhanced by a mutation associated with familial amyotrophic lateral sclerosis. J Neurosci *30*, 639-649.

Bartel, D.P. (2018). Metazoan MicroRNAs. Cell *173*, 20-51.

Beaulieu, J.M., and Julien, J.P. (2003). Peripherin-mediated death of motor neurons rescued by overexpression of neurofilament NF-H proteins. J Neurochem *85*, 248-256.

Beaulieu, J.M., Nguyen, M.D., and Julien, J.P. (1999). Late onset of motor neurons in mice overexpressing wild-type peripherin. J Cell Biol *147*, 531-544.

Behm-Ansmant, I., Rehwinkel, J., Doerks, T., Stark, A., Bork, P., and Izaurralde, E. (2006). mRNA degradation by miRNAs and GW182 requires both CCR4:NOT deadenylase and DCP1:DCP2 decapping complexes. Genes Dev *20*, 1885-1898.

Belzil, V.V., Valdmanis, P.N., Dion, P.A., Daoud, H., Kabashi, E., Noreau, A., Gauthier, J., team, S.D., Hince, P., Desjarlais, A.*, et al.* (2009). Mutations in FUS cause FALS and SALS in French and French Canadian populations. Neurology *73*, 1176-1179.

Benigni, M., Ricci, C., Jones, A.R., Giannini, F., Al-Chalabi, A., and Battistini, S. (2016). Identification of miRNAs as Potential Biomarkers in Cerebrospinal Fluid from Amyotrophic Lateral Sclerosis Patients. Neuromolecular Med *18*, 551-560.

Berezikov, E., Chung, W.J., Willis, J., Cuppen, E., and Lai, E.C. (2007). Mammalian mirtron genes. Mol Cell *28*, 328-336.

Bergeron, C., Beric-Maskarel, K., Muntasser, S., Weyer, L., Somerville, M.J., and Percy, M.E. (1994). Neurofilament light and polyadenylated mRNA levels are decreased in amyotrophic lateral sclerosis motor neurons. J Neuropathol Exp Neurol *53*, 221-230.

Bhinge, A., Namboori, S.C., Bithell, A., Soldati, C., Buckley, N.J., and Stanton, L.W. (2016). MiR-375 is Essential for Human Spinal Motor Neuron Development and May Be Involved in Motor Neuron Degeneration. Stem Cells *34*, 124-134.

Bisby, M.A., and Tetzlaff, W. (1992). Changes in cytoskeletal protein synthesis following axon injury and during axon regeneration. Mol Neurobiol *6*, 107-123.

Boehringer, A., Garcia-Mansfield, K., Singh, G., Bakkar, N., Pirrotte, P., and Bowser, R. (2017). ALS Associated Mutations in Matrin 3 Alter Protein-Protein Interactions and Impede mRNA Nuclear Export. Sci Rep *7*, 14529.

Bohnsack, M.T., Czaplinski, K., and Gorlich, D. (2004). Exportin 5 is a RanGTP-dependent dsRNA-binding protein that mediates nuclear export of pre-miRNAs. RNA *10*, 185-191.

Borchert, G.M., Lanier, W., and Davidson, B.L. (2006). RNA polymerase III transcribes human microRNAs. Nat Struct Mol Biol *13*, 1097-1101.

Bose, J.K., Wang, I.F., Hung, L., Tarn, W.Y., and Shen, C.K. (2008). TDP-43 overexpression enhances exon 7 inclusion during the survival of motor neuron pre-mRNA splicing. J Biol Chem *283*, 28852-28859.

Bose, M., and Bhattacharyya, S.N. (2016). Target-dependent biogenesis of cognate microRNAs in human cells. Nat Commun *7*, 12200.

Bramham, C.R., and Wells, D.G. (2007). Dendritic mRNA: transport, translation and function. Nat Rev Neurosci *8*, 776-789.

Braun, J.E., Huntzinger, E., Fauser, M., and Izaurralde, E. (2011). GW182 proteins directly recruit cytoplasmic deadenylase complexes to miRNA targets. Mol Cell *44*, 120-133.

Brenner, D., Yilmaz, R., Muller, K., Grehl, T., Petri, S., Meyer, T., Grosskreutz, J., Weydt, P., Ruf, W., Neuwirth, C.*, et al.* (2018). Hot-spot KIF5A mutations cause familial ALS. Brain *141*, 688-697.

Buchan, J.R. (2014). mRNP granules. Assembly, function, and connections with disease. RNA Biol *11*, 1019-1030.

Buchan, J.R., Kolaitis, R.M., Taylor, J.P., and Parker, R. (2013). Eukaryotic stress granules are cleared by autophagy and Cdc48/VCP function. Cell *153*, 1461-1474.

Buratti, E. (2015). Functional Significance of TDP-43 Mutations in Disease. Adv Genet *91*, 1-53.

Buratti, E., and Baralle, F.E. (2001). Characterization and functional implications of the RNA binding properties of nuclear factor TDP-43, a novel splicing regulator of CFTR exon 9. J Biol Chem *276*, 36337-36343.

Burghes, A.H., and Beattie, C.E. (2009). Spinal muscular atrophy: why do low levels of survival motor neuron protein make motor neurons sick? Nat Rev Neurosci *10*, 597-609.

Butovsky, O., Siddiqui, S., Gabriely, G., Lanser, A.J., Dake, B., Murugaiyan, G., Doykan, C.E., Wu, P.M., Gali, R.R., Iyer, L.K.*, et al.* (2012). Modulating inflammatory monocytes with a unique microRNA gene signature ameliorates murine ALS. J Clin Invest *122*, 3063-3087.

Cai, X., Hagedorn, C.H., and Cullen, B.R. (2004). Human microRNAs are processed from capped, polyadenylated transcripts that can also function as mRNAs. RNA *10*, 1957-1966.

Campos-Melo, D., Droppelmann, C.A., He, Z., Volkening, K., and Strong, M.J. (2013). Altered microRNA expression profile in Amyotrophic Lateral Sclerosis: a role in the regulation of NFL mRNA levels. Mol Brain *6*, 26.

Campos-Melo, D., Droppelmann, C.A., Volkening, K., and Strong, M.J. (2014). Comprehensive luciferase-based reporter gene assay reveals previously masked up-regulatory effects of miRNAs. Int J Mol Sci *15*, 15592-15602.

Carpenter, D.A., and Ip, W. (1996). Neurofilament triplet protein interactions: evidence for the preferred formation of NF-L-containing dimers and a putative function for the end domains. J Cell Sci *109 ( Pt 10)*, 2493-2498.

Castanotto, D., Lingeman, R., Riggs, A.D., and Rossi, J.J. (2009). CRM1 mediates nuclear-cytoplasmic shuttling of mature microRNAs. Proc Natl Acad Sci U S A *106*, 21655-21659.

Catapano, F., Zaharieva, I., Scoto, M., Marrosu, E., Morgan, J., Muntoni, F., and Zhou, H. (2016). Altered Levels of MicroRNA-9, -206, and -132 in Spinal Muscular Atrophy and Their Response to Antisense Oligonucleotide Therapy. Mol Ther Nucleic Acids *5*, e331.

Cazalla, D., Xie, M., and Steitz, J.A. (2011). A primate herpesvirus uses the integrator complex to generate viral microRNAs. Mol Cell *43*, 982-992.

Chadan, S., Le Gall, J.Y., Di Giamberardino, L., and Filliatreau, G. (1994). Axonal transport of type III intermediate filament protein peripherin in intact and regenerating motor axons of the rat sciatic nerve. J Neurosci Res *39*, 127-139.

Chang, H.M., Triboulet, R., Thornton, J.E., and Gregory, R.I. (2013). A role for the Perlman syndrome exonuclease Dis3l2 in the Lin28-let-7 pathway. Nature *497*, 244-248.

Chen, J.A., and Wichterle, H. (2012). Apoptosis of limb innervating motor neurons and erosion of motor pool identity upon lineage specific dicer inactivation. Front Neurosci *6*, 69.

Chen, K.W., and Chen, J.A. (2020). Functional Roles of Long Non-coding RNAs in Motor Neuron Development and Disease. J Biomed Sci *27*, 38.

Chen, S., Sayana, P., Zhang, X., and Le, W. (2013). Genetics of amyotrophic lateral sclerosis: an update. Mol Neurodegener *8*, 28.

Chen, Y.Z., Bennett, C.L., Huynh, H.M., Blair, I.P., Puls, I., Irobi, J., Dierick, I., Abel, A., Kennerson, M.L., Rabin, B.A.*, et al.* (2004). DNA/RNA helicase gene mutations in a form of juvenile amyotrophic lateral sclerosis (ALS4). Am J Hum Genet *74*, 1128-1135.

Chendrimada, T.P., Gregory, R.I., Kumaraswamy, E., Norman, J., Cooch, N., Nishikura, K., and Shiekhattar, R. (2005). TRBP recruits the Dicer complex to Ago2 for microRNA processing and gene silencing. Nature *436*, 740-744.

Cherkasov, V., Hofmann, S., Druffel-Augustin, S., Mogk, A., Tyedmers, J., Stoecklin, G., and Bukau, B. (2013). Coordination of translational control and protein homeostasis during severe heat stress. Curr Biol *23*, 2452-2462.

Choksi, D.K., Roy, B., Chatterjee, S., Yusuff, T., Bakhoum, M.F., Sengupta, U., Ambegaokar, S., Kayed, R., and Jackson, G.R. (2014). TDP-43 Phosphorylation by casein kinase Iepsilon promotes oligomerization and enhances toxicity in vivo. Hum Mol Genet *23*, 1025-1035.

Chou, C.C., Zhang, Y., Umoh, M.E., Vaughan, S.W., Lorenzini, I., Liu, F., Sayegh, M., Donlin-Asp, P.G., Chen, Y.H., Duong, D.M.*, et al.* (2018). TDP-43 pathology disrupts nuclear pore complexes and nucleocytoplasmic transport in ALS/FTD. Nat Neurosci *21*, 228-239.

Cifuentes, D., Xue, H., Taylor, D.W., Patnode, H., Mishima, Y., Cheloufi, S., Ma, E., Mane, S., Hannon, G.J., Lawson, N.D.*, et al.* (2010). A novel miRNA processing pathway independent of Dicer requires Argonaute2 catalytic activity. Science *328*, 1694-1698.

Colombrita, C., Zennaro, E., Fallini, C., Weber, M., Sommacal, A., Buratti, E., Silani, V., and Ratti, A. (2009). TDP-43 is recruited to stress granules in conditions of oxidative insult. J Neurochem *111*, 1051-1061.

Conicella, A.E., Zerze, G.H., Mittal, J., and Fawzi, N.L. (2016). ALS Mutations Disrupt Phase Separation Mediated by alpha-Helical Structure in the TDP-43 Low-Complexity C-Terminal Domain. Structure *24*, 1537-1549.

Cote, F., Collard, J.F., and Julien, J.P. (1993). Progressive neuronopathy in transgenic mice expressing the human neurofilament heavy gene: a mouse model of amyotrophic lateral sclerosis. Cell *73*, 35-46.

Couthouis, J., Hart, M.P., Erion, R., King, O.D., Diaz, Z., Nakaya, T., Ibrahim, F., Kim, H.J., Mojsilovic-Petrovic, J., Panossian, S.*, et al.* (2012). Evaluating the role of the FUS/TLS-related gene EWSR1 in amyotrophic lateral sclerosis. Hum Mol Genet *21*, 2899-2911.

Couthouis, J., Hart, M.P., Shorter, J., DeJesus-Hernandez, M., Erion, R., Oristano, R., Liu, A.X., Ramos, D., Jethava, N., Hosangadi, D.*, et al.* (2011). A yeast functional screen predicts new candidate ALS disease genes. Proc Natl Acad Sci U S A *108*, 20881-20890.

D'Ambrogio, A., Gu, W., Udagawa, T., Mello, C.C., and Richter, J.D. (2012). Specific miRNA stabilization by Gld2-catalyzed monoadenylation. Cell Rep *2*, 1537-1545.

Dajas-Bailador, F., Bonev, B., Garcez, P., Stanley, P., Guillemot, F., and Papalopulu, N. (2012). microRNA-9 regulates axon extension and branching by targeting Map1b in mouse cortical neurons. Nature Neurosci *15*, 667-669.

Davidson, T.J., and Hartmann, H.A. (1981). RNA content and volume of motor neurons in amyotrophic lateral sclerosis. II. The lumbar intumescence and nucleus dorsalis. J Neuropathol Exp Neurol *40*, 187-192.

Davidson, T.J., Hartmann, H.A., and Johnson, P.C. (1981). RNA content and volume of motor neurons in amyotrophic lateral sclerosis. I. The cervical swelling. J Neuropathol Exp Neurol *40*, 32-36.

Davis-Dusenbery, B.N., and Hata, A. (2010). Mechanisms of control of microRNA biogenesis. J Biochem *148*, 381-392.

Davis, B.N., and Hata, A. (2009). Regulation of MicroRNA Biogenesis: A miRiad of mechanisms. Cell Commun Signal *7*, 18.

de Andrade, H.M., de Albuquerque, M., Avansini, S.H., de, S.R.C., Dogini, D.B., Nucci, A., Carvalho, B., Lopes-Cendes, I., and Franca, M.C., Jr. (2016). MicroRNAs-424 and 206 are potential prognostic markers in spinal onset amyotrophic lateral sclerosis. J Neurol Sci *368*, 19-24.

De Felice, B., Annunziata, A., Fiorentino, G., Borra, M., Biffali, E., Coppola, C., Cotrufo, R., Brettschneider, J., Giordana, M.L., Dalmay, T.*, et al.* (2014). miR-338-3p is over-expressed in blood, CFS, serum and spinal cord from sporadic amyotrophic lateral sclerosis patients. Neurogenetics *15*, 243-253.

DeJesus-Hernandez, M., Mackenzie, I.R., Boeve, B.F., Boxer, A.L., Baker, M., Rutherford, N.J., Nicholson, A.M., Finch, N.A., Flynn, H., Adamson, J.*, et al.* (2011). Expanded GGGGCC hexanucleotide repeat in noncoding region of C9ORF72 causes chromosome 9p-linked FTD and ALS. Neuron *72*, 245-256.

Del Gatto-Konczak, F., Bourgeois, C.F., Le Guiner, C., Kister, L., Gesnel, M.C., Stevenin, J., and Breathnach, R. (2000). The RNA-binding protein TIA-1 is a novel mammalian splicing regulator acting through intron sequences adjacent to a 5' splice site. Mol Cell Biol *20*, 6287-6299.

Deng, H.X., Chen, W., Hong, S.T., Boycott, K.M., Gorrie, G.H., Siddique, N., Yang, Y., Fecto, F., Shi, Y., Zhai, H.*, et al.* (2011). Mutations in UBQLN2 cause dominant X-linked juvenile and adult-onset ALS and ALS/dementia. Nature *477*, 211-215.

Denli, A.M., Tops, B.B., Plasterk, R.H., Ketting, R.F., and Hannon, G.J. (2004). Processing of primary microRNAs by the Microprocessor complex. Nature *432*, 231-235.

Deshaies, J.E., Shkreta, L., Moszczynski, A.J., Sidibe, H., Semmler, S., Fouillen, A., Bennett, E.R., Bekenstein, U., Destroismaisons, L., Toutant, J.*, et al.* (2018). TDP-43 regulates the alternative splicing of hnRNP A1 to yield an aggregation-prone variant in amyotrophic lateral sclerosis. Brain *141*, 1320-1333.

Dixon, D.A., Balch, G.C., Kedersha, N., Anderson, P., Zimmerman, G.A., Beauchamp, R.D., and Prescott, S.M. (2003). Regulation of cyclooxygenase-2 expression by the translational silencer TIA-1. J Exp Med *198*, 475-481.

Dobrowolny, G., Bernardini, C., Martini, M., Baranzini, M., Barba, M., and Musaro, A. (2015). Muscle Expression of SOD1(G93A) Modulates microRNA and mRNA Transcription Pattern Associated with the Myelination Process in the Spinal Cord of Transgenic Mice. Front Cell Neurosci *9*, 463.

Dormann, D., Rodde, R., Edbauer, D., Bentmann, E., Fischer, I., Hruscha, A., Than, M.E., Mackenzie, I.R., Capell, A., Schmid, B.*, et al.* (2010). ALS-associated fused in sarcoma (FUS) mutations disrupt Transportin-mediated nuclear import. EMBO J *29*, 2841-2857.

Droppelmann, C.A., Campos-Melo, D., Volkening, K., and Strong, M.J. (2014). The emerging role of guanine nucleotide exchange factors in ALS and other neurodegenerative diseases. Front Cell Neurosci *8*, 282.

Droppelmann, C.A., Keller, B.A., Campos-Melo, D., Volkening, K., and Strong, M.J. (2013a). Rho guanine nucleotide exchange factor is an NFL mRNA destabilizing factor that forms cytoplasmic inclusions in amyotrophic lateral sclerosis. Neurobiol Aging *34*, 248-262.

Droppelmann, C.A., Wang, J., Campos-Melo, D., Keller, B., Volkening, K., Hegele, R.A., and Strong, M.J. (2013b). Detection of a novel frameshift mutation and regions with homozygosis within ARHGEF28 gene in familial amyotrophic lateral sclerosis. Amyotroph Lateral Scler Frontotemporal Degener *14*, 444-451.

Duan, R., Pak, C., and Jin, P. (2007). Single nucleotide polymorphism associated with mature miR-125a alters the processing of pri-miRNA. Hum Mol Genet *16*, 1124-1131.

Dum, R.P., and Strick, P.L. (2005). Frontal lobe inputs to the digit representations of the motor areas on the lateral surface of the hemisphere. J Neurosci *25*, 1375-1386.

Eichhorn, S.W., Guo, H., McGeary, S.E., Rodriguez-Mias, R.A., Shin, C., Baek, D., Hsu, S.H., Ghoshal, K., Villen, J., and Bartel, D.P. (2014). mRNA destabilization is the dominant effect of mammalian microRNAs by the time substantial repression ensues. Mol Cell *56*, 104-115.

Elden, A.C., Kim, H.J., Hart, M.P., Chen-Plotkin, A.S., Johnson, B.S., Fang, X., Armakola, M., Geser, F., Greene, R., Lu, M.M.*, et al.* (2010). Ataxin-2 intermediate-length

polyglutamine expansions are associated with increased risk for ALS. Nature *466*, 1069-1075.

Emde, A., Eitan, C., Liou, L.L., Libby, R.T., Rivkin, N., Magen, I., Reichenstein, I., Oppenheim, H., Eilam, R., Silvestroni, A.*, et al.* (2015). Dysregulated miRNA biogenesis downstream of cellular stress and ALS-causing mutations: a new mechanism for ALS. EMBO J *34*, 2633-2651.

Ender, C., Krek, A., Friedlander, M.R., Beitzinger, M., Weinmann, L., Chen, W., Pfeffer, S., Rajewsky, N., and Meister, G. (2008). A human snoRNA with microRNA-like functions. Mol Cell *32*, 519-528.

Fabian, M.R., Cieplak, M.K., Frank, F., Morita, M., Green, J., Srikumar, T., Nagar, B., Yamamoto, T., Raught, B., Duchaine, T.F.*, et al.* (2011). miRNA-mediated deadenylation is orchestrated by GW182 through two conserved motifs that interact with CCR4-NOT. Nat Struct Mol Biol *18*, 1211-1217.

Fallini, C., Rouanet, J.P., Donlin-Asp, P.G., Guo, P., Zhang, H., Singer, R.H., Rossoll, W., and Bassell, G.J. (2014). Dynamics of survival of motor neuron (SMN) protein interaction with the mRNA-binding protein IMP1 facilitates its trafficking into motor neuron axons. Dev Neurobiol *74*, 319-332.

Fallini, C., Zhang, H., Su, Y., Silani, V., Singer, R.H., Rossoll, W., and Bassell, G.J. (2011). The survival of motor neuron (SMN) protein interacts with the mRNA-binding protein HuD and regulates localization of poly(A) mRNA in primary motor neuron axons. J Neurosci *31*, 3914-3925.

Fareh, M., Yeom, K.H., Haagsma, A.C., Chauhan, S., Heo, I., and Joo, C. (2016). TRBP ensures efficient Dicer processing of precursor microRNA in RNA-crowded environments. Nat Commun *7*, 13694.

Farg, M.A., Soo, K.Y., Warraich, S.T., Sundaramoorthy, V., Blair, I.P., and Atkin, J.D. (2013). Ataxin-2 interacts with FUS and intermediate-length polyglutamine expansions enhance FUS-related pathology in amyotrophic lateral sclerosis. Hum Mol Genet *22*, 717-728.

Farhan, S.M.K., Gendron, T.F., Petrucelli, L., Hegele, R.A., and Strong, M.J. (2017). ARHGEF28 p.Lys280Metfs40Ter in an amyotrophic lateral sclerosis family with a C9orf72 expansion. Neurol Genet *3*, e190.

Farhan, S.M.K., Howrigan, D.P., Abbott, L.E., Klim, J.R., Topp, S.D., Byrnes, A.E., Churchhouse, C., Phatnani, H., Smith, B.N., Rampersaud, E.*, et al.* (2019). Exome sequencing in amyotrophic lateral sclerosis implicates a novel gene, DNAJC7, encoding a heat-shock protein. Nat Neurosci *22*, 1966-1974.

Fecto, F., Yan, J., Vemula, S.P., Liu, E., Yang, Y., Chen, W., Zheng, J.G., Shi, Y., Siddique, N., Arrat, H.*, et al.* (2011). SQSTM1 mutations in familial and sporadic amyotrophic lateral sclerosis. Arch Neurol *68*, 1440-1446.

Figueroa-Romero, C., Hur, J., Lunn, J.S., Paez-Colasante, X., Bender, D.E., Yung, R., Sakowski, S.A., and Feldman, E.L. (2016). Expression of microRNAs in human post-mortem amyotrophic lateral sclerosis spinal cords provides insight into disease mechanisms. Mol Cell Neurosci *71*, 34-45.

Fitch, M.T., and Silver, J. (1997). Glial cell extracellular matrix: boundaries for axon growth in development and regeneration. Cell Tissue Res *290*, 379-384.

Forch, P., Puig, O., Kedersha, N., Martinez, C., Granneman, S., Seraphin, B., Anderson, P., and Valcarcel, J. (2000). The apoptosis-promoting factor TIA-1 is a regulator of alternative pre-mRNA splicing. Mol Cell *6*, 1089-1098.

Forman, J.J., Legesse-Miller, A., and Coller, H.A. (2008). A search for conserved sequences in coding regions reveals that the let-7 microRNA targets Dicer within its coding sequence. Proc Natl Acad Sci U S A *105*, 14879-14884.

Fox, A.H., and Lamond, A.I. (2010). Paraspeckles. Cold Spring Harb Perspect Biol *2*, a000687.

Franzmann, T.M., and Alberti, S. (2019). Prion-like low-complexity sequences: Key regulators of protein solubility and phase behavior. J Biol Chem *294*, 7128-7136.

Fratta, P., Sivakumar, P., Humphrey, J., Lo, K., Ricketts, T., Oliveira, H., Brito-Armas, J.M., Kalmar, B., Ule, A., Yu, Y.*, et al.* (2018). Mice with endogenous TDP-43 mutations exhibit gain of splicing function and characteristics of amyotrophic lateral sclerosis. EMBO J *37*.

Freibaum, B.D., Lu, Y., Lopez-Gonzalez, R., Kim, N.C., Almeida, S., Lee, K.H., Badders, N., Valentine, M., Miller, B.L., Wong, P.C.*, et al.* (2015). GGGGCC repeat expansion in C9orf72 compromises nucleocytoplasmic transport. Nature *525*, 129-133.

Freischmidt, A., Muller, K., Zondler, L., Weydt, P., Mayer, B., von Arnim, C.A., Hubers, A., Dorst, J., Otto, M., Holzmann, K.*, et al.* (2015a). Serum microRNAs in sporadic amyotrophic lateral sclerosis. Neurobiol Aging *36*, 2660 e2615-2620.

Freischmidt, A., Wieland, T., Richter, B., Ruf, W., Schaeffer, V., Muller, K., Marroquin, N., Nordin, F., Hubers, A., Weydt, P.*, et al.* (2015b). Haploinsufficiency of TBK1 causes familial ALS and fronto-temporal dementia. Nat Neurosci *18*, 631-636.

Fu, S.Y., and Gordon, T. (1997). The cellular and molecular basis of peripheral nerve regeneration. Mol Neurobiol *14*, 67-116.

Fukao, A., Mishima, Y., Takizawa, N., Oka, S., Imataka, H., Pelletier, J., Sonenberg, N., Thoma, C., and Fujiwara, T. (2014). MicroRNAs trigger dissociation of eIF4AI and eIF4AII from target mRNAs in humans. Mol Cell *56*, 79-89.

Fukaya, T., Iwakawa, H.O., and Tomari, Y. (2014). MicroRNAs block assembly of eIF4F translation initiation complex in Drosophila. Mol Cell *56*, 67-78.

Funakoshi, H., Frisen, J., Barbany, G., Timmusk, T., Zachrisson, O., Verge, V.M., and Persson, H. (1993). Differential expression of mRNAs for neurotrophins and their receptors after axotomy of the sciatic nerve. J Cell Biol *123*, 455-465.

Giehl, K.M., and Tetzlaff, W. (1996). BDNF and NT-3, but not NGF, prevent axotomy-induced death of rat corticospinal neurons in vivo. Eur J Neurosci *8*, 1167-1175.

Gilks, N., Kedersha, N., Ayodele, M., Shen, L., Stoecklin, G., Dember, L.M., and Anderson, P. (2004). Stress granule assembly is mediated by prion-like aggregation of TIA-1. Mol Biol Cell *15*, 5383-5398.

Goulding, M. (1998). Specifying motor neurons and their connections. Neuron *21*, 943-946.

Gregory, R.I., Yan, K.P., Amuthan, G., Chendrimada, T., Doratotaj, B., Cooch, N., and Shiekhattar, R. (2004). The Microprocessor complex mediates the genesis of microRNAs. Nature *432*, 235-240.

Gu, J., Chen, F., Iqbal, K., Gong, C.X., Wang, X., and Liu, F. (2017). Transactive response DNA-binding protein 43 (TDP-43) regulates alternative splicing of tau exon 10: Implications for the pathogenesis of tauopathies. J Biol Chem *292*, 10600-10612.

Gubitz, A.K., Feng, W., and Dreyfuss, G. (2004). The SMN complex. Exp Cell Res *296*, 51-56.

Guil, S., and Caceres, J.F. (2007). The multifunctional RNA-binding protein hnRNP A1 is required for processing of miR-18a. Nat Struct Mol Biol *14*, 591-596.

Guo, H., Ingolia, N.T., Weissman, J.S., and Bartel, D.P. (2010). Mammalian microRNAs predominantly act to decrease target mRNA levels. Nature *466*, 835-840.

Guo, J., Lv, J., Liu, M., and Tang, H. (2015). miR-346 Up-regulates Argonaute 2 (AGO2) Protein Expression to Augment the Activity of Other MicroRNAs (miRNAs) and Contributes to Cervical Cancer Cell Malignancy. J Biol Chem *290*, 30342-30350.

Guthrie, S. (2007). Patterning and axon guidance of cranial motor neurons. Nat Rev Neurosci *8*, 859-871.

Ha, M., and Kim, V.N. (2014). Regulation of microRNA biogenesis. Nat Rev Mol Cell Biol *15*, 509-524.

Haase, A.D., Jaskiewicz, L., Zhang, H., Laine, S., Sack, R., Gatignol, A., and Filipowicz, W. (2005). TRBP, a regulator of cellular PKR and HIV-1 virus expression, interacts with Dicer and functions in RNA silencing. EMBO Rep *6*, 961-967.

Hadano, S., Hand, C.K., Osuga, H., Yanagisawa, Y., Otomo, A., Devon, R.S., Miyamoto, N., Showguchi-Miyata, J., Okada, Y., Singaraja, R.*, et al.* (2001). A gene encoding a putative GTPase regulator is mutated in familial amyotrophic lateral sclerosis 2. Nat Genet *29*, 166-173.

Hagan, J.P., Piskounova, E., and Gregory, R.I. (2009). Lin28 recruits the TUTase Zcchc11 to inhibit let-7 maturation in mouse embryonic stem cells. Nat Struct Mol Biol *16*, 1021-1025.

Han, J., Lee, Y., Yeom, K.H., Kim, Y.K., Jin, H., and Kim, V.N. (2004). The Drosha-DGCR8 complex in primary microRNA processing. Genes Dev *18*, 3016-3027.

Haramati, S., Chapnik, E., Sztainberg, Y., Eilam, R., Zwang, R., Gershoni, N., McGlinn, E., Heiser, P.W., Wills, A.M., Wirguin, I., *et al.* (2010). miRNA malfunction causes spinal motor neuron disease. Proc Nat Acad Sci U S A *107*, 13111-13116.

Hawley, Z.C.E., Campos-Melo, D., and Strong, M.J. (2017). Novel miR-b2122 regulates several ALS-related RNA-binding proteins. Mol Brain *10*, 46.

He, C.Z., and Hays, A.P. (2004). Expression of peripherin in ubiquinated inclusions of amyotrophic lateral sclerosis. J Neurol Sci *217*, 47-54.

Helwak, A., Kudla, G., Dudnakova, T., and Tollervey, D. (2013). Mapping the human miRNA interactome by CLASH reveals frequent noncanonical binding. Cell *153*, 654-665.

Hendrickson, D.G., Hogan, D.J., McCullough, H.L., Myers, J.W., Herschlag, D., Ferrell, J.E., and Brown, P.O. (2009). Concordant regulation of translation and mRNA abundance for hundreds of targets of a human microRNA. PLoS Biol *7*, e1000238.

Hentati, A., Ouahchi, K., Pericak-Vance, M.A., Nijhawan, D., Ahmad, A., Yang, Y., Rimmler, J., Hung, W., Schlotter, B., Ahmed, A., *et al.* (1998). Linkage of a commoner form of recessive amyotrophic lateral sclerosis to chromosome 15q15-q22 markers. Neurogenetics *2*, 55-60.

Heo, I., Ha, M., Lim, J., Yoon, M.J., Park, J.E., Kwon, S.C., Chang, H., and Kim, V.N. (2012). Mono-uridylation of pre-microRNA as a key step in the biogenesis of group II let-7 microRNAs. Cell *151*, 521-532.

Heo, I., Joo, C., Cho, J., Ha, M., Han, J., and Kim, V.N. (2008). Lin28 mediates the terminal uridylation of let-7 precursor MicroRNA. Mol Cell *32*, 276-284.

Heo, I., Joo, C., Kim, Y.K., Ha, M., Yoon, M.J., Cho, J., Yeom, K.H., Han, J., and Kim, V.N. (2009). TUT4 in concert with Lin28 suppresses microRNA biogenesis through pre-microRNA uridylation. Cell *138*, 696-708.

Hinckelmann, M.V., Zala, D., and Saudou, F. (2013). Releasing the brake: restoring fast axonal transport in neurodegenerative disorders. Trends Cell Biol *23*, 634-643.

Hirokawa, N., Niwa, S., and Tanaka, Y. (2010). Molecular motors in neurons: transport mechanisms and roles in brain function, development, and disease. Neuron *68*, 610-638.

Houlden, H., and Singleton, A.B. (2012). The genetics and neuropathology of Parkinson's disease. Acta Neuropathol *124*, 325-338.

Huang, V., Place, R.F., Portnoy, V., Wang, J., Qi, Z., Jia, Z., Yu, A., Shuman, M., Yu, J., and Li, L.C. (2012). Upregulation of Cyclin B1 by miRNA and its implications in cancer. Nucleic Acids Res *40*, 1695-1707.

Hubers, L., Valderrama-Carvajal, H., Laframboise, J., Timbers, J., Sanchez, G., and Cote, J. (2011). HuD interacts with survival motor neuron protein and can rescue spinal muscular atrophy-like neuronal defects. Hum Mol Genet *20*, 553-579.

Hutvagner, G., McLachlan, J., Pasquinelli, A.E., Balint, E., Tuschl, T., and Zamore, P.D. (2001). A cellular function for the RNA-interference enzyme Dicer in the maturation of the let-7 small temporal RNA. Science *293*, 834-838.

Ishtiaq, M., Campos-Melo, D., Volkening, K., and Strong, M.J. (2014). Analysis of novel NEFL mRNA targeting microRNAs in amyotrophic lateral sclerosis. PLoS One *9*, e85653.

Jain, S., Wheeler, J.R., Walters, R.W., Agrawal, A., Barsic, A., and Parker, R. (2016). ATPase-Modulated Stress Granules Contain a Diverse Proteome and Substructure. Cell *164*, 487-498.

Jiang, Y.Q., Pickett, J., and Oblinger, M.M. (1994). Long-term effects of axotomy on beta-tubulin and NF gene expression in rat DRG neurons. J Neural Trans Plast *5*, 103-114.

Johnson, J.O., Mandrioli, J., Benatar, M., Abramzon, Y., Van Deerlin, V.M., Trojanowski, J.Q., Gibbs, J.R., Brunetti, M., Gronka, S., Wuu, J.*, et al.* (2010). Exome sequencing reveals VCP mutations as a cause of familial ALS. Neuron *68*, 857-864.

Johnson, J.O., Pioro, E.P., Boehringer, A., Chia, R., Feit, H., Renton, A.E., Pliner, H.A., Abramzon, Y., Marangi, G., Winborn, B.J.*, et al.* (2014). Mutations in the Matrin 3 gene cause familial amyotrophic lateral sclerosis. Nat Neurosci *17*, 664-666.

Kamenska, A., Lu, W.T., Kubacka, D., Broomhead, H., Minshall, N., Bushell, M., and Standart, N. (2014). Human 4E-T represses translation of bound mRNAs and enhances microRNA-mediated silencing. Nucleic Acids Res *42*, 3298-3313.

Kapeli, K., Pratt, G.A., Vu, A.Q., Hutt, K.R., Martinez, F.J., Sundararaman, B., Batra, R., Freese, P., Lambert, N.J., Huelga, S.C.*, et al.* (2016). Distinct and shared functions of ALS-associated proteins TDP-43, FUS and TAF15 revealed by multisystem analyses. Nat Commun *7*, 12143.

Kaplan, M.P., Chin, S.S., Fliegner, K.H., and Liem, R.K. (1990). Alpha-internexin, a novel neuronal intermediate filament protein, precedes the low molecular weight neurofilament protein (NF-L) in the developing rat brain. J Neurosci *10*, 2735-2748.

Kato, M., Han, T.W., Xie, S., Shi, K., Du, X., Wu, L.C., Mirzaei, H., Goldsmith, E.J., Longgood, J., Pei, J.*, et al.* (2012). Cell-free formation of RNA granules: low complexity sequence domains form dynamic fibers within hydrogels. Cell *149*, 753-767.

Katoh, T., Sakaguchi, Y., Miyauchi, K., Suzuki, T., Kashiwabara, S., and Baba, T. (2009). Selective stabilization of mammalian microRNAs by 3' adenylation mediated by the cytoplasmic poly(A) polymerase GLD-2. Genes Dev *23*, 433-438.

Kaur, S.J., McKeown, S.R., and Rashid, S. (2016). Mutant SOD1 mediated pathogenesis of Amyotrophic Lateral Sclerosis. Gene *577*, 109-118.

Kawahara, Y., and Mieda-Sato, A. (2012). TDP-43 promotes microRNA biogenesis as a component of the Drosha and Dicer complexes. Proc Natl Acad Sci U S A *109*, 3347-3352.

Kawamata, T., and Tomari, Y. (2010). Making RISC. Trends Biochem Sci *35*, 368-376.

Kedersha, N., Chen, S., Gilks, N., Li, W., Miller, I.J., Stahl, J., and Anderson, P. (2002). Evidence that ternary complex (eIF2-GTP-tRNA(i)(Met))-deficient preinitiation complexes are core constituents of mammalian stress granules. Mol Biol Cell *13*, 195-210.

Kedersha, N., Cho, M.R., Li, W., Yacono, P.W., Chen, S., Gilks, N., Golan, D.E., and Anderson, P. (2000). Dynamic shuttling of TIA-1 accompanies the recruitment of mRNA to mammalian stress granules. J Cell Biol *151*, 1257-1268.

Kedersha, N., Panas, M.D., Achorn, C.A., Lyons, S., Tisdale, S., Hickman, T., Thomas, M., Lieberman, J., McInerney, G.M., Ivanov, P.*, et al.* (2016). G3BP-Caprin1-USP10 complexes mediate stress granule condensation and associate with 40S subunits. J Cell Biol *212*, 845-860.

Kedersha, N.L., Gupta, M., Li, W., Miller, I., and Anderson, P. (1999). RNA-binding proteins TIA-1 and TIAR link the phosphorylation of eIF-2 alpha to the assembly of mammalian stress granules. J Cell Biol *147*, 1431-1442.

Keller, B.A., Volkening, K., Droppelmann, C.A., Ang, L.C., Rademakers, R., and Strong, M.J. (2012). Co-aggregation of RNA binding proteins in ALS spinal motor neurons: evidence of a common pathogenic mechanism. Acta Neuropathol *124*, 733-747.

Kenna, K.P., van Doormaal, P.T., Dekker, A.M., Ticozzi, N., Kenna, B.J., Diekstra, F.P., van Rheenen, W., van Eijk, K.R., Jones, A.R., Keagle, P.*, et al.* (2016). NEK1 variants confer susceptibility to amyotrophic lateral sclerosis. Nat Genet *48*, 1037-1042.

Ketting, R.F., Fischer, S.E., Bernstein, E., Sijen, T., Hannon, G.J., and Plasterk, R.H. (2001). Dicer functions in RNA interference and in synthesis of small RNA involved in developmental timing in C. elegans. Genes Dev *15*, 2654-2659.

Kim, B., Ha, M., Loeff, L., Chang, H., Simanshu, D.K., Li, S., Fareh, M., Patel, D.J., Joo, C., and Kim, V.N. (2015). TUT7 controls the fate of precursor microRNAs by using three different uridylation mechanisms. EMBO J *34*, 1801-1815.

Kim, H.J., Kim, N.C., Wang, Y.D., Scarborough, E.A., Moore, J., Diaz, Z., MacLea, K.S., Freibaum, B., Li, S., Molliex, A.*, et al.* (2013). Mutations in prion-like domains in hnRNPA2B1 and hnRNPA1 cause multisystem proteinopathy and ALS. Nature *495*, 467-473.

Kim, H.K., Prokunina-Olsson, L., and Chanock, S.J. (2012). Common genetic variants in miR-1206 (8q24.2) and miR-612 (11q13.3) affect biogenesis of mature miRNA forms. PLoS One *7*, e47454.

Kim, K.Y., Hwang, Y.J., Jung, M.K., Choe, J., Kim, Y., Kim, S., Lee, C.J., Ahn, H., Lee, J., Kowall, N.W.*, et al.* (2014). A multifunctional protein EWS regulates the expression of Drosha and microRNAs. Cell Death Differ *21*, 136-145.

Kim, W.J., Kim, J.H., and Jang, S.K. (2007). Anti-inflammatory lipid mediator 15d-PGJ2 inhibits translation through inactivation of eIF4A. EMBO J *26*, 5020-5032.

Kim, Y.K., Kim, B., and Kim, V.N. (2016). Re-evaluation of the roles of DROSHA, Export in 5, and DICER in microRNA biogenesis. Proc Natl Acad Sci U S A *113*, E1881-1889.

Klim, J.R., Williams, L.A., Limone, F., Guerra San Juan, I., Davis-Dusenbery, B.N., Mordes, D.A., Burberry, A., Steinbaugh, M.J., Gamage, K.K., Kirchner, R.*, et al.* (2019). ALS-implicated protein TDP-43 sustains levels of STMN2, a mediator of motor neuron growth and repair. Nat Neurosci *22*, 167-179.

Kobayashi, N.R., Bedard, A.M., Hincke, M.T., and Tetzlaff, W. (1996). Increased expression of BDNF and trkB mRNA in rat facial motoneurons after axotomy. Eur J Neurosci *8*, 1018-1029.

Kobayashi, N.R., Fan, D.P., Giehl, K.M., Bedard, A.M., Wiegand, S.J., and Tetzlaff, W. (1997). BDNF and NT-4/5 prevent atrophy of rat rubrospinal neurons after cervical axotomy, stimulate GAP-43 and Talpha1-tubulin mRNA expression, and promote axonal regeneration. J Neurosci *17*, 9583-9595.

Kooshapur, H., Choudhury, N.R., Simon, B., Muhlbauer, M., Jussupow, A., Fernandez, N., Jones, A.N., Dallmann, A., Gabel, F., Camilloni, C.*, et al.* (2018). Structural basis for terminal loop recognition and stimulation of pri-miRNA-18a processing by hnRNP A1. Nat Commun *9*, 2479.

Kost, S.A., and Oblinger, M.M. (1993). Immature corticospinal neurons respond to axotomy with changes in tubulin gene expression. Brain Res Bull *30*, 469-475.

Koval, E.D., Shaner, C., Zhang, P., du Maine, X., Fischer, K., Tay, J., Chau, B.N., Wu, G.F., and Miller, T.M. (2013). Method for widespread microRNA-155 inhibition prolongs survival in ALS-model mice. Hum Mol Genet *22*, 4127-4135.

Koyama, A., Sugai, A., Kato, T., Ishihara, T., Shiga, A., Toyoshima, Y., Koyama, M., Konno, T., Hirokawa, S., Yokoseki, A.*, et al.* (2016). Increased cytoplasmic TARDBP mRNA in

affected spinal motor neurons in ALS caused by abnormal autoregulation of TDP-43. Nucleic Acids Res *44*, 5820-5836.

Kriz, J., Zhu, Q., Julien, J.P., and Padjen, A.L. (2000). Electrophysiological properties of axons in mice lacking neurofilament subunit genes: disparity between conduction velocity and axon diameter in absence of NF-H. Brain Res *885*, 32-44.

Kroschwald, S., Maharana, S., Mateju, D., Malinovska, L., Nuske, E., Poser, I., Richter, D., and Alberti, S. (2015). Promiscuous interactions and protein disaggregases determine the material state of stress-inducible RNP granules. Elife *4*, e06807.

Kwiatkowski, T.J., Jr., Bosco, D.A., Leclerc, A.L., Tamrazian, E., Vanderburg, C.R., Russ, C., Davis, A., Gilchrist, J., Kasarskis, E.J., Munsat, T.*, et al.* (2009). Mutations in the FUS/TLS gene on chromosome 16 cause familial amyotrophic lateral sclerosis. Science *323*, 1205-1208.

Kwon, I., Xiang, S., Kato, M., Wu, L., Theodoropoulos, P., Wang, T., Kim, J., Yun, J., Xie, Y., and McKnight, S.L. (2014). Poly-dipeptides encoded by the C9orf72 repeats bind nucleoli, impede RNA biogenesis, and kill cells. Science *345*, 1139-1145.

Kye, M.J., Niederst, E.D., Wertz, M.H., Goncalves Ido, C., Akten, B., Dover, K.Z., Peters, M., Riessland, M., Neveu, P., Wirth, B.*, et al.* (2014). SMN regulates axonal local translation via miR-183/mTOR pathway. Human Mol Genet *23*, 6318-6331.

Lagier-Tourenne, C., Polymenidou, M., Hutt, K.R., Vu, A.Q., Baughn, M., Huelga, S.C., Clutario, K.M., Ling, S.C., Liang, T.Y., Mazur, C.*, et al.* (2012). Divergent roles of ALS-linked proteins FUS/TLS and TDP-43 intersect in processing long pre-mRNAs. Nat Neurosci *15*, 1488-1497.

Laird, A.S., Mackovski, N., Rinkwitz, S., Becker, T.S., and Giacomotto, J. (2016). Tissue-specific models of spinal muscular atrophy confirm a critical role of SMN in motor neurons from embryonic to adult stages. Hum Mol Genet *25*, 1728-1738.

Lal, A., Navarro, F., Maher, C.A., Maliszewski, L.E., Yan, N., O'Day, E., Chowdhury, D., Dykxhoorn, D.M., Tsai, P., Hofmann, O.*, et al.* (2009). miR-24 Inhibits cell proliferation by targeting E2F2, MYC, and other cell-cycle genes via binding to "seedless" 3'UTR microRNA recognition elements. Mol Cell *35*, 610-625.

Le Ber, I., Camuzat, A., Guerreiro, R., Bouya-Ahmed, K., Bras, J., Nicolas, G., Gabelle, A., Didic, M., De Septenville, A., Millecamps, S.*, et al.* (2013). SQSTM1 mutations in French patients with frontotemporal dementia or frontotemporal dementia with amyotrophic lateral sclerosis. JAMA Neurol *70*, 1403-1410.

Leblond, C.S., Gan-Or, Z., Spiegelman, D., Laurent, S.B., Szuto, A., Hodgkinson, A., Dionne-Laporte, A., Provencher, P., de Carvalho, M., Orru, S.*, et al.* (2016). Replication study of MATR3 in familial and sporadic amyotrophic lateral sclerosis. Neurobiol Aging *37*, 209 e217-209 e221.

Lee, H.Y., Zhou, K., Smith, A.M., Noland, C.L., and Doudna, J.A. (2013). Differential roles of human Dicer-binding proteins TRBP and PACT in small RNA processing. Nucleic Acids Res *41*, 6568-6576.

Lee, M.K., Marszalek, J.R., and Cleveland, D.W. (1994). A mutant neurofilament subunit causes massive, selective motor neuron death: implications for the pathogenesis of human motor neuron disease. Neuron *13*, 975-988.

Lee, R.C., Feinbaum, R.L., and Ambros, V. (1993). The C. elegans heterochronic gene lin-4 encodes small RNAs with antisense complementarity to lin-14. Cell *75*, 843-854.

Lee, Y., Ahn, C., Han, J., Choi, H., Kim, J., Yim, J., Lee, J., Provost, P., Radmark, O., Kim, S.*, et al.* (2003). The nuclear RNase III Drosha initiates microRNA processing. Nature *425*, 415-419.

Lee, Y., Hur, I., Park, S.Y., Kim, Y.K., Suh, M.R., and Kim, V.N. (2006). The role of PACT in the RNA silencing pathway. EMBO J *25*, 522-532.

Lee, Y., Kim, M., Han, J., Yeom, K.H., Lee, S., Baek, S.H., and Kim, V.N. (2004). MicroRNA genes are transcribed by RNA polymerase II. EMBO J *23*, 4051-4060.

Lefebvre, S., Burglen, L., Reboullet, S., Clermont, O., Burlet, P., Viollet, L., Benichou, B., Cruaud, C., Millasseau, P., Zeviani, M.*, et al.* (1995). Identification and characterization of a spinal muscular atrophy-determining gene. Cell *80*, 155-165.

Lemon, R.N. (2008). Descending pathways in motor control. Annu Rev Neurosci *31*, 195-218.

Leung, A.K., and Sharp, P.A. (2013). Quantifying Argonaute proteins in and out of GW/P-bodies: implications in microRNA activities. Adv Exp Med Biol *768*, 165-182.

Lewin, G.R., and Barde, Y.A. (1996). Physiology of the neurotrophins. Annu Rev Neurosci *19*, 289-317.

Li, X., Lu, L., Bush, D.J., Zhang, X., Zheng, L., Suswam, E.A., and King, P.H. (2009). Mutant copper-zinc superoxide dismutase associated with amyotrophic lateral sclerosis binds to adenine/uridine-rich stability elements in the vascular endothelial growth factor 3'-untranslated region. J Neurochem *108*, 1032-1044.

Li, Y., Collins, M., Geiser, R., Bakkar, N., Riascos, D., and Bowser, R. (2015). RBM45 homo-oligomerization mediates association with ALS-linked proteins and stress granules. Sci Rep *5*, 14262.

Li, Y.R., King, O.D., Shorter, J., and Gitler, A.D. (2013). Stress granules as crucibles of ALS pathogenesis. J Cell Biol *201*, 361-372.

Liachko, N.F., Guthrie, C.R., and Kraemer, B.C. (2010). Phosphorylation promotes neurotoxicity in a Caenorhabditis elegans model of TDP-43 proteinopathy. J Neurosci *30*, 16208-16219.

Liang, H., Zhang, J., Zen, K., Zhang, C.Y., and Chen, X. (2013). Nuclear microRNAs and their unconventional role in regulating non-coding RNAs. Protein Cell *4*, 325-330.

Lin, H., Zhai, J., Canete-Soler, R., and Schlaepfer, W.W. (2004). 3' untranslated region in a light neurofilament (NF-L) mRNA triggers aggregation of NF-L and mutant superoxide dismutase 1 proteins in neuronal cells. J Neurosci *24*, 2716-2726.

Lin, M.Y., and Sheng, Z.H. (2015). Regulation of mitochondrial transport in neurons. Exp Cell Res *334*, 35-44.

Ling, S.C., Polymenidou, M., and Cleveland, D.W. (2013). Converging mechanisms in ALS and FTD: disrupted RNA and protein homeostasis. Neuron *79*, 416-438.

Liu-Yesucevitz, L., Bilgutay, A., Zhang, Y.J., Vanderweyde, T., Citro, A., Mehta, T., Zaarur, N., McKee, A., Bowser, R., Sherman, M.*, et al.* (2010). Tar DNA binding protein-43 (TDP-43) associates with stress granules: analysis of cultured cells and pathological brain tissue. PLoS One *5*, e13250.

Lu, C.S., Zhai, B., Mauss, A., Landgraf, M., Gygi, S., and Van Vactor, D. (2014). MicroRNA-8 promotes robust motor axon targeting by coordinate regulation of cell adhesion molecules during synapse development. Phil Transac Roy Soc Biol Sci *369*.

Lu, L., Zheng, L., Viera, L., Suswam, E., Li, Y., Li, X., Estevez, A.G., and King, P.H. (2007). Mutant Cu/Zn-superoxide dismutase associated with amyotrophic lateral sclerosis destabilizes vascular endothelial growth factor mRNA and downregulates its expression. J Neurosci *27*, 7929-7938.

Luisier, R., Tyzack, G.E., Hall, C.E., Mitchell, J.S., Devine, H., Taha, D.M., Malik, B., Meyer, I., Greensmith, L., Newcombe, J.*, et al.* (2018). Intron retention and nuclear loss of SFPQ are molecular hallmarks of ALS. Nat Commun *9*, 2010.

Lund, E., Guttinger, S., Calado, A., Dahlberg, J.E., and Kutay, U. (2004). Nuclear export of microRNA precursors. Science *303*, 95-98.

Luxenhofer, G., Helmbrecht, M.S., Langhoff, J., Giusti, S.A., Refojo, D., and Huber, A.B. (2014). MicroRNA-9 promotes the switch from early-born to late-born motor neuron populations by regulating Onecut transcription factor expression. Devel Biol *386*, 358-370.

Ma, F., Liu, X., Li, D., Wang, P., Li, N., Lu, L., and Cao, X. (2010). MicroRNA-466l upregulates IL-10 expression in TLR-triggered macrophages by antagonizing RNA-binding protein tristetraprolin-mediated IL-10 mRNA degradation. J Immunol *184*, 6053-6059.

Ma, Y., Tang, L., Chen, L., Zhang, B., Deng, P., Wang, J., Yang, Y., Liu, R., Yang, Y., Ye, S.*, et al.* (2014). ARHGEF28 gene exon 6/intron 6 junction mutations in Chinese amyotrophic lateral sclerosis cohort. Amyotroph Lateral Scler Frontotemporal Degener *15*, 309-311.

Mackenzie, I.R., Nicholson, A.M., Sarkar, M., Messing, J., Purice, M.D., Pottier, C., Annu, K., Baker, M., Perkerson, R.B., Kurti, A.*, et al.* (2017). TIA1 Mutations in Amyotrophic Lateral Sclerosis and Frontotemporal Dementia Promote Phase Separation and Alter Stress Granule Dynamics. Neuron *95*, 808-816 e809.

Maharjan, N., Kunzli, C., Buthey, K., and Saxena, S. (2017). C9ORF72 Regulates Stress Granule Formation and Its Deficiency Impairs Stress Granule Assembly, Hypersensitizing Cells to Stress. Mol Neurobiol *54*, 3062-3077.

Maimon, R., Ionescu, A., Bonnie, A., Sweetat, S., Wald-Altman, S., Inbar, S., Gradus, T., Trotti, D., Weil, M., Behar, O.*, et al.* (2018). miR126-5p Downregulation Facilitates Axon Degeneration and NMJ Disruption via a Non-Cell-Autonomous Mechanism in ALS. J Neurosci *38*, 5478-5494.

Majounie, E., Renton, A.E., Mok, K., Dopper, E.G., Waite, A., Rollinson, S., Chio, A., Restagno, G., Nicolaou, N., Simon-Sanchez, J.*, et al.* (2012). Frequency of the C9orf72 hexanucleotide repeat expansion in patients with amyotrophic lateral sclerosis and frontotemporal dementia: a cross-sectional study. Lancet Neurol *11*, 323-330.

Majounie, E., Wardle, M., Muzaimi, M., Cross, W.C., Robertson, N.P., Williams, N.M., and Morris, H.R. (2007). Case control analysis of repeat expansion size in ataxia. Neurosci Lett *429*, 28-32.

Malik, A.M., Miguez, R.A., Li, X., Ho, Y.S., Feldman, E.L., and Barmada, S.J. (2018). Matrin 3-dependent neurotoxicity is modified by nucleic acid binding and nucleocytoplasmic localization. Elife *7*.

Marcuzzo, S., Kapetis, D., Mantegazza, R., Baggi, F., Bonanno, S., Barzago, C., Cavalcante, P., Kerlero de Rosbo, N., and Bernasconi, P. (2014). Altered miRNA expression is associated with neuronal fate in G93A-SOD1 ependymal stem progenitor cells. Exp Neurol *253*, 91-101.

Markmiller, S., Soltanieh, S., Server, K.L., Mak, R., Jin, W., Fang, M.Y., Luo, E.C., Krach, F., Yang, D., Sen, A.*, et al.* (2018). Context-Dependent and Disease-Specific Diversity in Protein Interactions within Stress Granules. Cell *172*, 590-604 e513.

Maruyama, H., Morino, H., Ito, H., Izumi, Y., Kato, H., Watanabe, Y., Kinoshita, Y., Kamada, M., Nodera, H., Suzuki, H.*, et al.* (2010). Mutations of optineurin in amyotrophic lateral sclerosis. Nature *465*, 223-226.

Mathis, S., Goizet, C., Soulages, A., Vallat, J.M., and Masson, G.L. (2019). Genetics of amyotrophic lateral sclerosis: A review. J Neurol Sci *399*, 217-226.

McEwen, E., Kedersha, N., Song, B., Scheuner, D., Gilks, N., Han, A., Chen, J.J., Anderson, P., and Kaufman, R.J. (2005). Heme-regulated inhibitor kinase-mediated phosphorylation of eukaryotic translation initiation factor 2 inhibits translation, induces stress granule formation, and mediates survival upon arsenite exposure. J Biol Chem *280*, 16925-16933.

McNeill, E.M., Warinner, C., Alkins, S., Taylor, A., Heggeness, H., DeLuca, T.F., Fulga, T.A., Wall, D.P., Griffith, L.C., and Van Vactor, D. (2020). The conserved microRNA miR-34 regulates synaptogenesis via coordination of distinct mechanisms in presynaptic and postsynaptic cells. Nat Commun *11*, 1092.

Meijer, H.A., Kong, Y.W., Lu, W.T., Wilczynska, A., Spriggs, R.V., Robinson, S.W., Godfrey, J.D., Willis, A.E., and Bushell, M. (2013). Translational repression and eIF4A2 activity are critical for microRNA-mediated gene regulation. Science *340*, 82-85.

Melamed, Z., Lopez-Erauskin, J., Baughn, M.W., Zhang, O., Drenner, K., Sun, Y., Freyermuth, F., McMahon, M.A., Beccari, M.S., Artates, J.W.*, et al.* (2019). Premature polyadenylation-mediated loss of stathmin-2 is a hallmark of TDP-43-dependent neurodegeneration. Nat Neurosci *22*, 180-190.

Mendonca, D.M., Chimelli, L., and Martinez, A.M. (2005). Quantitative evidence for neurofilament heavy subunit aggregation in motor neurons of spinal cords of patients with amyotrophic lateral sclerosis. Braz J Med Biol Res *38*, 925-933.

Menzies, F.M., Grierson, A.J., Cookson, M.R., Heath, P.R., Tomkins, J., Figlewicz, D.A., Ince, P.G., and Shaw, P.J. (2002). Selective loss of neurofilament expression in Cu/Zn superoxide dismutase (SOD1) linked amyotrophic lateral sclerosis. J Neurochem *82*, 1118-1128.

Meyer, H., and Weihl, C.C. (2014). The VCP/p97 system at a glance: connecting cellular function to disease pathogenesis. J Cell Sci *127*, 3877-3883.

Migheli, A., Pezzulo, T., Attanasio, A., and Schiffer, D. (1993). Peripherin immunoreactive structures in amyotrophic lateral sclerosis. Lab Invest *68*, 185-191.

Miller, K.E., and Sheetz, M.P. (2004). Axonal mitochondrial transport and potential are correlated. J Cell Sci *117*, 2791-2804.

Mitchell, J.C., Constable, R., So, E., Vance, C., Scotter, E., Glover, L., Hortobagyi, T., Arnold, E.S., Ling, S.C., McAlonis, M.*, et al.* (2015). Wild type human TDP-43 potentiates ALS-linked mutant TDP-43 driven progressive motor and cortical neuron degeneration with pathological features of ALS. Acta Neuropathol Commun *3*, 36.

Mitchell, J.C., McGoldrick, P., Vance, C., Hortobagyi, T., Sreedharan, J., Rogelj, B., Tudor, E.L., Smith, B.N., Klasen, C., Miller, C.C.*, et al.* (2013). Overexpression of human wild-type FUS causes progressive motor neuron degeneration in an age- and dose-dependent fashion. Acta Neuropathol *125*, 273-288.

Miura, P., Amirouche, A., Clow, C., Belanger, G., and Jasmin, B.J. (2012). Brain-derived neurotrophic factor expression is repressed during myogenic differentiation by miR-206. J Neurochem *120*, 230-238.

Mizuno, Y., Fujita, Y., Takatama, M., and Okamoto, K. (2011). Peripherin partially localizes in Bunina bodies in amyotrophic lateral sclerosis. J Neurol Sci *302*, 14-18.

Molliex, A., Temirov, J., Lee, J., Coughlin, M., Kanagaraj, A.P., Kim, H.J., Mittag, T., and Taylor, J.P. (2015). Phase separation by low complexity domains promotes stress granule assembly and drives pathological fibrillization. Cell *163*, 123-133.

Moloney, C., Rayaprolu, S., Howard, J., Fromholt, S., Brown, H., Collins, M., Cabrera, M., Duffy, C., Siemienski, Z., Miller, D.*, et al.* (2018). Analysis of spinal and muscle pathology in transgenic mice overexpressing wild-type and ALS-linked mutant MATR3. Acta Neuropathol Commun *6*, 137.

Moretti, F., Kaiser, C., Zdanowicz-Specht, A., and Hentze, M.W. (2012). PABP and the poly(A) tail augment microRNA repression by facilitated miRISC binding. Nat Struct Mol Biol *19*, 603-608.

Moretti, F., Thermann, R., and Hentze, M.W. (2010). Mechanism of translational regulation by miR-2 from sites in the 5' untranslated region or the open reading frame. RNA *16*, 2493-2502.

Mori, K., Arzberger, T., Grasser, F.A., Gijselinck, I., May, S., Rentzsch, K., Weng, S.M., Schludi, M.H., van der Zee, J., Cruts, M.*, et al.* (2013a). Bidirectional transcripts of the expanded C9orf72 hexanucleotide repeat are translated into aggregating dipeptide repeat proteins. Acta Neuropathol *126*, 881-893.

Mori, K., Weng, S.M., Arzberger, T., May, S., Rentzsch, K., Kremmer, E., Schmid, B., Kretzschmar, H.A., Cruts, M., Van Broeckhoven, C.*, et al.* (2013b). The C9orf72 GGGGCC repeat is translated into aggregating dipeptide-repeat proteins in FTLD/ALS. Science *339*, 1335-1338.

Morlando, M., Dini Modigliani, S., Torrelli, G., Rosa, A., Di Carlo, V., Caffarelli, E., and Bozzoni, I. (2012). FUS stimulates microRNA biogenesis by facilitating co-transcriptional Drosha recruitment. EMBO J *31*, 4502-4510.

Munoz, D.G., Greene, C., Perl, D.P., and Selkoe, D.J. (1988). Accumulation of phosphorylated neurofilaments in anterior horn motoneurons of amyotrophic lateral sclerosis patients. J Neuropathol Exp Neurol *47*, 9-18.

Murakami, T., Qamar, S., Lin, J.Q., Schierle, G.S., Rees, E., Miyashita, A., Costa, A.R., Dodd, R.B., Chan, F.T., Michel, C.H.*, et al.* (2015). ALS/FTD Mutation-Induced Phase Transition of FUS Liquid Droplets and Reversible Hydrogels into Irreversible Hydrogels Impairs RNP Granule Function. Neuron *88*, 678-690.

Murray, D.T., Kato, M., Lin, Y., Thurber, K.R., Hung, I., McKnight, S.L., and Tycko, R. (2017). Structure of FUS Protein Fibrils and Its Relevance to Self-Assembly and Phase Separation of Low-Complexity Domains. Cell *171*, 615-627 e616.

Nachev, P., Kennard, C., and Husain, M. (2008). Functional role of the supplementary and pre-supplementary motor areas. Nat Rev Neurosci *9*, 856-869.

Nagata, K., Hama, I., Kiryu-Seo, S., and Kiyama, H. (2014). microRNA-124 is down regulated in nerve-injured motor neurons and it potentially targets mRNAs for KLF6 and STAT3. Neuroscience *256*, 426-432.

Nasser, M.W., Datta, J., Nuovo, G., Kutay, H., Motiwala, T., Majumder, S., Wang, B., Suster, S., Jacob, S.T., and Ghoshal, K. (2008). Down-regulation of micro-RNA-1 (miR-1) in lung cancer. Suppression of tumorigenic property of lung cancer cells and their sensitization to doxorubicin-induced apoptosis by miR-1. J Biol Chem *283*, 33394-33405.

Nesler, K.R., Sand, R.I., Symmes, B.A., Pradhan, S.J., Boin, N.G., Laun, A.E., and Barbee, S.A. (2013). The miRNA pathway controls rapid changes in activity-dependent synaptic structure at the Drosophila melanogaster neuromuscular junction. PLoS One *8*, e68385.

Neumann, M., Kwong, L.K., Lee, E.B., Kremmer, E., Flatley, A., Xu, Y., Forman, M.S., Troost, D., Kretzschmar, H.A., Trojanowski, J.Q.*, et al.* (2009a). Phosphorylation of S409/410 of TDP-43 is a consistent feature in all sporadic and familial forms of TDP-43 proteinopathies. Acta Neuropathol *117*, 137-149.

Neumann, M., Roeber, S., Kretzschmar, H.A., Rademakers, R., Baker, M., and Mackenzie, I.R. (2009b). Abundant FUS-immunoreactive pathology in neuronal intermediate filament inclusion disease. Acta Neuropathol *118*, 605-616.

Neumann, M., Sampathu, D.M., Kwong, L.K., Truax, A.C., Micsenyi, M.C., Chou, T.T., Bruce, J., Schuck, T., Grossman, M., Clark, C.M.*, et al.* (2006). Ubiquitinated TDP-43 in frontotemporal lobar degeneration and amyotrophic lateral sclerosis. Science *314*, 130-133.

Nicolas, A., Kenna, K.P., Renton, A.E., Ticozzi, N., Faghri, F., Chia, R., Dominov, J.A., Kenna, B.J., Nalls, M.A., Keagle, P.*, et al.* (2018). Genome-wide Analyses Identify KIF5A as a Novel ALS Gene. Neuron *97*, 1268-1283 e1266.

Nishimoto, Y., Nakagawa, S., Hirose, T., Okano, H.J., Takao, M., Shibata, S., Suyama, S., Kuwako, K., Imai, T., Murayama, S.*, et al.* (2013). The long non-coding RNA nuclear-enriched abundant transcript 1_2 induces paraspeckle formation in the motor neuron during the early phase of amyotrophic lateral sclerosis. Mol Brain *6*, 31.

Nishimura, A.L., Mitne-Neto, M., Silva, H.C., Richieri-Costa, A., Middleton, S., Cascio, D., Kok, F., Oliveira, J.R., Gillingwater, T., Webb, J.*, et al.* (2004). A mutation in the vesicle-trafficking protein VAPB causes late-onset spinal muscular atrophy and amyotrophic lateral sclerosis. Am J Hum Genet *75*, 822-831.

Nonhoff, U., Ralser, M., Welzel, F., Piccini, I., Balzereit, D., Yaspo, M.L., Lehrach, H., and Krobitsch, S. (2007). Ataxin-2 interacts with the DEAD/H-box RNA helicase DDX6 and interferes with P-bodies and stress granules. Mol Biol Cell *18*, 1385-1396.

Oosthuyse, B., Moons, L., Storkebaum, E., Beck, H., Nuyens, D., Brusselmans, K., Van Dorpe, J., Hellings, P., Gorselink, M., Heymans, S.*, et al.* (2001). Deletion of the hypoxia-

response element in the vascular endothelial growth factor promoter causes motor neuron degeneration. Nat Genet *28*, 131-138.

Orlacchio, A., Babalini, C., Borreca, A., Patrono, C., Massa, R., Basaran, S., Munhoz, R.P., Rogaeva, E.A., St George-Hyslop, P.H., Bernardi, G.*, et al.* (2010). SPATACSIN mutations cause autosomal recessive juvenile amyotrophic lateral sclerosis. Brain *133*, 591-598.

Orozco, D., and Edbauer, D. (2013). FUS-mediated alternative splicing in the nervous system: consequences for ALS and FTLD. J Mol Med (Berl) *91*, 1343-1354.

Ostrowski, L.A., Hall, A.C., and Mekhail, K. (2017). Ataxin-2: From RNA Control to Human Health and Disease. Genes (Basel) *8*.

Otaegi, G., Pollock, A., Hong, J., and Sun, T. (2011). MicroRNA miR-9 modifies motor neuron columns by a tuning regulation of FoxP1 levels in developing spinal cords. J Neurosci *31*, 809-818.

Ozsolak, F., Poling, L.L., Wang, Z., Liu, H., Liu, X.S., Roeder, R.G., Zhang, X., Song, J.S., and Fisher, D.E. (2008). Chromatin structure analyses identify miRNA promoters. Genes Dev *22*, 3172-3183.

Parisi, C., Arisi, I., D'Ambrosi, N., Storti, A.E., Brandi, R., D'Onofrio, M., and Volonte, C. (2013). Dysregulated microRNAs in amyotrophic lateral sclerosis microglia modulate genes linked to neuroinflammation. Cell Death Dis *4*, e959.

Park, J.E., Heo, I., Tian, Y., Simanshu, D.K., Chang, H., Jee, D., Patel, D.J., and Kim, V.N. (2011). Dicer recognizes the 5' end of RNA for efficient and accurate processing. Nature *475*, 201-205.

Patel, A., Lee, H.O., Jawerth, L., Maharana, S., Jahnel, M., Hein, M.Y., Stoynov, S., Mahamid, J., Saha, S., Franzmann, T.M.*, et al.* (2015). A Liquid-to-Solid Phase Transition of the ALS Protein FUS Accelerated by Disease Mutation. Cell *162*, 1066-1077.

Perrone, B., La Cognata, V., Sprovieri, T., Ungaro, C., Conforti, F.L., Ando, S., and Cavallaro, S. (2020). Alternative Splicing of ALS Genes: Misregulation and Potential Therapies. Cell Mol Neurobiol *40*, 1-14.

Pfeffer, S., Sewer, A., Lagos-Quintana, M., Sheridan, R., Sander, C., Grasser, F.A., van Dyk, L.F., Ho, C.K., Shuman, S., Chien, M.*, et al.* (2005). Identification of microRNAs of the herpesvirus family. Nat Methods *2*, 269-276.

Piazzon, N., Rage, F., Schlotter, F., Moine, H., Branlant, C., and Massenet, S. (2008). In vitro and in cellulo evidences for association of the survival of motor neuron complex with the fragile X mental retardation protein. J Biol Chem *283*, 5598-5610.

Piecyk, M., Wax, S., Beck, A.R., Kedersha, N., Gupta, M., Maritim, B., Chen, S., Gueydan, C., Kruys, V., Streuli, M.*, et al.* (2000). TIA-1 is a translational silencer that selectively regulates the expression of TNF-alpha. EMBO J *19*, 4154-4163.

Protter, D.S.W., and Parker, R. (2016). Principles and Properties of Stress Granules. Trends Cell Biol *26*, 668-679.

Raman, R., Allen, S.P., Goodall, E.F., Kramer, S., Ponger, L.L., Heath, P.R., Milo, M., Hollinger, H.C., Walsh, T., Highley, J.R.*, et al.* (2015). Gene expression signatures in motor neurone disease fibroblasts reveal dysregulation of metabolism, hypoxia-response and RNA processing functions. Neuropathol Appl Neurobiol *41*, 201-226.

Ratti, A., and Buratti, E. (2016). Physiological functions and pathobiology of TDP-43 and FUS/TLS proteins. J Neurochem *138 Suppl 1*, 95-111.

Reber, S., Stettler, J., Filosa, G., Colombo, M., Jutzi, D., Lenzken, S.C., Schweingruber, C., Bruggmann, R., Bachi, A., Barabino, S.M.*, et al.* (2016). Minor intron splicing is regulated by FUS and affected by ALS-associated FUS mutants. EMBO J *35*, 1504-1521.

Rehwinkel, J., Behm-Ansmant, I., Gatfield, D., and Izaurralde, E. (2005). A crucial role for GW182 and the DCP1:DCP2 decapping complex in miRNA-mediated gene silencing. RNA *11*, 1640-1647.

Reichenstein, I., Eitan, C., Diaz-Garcia, S., Haim, G., Magen, I., Siany, A., Hoye, M.L., Rivkin, N., Olender, T., Toth, B.*, et al.* (2019). Human genetics and neuropathology suggest a link between miR-218 and amyotrophic lateral sclerosis pathophysiology. Sci Transl Med *11*.

Renaud, L., Harris, L.G., Mani, S.K., Kasiganesan, H., Chou, J.C., Baicu, C.F., Van Laer, A., Akerman, A.W., Stroud, R.E., Jones, J.A.*, et al.* (2015). HDACs Regulate miR-133a Expression in Pressure Overload-Induced Cardiac Fibrosis. Circ Heart Fail *8*, 1094-1104.

Renton, A.E., Majounie, E., Waite, A., Simon-Sanchez, J., Rollinson, S., Gibbs, J.R., Schymick, J.C., Laaksovirta, H., van Swieten, J.C., Myllykangas, L.*, et al.* (2011). A hexanucleotide repeat expansion in C9ORF72 is the cause of chromosome 9p21-linked ALS-FTD. Neuron *72*, 257-268.

Riva, N., Clarelli, F., Domi, T., Cerri, F., Gallia, F., Trimarco, A., Brambilla, P., Lunetta, C., Lazzerini, A., Lauria, G.*, et al.* (2016). Unraveling gene expression profiles in peripheral motor nerve from amyotrophic lateral sclerosis patients: insights into pathogenesis. Sci Rep *6*, 39297.

Robertson, J., Kriz, J., Nguyen, M.D., and Julien, J.P. (2002). Pathways to motor neuron degeneration in transgenic mouse models. Biochimie *84*, 1151-1160.

Rodriguez, A., Griffiths-Jones, S., Ashurst, J.L., and Bradley, A. (2004). Identification of mammalian microRNA host genes and transcription units. Genome Res *14*, 1902-1910.

Rogelj, B., Easton, L.E., Bogu, G.K., Stanton, L.W., Rot, G., Curk, T., Zupan, B., Sugimoto, Y., Modic, M., Haberman, N.*, et al.* (2012). Widespread binding of FUS along nascent RNA regulates alternative splicing in the brain. Sci Rep *2*, 603.

Rosen, D.R., Siddique, T., Patterson, D., Figlewicz, D.A., Sapp, P., Hentati, A., Donaldson, D., Goto, J., O'Regan, J.P., Deng, H.X.*, et al.* (1993). Mutations in Cu/Zn superoxide dismutase gene are associated with familial amyotrophic lateral sclerosis. Nature *362*, 59-62.

Rubino, E., Mancini, C., Boschi, S., Ferrero, P., Ferrone, M., Bianca, S., Zucca, M., Orsi, L., Pinessi, L., Govone, F.*, et al.* (2019). ATXN2 intermediate repeat expansions influence the clinical phenotype in frontotemporal dementia. Neurobiol Aging *73*, 231 e237-231 e239.

Ruby, J.G., Jan, C.H., and Bartel, D.P. (2007). Intronic microRNA precursors that bypass Drosha processing. Nature *448*, 83-86.

Russell, A.P., Wada, S., Vergani, L., Hock, M.B., Lamon, S., Leger, B., Ushida, T., Cartoni, R., Wadley, G.D., Hespel, P.*, et al.* (2013). Disruption of skeletal muscle mitochondrial network genes and miRNAs in amyotrophic lateral sclerosis. Neurobiol Dis *49*, 107-117.

Saito, Y., and Jones, P.A. (2006). Epigenetic activation of tumor suppressor microRNAs in human cancer cells. Cell Cycle *5*, 2220-2222.

Sapp, P.C., Hosler, B.A., McKenna-Yasek, D., Chin, W., Gann, A., Genise, H., Gorenstein, J., Huang, M., Sailer, W., Scheffler, M.*, et al.* (2003). Identification of two novel loci for dominantly inherited familial amyotrophic lateral sclerosis. Am J Hum Genet *73*, 397-403.

Schwab, M.E. (1996). Molecules inhibiting neurite growth: a minireview. Neurochem Res *21*, 755-761.

Scott, G.K., Mattie, M.D., Berger, C.E., Benz, S.C., and Benz, C.C. (2006). Rapid alteration of microRNA levels by histone deacetylase inhibition. Cancer Res *66*, 1277-1281.

Shenton, D., Smirnova, J.B., Selley, J.N., Carroll, K., Hubbard, S.J., Pavitt, G.D., Ashe, M.P., and Grant, C.M. (2006). Global translational responses to oxidative stress impact upon multiple levels of protein synthesis. J Biol Chem *281*, 29011-29021.

Shi, K.Y., Mori, E., Nizami, Z.F., Lin, Y., Kato, M., Xiang, S., Wu, L.C., Ding, M., Yu, Y., Gall, J.G.*, et al.* (2017). Toxic PRn poly-dipeptides encoded by the C9orf72 repeat expansion block nuclear import and export. Proc Natl Acad Sci U S A *114*, E1111-E1117.

Shi, Y., Chichung Lie, D., Taupin, P., Nakashima, K., Ray, J., Yu, R.T., Gage, F.H., and Evans, R.M. (2004). Expression and function of orphan nuclear receptor TLX in adult neural stem cells. Nature *427*, 78-83.

Slack, F.J., Basson, M., Liu, Z., Ambros, V., Horvitz, H.R., and Ruvkun, G. (2000). The lin-41 RBCC gene acts in the C. elegans heterochronic pathway between the let-7 regulatory RNA and the LIN-29 transcription factor. Mol Cell *5*, 659-669.

Solomon, S., Xu, Y., Wang, B., David, M.D., Schubert, P., Kennedy, D., and Schrader, J.W. (2007). Distinct structural features of caprin-1 mediate its interaction with G3BP-1 and its induction of phosphorylation of eukaryotic translation initiation factor 2alpha, entry to cytoplasmic stress granules, and selective interaction with a subset of mRNAs. Mol Cell Biol *27*, 2324-2342.

Song, G., Wang, R., Guo, J., Liu, X., Wang, F., Qi, Y., Wan, H., Liu, M., Li, X., and Tang, H. (2015). miR-346 and miR-138 competitively regulate hTERT in GRSF1- and AGO2-dependent manners, respectively. Sci Rep *5*, 15793.

Song, Y., Lin, F., Ye, C.H., Huang, H., Li, X., Yao, X., Xu, Y., and Wang, C. (2020). Rare, low-frequency and common coding variants of ARHGEF28 gene and their association with sporadic amyotrophic lateral sclerosis. Neurobiol Aging *87*, 138 e131-138 e136.

Sreedharan, J., Blair, I.P., Tripathi, V.B., Hu, X., Vance, C., Rogelj, B., Ackerley, S., Durnall, J.C., Williams, K.L., Buratti, E.*, et al.* (2008). TDP-43 mutations in familial and sporadic amyotrophic lateral sclerosis. Science *319*, 1668-1672.

Strong, M.J. (2017). Revisiting the concept of amyotrophic lateral sclerosis as a multisystems disorder of limited phenotypic expression. Curr Opin Neurol *30*, 599-607.

Strong, M.J., Abrahams, S., Goldstein, L.H., Woolley, S., McLaughlin, P., Snowden, J., Mioshi, E., Roberts-South, A., Benatar, M., HortobaGyi, T.*, et al.* (2017). Amyotrophic lateral sclerosis - frontotemporal spectrum disorder (ALS-FTSD): Revised diagnostic criteria. Amyotroph Lateral Scler Frontotemporal Degener *18*, 153-174.

Strong, M.J., Kesavapany, S., and Pant, H.C. (2005). The pathobiology of amyotrophic lateral sclerosis: a proteinopathy? Journal Neuropath Exp Neurol *64*, 649-664.

Sun, X., Zhou, Z., Fink, D.J., and Mata, M. (2013). HspB1 silences translation of PDZ-RhoGEF by enhancing miR-20a and miR-128 expression to promote neurite extension. Mol Cell Neurosci *57*, 111-119.

Sutton, M.A., and Schuman, E.M. (2006). Dendritic protein synthesis, synaptic plasticity, and memory. Cell *127*, 49-58.

Suzuki, H., Shibagaki, Y., Hattori, S., and Matsuoka, M. (2018). The proline-arginine repeat protein linked to C9-ALS/FTD causes neuronal toxicity by inhibiting the DEAD-box RNA helicase-mediated ribosome biogenesis. Cell Death Dis *9*, 975.

Svetoni, F., Frisone, P., and Paronetto, M.P. (2016). Role of FET proteins in neurodegenerative disorders. RNA Biol *13*, 1089-1102.

Swarup, V., Phaneuf, D., Dupre, N., Petri, S., Strong, M., Kriz, J., and Julien, J.P. (2011). Deregulation of TDP-43 in amyotrophic lateral sclerosis triggers nuclear factor kappaB-mediated pathogenic pathways. J Exp Med *208*, 2429-2447.

Szaro, B.G., and Strong, M.J. (2010). Post-transcriptional control of neurofilaments: New roles in development, regeneration and neurodegenerative disease. Trend Neurosci *33*, 27-37.

Tada, M., Doi, H., Koyano, S., Kubota, S., Fukai, R., Hashiguchi, S., Hayashi, N., Kawamoto, Y., Kunii, M., Tanaka, K.*, et al.* (2018). Matrin 3 Is a Component of Neuronal Cytoplasmic Inclusions of Motor Neurons in Sporadic Amyotrophic Lateral Sclerosis. Am J Pathol *188*, 507-514.

Tadesse, H., Deschenes-Furry, J., Boisvenue, S., and Cote, J. (2008). KH-type splicing regulatory protein interacts with survival motor neuron protein and is misregulated in spinal muscular atrophy. Hum Mol Genet *17*, 506-524.

Takahashi, I., Hama, Y., Matsushima, M., Hirotani, M., Kano, T., Hohzen, H., Yabe, I., Utsumi, J., and Sasaki, H. (2015). Identification of plasma microRNAs as a biomarker of sporadic Amyotrophic Lateral Sclerosis. Mol Brain *8*, 67.

Tan, S.L., Ohtsuka, T., Gonzalez, A., and Kageyama, R. (2012). MicroRNA9 regulates neural stem cell differentiation by controlling Hes1 expression dynamics in the developing brain. Genes Cells *17*, 952-961.

Tang, Y., Fu, R., Ling, Z.M., Liu, L.L., Yu, G.Y., Li, W., Fang, X.Y., Zhu, Z., Wu, W.T., and Zhou, L.H. (2018). MiR-137-3p rescue motoneuron death by targeting calpain-2. Nitric Oxide *74*, 74-85.

Taylor, J.P., Brown, R.H., Jr., and Cleveland, D.W. (2016). Decoding ALS: from genes to mechanism. Nature *539*, 197-206.

Tetzlaff, W., Alexander, S.W., Miller, F.D., and Bisby, M.A. (1991). Response of facial and rubrospinal neurons to axotomy: changes in mRNA expression for cytoskeletal proteins and GAP-43. J Neurosci *11*, 2528-2544.

Tetzlaff, W., Leonard, C., Krekoski, C.A., Parhad, I.M., and Bisby, M.A. (1996). Reductions in motoneuronal neurofilament synthesis by successive axotomies: a possible explanation for the conditioning lesion effect on axon regeneration. Exp Neurol *139*, 95-106.

Therrien, M., Dion, P.A., and Rouleau, G.A. (2016). ALS: Recent Developments from Genetics Studies. Curr Neurol Neurosci Rep *16*, 59.

Thiebes, K.P., Nam, H., Cambronne, X.A., Shen, R., Glasgow, S.M., Cho, H.H., Kwon, J.S., Goodman, R.H., Lee, J.W., Lee, S.*, et al.* (2015). miR-218 is essential to establish motor neuron fate as a downstream effector of Isl1-Lhx3. Nature Commun *6*, 7718.

Ticozzi, N., Vance, C., Leclerc, A.L., Keagle, P., Glass, J.D., McKenna-Yasek, D., Sapp, P.C., Silani, V., Bosco, D.A., Shaw, C.E.*, et al.* (2011). Mutational analysis reveals the FUS

homolog TAF15 as a candidate gene for familial amyotrophic lateral sclerosis. Am J Med Genet B Neuropsychiatr Genet *156B*, 285-290.

Toivonen, J.M., Manzano, R., Olivan, S., Zaragoza, P., Garcia-Redondo, A., and Osta, R. (2014). MicroRNA-206: a potential circulating biomarker candidate for amyotrophic lateral sclerosis. PLoS One *9*, e89065.

Trabucchi, M., Briata, P., Filipowicz, W., Rosenfeld, M.G., Ramos, A., and Gherzi, R. (2009). How to control miRNA maturation? RNA Biol *6*, 536-540.

Treiber, T., Treiber, N., Plessmann, U., Harlander, S., Daiss, J.L., Eichner, N., Lehmann, G., Schall, K., Urlaub, H., and Meister, G. (2017). A Compendium of RNA-Binding Proteins that Regulate MicroRNA Biogenesis. Mol Cell *66*, 270-284 e213.

Tsurudome, K., Tsang, K., Liao, E.H., Ball, R., Penney, J., Yang, J.S., Elazzouzi, F., He, T., Chishti, A., Lnenicka, G.*, et al.* (2010). The Drosophila miR-310 cluster negatively regulates synaptic strength at the neuromuscular junction. Neuron *68*, 879-893.

Ustianenko, D., Hrossova, D., Potesil, D., Chalupnikova, K., Hrazdilova, K., Pachernik, J., Cetkovska, K., Uldrijan, S., Zdrahal, Z., and Vanacova, S. (2013). Mammalian DIS3L2 exoribonuclease targets the uridylated precursors of let-7 miRNAs. RNA *19*, 1632-1638.

Valinezhad Orang, A., Safaralizadeh, R., and Kazemzadeh-Bavili, M. (2014). Mechanisms of miRNA-Mediated Gene Regulation from Common Downregulation to mRNA-Specific Upregulation. Int J Genomics *2014*, 970607.

Valsecchi, V., Boido, M., De Amicis, E., Piras, A., and Vercelli, A. (2015). Expression of Muscle-Specific MiRNA 206 in the Progression of Disease in a Murine SMA Model. PLoS One *10*, e0128560.

van Horck, F.P., Ahmadian, M.R., Haeusler, L.C., Moolenaar, W.H., and Kranenburg, O. (2001). Characterization of p190RhoGEF, a RhoA-specific guanine nucleotide exchange factor that interacts with microtubules. J Biol Chem *276*, 4948-4956.

van Rooij, E., Sutherland, L.B., Qi, X., Richardson, J.A., Hill, J., and Olson, E.N. (2007). Control of stress-dependent cardiac growth and gene expression by a microRNA. Science *316*, 575-579.

Vance, C., Rogelj, B., Hortobagyi, T., De Vos, K.J., Nishimura, A.L., Sreedharan, J., Hu, X., Smith, B., Ruddy, D., Wright, P.*, et al.* (2009). Mutations in FUS, an RNA processing protein, cause familial amyotrophic lateral sclerosis type 6. Science *323*, 1208-1211.

Vasudevan, S., Tong, Y., and Steitz, J.A. (2007). Switching from repression to activation: microRNAs can up-regulate translation. Science *318*, 1931-1934.

Visvanathan, J., Lee, S., Lee, B., Lee, J.W., and Lee, S.K. (2007). The microRNA miR-124 antagonizes the anti-neural REST/SCP1 pathway during embryonic CNS development. Genes Dev *21*, 744-749.

Volkening, K., Leystra-Lantz, C., and Strong, M.J. (2010). Human low molecular weight neurofilament (NFL) mRNA interacts with a predicted p190RhoGEF homologue (RGNEF) in humans. Amyotroph Lateral Scler *11*, 97-103.

Volkening, K., Leystra-Lantz, C., Yang, W., Jaffee, H., and Strong, M.J. (2009). Tar DNA binding protein of 43 kDa (TDP-43), 14-3-3 proteins and copper/zinc superoxide dismutase (SOD1) interact to modulate NFL mRNA stability. Implications for altered RNA processing in amyotrophic lateral sclerosis (ALS). Brain Res *1305*, 168-182.

Vuppalanchi, D., Willis, D.E., and Twiss, J.L. (2009). Regulation of mRNA transport and translation in axons. Results Probl Cell Differ *48*, 193-224.

Waghray, S., Williams, C., Coon, J.J., and Wickens, M. (2015). Xenopus CAF1 requires NOT1-mediated interaction with 4E-T to repress translation in vivo. RNA *21*, 1335-1345.

Wakabayashi, K., Mori, F., Kakita, A., Takahashi, H., Utsumi, J., and Sasaki, H. (2014). Analysis of microRNA from archived formalin-fixed paraffin-embedded specimens of amyotrophic lateral sclerosis. Acta Neuropathol Commun *2*, 173.

Wang, L.T., Chiou, S.S., Liao, Y.M., Jong, Y.J., and Hsu, S.H. (2014). Survival of motor neuron protein downregulates miR-9 expression in patients with spinal muscular atrophy. Kaohsiung J Med Sci *30*, 229-234.

Wee, E.J., Peters, K., Nair, S.S., Hulf, T., Stein, S., Wagner, S., Bailey, P., Lee, S.Y., Qu, W.J., Brewster, B.*, et al.* (2012). Mapping the regulatory sequences controlling 93 breast cancer-associated miRNA genes leads to the identification of two functional promoters of the Hsa-mir-200b cluster, methylation of which is associated with metastasis or hormone receptor status in advanced breast cancer. Oncogene *31*, 4182-4195.

Wei, C., Thatcher, E.J., Olena, A.F., Cha, D.J., Perdigoto, A.L., Marshall, A.F., Carter, B.D., Broadie, K., and Patton, J.G. (2013). miR-153 regulates SNAP-25, synaptic transmission, and neuronal development. PLoS One *8*, e57080.

Weinmann, L., Hock, J., Ivacevic, T., Ohrt, T., Mutze, J., Schwille, P., Kremmer, E., Benes, V., Urlaub, H., and Meister, G. (2009). Importin 8 is a gene silencing factor that targets argonaute proteins to distinct mRNAs. Cell *136*, 496-507.

Welniarz, Q., Dusart, I., and Roze, E. (2016). The corticospinal tract: Evolution, development, and human disorders. Dev Neurobiol. *77*, 810-829.

Wen, X., Tan, W., Westergard, T., Krishnamurthy, K., Markandaiah, S.S., Shi, Y., Lin, S., Shneider, N.A., Monaghan, J., Pandey, U.B.*, et al.* (2014). Antisense proline-arginine RAN dipeptides linked to C9ORF72-ALS/FTD form toxic nuclear aggregates that initiate in vitro and in vivo neuronal death. Neuron *84*, 1213-1225.

Wertz, M.H., Winden, K., Neveu, P., Ng, S.Y., Ercan, E., and Sahin, M. (2016). Cell-type-specific miR-431 dysregulation in a motor neuron model of spinal muscular atrophy. Hum Mol Genet *25*, 2168-2181.

Wheeler, J.R., Matheny, T., Jain, S., Abrisch, R., and Parker, R. (2016). Distinct stages in stress granule assembly and disassembly. Elife *5*.

Wilczynska, A., and Bushell, M. (2015). The complexity of miRNA-mediated repression. Cell Death Differ *22*, 22-33.

Williams, A.H., Valdez, G., Moresi, V., Qi, X., McAnally, J., Elliott, J.L., Bassel-Duby, R., Sanes, J.R., and Olson, E.N. (2009). MicroRNA-206 delays ALS progression and promotes regeneration of neuromuscular synapses in mice. Science *326*, 1549-1554.

Wirth, B., Brichta, L., and Hahnen, E. (2006). Spinal muscular atrophy: from gene to therapy. Semin Pediatr Neurol *13*, 121-131.

Wong, N.K., He, B.P., and Strong, M.J. (2000). Characterization of neuronal intermediate filament protein expression in cervical spinal motor neurons in sporadic amyotrophic lateral sclerosis (ALS). J Neuropathol Exp Neurol *59*, 972-982.

Wu, C.H., Fallini, C., Ticozzi, N., Keagle, P.J., Sapp, P.C., Piotrowska, K., Lowe, P., Koppers, M., McKenna-Yasek, D., Baron, D.M.*, et al.* (2012). Mutations in the profilin 1 gene cause familial amyotrophic lateral sclerosis. Nature *488*, 499-503.

Wu, L., Fan, J., and Belasco, J.G. (2006). MicroRNAs direct rapid deadenylation of mRNA. Proc Natl Acad Sci U S A *103*, 4034-4039.

Xhemalce, B., Robson, S.C., and Kouzarides, T. (2012). Human RNA methyltransferase BCDIN3D regulates microRNA processing. Cell *151*, 278-288.

Xu, Y., An, B.Y., Xi, X.B., Li, Z.W., and Li, F.Y. (2016). MicroRNA-9 controls apoptosis of neurons by targeting monocyte chemotactic protein-induced protein 1 expression in rat acute spinal cord injury model. Brain Res Bull *121*, 233-240.

Xu, Y.F., Gendron, T.F., Zhang, Y.J., Lin, W.L., D'Alton, S., Sheng, H., Casey, M.C., Tong, J., Knight, J., Yu, X.*, et al.* (2010). Wild-type human TDP-43 expression causes TDP-43 phosphorylation, mitochondrial aggregation, motor deficits, and early mortality in transgenic mice. J Neurosci *30*, 10851-10859.

Yamazaki, T., Chen, S., Yu, Y., Yan, B., Haertlein, T.C., Carrasco, M.A., Tapia, J.C., Zhai, B., Das, R., Lalancette-Hebert, M.*, et al.* (2012). FUS-SMN protein interactions link the motor neuron diseases ALS and SMA. Cell Rep *2*, 799-806.

Yang, Y., Hentati, A., Deng, H.X., Dabbagh, O., Sasaki, T., Hirano, M., Hung, W.Y., Ouahchi, K., Yan, J., Azim, A.C.*, et al.* (2001). The gene encoding alsin, a protein with three guanine-nucleotide exchange factor domains, is mutated in a form of recessive amyotrophic lateral sclerosis. Nat Genet *29*, 160-165.

Yi, R., Qin, Y., Macara, I.G., and Cullen, B.R. (2003). Exportin-5 mediates the nuclear export of pre-microRNAs and short hairpin RNAs. Genes Dev *17*, 3011-3016.

Yin, H., Song, P., Su, R., Yang, G., Dong, L., Luo, M., Wang, B., Gong, B., Liu, C., Song, W.*, et al.* (2016). DNA Methylation mediated down-regulating of MicroRNA-33b and its role in gastric cancer. Sci Rep *6*, 18824.

Yoda, M., Cifuentes, D., Izumi, N., Sakaguchi, Y., Suzuki, T., Giraldez, A.J., and Tomari, Y. (2013). Poly(A)-specific ribonuclease mediates 3'-end trimming of Argonaute2-cleaved precursor microRNAs. Cell Rep *5*, 715-726.

Yu, Y., and Reed, R. (2015). FUS functions in coupling transcription to splicing by mediating an interaction between RNAP II and U1 snRNP. Proc Natl Acad Sci U S A *112*, 8608-8613.

Yuan, A., Rao, M.V., Sasaki, T., Chen, Y., Kumar, A., Veeranna, Liem, R.K., Eyer, J., Peterson, A.C., Julien, J.P.*, et al.* (2006). Alpha-internexin is structurally and functionally associated with the neurofilament triplet proteins in the mature CNS. J Neurosci *26*, 10006-10019.

Yuan, A., Sasaki, T., Kumar, A., Peterhoff, C.M., Rao, M.V., Liem, R.K., Julien, J.P., and Nixon, R.A. (2012). Peripherin is a subunit of peripheral nerve neurofilaments: implications for differential vulnerability of CNS and peripheral nervous system axons. J Neurosci *32*, 8501-8508.

Yuan, Z., Jiao, B., Hou, L., Xiao, T., Liu, X., Wang, J., Xu, J., Zhou, L., Yan, X., Tang, B.*, et al.* (2018). Mutation analysis of the TIA1 gene in Chinese patients with amyotrophic lateral sclerosis and frontotemporal dementia. Neurobiol Aging *64*, 160 e169-160 e112.

Zarei, S., Carr, K., Reiley, L., Diaz, K., Guerra, O., Altamirano, P.F., Pagani, W., Lodin, D., Orozco, G., and Chinea, A. (2015). A comprehensive review of amyotrophic lateral sclerosis. Surg Neurol Int *6*, 171.

Zekri, L., Kuzuoglu-Ozturk, D., and Izaurralde, E. (2013). GW182 proteins cause PABP dissociation from silenced miRNA targets in the absence of deadenylation. EMBO J *32*, 1052-1065.

Zhang, K., Daigle, J.G., Cunningham, K.M., Coyne, A.N., Ruan, K., Grima, J.C., Bowen, K.E., Wadhwa, H., Yang, P., Rigo, F.*, et al.* (2018a). Stress Granule Assembly Disrupts Nucleocytoplasmic Transport. Cell *173*, 958-971 e917.

Zhang, K., Donnelly, C.J., Haeusler, A.R., Grima, J.C., Machamer, J.B., Steinwald, P., Daley, E.L., Miller, S.J., Cunningham, K.M., Vidensky, S.*, et al.* (2015). The C9orf72 repeat expansion disrupts nucleocytoplasmic transport. Nature *525*, 56-61.

Zhang, K., Liu, Q., Shen, D., Tai, H., Fu, H., Liu, S., Wang, Z., Shi, J., Ding, Q., Li, X.*, et al.* (2018b). Genetic analysis of TIA1 gene in Chinese patients with amyotrophic lateral sclerosis. Neurobiol Aging *67*, 201 e209-201 e210.

Zhang, M., Xi, Z., Ghani, M., Jia, P., Pal, M., Werynska, K., Moreno, D., Sato, C., Liang, Y., Robertson, J.*, et al.* (2016). Genetic and epigenetic study of ALS-discordant identical

twins with double mutations in SOD1 and ARHGEF28. J Neurol Neurosurg Psychiatry *87*, 1268-1270.

Zhang, Y.J., Gendron, T.F., Ebbert, M.T.W., O'Raw, A.D., Yue, M., Jansen-West, K., Zhang, X., Prudencio, M., Chew, J., Cook, C.N.*, et al.* (2018c). Poly(GR) impairs protein translation and stress granule dynamics in C9orf72-associated frontotemporal dementia and amyotrophic lateral sclerosis. Nat Med *24*, 1136-1142.

Zhao, C., Sun, G., Li, S., and Shi, Y. (2009). A feedback regulatory loop involving microRNA-9 and nuclear receptor TLX in neural stem cell fate determination. Nat Struct Mol Biol *16*, 365-371.

Zhao, M., Kim, J.R., van Bruggen, R., and Park, J. (2018). RNA-Binding Proteins in Amyotrophic Lateral Sclerosis. Mol Cell *41*, 818-829.

Zhou, F., Guan, Y., Chen, Y., Zhang, C., Yu, L., Gao, H., Du, H., Liu, B., and Wang, X. (2013a). miRNA-9 expression is upregulated in the spinal cord of G93A-SOD1 transgenic mice. Int J Clin Exp Pathol *6*, 1826-1838.

Zhou, Y., Liu, S., Liu, G., Ozturk, A., and Hicks, G.G. (2013b). ALS-associated FUS mutations result in compromised FUS alternative splicing and autoregulation. PLoS Genet *9*, e1003895.

Zhou, Z., Licklider, L.J., Gygi, S.P., and Reed, R. (2002). Comprehensive proteomic analysis of the human spliceosome. Nature *419*, 182-185.

Zhu, Q., Couillard-Despres, S., and Julien, J.P. (1997). Delayed maturation of regenerating myelinated axons in mice lacking neurofilaments. Exp Neurol *148*, 299-316.

Zhu, Q., Lindenbaum, M., Levavasseur, F., Jacomy, H., and Julien, J.P. (1998). Disruption of the NF-H gene increases axonal microtubule content and velocity of neurofilament transport: relief of axonopathy resulting from the toxin beta,beta'-iminodipropionitrile. J Cell Biol *143*, 183-193.

Zipeto, M.A., Court, A.C., Sadarangani, A., Delos Santos, N.P., Balaian, L., Chun, H.J., Pineda, G., Morris, S.R., Mason, C.N., Geron, I.*, et al.* (2016). ADAR1 Activation Drives Leukemia Stem Cell Self-Renewal by Impairing Let-7 Biogenesis. Cell Stem Cell *19*, 177-191.

**Chapter 2**

**MiR-105 and miR-9 regulate the mRNA stability of neuronal intermediate filaments. Implications for the pathogenesis of amyotrophic lateral sclerosis (ALS).**

Zachary C. E. Hawley, Danae Campos-Melo and Michael J. Strong

A version of this chapter was published in *Brain Research*

Hawley, ZCE., Campos-Melo, D., Strong MJ. MiR-105 and miR-9 regulate the mRNA stability of neuronal intermediate filaments. Implications for the pathogenesis of amyotrophic lateral sclerosis (ALS). *Brain Res*. 1706: 93-100 (2019). PMID: 30385300.

**2.1 Abstract**

Intermediate filament aggregation within motor neurons is a hallmark of ALS pathogenesis. Changes to intermediate filament stoichiometry due to altered mRNA steady-state levels of *NEFL*, *PRPH* and *INA* is thought to drive protein aggregation, yet the exact cause of these changes is unknown. MicroRNAs (miRNAs)—master regulators of gene expression—are largely dysregulated within ALS motor neurons and are known to be major contributors to the disease. We show that miR-105 and miR-9 are downregulated within the spinal cord of ALS patients and target *NEFL*, *PRPH* and *INA* 3'UTRs to regulate gene expression. Further, both miR-105 and miR-9 were observed to regulate the mRNA stability of these three intermediate filaments endogenously within a neuronal-derived cell line. Our data demonstrates that miR-105 and miR-9 can regulate the mRNA stability of these key intermediate filaments whose metabolism is dysregulated in ALS, and thus, these miRNAs likely contribute to their pathogenesis.

**2.2 Introduction**

Amyotrophic lateral sclerosis (ALS) is a fatal disease which is characterized by progressive degeneration of motor neurons (Strong, 2017). One major neuropathological hallmark of the disease is the formation of neuronal cytoplasmic inclusions (NCIs) containing intermediate filaments, which include neurofilament light, medium and heavy (NFL, NFM, and NFH, respectively), and peripherin (PRPH) (He and Hays, 2004; Hirano et al., 1984; Keller et al., 2012; Kondo et al., 1986; Xiao et al., 2006)

In general, intermediate filaments are essential proteins that make up the cytoskeleton and are needed for proper cellular structure and signaling within neurons. Neurofilament assembly requires NFL to form homopolymers, and as well as heteropolymers with NFM and NFH, to form a triplet protein structure (Carpenter and Ip, 1996; Szaro and Strong, 2010). Further, PRPH and α-internexin (INA) intermediate filaments are responsible for the formation of the early cytoskeleton within developing neurons, but both also interact with the neurofilament triplet protein structure within mature neurons (Yuan et al., 2006; Yuan et al., 2012). Together these intermediate filaments maintain a specific stoichiometry that ensures appropriate cell structure, axonal transport, and overall neuronal health (Lariviere and Julien, 2004; Szaro and Strong, 2010).

Alterations to intermediate filament stoichiometry within motor neurons of mammalian ALS-models induces the formation of NCIs similar to those observed in ALS spinal motor neurons (Beaulieu et al., 1999; Kriz et al., 2000; Lee et al., 1994; Zhu et al., 1997). Further, in motor neurons of sporadic ALS (sALS) patients with no known genetic background, *NEFL*, *PRPH* and *INA* mRNA steady-state levels are selectively reduced with no effect on *NEFM* or *NEFH* (Wong et al., 2000), suggesting that the loss of intermediate filament stoichiometry results

from the loss of proper regulation of intermediate filament mRNA metabolism (Strong, 2010; Strong et al., 2004; Szaro and Strong, 2010; Thyagarajan et al., 2007).

While alterations in mRNA metabolism seem to be critical to the pathogenesis of ALS (Strong, 2010), it is still unclear the etiology of neuronal intermediate filament mRNA dysregulation. However, microRNAs (miRNAs)—critical regulators of gene expression generally through interactions with the 3' untranslated region (UTR)—have been shown to be largely dysregulated within the spinal cord and motor neurons of sALS patients (Campos-Melo et al., 2013; Emde et al., 2015; Figueroa-Romero et al., 2016). Several of these ALS-linked miRNAs have been shown to regulate ALS-associated RNA-binding proteins (Dini Modigliani et al., 2014; Hawley et al., 2017b), suggesting that the loss of proper miRNA regulation is a contributing factor to the disease. Further, several miRNAs have been shown to regulate the mRNA levels of *NEFL* (Campos-Melo et al., 2013; Ishtiaq et al., 2014), which may explain the selective reduction of *NEFL* mRNA steady-state levels in sALS. However, the cause of *PRPH* and *INA* mRNA reduction, and whether the selective reduction of *NEFL*, *PRPH* and *INA* mRNA in sALS is caused by a common mechanism is still unknown.

In this study, we aim to identify a specific pool of ALS-linked miRNAs that may explain the selective reduction of *NEFL*, *PRPH* and *INA* mRNA steady-state levels. Our data revealed that within the pool of miRNAs that is dysregulated in sALS, miR-105 and miR-9 are critical regulators of neuronal intermediate filaments; however, only miR-105 directly interacts with the *NEFL*, *PRPH* and *INA* 3'UTRs to regulate mRNA levels, suggesting that its dysregulation is a key part to the etiology of altered intermediate filament mRNA expression in sALS.

## 2.3 Methods and Materials

### 2.3.1 Tissue Samples

ALS patient and neuropathologically healthy, age-matched control spinal cord tissue was collected and stored at -80ºC, or formalin-fixed and paraffin-embedded (**Table 2.1**). All ALS cases used in this study were clinically and neuropathologically confirmed using the El Escorial Criteria (World Federation of Neurology Research Group on Neuromuscular Disease, 1994). The research was approved by "The University of Western Ontario Research Ethics Board for Health Sciences Research Involving Human Subjects (HSREB)". Written consent for autopsy was either received from the patient antemortem, or the next of kin in accordance with the London Health Sciences Center consent for autopsy. All ALS patients were genetically screened and confirmed to have no mutations in *SOD1*, *TARDBP*, *FUS*, or expanded repeats in *C9ORF72*.

**2.3.2 MiRNA Selection**

Candidate miRNAs were selected if they had predicted miRNA recognition elements (MREs) within the 3'UTRs identified in human spinal cord using miRanda software, and if they meant the criteria that we have previously reported (Hawley et al., 2017b).

**2.3.3 Real-time PCR**

In order to determine miRNA changes in the spinal cord, total miRNA extraction was done on ventral lumbar human spinal cord using the mirVana miRNA extraction kit (Life Technologies Inc., Ambion, Carlsbad, CA, USA) in accordance with the manufactures protocol. Reverse transcription and real-time PCR was performed on miRNA extracts using miRCURY LNA™ Universal RT microRNA PCR (Exiqon, Woburn, MA, USA) and ExiLENT SYBR Green master mix (Exiqon, Woburn, MA, USA) kits, respectively, in accordance with the manufacturer's instructions. Candidate miRNA expression was normalized and examined between ALS patients and control subjects as previously described (Hawley et al., 2017b).

**Table 2.1**. Patient demographics.

| Cases | Gender | Age of symptom onset | Symptom onset | Age of death | Cause of Death |
|---|---|---|---|---|---|
| Control | F | - | - | 62 | Heart Attack |
| | M | - | - | 74 | Stroke |
| | F | - | - | 68 | Unknown |
| | M | - | - | 68 | Brain Tumor |
| | M | - | - | 75 | Unknown |
| | F | - | - | 53 | Pneumonia |
| | F | - | - | 74 | Leukemia |
| | M | - | - | 67 | Unknown |
| ALS | F | 58 | Unknown | 60 | Unknown |
| | M | 69 | Upper/lower limbs | 72 | Unknown |
| | F | 40 | Bulbar | 41 | Systemic Failure |
| | M | 55 | Unknown | 61 | Pneumonia |
| | M | 64 | Upper/lower limbs | 67 | Respiratory Failure |
| | F | 69 | Respiratory Symptoms | 71 | Respiratory Failure |
| | M | 63 | Unknown | 64 | Unknown |
| | F | 47 | Bulbar | 49 | Respiratory Failure |

Total RNA extraction from IMR-32 cells was done using TRIzol reagent (Life Technologies

Inc., Ambion, Carlsbad, CA, USA) followed by cDNA synthesis using the SuperScript IV VILO

reverse transcriptase according to the manufactures protocol (Invitrogen, Life Technologies Inc.,

Mississauga, ON, Canada). Changes to *NEFL*, *PRPH*, or *INA* mRNA levels were measured via

real-time PCR using the TaqMan Fast Advanced Master Mix and TaqMan Gene Expression

Assays (Applied Biosystems, Thermo Fisher Scientific). Intermediate filament expression levels

were normalized to 18S, and then quantified using the $2^{-\Delta\Delta CT}$ method.

### 2.3.4 Fluorescent *In Situ* Hybridization (FISH)

Neuropathologically intact human spinal cord was examined for candidate miRNA

expression within motor neurons. Spinal cord tissue was formalin-fixed, paraffin embedded, and

then cut into 7µm sections. Samples were UV treated overnight prior to experiment to reduce

autofluorescent lipofuscin signaling. MiRNA FISH was performed as previously described (de

Planell-Saguer et al., 2010).  MiRNA probes were double DIG tagged (Exiqon, Woburn, MA,

USA), and were targeted using a DIG-HRP secondary antibody (1:100; Roche, Indianapolis, IN,

USA) and Tyramide Signal Amplification tagged with a Cy3 fluorophore (PerkinElmer,

Waltham, MA, USA). Spinal motor neurons were examined for positive expression of candidate

miRNAs using the Olympus FV1000 confocal microscope.

### 2.3.5 Cell Culture and Plasmid Construction

HEK293T and IMR-32 cells were cultured in Dulbecco's Modified Eagle's Media

(DMEM) and Eagle's Minimum Essential Medium (EMEM), respectively, with 10% Fetal

Bovine Serum (FBS) and incubated at 37°C with 5% $CO_2$.

*NEFL*, *PRPH*, and *INA* 3'UTRs identified in human spinal cord were individually cloned

into the pmirGLO vector in between SalI and NheI restriction enzyme sites and downstream of

the firefly luciferase gene (Promega, Madison, WI, USA). Mutations made within the 3'UTRs were done as previously reported (Hawley et al., 2017b) using the Site-Directed Mutagenesis Kit II (Aligent Technologies Canada Inc., Missasauga, ON, Canada) in accordance with the manufacturer's instructions. Cloned fragments and mutated sites were confirmed with Sanger sequencing.

**2.3.6 Luciferase Assay and Relative Quantitative RT-PCR**

HEK293T cells were seeded 24 and 48 hours prior to transfection for luciferase and RT-qPCR assays, respectively, as previously reported (Hawley et al., 2017b). PmirGLO vectors containing either the *NEFL*, *PRPH*, or *INA* 3'UTR were transfected into HEK293T cells either with or without miRNA mimics for luciferase and relative quantitative RT-PCR assays in accordance to what has been previously done (Campos-Melo et al., 2013; Hawley et al., 2017b) using the Lipofectamine 2000 protocol (Life Technologies Inc., Invitrogen, Burlington, ON, Canada). Luciferase activity was measured 24 hours post-transfection using the Dual-GLO Luciferase Assay System (Promega, Madison, WI, USA). For RT-PCRs firefly and renilla cDNAs were amplified and data was normalized in accordance to what has been previously described (Campos-Melo et al., 2013). Data for luciferase and RT-qPCR assays was quantified and plotted as relative difference of firefly expression from the control when in the presence of miR-105, miR-140-5p, miR-9, or let-7a (negative control) and is represented as mean ± SEM.

**2.3.7 Statistical Analysis**

Student's t-test was performed when comparing two conditions. One-way ANOVA followed by Tukey's post-hoc was done when doing multiple comparisons between groups. Data was considered significant if $p<0.05$.

**2.4 Results**

**2.4.1 MiR-105 and miR-140-5p are downregulated in sALS and expressed in motor neurons.**

Spinal cord obtained from neuropathologically intact subjects was used to identify *NEFL*, *PRPH* and *INA* 3'UTRs isoforms expressed within this tissue. We confirmed that already known 3'UTRs of *NEFL* [1838 bases – GenBank NM_006158], *PRPH* [325 bases – GenBank NM_006262] and *INA* [1638 bases – GenBank NM_032727] were present in human spinal cord (data not shown).

Subsequently, using the miRanda prediction tool, 15 miRNAs were identified to have MREs within the *NEFL*, *PRPH* and *INA* 3'UTRs expressed in human spinal cord. However, we previously demonstrated that the expression of 6 of these miRNAs are not dysregulated in sALS (Campos-Melo et al., 2013). Thus, we focused on those 9 miRNAs that we previously reported to be dysregulated in sALS, or possessed MREs in the *NEFL*, *PRPH* or *INA* 3'UTR, but for which expression levels had not been characterized in sALS (**Fig. 2.1**). Of note, miR-9 has a non-canonical binding site within the *PRPH* 3'UTR (seed region is from +3 to +8, rather than +2 to +7). Since miR-9 is predicted to regulate all intermediate filaments of interest, and several labs have shown its relationship to sALS (Campos-Melo et al., 2013; Campos-Melo et al., 2018; Emde et al., 2015; Haramati et al., 2010; Hawley et al., 2017a; Zhang et al., 2013), we decided miR-9 was critical to examine.

Our previous work has shown that miR-9 is expressed within motor neurons and significantly downregulated within the spinal cord of sALS patients (Campos-Melo et al., 2013; Campos-Melo et al., 2018), and others have shown this downregulation is specific to motor neurons (Emde et al., 2015). Thus, the remaining 8 miRNA candidates were further examined within the spinal cord tissue of sALS patients (n=8) and control subjects (n=5). Real-time PCR

A

Known dysregulation in ALS
miR-105
miR-140-5p
miR-185

Uncharacterized in ALS
miR-1297
miR-1179
miR-3120
miR-4306
miR-b4335

Not differentially expressed in ALS
miR-26a
miR-26b
miR-376c
miR-543
miR-607
miR-942
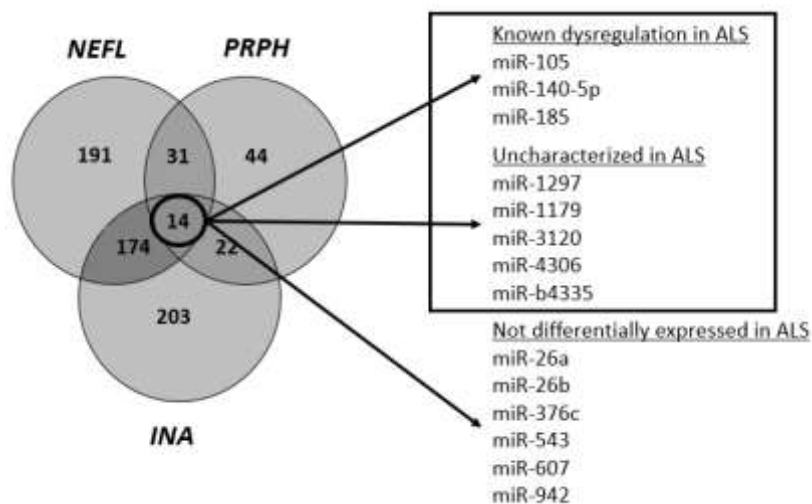
B
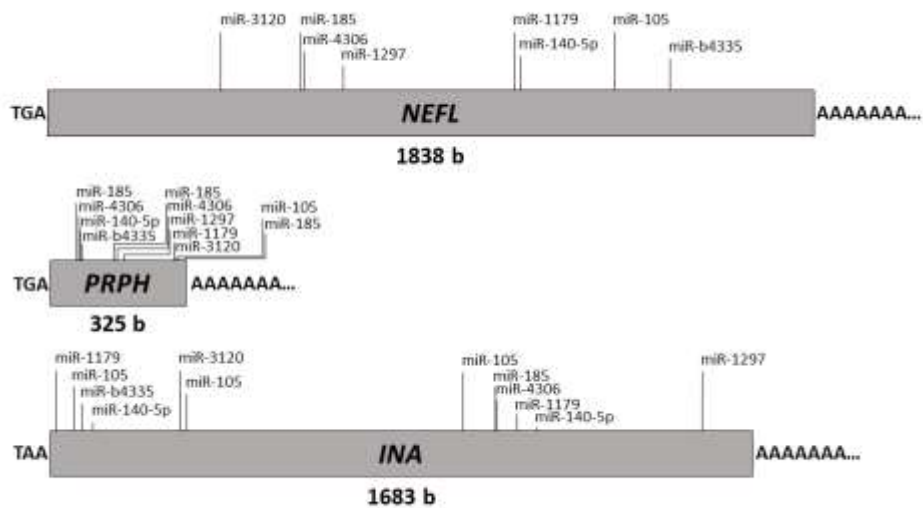
**Figure 2.1. MiRanda predicted 15 miRNAs to have MREs in *NEFL*, *PRPH*, and *INA* 3'UTRs.** A) Venn diagram showing 15 miRNAs that have MRE sites within the *NEFL*, *PRPH* and *INA* 3'UTRs according to miRanda software. However, we have shown previously that six miRNAs are not dysregulated in sALS (Campos-Melo et al., 2013). Thus, only those outlined in the black box were considered for further analysis. B) Schematic showing *NEFL*, *PRPH* and *INA* 3'UTRs expressed in neuropathologically intact human spinal cord (n=3), and the location of the MREs of miRNA candidates within each 3'UTR.

confirmed our previous reports that miR-105 and miR-140-5p were significantly downregulated within the spinal cord tissue of sALS patients (Campos-Melo et al., 2013), while miR-185, miR-1179, miR-1297, miR-3120, miR-4306 and miR-b4335 showed no significant change (**Fig. 2.2**).

Since miR-105 and miR-140-5p were both downregulated in the spinal cord of sALS patients, we wanted to determine if these miRNAs were normally expressed within human motor neurons, as what has been seen with miR-9 (Campos-Melo et al., 2018; Emde et al., 2015). Both miR-105 and miR-140-5p are highly expressed within motor neurons (**Fig. 2.3**), suggesting that the observed downregulation of these two miRNAs is likely occurring in motor neurons.

**2.4.2 MiR-105 regulates a reporter linked to *NEFL*, *PRPH* and *INA* 3'UTRs.**

*NEFL*, *PRPH* and *INA* 3'UTRs were individually linked to the firefly luciferase reporter gene to determine if candidate miRNAs altered the expression of the reporter gene. Both miR-105 and miR-140-5p significantly increased luciferase activity when in the presence of the *NEFL* 3'UTR strongly suggesting that miR-105 upregulates *NEFL* levels. Further, miR-105 significantly increased or decreased luciferase activity when in the presence of either the *PRPH* or *INA* 3'UTRs, respectively, while miR-140-5p had no effect. Further, miR-9 significantly reduced luciferase activity when in the presence of either the *NEFL*, *PRPH*, or *INA* 3'UTR (**Fig. 2.4A**). Let-7a was used as negative control and had no effect on luciferase activity when in the presence of any intermediate filament 3'UTR.

Subsequently, we determined whether the changes observed in luciferase activity were due to changes at the mRNA level (**Fig. 2.4B**). Changes to luciferase mRNA levels when linked to either the *NEFL*, *PRPH*, or *INA* 3'UTR matched changes seen to luciferase activity when in the presence of miR-105. MiR-9 significantly reduced luciferase mRNA levels in the presence of either the *NEFL* or *PRPH* 3'UTR, but had no effect on the luciferase mRNA levels when in the

presence of the *INA* 3'UTR. MiR-140-5p had no effect on the mRNA levels of the luciferase gene when in the presence of either the *NEFL*, *PRPH*, or *INA* 3'UTR (**Fig. 2.4B**). Since miR-140-5p had no effect on the mRNA levels when interacting with *NEFL*, *PRPH* or *INA* 3'UTRs, only miR-105 and miR-9 were further examined.

**2.4.3 MiR-105 directly interacts with the *NEFL*, *PRPH* and *INA* 3'UTRs to regulate reporter expression.**

MREs of miR-105 and miR-9 were mutated at the +2 and +3 positions in the *NEFL*, *PRPH* and *INA* 3'UTRs to determine if these miRNAs needed to directly interact with the 3'UTRs to regulate luciferase activity. Indeed, miR-105 had significantly reduced effects on increasing luciferase activity when the *NEFL* 3'UTR was lacking the miR-105 MRE; however, the effect was not completely abolished. This indicates miR-105 likely stabilizes *NEFL* by binding to the 3'UTR, but possibly also through an indirect mechanism by which miR-105 regulates another target that stabilizes *NEFL*. Further, the *PRPH* 3'UTR lacking the miR-105 MRE completely abolished the ability for miR-105 to upregulate luciferase activity (**Fig. 2.5A**). Interestingly, miR-105 has multiple MREs within the *INA* 3'UTR, and thus, we aimed to determine if miR-105 targeted a specific MRE to reduce luciferase activity. Indeed, mutations only in the MRE closest to the 5'end of the 3'UTR, or site 1 (S1), abolished the ability of miR-105 to reduce luciferase activity. Mutations in the MREs closer to the 3'end, or sites 2 and 3 (S2 and S3, respectively), had no effect on the ability of miR-105 to reduce luciferase activity, indicating the S1 MRE is critical for miR-105 function (**Fig. 2.5A**).

MiR-9 has two MREs within the *NEFL* 3'UTR, but only one MRE in the *PRPH* and *INA* 3'UTRs. Removal of the S1 MRE within the *NEFL* 3'UTR lead to a significant reversal in the reduction of luciferase activity via miR-9, but the effect was not completely abolished. It was
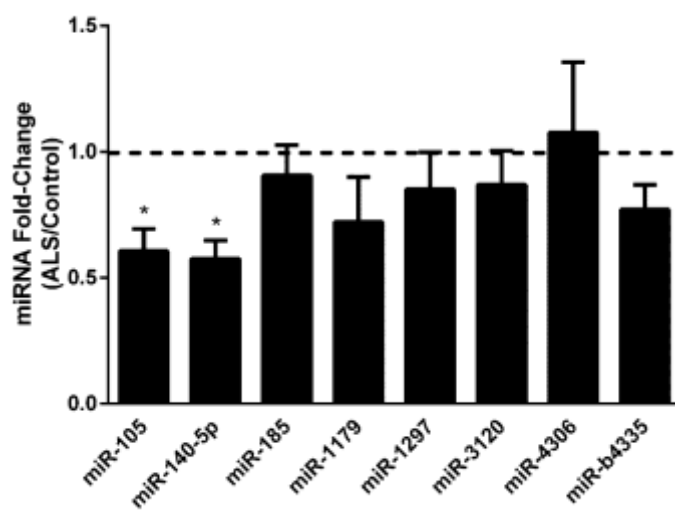
**Figure 2.2. Differential expression of miRNA candidates within sALS spinal cord tissue.**

We examined the expression of candidate miRNAs in the spinal cord of sALS patients (n=8) compared to control subjects (n=5) using real-time PCR. MiR-105 and miR-140-5p are significantly downregulated in the spinal cord of sALS patients, while all other candidates showed no significant change in expression compared to the control population. Data was expressed miRNA fold-change (ALS/Control) ± SEM, and significance was determined using a Student's t-test (* = p<0.05).

miR-105     miR-140-5p     Negative Control (miR-548c)
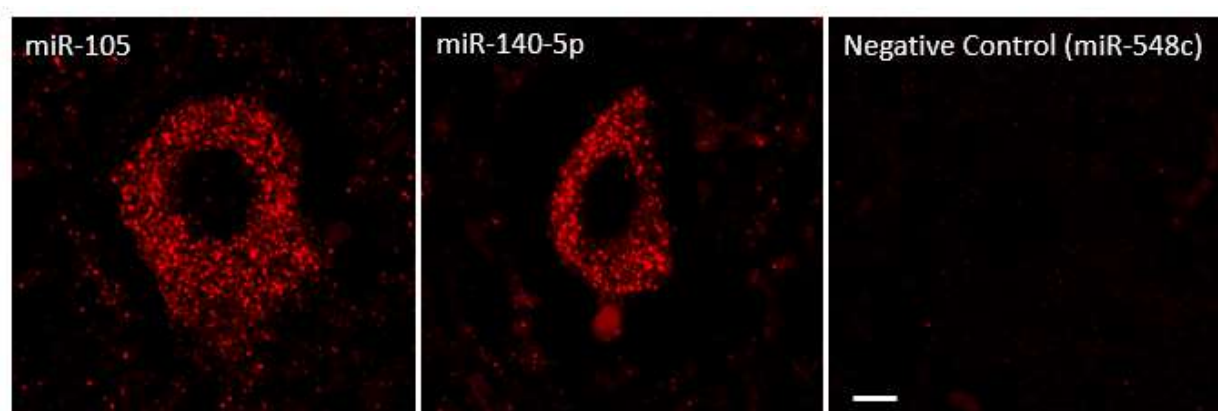
**Figure 2.3. MiR-105 and miR-140-5p are expressed in human spinal motor neurons.** FISH was used to examine the expression of both miR-105 and miR-140-5p within human ventral lumbar spinal cord. Both miRNAs showed strong expression within motor neurons of a control case (n=1). MiR-548c was used as a negative control. Motors neurons were identified based on size, as they are the only cells 50-70µm in size within the ventral spinal cord. Scale bar represents 10µm.

**A**
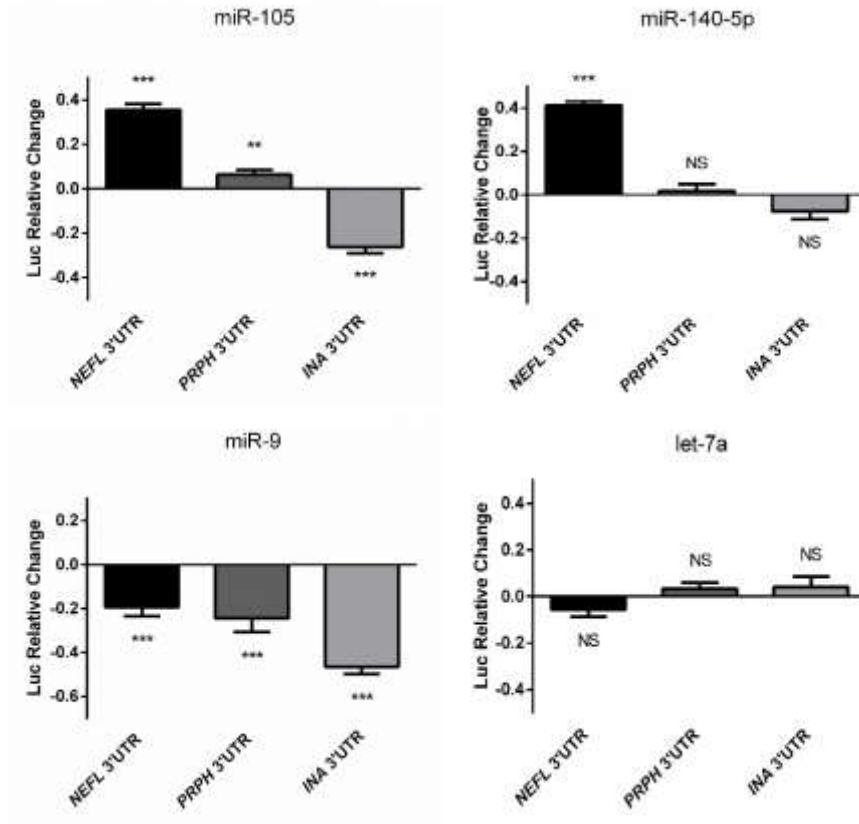


**B**
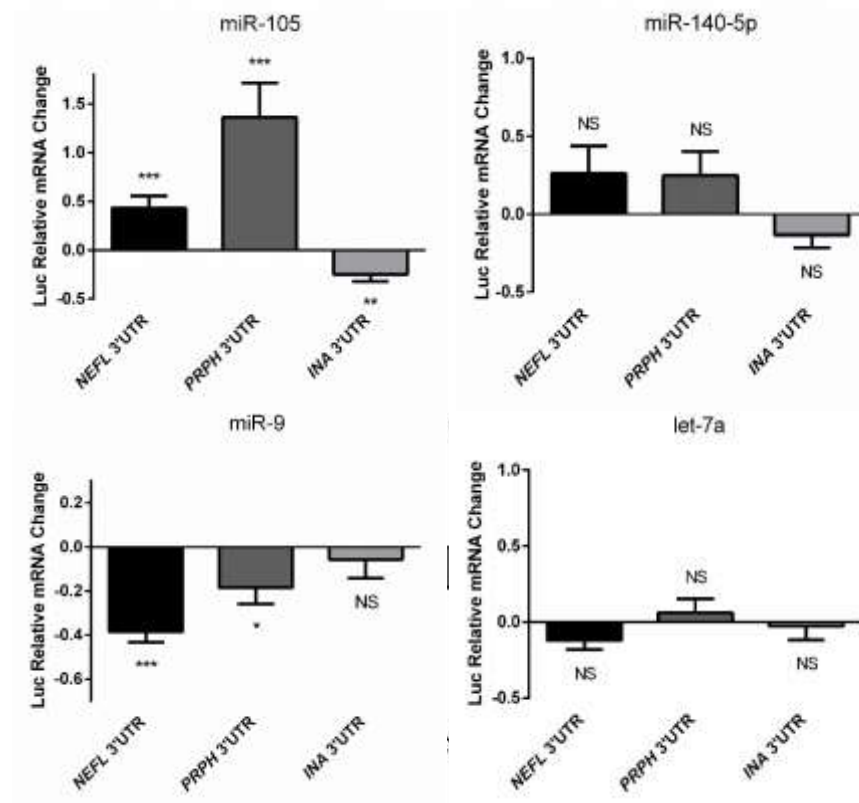
**Figure 2.4. MiR-105 regulates luciferase activity and mRNA expression when it contains either the *NEFL, PRPH,* or *INA* 3'UTR.** HEK293T cells were transfected with the pmirGLO plasmid containing either the *NEFL*, *PRPH*, or *INA* 3'UTR, or cells were co-transfected with the pmirGLO plasmid containing the intermediate filament 3'UTRs and either miR-105, miR-140-5p, or miR-9. A) Reporter gene assay showing changes in luciferase activity from control when either miR-105, miR-140-5p, or miR-9 interact with either the *NEFL*, *PRPH* or *INA* 3'UTR. B) Relative quantitative RT-qPCR showing changes in luciferase mRNA levels from control when either miR-105, miR-140-5p, or miR-9 interact with either the *NEFL*, *PRPH* or *INA* 3'UTR. Positive and negative values represent up- and downregulation, respectively. Let-7a was used as a negative control. Firefly luciferase expression was normalized to renilla luciferase expression, and then further normalized to account for the effect of the miRNA on the pmirGLO plasmid itself to determine the exact effect of the miRNA when it interacts with the respective intermediate filament 3'UTR. Data is represented as mean (n=3) $\pm$ SEM. Significance was determined using a Student's t-test (*** = $p<0.001$; ** = $p<0.01$; * = $p<0.05$; NS = $p>0.05$).

only when the S2 MRE was removed that miR-9 no longer silenced luciferase activity (**Fig. 2.5B**), indicating the S2 MRE within the *NEFL* 3'UTR is crucial for miR-9 mediated silencing. Mutations within the MRE of miR-9 in the *PRPH* 3'UTR lead to the eradication of the ability of miR-9 to reduce luciferase activity. However, elimination of the miR-9 MRE in the *INA* 3'UTR had no effect on its ability to reduce luciferase levels, indicating that miR-9 regulates *INA* expression through an indirect mechanism (**Fig. 2.5B**). Overall, these data indicate that miR-105 directly binds to the 3'UTR of *NEFL*, *PRPH* and *INA* to regulate expression, while miR-9 only directly targets the *NEFL* and *PRPH* 3'UTRs.

### 2.4.4 MiR-105 and miR-9 regulate the mRNA stability of endogenous *NEFL*, *PRPH* and *INA*.

The human neuron-derived cell line IMR-32, endogenously expresses *NEFL*, *PRPH* and *INA*, as well as miR-105 and miR-9 (**Fig. 2.6**). Therefore, we decided to determine whether miR-105 and miR-9 regulated these intermediate filaments endogenously. Overexpression of miR-105 lead to a significant increase in *NEFL*, while inhibition of miR-105 had a significant decrease on *NEFL* mRNA levels. Interestingly, overexpression of miR-105 was observed to have little effect on *PRPH* mRNA levels, yet its inhibition drastically reduced *PRPH* expression, which suggests that miR-105 is needed to stabilize the *PRPH* transcript. In contrast, miR-105 overexpression lead to a significant decrease, while miR-105 inhibition lead to a 2-fold increase ($p = 0.08$) in *INA* mRNA levels (**Fig. 2.7A**). This data indicates that miR-105 is a stabilizer of *NEFL* and *PRPH*, and a destabilizer of *INA* mRNA, consistent with what we observed in our luciferase assays.

Further, overexpression of miR-9 within IMR-32 cells lead to a significant decrease in *NEFL* and *PRPH* mRNA levels which is consistent with alterations seen in the relative quantitative RT-PCR and the luciferase assay, while the inhibition of miR-9 lead to a significant

increase in *NEFL* and *PRPH* mRNA (**Fig. 2.7B**). As expected, based on our relative quantitative RT-PCR, overexpression of miR-9 had little effect on *INA* mRNA stability. However, inhibition of miR-9 within IMR-32 cells lead to a significant increase in *INA* mRNA. This could indicate that the indirect mechanism by which miR-9 suppresses *INA* expression, as suggested by our luciferase and site-directed mutagenesis assays, is lost upon inhibition of miR-9 (**Fig. 2.7B**). This data shows that both miR-105 and miR-9 regulate this network on intermediate filaments within a human neuronal-derived cell line, further emphasizing that alterations to these miRNAs is a major contributing factor to aberrant intermediate filament stoichiometry seen in sALS spinal cord.

## 2.5 Discussion

In this study, we aimed to determine whether a specific pool of ALS-associated miRNAs contributes to changes in the mRNA metabolism of intermediate filaments that is observed in ALS spinal motor neurons. We identified two miRNAs—miR-105 and miR-9—to be central regulators of NFL, PRPH and INA, but only miR-105 binds directly to all intermediate filament 3'UTRs. Further, we showed that miR-105 is highly expressed in motor neurons and has reduced levels within the spinal cord of sALS patients, suggesting that the regulation of these intermediate filaments in spinal motor neurons is disrupted in sALS via miR-105.

Elucidating the mechanism that causes the selective reduction of *NEFL*, *PRPH* and *INA* has major significance in understanding ALS progression for several reasons. First, NFL is a necessary component of the neurofilament triplet protein structure, as NFM and NFH alone could not form a stable cytoskeleton (Szaro and Strong, 2010). Second, both INA and PRPH provide the early cytoskeleton for developing neurons, and thus, without the neurofilament triplet protein structure, INA and PRPH could potentially act as replacements for the neuronal
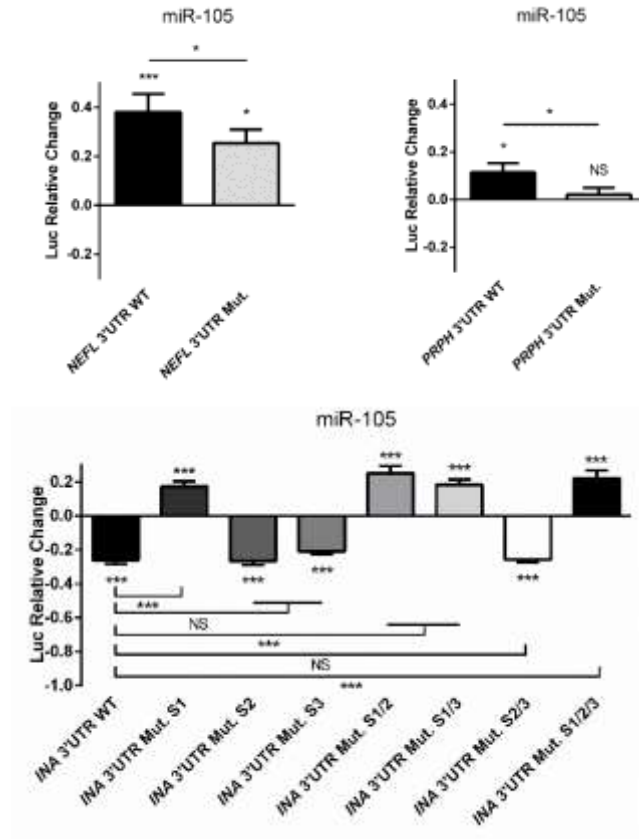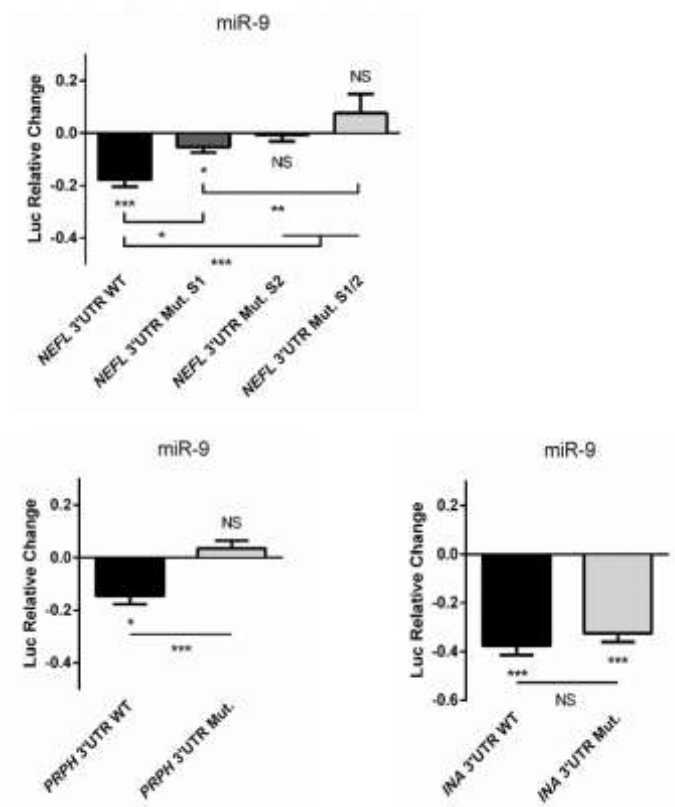
**Figure 2.5. MiR-105 regulates firefly luciferase expression through direct interactions with the *NEFL*, *PRPH*, and *INA* 3'UTR.** HEK293T cells were co-transfected with either the pmirGLO plasmid containing the wild-type 3'UTR, or mutated form, and either with or without miR-105 or miR-9. A) Changes to luciferase activity from control when miR-105 either contains or lacks MREs within either the *NEFL*, *PRPH,* or *INA* 3'UTR. MiR-105 has three MREs within the *INA* 3'UTR, and thus each MRE was individually examined. B) Changes to luciferase activity from control when miR-9 either contains or lacks MREs within either the *NEFL*, *PRPH,* or *INA* 3'UTR. MiR-9 has two MREs within the *NEFL* 3'UTR, and thus each MRE was individually examined. Firefly luciferase expression was normalized to renilla luciferase expression, and then further normalized to account for the effect of the miRNA on the pmirGLO plasmid to determine the exact effect of the miRNA when it interacts with the respective 3'UTR. Data is represented as mean (n=3) ± SEM. Significance was determined using a one-way ANOVA followed by a Tukey's post-hoc (*** = $p<0.001$; ** = $p<0.01$; * = $p<0.05$; NS = $p>0.05$).
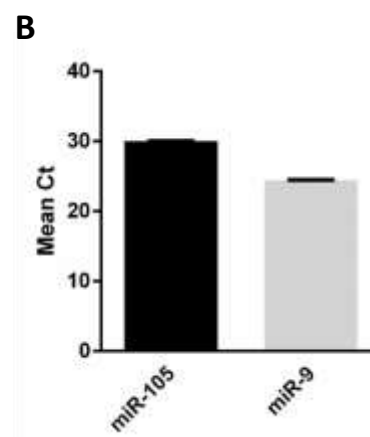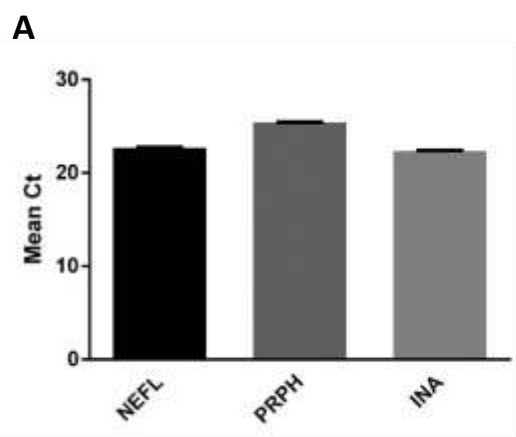
**Figure 2.6. Real-time PCR indicating expression of intermediate filaments and miRNAs of interest in IMR-32 cells.** A) Expression of *NEFL*, *PRPH* and *INA* mRNA within IMR-32 cells. B) Expression of miR-105 and miR-9 in IMR-32 cells. Values represented as mean (n=3) CT ± SEM.

**A**
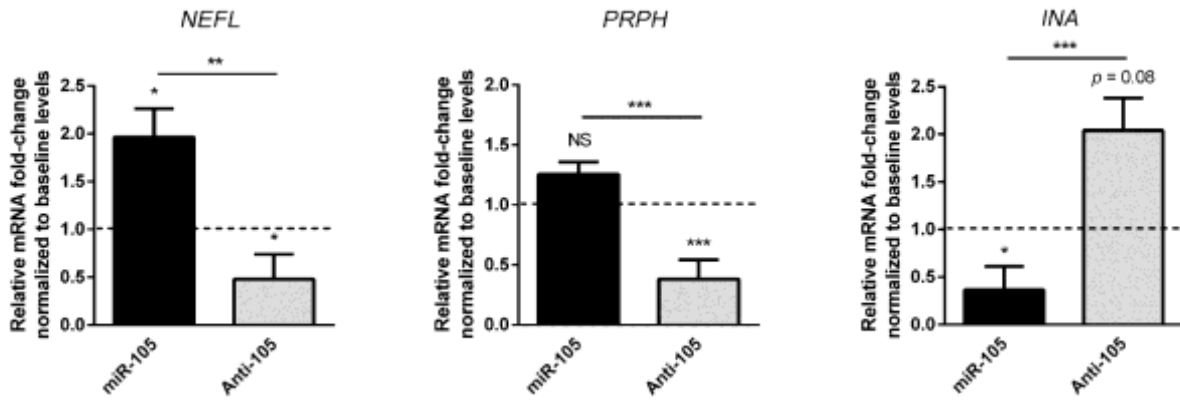


**B**
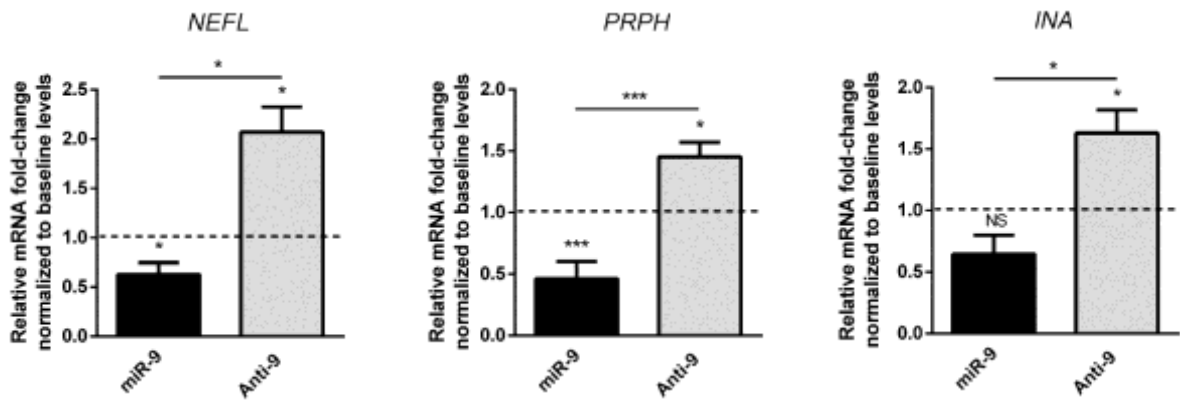
**Figure 2.7. MiR-105 and miR-9 regulate the endogenous mRNA expression of *NEFL*,**

***PRPH* and *INA*.** IMR-32 cells were transfected with either a miR-105 or miR-9, or let-7a

(negative control) mimics, or inhibitors. Basal levels of intermediate filament mRNAs were

measured in IMR-32 cells transfected with let-7a. Values above and below one represents either

an increase or decrease in expression, respectively. Changes to the expression of intermediate

filaments was measured using real-time PCR, and quantified using the $2^{-\Delta\Delta CT}$ method, where

values were first normalized to 18S RNA levels prior to comparison. Data was represented as

mean (n=5) ± SEM.  Significance was calculated using a one-way ANOVA followed by a

Tukey's post-hoc (*** = $p<0.001$; ** = $p<0.01$; * = $p<0.05$; NS = $p>0.05$).

cytoskeleton (Athlan and Mushynski, 1997; Kaplan et al., 1990; Yuan et al., 2006; Yuan et al.,

2012). In fact, there is an increase in INA and PRPH expression within injured neurons which

allows for replacement of the cytoskeleton structure at the injured site (McGraw et al., 2002;

Troy et al., 1990). However, since there is a selective reduction of *NEFL*, *PRPH*, and *INA*

expression within spinal motor neurons of ALS patients (Wong et al., 2000), these motor

neurons have no mechanism by which they can support and/or replace their cytoskeleton

structure.

Reduction of miR-105 has generally been associated with tumor and cancer formation as

it is responsible for regulating several tumor suppressor genes (Honeywell et al., 2013; Liu et al.,

2016; Lu et al., 2017; Zhang et al., 2017). However, this is the first time, to our knowledge, that

miR-105 has been associated with the regulation of neuronal intermediate filaments. According

to our results, reduced levels of miR-105 leads to decreased levels of *NEFL* and *PRPH*, and

increased levels of *INA* mRNA. However, this does not match what is actually seen in sALS

motor neurons, as all three intermediate filaments show decreased levels (Wong et al., 2000).

Thus, while miR-105 appears to be a central regulator of ALS-linked intermediate filaments, the

dysregulation of this miRNA in sALS is probably a contributing factor to the dysregulation of

intermediate filaments, and not the sole cause.

Beyond miR-105, we examined miR-9 given that it had previously been shown to be

reduced in ALS spinal cord and motor neurons. We observed that miR-9 also was capable of

reducing the expression of *NEFL*, *PRPH* and *INA*. Previous work has shown that miR-9 is a

critical part of the intermediate filament pathway through the regulation of *NEFH* (Campos-Melo

et al., 2018; Haramati et al., 2010). While Haramati et al. had also observed that miR-9 does not

regulate mouse *Nefl,* it is noteworthy that miR-9 lacks MREs within the mouse *Nefl* 3'UTR. In

contrast, human *NEFL* 3'UTR has two sites for miR-9 binding. Further, our results suggest that loss of miR-9 expression in ALS would lead to an increase in all three of these intermediate filaments, which does not match what we have previously observed in sALS motor neurons (Wong et al., 2000). However, based on our data, loss of miR-9 expression would still alter the intermediate filament stoichiometry, which is the main factor that drives intermediate filament pathogenesis (Szaro and Strong, 2010). Overall, our findings indicate that miR-105 and miR-9 are necessary components to maintain intermediate filament stoichiometry, and thus, loss of these miRNAs in sALS likely contribute to intermediate filament dysregulation.

An intriguing finding in this study was the MRE site preference of miR-105 and miR-9 within the *INA* and *NEFL* 3'UTRs, respectively. Despite having three MREs within the *INA* 3'UTR, miR-105 only bound to one site (S1) to regulate mRNA stability, while miR-9 binds both MREs to reduce *NEFL* levels, with binding to the S2 MRE having a greater effect on *NEFL* downregulation than binding to the S1 MRE. It is a common phenomenon for a single miRNA to have multiple MREs within a transcript, where interactions with each MRE has either a synergistic or differential effect on transcript stability and translational output (Jangra et al., 2010; Nasheri et al., 2011; Ott et al., 2011). For example, miR-122 has four MREs within the Hepatitis C Virus (HCV). When miR-122 binds to the S1 or S2 MRE it promotes viral translation (Jangra et al., 2010). In contrast, interactions with the S4 MRE suppresses viral translation while binding to the S3 MRE has no effect on overall translational output of the virus (Henke et al., 2008; Nasheri et al., 2011). The exact reason why a miRNA binds to some MREs and not others or has differential effects on transcript stability at different MREs is unknown. Considering there are other *trans*-acting factors that regulate mRNA stability, how a miRNA

functions at a particular MRE is likely affected by the other *trans*-acting factors that are binding within that area.

Further, while removing the miR-105 binding site from the *NEFL* 3'UTR reduced the stabilizing effect it had on the luciferase transcript, it did not completely abolish the effect. This could indicate that miR-105 regulates the expression of another target that is responsible for regulating *NEFL* stability. TDP-43 and RGNEF are two ALS-associated RNA-binding proteins known to regulate *NEFL* mRNA stability (Droppelmann et al., 2013; Volkening et al., 2009), and thus, it would be worth investigating whether the expression of these RNA-binding proteins are affected by changes to miR-105 levels.

Both miR-9 and miR-105 downregulation in sALS likely contributes to the loss of intermediate filament stoichiometry, ultimately leading to intermediate filament aggregation and eventual neuronal death. MiRNAs are ideal therapeutic targets as they are known to regulate several genes within a network. For example, miR-506 and miR-146a are negative regulators of several genes involved in cancer metastasis and inflammation, respectively (Sun et al., 2015; Wu et al., 2015). Thus, rather than targeting individual genes that contribute to the disease, miRNAs offer an avenue in which we can target multiple genes involved in a disease process (Rupaimoole and Slack, 2017). Our data suggests that both miR-105 and miR-9 regulate a network of ALS-associated neuronal intermediate filaments, and thus recovery of these miRNAs within sALS patients could slow disease progression by mitigating the alterations seen to intermediate filament stoichiometry. Further work within *in vivo* models is still needed to confirm this hypothesis.

## 2.6 References

Athlan, E.S., and Mushynski, W.E. (1997). Heterodimeric associations between neuronal intermediate filament proteins. J Biol Chem *272*, 31073-31078.

Beaulieu, J.M., Nguyen, M.D., and Julien, J.P. (1999). Late onset of motor neurons in mice overexpressing wild-type peripherin. J Cell Biol *147*, 531-544.

Campos-Melo, D., Droppelmann, C.A., He, Z., Volkening, K., and Strong, M.J. (2013). Altered microRNA expression profile in Amyotrophic Lateral Sclerosis: a role in the regulation of NFL mRNA levels. Mol Brain *6*, 26.

Campos-Melo, D., Hawley, Z.C.E., and Strong, M.J. (2018). Dysregulation of human NEFM and NEFH mRNA stability by ALS-linked miRNAs. Mol Brain *11*, 43.

Carpenter, D.A., and Ip, W. (1996). Neurofilament triplet protein interactions: evidence for the preferred formation of NF-L-containing dimers and a putative function for the end domains. J Cell Sci *109 ( Pt 10)*, 2493-2498.

de Planell-Saguer, M., Rodicio, M.C., and Mourelatos, Z. (2010). Rapid in situ codetection of noncoding RNAs and proteins in cells and formalin-fixed paraffin-embedded tissue sections without protease treatment. Nat Protoc *5*, 1061-1073.

Dini Modigliani, S., Morlando, M., Errichelli, L., Sabatelli, M., and Bozzoni, I. (2014). An ALS-associated mutation in the FUS 3'-UTR disrupts a microRNA-FUS regulatory circuitry. Nat Commun *5*, 4335.

Droppelmann, C.A., Keller, B.A., Campos-Melo, D., Volkening, K., and Strong, M.J. (2013). Rho guanine nucleotide exchange factor is an NFL mRNA destabilizing factor that forms cytoplasmic inclusions in amyotrophic lateral sclerosis. Neurobiol Aging *34*, 248-262.

Emde, A., Eitan, C., Liou, L.L., Libby, R.T., Rivkin, N., Magen, I., Reichenstein, I., Oppenheim, H., Eilam, R., Silvestroni, A.*, et al.* (2015). Dysregulated miRNA biogenesis downstream of cellular stress and ALS-causing mutations: a new mechanism for ALS. EMBO J *34*, 2633-2651.

Figueroa-Romero, C., Hur, J., Lunn, J.S., Paez-Colasante, X., Bender, D.E., Yung, R., Sakowski, S.A., and Feldman, E.L. (2016). Expression of microRNAs in human post-mortem amyotrophic lateral sclerosis spinal cords provides insight into disease mechanisms. Mol Cell Neurosci *71*, 34-45.

Haramati, S., Chapnik, E., Sztainberg, Y., Eilam, R., Zwang, R., Gershoni, N., McGlinn, E., Heiser, P.W., Wills, A.M., Wirguin, I.*, et al.* (2010). miRNA malfunction causes spinal motor neuron disease. Proc Nat Acad Sci USA *107*, 13111-13116.

Hawley, Z.C.E., Campos-Melo, D., Droppelmann, C.A., and Strong, M.J. (2017a). MotomiRs: miRNAs in Motor Neuron Function and Disease. Front Mol Neurosci *10*, 127.

Hawley, Z.C.E., Campos-Melo, D., and Strong, M.J. (2017b). Novel miR-b2122 regulates several ALS-related RNA-binding proteins. Mol Brain *10*, 46.

He, C.Z., and Hays, A.P. (2004). Expression of peripherin in ubiquinated inclusions of amyotrophic lateral sclerosis. J Neurol Sci *217*, 47-54.

Henke, J.I., Goergen, D., Zheng, J., Song, Y., Schuttler, C.G., Fehr, C., Junemann, C., and Niepmann, M. (2008). microRNA-122 stimulates translation of hepatitis C virus RNA. EMBO J *27*, 3300-3310.

Hirano, A., Nakano, I., Kurland, L.T., Mulder, D.W., Holley, P.W., and Saccomanno, G. (1984). Fine structural study of neurofibrillary changes in a family with amyotrophic lateral sclerosis. J Neuropathol Exp Neurol *43*, 471-480.

Honeywell, D.R., Cabrita, M.A., Zhao, H., Dimitroulakos, J., and Addison, C.L. (2013). miR-105 inhibits prostate tumour growth by suppressing CDK6 levels. PLoS One *8*, e70515.

Ishtiaq, M., Campos-Melo, D., Volkening, K., and Strong, M.J. (2014). Analysis of novel NEFL mRNA targeting microRNAs in amyotrophic lateral sclerosis. PLoS One *9*, e85653.

Jangra, R.K., Yi, M., and Lemon, S.M. (2010). Regulation of hepatitis C virus translation and infectious virus production by the microRNA miR-122. J Virol *84*, 6615-6625.

Kaplan, M.P., Chin, S.S., Fliegner, K.H., and Liem, R.K. (1990). Alpha-internexin, a novel neuronal intermediate filament protein, precedes the low molecular weight neurofilament protein (NF-L) in the developing rat brain. J Neurosci *10*, 2735-2748.

Keller, B.A., Volkening, K., Droppelmann, C.A., Ang, L.C., Rademakers, R., and Strong, M.J. (2012). Co-aggregation of RNA binding proteins in ALS spinal motor neurons: evidence of a common pathogenic mechanism. Acta Neuropathol *124*, 733-747.

Kondo, A., Iwaki, T., Tateishi, J., Kirimoto, K., Morimoto, T., and Oomura, I. (1986). Accumulation of neurofilaments in a sporadic case of amyotrophic lateral sclerosis. Jpn J Psychiatry Neurol *40*, 677-684.

Kriz, J., Meier, J., Julien, J.P., and Padjen, A.L. (2000). Altered ionic conductances in axons of transgenic mouse expressing the human neurofilament heavy gene: A mouse model of amyotrophic lateral sclerosis. Exp Neurol *163*, 414-421.

Lariviere, R.C., and Julien, J.P. (2004). Functions of intermediate filaments in neuronal development and disease. J Neurobiol *58*, 131-148.

Lee, M.K., Marszalek, J.R., and Cleveland, D.W. (1994). A mutant neurofilament subunit causes massive, selective motor neuron death: implications for the pathogenesis of human motor neuron disease. Neuron *13*, 975-988.

Liu, X., Wang, H., Zhu, Z., Ye, Y., Mao, H., and Zhang, S. (2016). MicroRNA-105 targets SOX9 and inhibits human glioma cell progression. FEBS Lett *590*, 4329-4342.

Lu, G., Fu, D., Jia, C., Chai, L., Han, Y., Liu, J., Wu, T., Xie, R., Chang, Z., Yang, H.*, et al.* (2017). Reduced miR-105-1 levels are associated with poor survival of patients with non-small cell lung cancer. Oncol Lett *14*, 7842-7848.

McGraw, T.S., Mickle, J.P., Shaw, G., and Streit, W.J. (2002). Axonally transported peripheral signals regulate alpha-internexin expression in regenerating motoneurons. J Neurosci *22*, 4955-4963.

Nasheri, N., Singaravelu, R., Goodmurphy, M., Lyn, R.K., and Pezacki, J.P. (2011). Competing roles of microRNA-122 recognition elements in hepatitis C virus RNA. Virology *410*, 336-344.

Ott, C.E., Grunhagen, J., Jager, M., Horbelt, D., Schwill, S., Kallenbach, K., Guo, G., Manke, T., Knaus, P., Mundlos, S.*, et al.* (2011). MicroRNAs differentially expressed in postnatal aortic development downregulate elastin via 3' UTR and coding-sequence binding sites. PLoS One *6*, e16250.

Rupaimoole, R., and Slack, F.J. (2017). MicroRNA therapeutics: towards a new era for the management of cancer and other diseases. Nat Rev Drug Discov *16*, 203-222.

Strong, M.J. (2010). The evidence for altered RNA metabolism in amyotrophic lateral sclerosis (ALS). J Neurol Sci *288*, 1-12.

Strong, M.J. (2017). Revisiting the concept of amyotrophic lateral sclerosis as a multisystems disorder of limited phenotypic expression. Curr Opin Neurol *30*, 599-607.

Strong, M.J., Leystra-Lantz, C., and Ge, W.W. (2004). Intermediate filament steady-state mRNA levels in amyotrophic lateral sclerosis. Biochem Biophys Res Commun *316*, 317-322.

Sun, Y., Hu, L., Zheng, H., Bagnoli, M., Guo, Y., Rupaimoole, R., Rodriguez-Aguayo, C., Lopez-Berestein, G., Ji, P., Chen, K.*, et al.* (2015). MiR-506 inhibits multiple targets in the epithelial-to-mesenchymal transition network and is associated with good prognosis in epithelial ovarian cancer. J Pathol *235*, 25-36.

Szaro, B.G., and Strong, M.J. (2010). Post-transcriptional control of neurofilaments: New roles in development, regeneration and neurodegenerative disease. Trends Neurosci *33*, 27-37.

Thyagarajan, A., Strong, M.J., and Szaro, B.G. (2007). Post-transcriptional control of neurofilaments in development and disease. Exp Cell Res *313*, 2088-2097.

Troy, C.M., Muma, N.A., Greene, L.A., Price, D.L., and Shelanski, M.L. (1990). Regulation of peripherin and neurofilament expression in regenerating rat motor neurons. Brain Res *529*, 232-238.

Volkening, K., Leystra-Lantz, C., Yang, W., Jaffee, H., and Strong, M.J. (2009). Tar DNA binding protein of 43 kDa (TDP-43), 14-3-3 proteins and copper/zinc superoxide dismutase (SOD1) interact to modulate NFL mRNA stability. Implications for altered RNA processing in amyotrophic lateral sclerosis (ALS). Brain Res *1305*, 168-182.

Wong, N.K., He, B.P., and Strong, M.J. (2000). Characterization of neuronal intermediate filament protein expression in cervical spinal motor neurons in sporadic amyotrophic lateral sclerosis (ALS). J Neuropathol Exp Neurol *59*, 972-982.

Wu, D., Cerutti, C., Lopez-Ramirez, M.A., Pryce, G., King-Robson, J., Simpson, J.E., van der Pol, S.M., Hirst, M.C., de Vries, H.E., Sharrack, B.*, et al.* (2015). Brain endothelial miR-146a negatively modulates T-cell adhesion through repressing multiple targets to inhibit NF-kappaB activation. J Cereb Blood Flow Metab *35*, 412-423.

Xiao, S., McLean, J., and Robertson, J. (2006). Neuronal intermediate filaments and ALS: a new look at an old question. Biochim Biophys Acta *1762*, 1001-1012.

Yuan, A., Rao, M.V., Sasaki, T., Chen, Y., Kumar, A., Veeranna, Liem, R.K., Eyer, J., Peterson, A.C., Julien, J.P.*, et al.* (2006). Alpha-internexin is structurally and functionally associated with the neurofilament triplet proteins in the mature CNS. J Neurosci *26*, 10006-10019.

Yuan, A., Sasaki, T., Kumar, A., Peterhoff, C.M., Rao, M.V., Liem, R.K., Julien, J.P., and Nixon, R.A. (2012). Peripherin is a subunit of peripheral nerve neurofilaments: implications for differential vulnerability of CNS and peripheral nervous system axons. J Neurosci *32*, 8501-8508.

Zhang, J., Wu, W., Xu, S., Zhang, J., Zhang, J., Yu, Q., Jiao, Y., Wang, Y., Lu, A., You, Y.*, et al.* (2017). MicroRNA-105 inhibits human glioma cell malignancy by directly targeting SUZ12. Tumour Biol *39*, 1010428317705766.

Zhang, Z., Almeida, S., Lu, Y., Nishimura, A.L., Peng, L., Sun, D., Wu, B., Karydas, A.M., Tartaglia, M.C., Fong, J.C.*, et al.* (2013). Downregulation of microRNA-9 in iPSC-derived neurons of FTD/ALS patients with TDP-43 mutations. PLoS One *8*, e76055.

Zhu, Q., Couillard-Despres, S., and Julien, J.P. (1997). Delayed maturation of regenerating myelinated axons in mice lacking neurofilaments. Exp Neurol *148*, 299-316.

# Chapter 3

## Dysregulation of human *NEFM* and *NEFH* mRNA stability by ALS-linked miRNAs

Danae Campos-Melo\*, Zachary C. E. Hawley\*, and Michael J. Strong

A version of this chapter was published in *Molecular Brain*

## 3.1 Abstract

Neurofilaments (NFs) are the most abundant cytoskeletal component of vertebrate myelinated axons. NFs function by determining axonal caliber, promoting axonal growth and forming a 3-dimensional lattice that supports the organization of cytoplasmic organelles. The stoichiometry of NF protein subunits (NFL, NFM and NFH) must be tightly controlled to avoid the formation of NF neuronal cytoplasmic inclusions (NCIs), axonal degeneration and neuronal death, all pathological hallmarks of amyotrophic lateral sclerosis (ALS). The post-transcriptional control of NF transcripts is critical for regulating normal levels of NF proteins. Previously, we showed that miRNAs that are dysregulated in ALS spinal cord regulate the levels of *NEFL* mRNA. In order to complete the understanding of altered NF expression in ALS, in this study we have investigated the regulation of *NEFM* and *NEFH* mRNA levels by miRNAs. We observed that a small group of ALS-linked miRNAs that are expressed in human spinal motor neurons directly regulate *NEFM* and *NEFH* transcript levels in a manner that is associated with an increase in NFM and NFH protein levels in ALS spinal cord homogenates. In concert with previous observations demonstrating the suppression of *NEFL* mRNA steady state levels in ALS, these observations provide support for the hypothesis that the dysregulation of miRNAs in spinal motor neurons in ALS fundamentally alters the stoichiometry of NF expression, leading to the formation of pathological NCIs.

**3.2 Introduction**

Neurofilaments (NFs) are unique neuron-specific intermediate filaments in vertebrates. They are highly dynamic structures that determine axonal caliber, promote axonal growth and organize the cytoplasm to form a stable 3-dimensional lattice that supports the organization of organelles and cytoplasmic proteins (Szaro and Strong, 2010; Walker et al., 2001).

NF subunit proteins (low, medium and high molecular weight neurofilaments; NFL, NFM and NFH, respectively) form homo- and hetero-polymers following a specific stoichiometry and tight spatiotemporal regulation. Conserving NF stoichiometry by controlling the levels of expression of individual NF subunits is critical for the maintenance of healthy neurons. Alterations of NF mRNA steady stoichiometry and the associated formation of neuronal cytoplasmic inclusions (NCIs) composed of NF proteins are neuropathological markers of degenerating motor neurons in amyotrophic lateral sclerosis (ALS), a progressive neurodegenerative disease (Szaro and Strong, 2010; Thyagarajan et al., 2007; Xiao et al., 2006). Although the exact mechanism by which NF NCIs exert toxicity is unknown, it has been suggested that they alter the internal structure of axons and disrupt axonal transport, in addition to impairing NMDA-mediated calcium influx, compromising the survival of neurons (Sanelli et al., 2004; Thyagarajan et al., 2007).

Post-transcriptional control is crucial for preserving NF subunit expression in neuronal homeostasis and also during axonal outgrowth in development and regeneration (Ananthakrishnan et al., 2008; Ananthakrishnan and Szaro, 2009; Schwartz et al., 1994). MiRNAs are evolutionary conserved non-coding RNAs that control the expression of the majority of the mammalian transcriptome and have been increasingly linked to neurodegenerative disorders. We and others have described a profound dysregulation of miRNAs in spinal cord and motor cortex of ALS patients (Campos-Melo et al., 2013; Emde

et al., 2015; Figueroa-Romero et al., 2016; Wakabayashi et al., 2014). We previously demonstrated that a selective group of these miRNAs directly regulate *NEFL* mRNA stability (Campos-Melo et al., 2013), and postulated that this dysregulation of miRNA expression would contribute to the selective suppression of *NEFL* mRNA levels observed in ventral lateral spinal cord motor neurons in ALS (Bergeron et al., 1994; Wong et al., 2000). Proper control of the levels of the NF triplet is critical because the backbone of the NF is mainly formed by NFL (Leermakers and Zhulina, 2010) and the stoichiometry of NFL/NFM/NFH (4:2:1) has to be carefully maintained (Scott et al., 1985). The miRNAs responsible for regulating human *NEFM* and *NEFH* mRNA stability are however unknown. In this study we observed that a limited number of ALS-linked miRNAs that are expressed in spinal motor neurons directly regulate *NEFM* and *NEFH* mRNA levels, in a way that might explain the increase in NFM and NFH protein levels that we observed in ALS spinal cords and thus contribute directly to the formation of NF NCIs.

## 3.3 Materials and Methods

### 3.3.1 Tissue Collection

Spinal cord samples from sALS patients and age-matched, neurologically intact control individuals were used. All ALS cases were both clinically and neuropathologically confirmed using the El Escorial Criteria (World Federation of Neurology Research Group on Neuromuscular Disease, 1994). Written consent for autopsy was obtained from the next of kin at the time of death or from the patient antemortem in accordance with the London Health Sciences Centre consent for autopsy. Cases were genotyped and confirmed to have no known mutations in *SOD1, TARDBP, FUS* or expanded repeats in *C9ORF72* (**Table 3.1**).

**Table 3.1**. Patient demographics.

| Cases | Gender | Age of symptom onset | Symptom onset | Age of death | Cause of Death |
|---|---|---|---|---|---|
| Control | F | - | - | 62 | Heart Attack |
| | M | - | - | 74 | Stroke |
| | F | - | - | 68 | Unknown |
| | M | - | - | 68 | Brain Tumor |
| | M | - | - | 75 | Unknown |
| | F | - | - | 53 | Pneumonia |
| | F | - | - | 74 | Leukemia |
| | M | - | - | 67 | Unknown |
| ALS | F | 58 | Unknown | 60 | Unknown |
| | M | 69 | Upper/lower limbs | 72 | Unknown |
| | F | 40 | Bulbar | 41 | Systemic Failure |
| | M | 55 | Unknown | 61 | Pneumonia |
| | M | 64 | Upper/lower limbs | 67 | Respiratory Failure |
| | F | 69 | Respiratory Symptoms | 71 | Respiratory Failure |
| | M | 63 | Unknown | 64 | Unknown |
| | F | 47 | Bulbar | 49 | Respiratory Failure |

**3.3.2 3'RACE PCR, cloning and miRNA target prediction**

*NEFM* and *NEFH* mRNA 3'UTRs were obtained using 3'RACE PCR. Briefly, TRIzol reagent (Thermo Fisher Scientific) was used for total RNA extraction from human spinal cord tissue. 3'RACE PCR was performed using SMARTer RACE 5'/3' RACE Kit (Takara Bio. Inc., Clontech) and primers hNEFM_3RACE_F1D: 5'CACTTCACACGCCATAGTAAAGGAAGTCACC3' and hNEFH_3RACE_F2: 5'GAGAAGGCCACAGAAGACAAGGCCGCCAAG3' for *NEFM* and *NEFH* 3'UTRs, respectively. 3'UTR isoforms were cloned into pGEMT-Easy vector and sequenced. For luciferase assays, 3'UTRs were subcloned into pmirGLO vector between NheI and SalI sites and linked to the firefly luciferase coding region. Mutations in two nucleotides at the 3'end of each miRNA recognition element (MRE) within the *NEFM* and *NEFH* 3'UTRs were made using QuikChange Site-Directed Mutagenesis Kit II (Agilent) according to the manufacturer's instructions. Mutations were carefully designed to ensure no changes were made in the secondary structures of the transcripts using the RNAFold WebServer (http://rna.tbi.univie.ac.at/cgi-bin/RNAfold.cgi). Both TargetScan (http://www.targetscan.org/) and miRanda (http://www.microrna.org/microrna/getGeneForm.do) software programs were used to determine miRNAs with predicted MREs in either *NEFM* or *NEFH* 3'UTRs.

**3.3.3 miRNA extraction and real-time PCR**

Total miRNA extraction using the mirVana miRNA isolation kit (Thermo Fisher Scientific) was performed from human ventral lumbar spinal cord using 5 controls and 8 ALS tissue samples according to the manufacturer's instruction. Yield and purity of the miRNA solution was determined using spectrophotometry while RNA integrity was measured using a bioanalyzer instrument.

MiRNA extracts from the spinal cord of ALS patients or controls were reversed transcribed and then subjected to real-time PCR using the miRCURY LNA™ Universal RT microRNA PCR (Exiqon) and ExiLENT SYBR Green master mix (Exiqon), according to the manufacturer's instructions. PCRs were performed using the 7900 HT real-time PCR system. Relative expression of miRNAs was normalized to miR-16-5p, a miRNA previously demonstrated to have the same expression in sALS and controls (Campos-Melo et al., 2013). The analysis of the relative expression of candidate miRNAs between sALS and controls was done using the $2^{-\Delta\Delta CT}$ method. All experiments were run in triplicate and significance was determined using Student's *t*-test.

### 3.3.4 TaqMan real-time PCR

To examine the expression levels of *NEFM* and *NEFH* mRNA, total RNA extraction was performed on ALS patient and control lumbar spinal cord tissue using TRIzol reagent (Ambion, Life Technologies). RNA samples were subjected to a cDNA synthesis reaction using the SuperScript IV VILO reverse transcriptase (Invitrogen, Thermo Fisher Scientific) in accordance to the manufacture's instructions. Real-time PCR was done on the cDNA templates using the TaqMan Fast Advanced Master Mix and TaqMan Gene Expression Assays (Applied Biosystems, Thermo Fisher Scientific) targeting either *NEFM* or *NEFH*. Assays were performed in accordance to the manufacture's instructions. TaqMan probes that targeted either *NEFM* or *NEFH* were designed with a FAM fluorophore. The expression of *NEFM* and *NEFH* was normalized to the expression of a reference gene (HPRT1), which was targeted by a TaqMan probe containing a VIC fluorophore. Changes in *NEFM* and *NEFH* mRNA expression between ALS patients and control subjects were determined using the $2^{-\Delta\Delta CT}$ method. Experiments were run in triplicate and determined to be significantly different using a Student's *t*-test.

### 3.3.5 Fluorescent *in situ* hybridization (FISH)

To ensure that the miRNAs of interest are expressed in human motor neurons, neuropathologically normal lumbar spinal cord from control subjects was examined for miRNA expression. Tissue sections were formalin-fixed, paraffin embedded (FFPE) and cut into 7μm sections. Samples were UV treated overnight to reduce the lipofuscin-induced auto-fluorescent signal. FISH was performed as described previously (Planell-Sauger et al 2010). LNA probes were designed with double DIG-labels that targeted the miRNA of interest (Exiqon). DIG-HRP secondary antibody, and Tyramide Signal Amplification (TSA) Systems tagged with a Cy3 fluorophore (PerkinElmer) were used to obtain a fluorescent signal of the miRNA target. Ventral horn of human lumbar spinal cord tissue was examined for positive staining within motor neurons using the Olympus FV1000 confocal microscope.

### 3.3.6 Cell culture, luciferase assay and relative quantitative RT-PCR

HEK293T cells were maintained in Dulbecco's Modified Eagle's Medium (DMEM) containing 10% fetal bovine serum (FBS), at 37$^{o}$C with 5% $CO_2$. HEK293T cells were plated on 96-well plates with a density of 10,000 cells/well 24 hours prior to transfection. 100 nM of miRNA mimics (Thermo Fisher Scientific) and 3.47 fmol of pmirGLO containing *NEFM* or *NEFH* 3'UTR were co-transfected into the cells using Lipofectamine 2000 reagent (Thermo Fisher Scientific).

Luciferase assays and relative quantitative RT-PCR were performed 24 hours post-transfection as was described previously (Campos-Melo et al., 2014). Data show positive values as upregulation and negative values as downregulation. All experiments were run in triplicate, and significance was determined using a Student's *t*-test or one-way ANOVA followed by Turkey's post hoc test.

### 3.3.7 Western blot

Total protein extraction from ventral lumbar spinal cord of 3 controls and 7 ALS patients was performed using NP40 lysis buffer containing proteinase inhibitors. Samples

were sonicated, resuspended in loading buffer, denatured at 90°C and run on an 8% SDS-gel. After transfer, the nitrocellulose membrane was probed with either mouse anti-NFM (1:1000; Boehringer Mannheim, 814-334), mouse anti-NFH (1:1000; Boehringer Mannheim, 814-342), or rabbit anti-GAPDH (1:5000; Abcam, ab9485) and later with HRP-secondary antibody (goat anti-mouse 1:3000, or goat anti-rabbit 1:5000; BioRad and Invitrogen, respectively). Relative protein expression of NFM and NFH were normalized to GAPDH expression levels. Student's *t*-test was used to determine statistical differences in endogenous protein expression.

## 3.4 Results

### 3.4.1 Only one 3'UTR isoform of either *NEFM* are *NEFH* is expressed in human spinal cord

Considering that 3'UTR polymorphisms have been increasingly reported in the literature, we determined if 3'UTR variants of *NEFM* and *NEFH* mRNAs are expressed in human spinal cord. A single variant form of *NEFM* and *NEFH* 3'UTRs (486 and 583 nt, respectively) was detected in lumbar spinal cord control tissue (**Fig. 3.1**). Analysis of ALS patients showed no difference in the 3'UTR variants of *NEFM* and *NEFH* expressed in spinal cord compared to control samples (data not shown).

### 3.4.2 Several ALS-linked miRNAs have MREs within the *NEFM* and *NEFH* 3'UTRs

Prediction algorithms showed that *NEFM* and *NEFH* 3'UTRs have multiple MREs for different pools of miRNAs. However, for this study we only considered those miRNAs that we previously observed to be differentially expressed in ALS tissue versus controls using the TaqMan assay (Campos-Melo et al., 2013). We performed real-time PCR using SYBR green of 40 miRNAs to validate differential expression of 6 miRNAs that have MREs in *NEFM* or *NEFH* 3'UTRs (**Fig. 3.2A**). Each miRNA, (miR-92a-3p, miR-125b-5p, miR-9-5p, miR-20b-
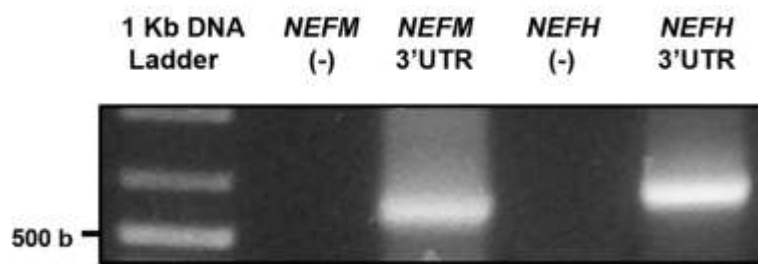
**Figure 3.1. Single *NEFM* and *NEFH* mRNA 3'UTR variants are expressed in human spinal cord**. 3'RACE-PCR was performed from spinal cord tissue samples of control individuals using specific primers to amplify *NEFM* and *NEFH* 3'UTRs. 3'UTRs were cloned and sequenced. One 3'UTR variant for each *NEFM* (486 nt) and *NEFH* (583 nt) transcript was observed in human spinal cord. *NEFM* specific primer anneals to a region 40 nt upstream the stop codon.

5p and miR-223-3p and miR-519d-3p) showed significant downregulation of expression in ALS spinal cord versus controls (**Fig. 3.2B**).

Next, we examined the neuronal expression of the group of miRNAs that potentially regulate *NEFM* and *NEFH* transcripts in human spinal cord motor neurons of control tissue through FISH. MiR-92a-3p is almost exclusively expressed in motor neurons of the spinal cord. MiR-125b-5p, miR-9-5p, miR-20b-5p and miR-519d-3p showed higher expression in motor neurons than in other cell types within the spinal cord. MiR-223-3p showed similar expression in motor neurons and surrounding cells. MiR-548c-3p was used as a negative control and miR-124-3p, which is highly expressed in neurons, was used as positive control. In summary, we observed that the 6 ALS-linked miRNAs that are predicted to regulate *NEFM* and *NEFH* mRNAs are expressed in motor neurons of human spinal cord (**Fig. 3.3**).

### 3.4.3 MiRNA candidates interact with *NEFM* and *NEFH* 3'UTRs to regulate gene expression

Functionality assays of these 6 miRNAs showed that miR-92a-3p and miR-125b-5p downregulate the levels of a luciferase reporter linked to *NEFM* 3'UTR (**Fig. 3.4A**). MiR-9-5p, miR-20b-5p, miR-92a-3p and miR-223-3p downregulate the levels of the luciferase reporter coupled to *NEFH* 3'UTR (**Fig. 3.4B**). We observed that most of these miRNAs also significantly downregulate mRNA levels of the luciferase reporter bound to either *NEFM* or *NEFH* 3'UTR (**Fig. 3.4C and D**), which implies that miRNAs are dysregulating the stability of *NEFM* and *NEFH* transcripts. Reporter gene assay using *NEFM* or *NEFH* 3'UTR MRE mutants showed a decrease in the downregulatory effect of each miRNA compared with the wild type, indicating that miR-9-5p, miR-20b-5p, miR-92a-3p, miR-125b-5p and miR-223-3p directly regulate *NEFM* or *NEFH* 3'UTRs stability (**Fig. 3.5**).

### 3.4.4 *NEFM* and *NEFH* mRNA and protein are increased in ALS spinal cord

Finally, considering the reduced expression of this group of 5 miRNAs in ALS spinal cords and the downregulatory function they showed on *NEFM* and *NEFH*, we should expect an increase of *NEFM* and *NEFH* transcript and protein levels in ALS spinal cord tissue compared to controls. Consistent with this, we observed an increase in both *NEFM* and *NEFH* transcript and protein levels in ALS ventral lumbar spinal cords (**Fig. 3.6**).

### 3.5 Discussion

In this study, we have shown that a small group of miRNAs that are dysregulated in the spinal cord of ALS patients directly regulate *NEFM* and *NEFH* mRNA stability and that this is associated with an increase in NFM and NFH protein levels in ALS spinal cord homogenates compared to neurological intact control spinal cord homogenates.

The post-transcriptional control of NF transcripts is critical for establishing, consolidating and maintaining normal levels of NF proteins. The stoichiometry of NF subunits has to be tightly controlled to promote axonal outgrowth, control axon caliber and avoid the formation of NF aggregates, axonal degeneration and neuronal death (Julien, 1999; Thyagarajan et al., 2007). The regulation of NF transcripts expression occurs at multiple levels. It has been reported that splicing of the last intron of *Xenopus NEFM* increases nucleocytoplasmic export of the transcript which allows for robust gene expression (Wang and Szaro, 2016). Another level of regulation is at the mRNA transport. One study observed that the mRNAs of each NF subunit are present and translated within intact and regenerating rat sciatic nerve, demonstrating that NF transcripts are transported through axons (Sotelo-Silveira et al., 2000). At the final stage of mRNA regulation, it has been shown that the RNA-binding protein HuB increases the translation of *NEFM* transcript (Antic et al., 1999).

**A**

```
3' uguccggcccuguuCACGUUAu 5'        hsa-miR-92a-3p
                | | | | | | |
5' uuguauuuuacuuuGUGCAAUa 3'        NEFM 3'UTR


3' aguguucaaucccaGAGUCCCu 5'        hsa-miR-125b-5p
                | | | | | | |
5' ggacugcaugcaagCUCAGGGu 3'        NEFM 3'UTR
```

```
3' aguaUGUCGAUC-UAUUGGUUUCu 5'      hsa-miR-9-5p
       | | |  | :|  |  |  |:| | | | | |
5' aggaACAUCCGGAACAGCCAAAGa 3'      NEFH 3'UTR


3' gaugGACGUGAUAC--U----CGUGAAAc 5' hsa-miR-20b-5p
       | | |  |:| | | |    |   | | | | | | |
5' gccaCUGAAUUAUGCCAGGGCGCACUUUc 3' NEFH 3'UTR


3' uguccggcccuguuCACGUUAu 5'        hsa-miR-92a-3p
                | | | | | | |
5' uuucaauugcuucuGUGCAAUa 3'        NEFH 3'UTR


3' accccAUAAACUGUUUGACUGu 5'        hsa-miR-223-3p
        | | |  | |   |  | | | | | |
5' gccucUAUGUG-C-AACUGACa 3'        NEFH 3'UTR


3' gugagauuucCCUCCGUGAAAc 5'        hsa-miR-519d-3p
            | |:  | | | | | | |
5' aauuaugccaGGGCGCACUUUc 3'        NEFH 3'UTR
```

**B**
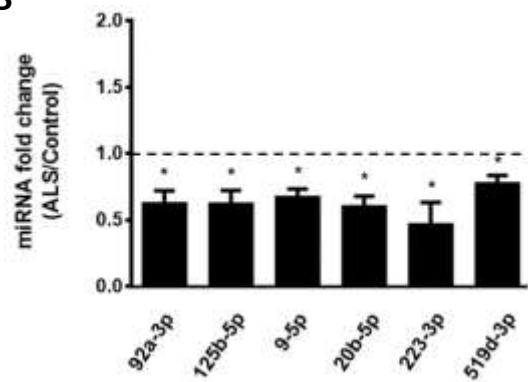
**Figure 3.2**. **MiRNAs that have MREs in *NEFM* or *NEFH* 3'UTRs are downregulated in the spinal cord of ALS patients.** (A) MREs within *NEFM* and *NEFH* 3'UTRs of ALS-linked miRNAs. (B) Real-time PCR using SYBR green. Validation of differential expression in ALS versus control spinal cords of 6 miRNAs that have MREs in *NEFM* or *NEFH* mRNA 3'UTRs is shown. Experiments were performed in triplicate. Values below 1 indicate downregulation. Results are shown as mean (n=3) ± SEM (Student *t*-test: **** $p < 0.0001$, *** $p < 0.001$, ** $p < 0.01$, * $p < 0.05$. MiR-9-5p, p = 0.0229; miR-20b-5p, p = 0.0230; miR-92a-3p, p = 0.0234; miR-125b-5p, p = 0.0412; miR-223-3p, p = 0.0215 and miR-519d-3p, p = 0.0232).
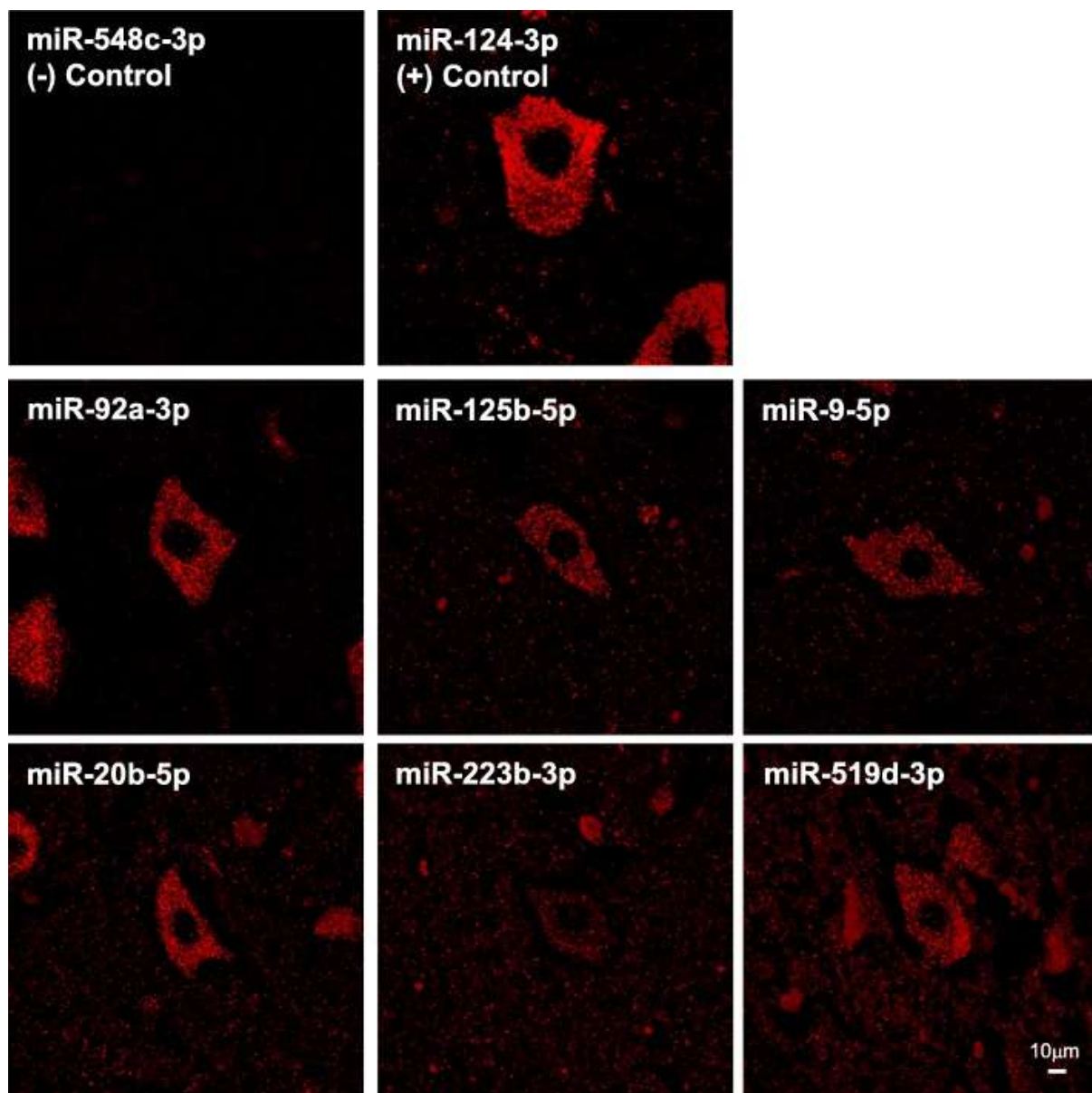
**Figure 3.3. MiRNAs that have MREs within *NEFM* or *NEFH* 3'UTRs are expressed in motor neurons of human spinal cord control tissue.** FISH was performed using FFPE control spinal cord tissue and LNA$^{TM}$-enhanced detection probes 5`-DIG and 3`-DIG labeled for miRNAs. Amplification was performed using anti-DIG-HRP and TSA Plus Cy3. MiR-548c-3p, which is not expressed in human spinal cord, was used as negative control. MiR-124-3p, which is known as highly expressed in neurons, was used as positive control.
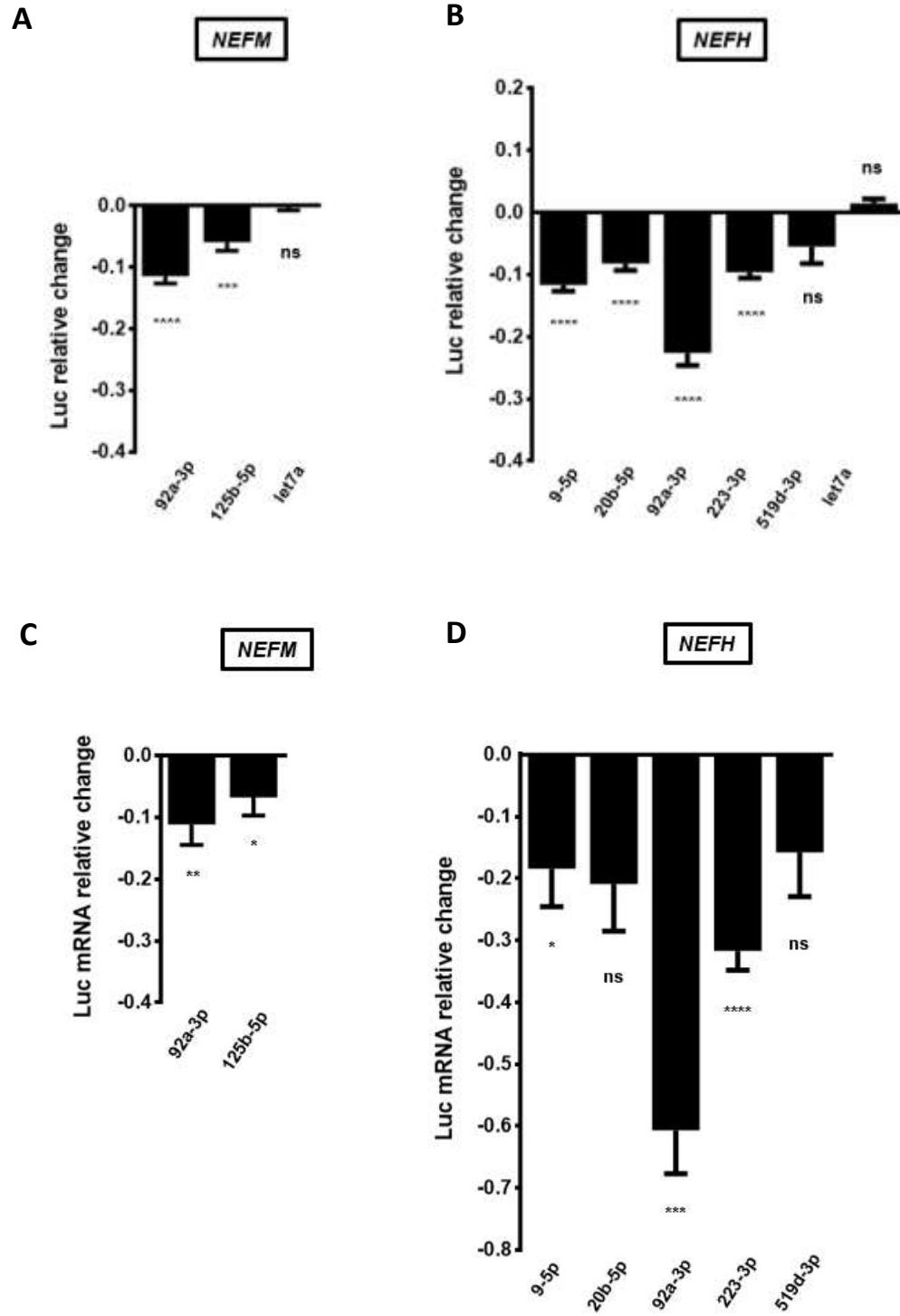
**Figure 3.4. A group of ALS-linked miRNAs regulate a luciferase reporter linked to**

*NEFM* **or** *NEFH* **3'UTRs.** HEK293T cells were co-transfected with a reporter plasmid

containing *NEFM* or *NEFH* 3'UTRs and miRNA mimics. (A, B) Reporter gene assays were

performed 24 hours after transfection. Data are expressed as relative change and plotted in

logarithmic scale. (C, D) Relative quantitative RT-PCRs were performed after RNA

extraction, 24 hours post-transfection. Data are expressed as relative mRNA level change and

plotted in logarithmic scale. All experiments were performed in triplicate. Results are shown

as mean (n=3) $\pm$ SEM (Student *t*-test: **** $p < 0.0001$, *** $p < 0.001$, ** $p < 0.01$, * $p <$

0.05, relative to the pmirGLO vector control). Reporter gene assays: miR-92a-3p/*NEFM*, $p <$

0.0001; miR-125b-5p/*NEFM*, $p = 0.0005$; miR-let-7a/*NEFM*, $p = 0.6015$; miR-9-5p/*NEFH*,

miR-20b-5p/*NEFH*, miR-92a-3p/*NEFH* and miR-223-3p/*NEFH*, $p < 0.0001$; miR-519d-

3p/*NEFH*, $p = 0.0723$; miR-let-7a/*NEFH*, $p = 0.0893$. RT-PCRs:  miR-92a-3p/*NEFM*, $p =$

0.0052; miR-125b-5p/*NEFM*, $p = 0.0429$; miR-9-5p/*NEFH*, $p = 0.0431$; miR-20b-5p/*NEFH*,

$p = 0.0518$; miR-92a-3p/*NEFH*, $p = 0.0003$; miR-223-3p/*NEFH*, $p < 0.001$; miR-519d-

3p/*NEFH*, $p = 0.0903$).
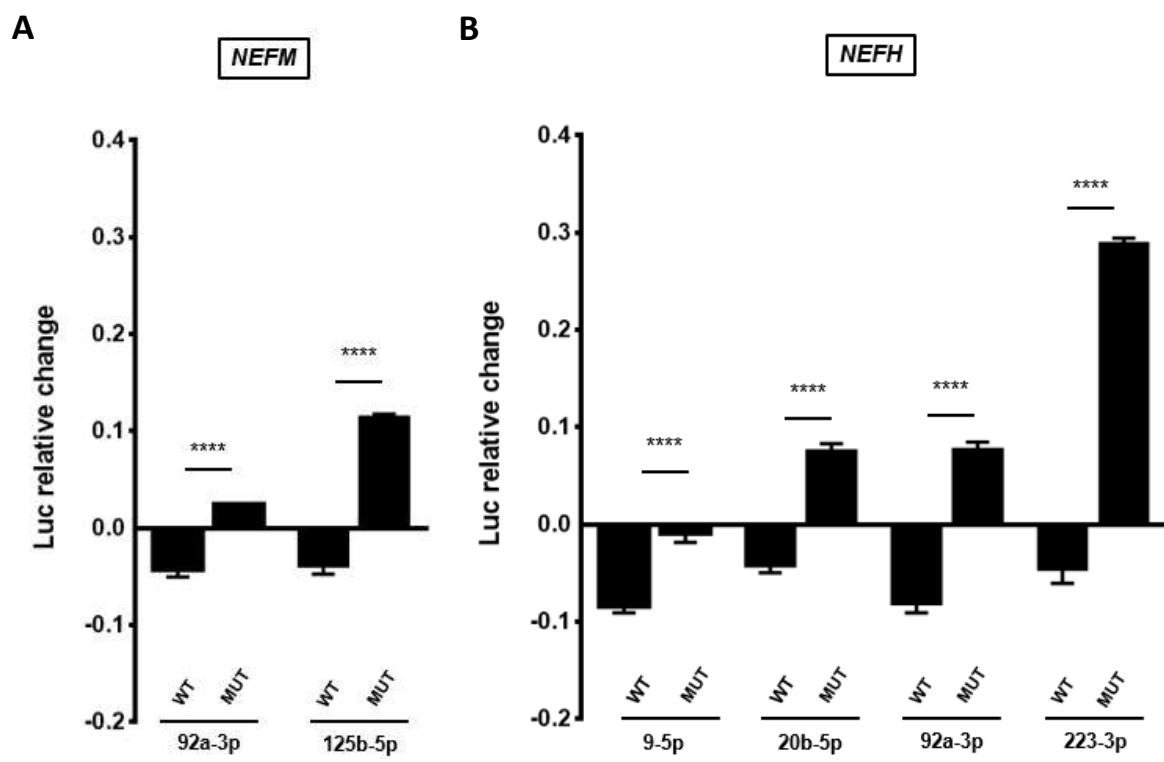
**Figure 3.5. MiRNAs directly regulate luciferase transcripts linked to *NEFM* or *NEFH* 3'UTRs.** HEK293T cells were co-transfected with a reporter plasmid containing mutant *NEFM* (A) or *NEFH* (B) 3'UTRs and miRNA mimics. Reporter gene assays were performed 24h after transfection. Data are expressed as relative change and plotted in logarithmic scale. All experiments were performed in triplicate. Result are shown as mean (n=3) ± SEM (One-way ANOVA followed by Tukey's post hoc test: **** $p < 0.0001$, *** $p < 0.001$, ** $p < 0.01$, * $p < 0.05$, relative to the pmirGLO vector control). MiR-92a-3p/NEFM, miR-125b-5p/NEFM, miR-9-5p/NEFH, miR-20b-5p/NEFH, miR-92a-3p/NEFH and miR-223-3p/NEFH, $p < 0.0001$).

**A**



**C**



**B**
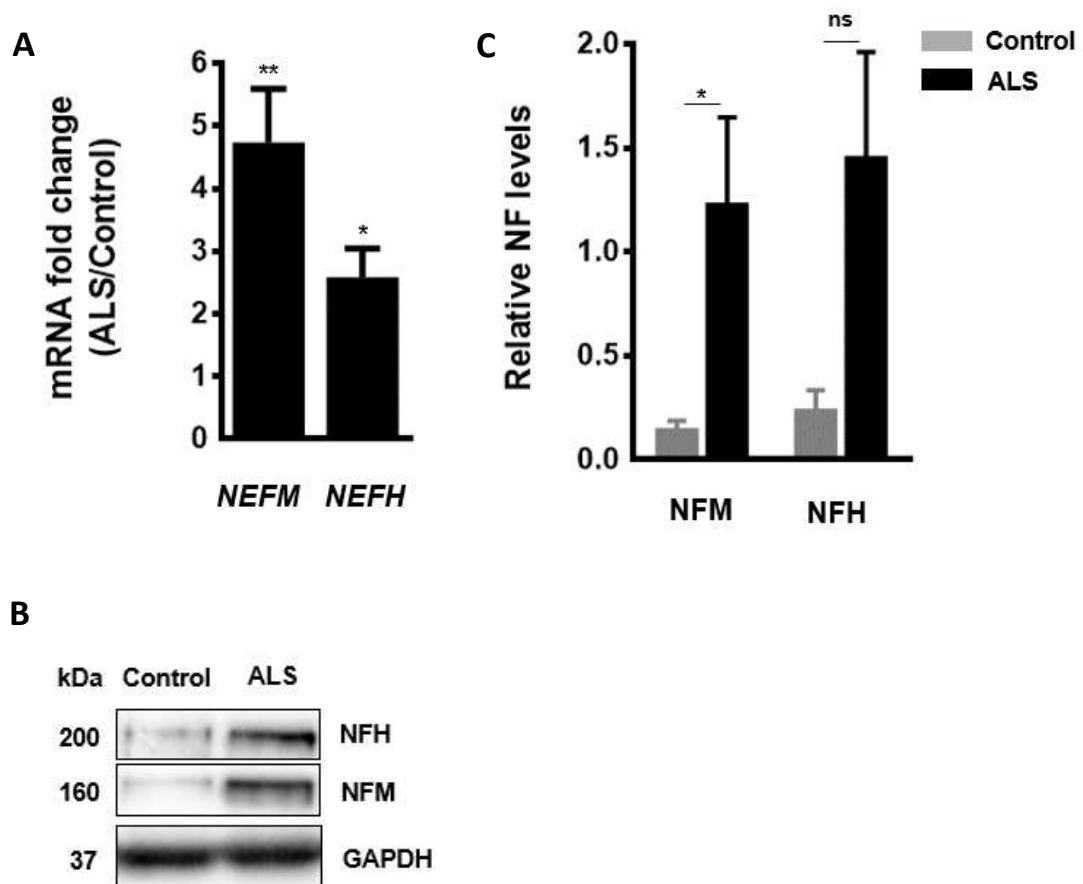
**Figure 3.6.** *NEFM* **and** *NEFH* **transcript and protein levels are increased in spinal cord**

**of ALS patients.** (A) Real-time PCR using TaqMan and (B) Western blots were performed

using ventral lumbar spinal cord samples of 5 controls and 7 ALS patients. (C) Quantification

by densitometry of Western blots in A. Protein levels were normalized to GAPDH. Data was

expressed as the mean ± SEM (Student *t*-test: **** $p < 0.0001$, *** $p < 0.001$, ** $p < 0.01$, *

$p < 0.05$. Real-time PCR: *NEFM*, $p = 0.0027$: *NEFH*, $p = 0.0239$. Western blot: NFM, $p =$

0.0238; NFH, $p = 0.4762$).

mRNA stability is the regulatory process of NF transcripts most extensively studied in which multiple *trans*-acting factors participate. In mice, it has been shown that the RNA-binding protein p190RhoGEF stabilizes and that glycolytic isoenzymes aldolases A and C directly destabilize *Nefl* mRNA (Canete-Soler et al., 2005; Canete-Soler et al., 2001). Our previous studies have shown that the stability of *NEFL* is regulated by ALS-associated RNA-binding proteins. Mutant copper/zinc superoxide dismutase (mtSOD1) and Rho Guanine Nucleotide Exchange Factor (RGNEF; the human homologue of p190RhoGEF) mediate the destabilization and TAR DNA binding protein 43 kDa (TDP-43) the stabilization of *NEFL* mRNA (Droppelmann et al., 2013; Ge et al., 2005; Strong et al., 2007). In addition, fused in sarcoma/translocated in liposarcoma (FUS/TLS), another ALS-associated protein, has been shown to bind to murine *Nefl*, *Nefm* and *Nefh* transcripts (Lagier-Tourenne et al., 2012).

The most prominent mechanism of RNA mediated gene silencing involves the interaction of miRNAs with their target mRNAs in which most, but not all, interactions between the miRNA and MREs leads to a degradation of the mRNA. Previously, we and others have observed a massive downregulation of miRNAs in ALS spinal cord (Campos-Melo et al., 2014; Emde et al., 2015; Figueroa-Romero et al., 2016). We also showed that three miRNAs that are dysregulated in ALS, miR-146a*, miR-524-5p and miR-582-3p, regulate levels of *NEFL* mRNA (Campos-Melo et al., 2013). In this paper, we extended our study to miRNAs responsible for *NEFM* and *NEFH* post-transcriptional regulation. We created a list of miRNAs that are downregulated in ALS spinal cord and that also possess MREs within *NEFM* and *NEFH* 3'UTRs. From the published literature, we observed that two miRNAs of this group (miR-9 and miR-125b-5p) were confirmed to be reduced in ALS spinal cord (Emde et al., 2015; Figueroa-Romero et al., 2016). We established that a small group of ALS-linked miRNAs (miR-9-5p, miR-20b-5p, miR-92a-3p, miR-125b-5p and miR-223-3p) directly downregulate human *NEFM* and *NEFH* mRNA levels, an effect that is

translated into a reduction of NFM and NFH protein levels within spinal cord homogenates. From this group of miRNAs that regulate *NEFM* and *NEFH* mRNA levels, only miR-9 has been reported to have a role in neuronal function. More specifically, by regulating several targets including *OC1, FoxP1, MAP1B,* and *MCPIP1,* miR-9 is critical for motor neuron development, function and survival (Hawley et al., 2017).

As these group of miRNAs that regulate *NEFM* and *NEFH* are reduced in spinal cord of ALS tissue, we predicted that the net effect would be an increase of NFM and NFH protein levels in ALS-spinal cords. Several groups have shown that NFL, NFM and/or p-NFH levels are increased in biological fluids of ALS patients (Feneberg et al., 2018; Ganesalingam et al., 2013; Haggmark et al., 2014; Rosengren et al., 1996; Xu et al., 2016), but there are no reports of NFs protein levels in spinal cord tissue. In this study we showed that both NFM and NFH levels are increased in ventral lumbar spinal cord of ALS patients compared to controls. This observation is in agreement with the increased in *NEFM* and *NEFH* transcripts in ALS ventral lumbar spinal cord homogenates that we observed here using real-time PCR and reported previously using RNase protection assay (Strong et al., 2004).

A selective reduction of *NEFL* steady-state mRNA levels in spinal motor neurons of ALS patients has been well documented (Bergeron et al., 1994; Menzies et al., 2002; Wong et al., 2000) a finding that we have proposed is due to alterations in the expression of *NEFL*-linked miRNAs (Campos-Melo et al., 2013). In concert with the observations of this study, we hypothesize that in ALS spinal cords the sustained dysregulation in time of the expression of groups of miRNAs that control NF levels fundamentally alters the expression of all three NF transcripts in a manner that induces an alteration in the stoichiometry of the individual NF proteins, favoring the formation of pathological NCIs.

While this hypothesis supports the critical role of the alteration of miRNA expression in ALS, miRNAs alone are not the sole mediators of RNA stability. Indeed, understanding

the fundamental relationship between alterations in RNA-binding proteins and how this interacts with alterations in miRNAs expression will be critical to understanding the process of perturbed RNA-mediated gene silencing which appears to lie at the core of a majority of ALS cases.

## 3.6 References

Ananthakrishnan, L., Gervasi, C., and Szaro, B.G. (2008). Dynamic regulation of middle neurofilament RNA pools during optic nerve regeneration. Neuroscience *153*, 144-153.

Ananthakrishnan, L., and Szaro, B.G. (2009). Transcriptional and translational dynamics of light neurofilament subunit RNAs during Xenopus laevis optic nerve regeneration. Brain Res *1250*, 27-40.

Antic, D., Lu, N., and Keene, J.D. (1999). ELAV tumor antigen, Hel-N1, increases translation of neurofilament M mRNA and induces formation of neurites in human teratocarcinoma cells. Genes Dev *13*, 449-461.

Bergeron, C., Beric-Maskarel, K., Muntasser, S., Weyer, L., Somerville, M.J., and Percy, M.E. (1994). Neurofilament light and polyadenylated mRNA levels are decreased in amyotrophic lateral sclerosis motor neurons. J Neuropathol Exp Neurol *53*, 221-230.

Campos-Melo, D., Droppelmann, C.A., He, Z., Volkening, K., and Strong, M.J. (2013). Altered microRNA expression profile in Amyotrophic Lateral Sclerosis: a role in the regulation of NFL mRNA levels. Mol Brain *6*, 26.

Campos-Melo, D., Droppelmann, C.A., Volkening, K., and Strong, M.J. (2014). Comprehensive luciferase-based reporter gene assay reveals previously masked up-regulatory effects of miRNAs. Int J Mol Sci *15*, 15592-15602.

Canete-Soler, R., Reddy, K.S., Tolan, D.R., and Zhai, J. (2005). Aldolases a and C are ribonucleolytic components of a neuronal complex that regulates the stability of the light-neurofilament mRNA. J Neurosci *25*, 4353-4364.

Canete-Soler, R., Wu, J., Zhai, J., Shamim, M., and Schlaepfer, W.W. (2001). p190RhoGEF Binds to a destabilizing element in the 3' untranslated region of light neurofilament subunit mRNA and alters the stability of the transcript. J Biol Chem *276*, 32046-32050.

Droppelmann, C.A., Keller, B.A., Campos-Melo, D., Volkening, K., and Strong, M.J. (2013). Rho guanine nucleotide exchange factor is an NFL mRNA destabilizing factor that forms cytoplasmic inclusions in amyotrophic lateral sclerosis. Neurobiol Aging *34*, 248-262.

Emde, A., Eitan, C., Liou, L.L., Libby, R.T., Rivkin, N., Magen, I., Reichenstein, I., Oppenheim, H., Eilam, R., Silvestroni, A.*, et al.* (2015). Dysregulated miRNA biogenesis downstream of cellular stress and ALS-causing mutations: a new mechanism for ALS. EMBO J *34*, 2633-2651.

Feneberg, E., Oeckl, P., Steinacker, P., Verde, F., Barro, C., Van Damme, P., Gray, E., Grosskreutz, J., Jardel, C., Kuhle, J.*, et al.* (2018). Multicenter evaluation of neurofilaments in early symptom onset amyotrophic lateral sclerosis. Neurology *90*, e22-e30.

Figueroa-Romero, C., Hur, J., Lunn, J.S., Paez-Colasante, X., Bender, D.E., Yung, R., Sakowski, S.A., and Feldman, E.L. (2016). Expression of microRNAs in human post-mortem amyotrophic lateral sclerosis spinal cords provides insight into disease mechanisms. Mol Cell Neurosci *71*, 34-45.

Ganesalingam, J., An, J., Bowser, R., Andersen, P.M., and Shaw, C.E. (2013). pNfH is a promising biomarker for ALS. Amyotroph Lateral Scler Frontotemporal Degener *14*, 146-149.

Ge, W.W., Wen, W., Strong, W., Leystra-Lantz, C., and Strong, M.J. (2005). Mutant copper-zinc superoxide dismutase binds to and destabilizes human low molecular weight neurofilament mRNA. J Biol Chem *280*, 118-124.

Haggmark, A., Mikus, M., Mohsenchian, A., Hong, M.G., Forsstrom, B., Gajewska, B., Baranczyk-Kuzma, A., Uhlen, M., Schwenk, J.M., Kuzma-Kozakiewicz, M.*, et al.* (2014). Plasma profiling reveals three proteins associated to amyotrophic lateral sclerosis. Ann Clin Transl Neurol *1*, 544-553.

Hawley, Z.C.E., Campos-Melo, D., Droppelmann, C.A., and Strong, M.J. (2017). MotomiRs: miRNAs in Motor Neuron Function and Disease. Front Mol Neurosci *10*, 127.

Julien, J.P. (1999). Neurofilament functions in health and disease. Curr Opin Neurobiol *9*, 554-560.

Lagier-Tourenne, C., Polymenidou, M., Hutt, K.R., Vu, A.Q., Baughn, M., Huelga, S.C., Clutario, K.M., Ling, S.C., Liang, T.Y., Mazur, C.*, et al.* (2012). Divergent roles of ALS-linked proteins FUS/TLS and TDP-43 intersect in processing long pre-mRNAs. Nat Neurosci *15*, 1488-1497.

Leermakers, F.A., and Zhulina, E.B. (2010). How the projection domains of NF-L and alpha-internexin determine the conformations of NF-M and NF-H in neurofilaments. Eur Biophys J *39*, 1323-1334.

Menzies, F.M., Grierson, A.J., Cookson, M.R., Heath, P.R., Tomkins, J., Figlewicz, D.A., Ince, P.G., and Shaw, P.J. (2002). Selective loss of neurofilament expression in Cu/Zn superoxide dismutase (SOD1) linked amyotrophic lateral sclerosis. J Neurochem *82*, 1118-1128.

Rosengren, L.E., Karlsson, J.E., Karlsson, J.O., Persson, L.I., and Wikkelso, C. (1996). Patients with amyotrophic lateral sclerosis and other neurodegenerative diseases have increased levels of neurofilament protein in CSF. J Neurochem *67*, 2013-2018.

Sanelli, T.R., Sopper, M.M., and Strong, M.J. (2004). Sequestration of nNOS in neurofilamentous aggregate bearing neurons in vitro leads to enhanced NMDA-mediated calcium influx. Brain Res *1004*, 8-17.

Schwartz, M.L., Shneidman, P.S., Bruce, J., and Schlaepfer, W.W. (1994). Stabilization of neurofilament transcripts during postnatal development. Brain Res Mol Brain Res *27*, 215-220.

Scott, D., Smith, K.E., O'Brien, B.J., and Angelides, K.J. (1985). Characterization of mammalian neurofilament triplet proteins. Subunit stoichiometry and morphology of native and reconstituted filaments. J Biol Chem *260*, 10736-10747.

Sotelo-Silveira, J.R., Calliari, A., Kun, A., Benech, J.C., Sanguinetti, C., Chalar, C., and Sotelo, J.R. (2000). Neurofilament mRNAs are present and translated in the normal and severed sciatic nerve. J Neurosci Res *62*, 65-74.

Strong, M.J., Leystra-Lantz, C., and Ge, W.W. (2004). Intermediate filament steady-state mRNA levels in amyotrophic lateral sclerosis. Biochem Biophys Res Commun *316*, 317-322.

Strong, M.J., Volkening, K., Hammond, R., Yang, W., Strong, W., Leystra-Lantz, C., and Shoesmith, C. (2007). TDP43 is a human low molecular weight neurofilament (hNFL) mRNA-binding protein. Mol Cell Neurosci *35*, 320-327.

Szaro, B.G., and Strong, M.J. (2010). Post-transcriptional control of neurofilaments: New roles in development, regeneration and neurodegenerative disease. Trends Neurosci *33*, 27-37.

Thyagarajan, A., Strong, M.J., and Szaro, B.G. (2007). Post-transcriptional control of neurofilaments in development and disease. Exp Cell Res *313*, 2088-2097.

Wakabayashi, K., Mori, F., Kakita, A., Takahashi, H., Utsumi, J., and Sasaki, H. (2014). Analysis of microRNA from archived formalin-fixed paraffin-embedded specimens of amyotrophic lateral sclerosis. Acta Neuropathol Commun *2*, 173.

Walker, K.L., Yoo, H.K., Undamatla, J., and Szaro, B.G. (2001). Loss of neurofilaments alters axonal growth dynamics. J Neurosci *21*, 9655-9666.

Wang, C., and Szaro, B.G. (2016). Using Xenopus Embryos to Study Transcriptional and Posttranscriptional Gene Regulatory Mechanisms of Intermediate Filaments. Methods Enzymol *568*, 635-660.

Wong, N.K., He, B.P., and Strong, M.J. (2000). Characterization of neuronal intermediate filament protein expression in cervical spinal motor neurons in sporadic amyotrophic lateral sclerosis (ALS). J Neuropathol Exp Neurol *59*, 972-982.

Xiao, S., McLean, J., and Robertson, J. (2006). Neuronal intermediate filaments and ALS: a new look at an old question. Biochim Biophys Acta *1762*, 1001-1012.

Xu, Z., Henderson, R.D., David, M., and McCombe, P.A. (2016). Neurofilaments as Biomarkers for Amyotrophic Lateral Sclerosis: A Systematic Review and Meta-Analysis. PLoS One *11*, e0164625.

# Chapter 4

## Novel miR-b2122 regulates several ALS-related RNA-binding proteins

Zachary C. E. Hawley, Danae Campos-Melo, and Michael J. Strong

A version of this chapter was published in *Molecular Brain*

**4.1 Abstract**

Common pathological features of amyotrophic lateral sclerosis (ALS) include cytoplasmic aggregation of several RNA-binding proteins. Out of these RNA-binding proteins, TDP-43, FUS and RGNEF have been known to co-aggregate with one another within motor neurons of sporadic ALS (sALS) patients suggesting there may be a common regulatory network disrupted. MiRNAs have been a recent focus in ALS research, as they have been identified to be globally downregulated in the spinal cord of ALS patients. The objective of this study was to identify if there were miRNA(s) dysregulated in sALS that are responsible for regulating the TDP-43, FUS and RGNEF network. In this study, we identify miR-194 and miR-b2122 to be significantly downregulated in sALS patients, and were predicted to regulate *TARDBP*, *FUS* and *RGNEF* expression. Reporter gene assays and RT-qPCR revealed that miR-b2122 downregulates the reporter gene through direct interactions with either the *TARDBP*, *FUS*, or *RGNEF* 3'UTR, while miR-194 downregulates firefly expression when it contained either the *TARDBP* or *FUS* 3'UTR. Further, we showed that miR-b2122 regulates endogenous expression of all three of these genes in a neuron-derived cell line. Also, an ALS-associated mutation in the *FUS* 3'UTR ablates the ability of miR-b2122 to regulate a reporter gene linked to the *FUS* 3'UTR, and sALS samples which showed a downregulation in miR-b2122 also showed an increase in FUS protein expression. Overall, we have identified a novel miRNA that is downregulated in sALS that appears to be a central regulator of disease-related RNA-binding proteins, and thus, its dysregulation likely contributes to TDP-43, FUS and RGNEF pathogenesis in sALS.

**4.2 Introduction**

Amyotrophic lateral sclerosis (ALS) is a progressive motor neurodegenerative disease resulting in paralysis and death within 2-5 years after diagnosis (Taylor et al., 2016; Zarei et al., 2015). 5-10% of ALS cases are familial (fALS), while the remaining are sporadic (sALS) although ~10-12% of these latter cases also have a genetic basis (Al-Chalabi et al., 2017; Chen et al., 2013; Taylor et al., 2016). While our understanding of ALS pathogenesis has advanced significantly in recent years, this understanding, and in particular the relationship amongst the individual genetic defects and the associated formation of pathological intraneuronal inclusions which are a hallmark of the disease, remains in its early phases (Blokhuis et al., 2013; Keller et al., 2012; Xiao et al., 2006).

Defects in mRNA metabolism have been suggested to be a major driver in the genesis of pathological inclusions in ALS (Cestra et al., 2017; Droppelmann et al., 2014; Freibaum et al., 2010; Hideyama et al., 2012; Tsuiji et al., 2013). Further, it has been shown that miRNAs, essential regulators of mRNA expression and protein synthesis, are globally downregulated within the spinal cord tissue of sALS patients (Campos-Melo et al., 2013; Figueroa-Romero et al., 2016). This downregulation of miRNA expression has been shown to be motor neuron specific (Emde et al., 2015), contributing to the concept that altered miRNA homeostasis is a major contributor to the pathogenesis of ALS (Hawley et al., 2017; Rinchetti et al., 2017). The finding of this global downregulation of miRNAs within sALS patients is intriguing, as TDP-43 and FUS, two proteins often found to be dysregulated in sALS, are known to be essential components of miRNA biogenesis (Kawahara and Mieda-Sato, 2012; Morlando et al., 2012). Further, ALS mutations within the FUS 3' untranslated region (UTR) have been shown to disrupt a negative feedback network between miR-141/200a and FUS, leading to an

accumulation of FUS within the cell (Dini Modigliani et al., 2014; Sabatelli et al., 2013). This suggests that there may be a disruption in the feedback networks between miRNAs and RNA-binding proteins in ALS, including TDP-43 and FUS.

Beyond TDP-43 and FUS, we have described RGNEF, another RNA-binding protein, that forms pathological aggregates within sALS spinal motor neurons and has mutations associated with ALS (Droppelmann et al., 2013a; Droppelmann et al., 2013b; Keller et al., 2012; Ma et al., 2014). Interestingly, we observed that TDP-43, FUS and RGNEF co-aggregate with each other within the motor neurons of sALS patients, suggesting a co-dysregulation of these three RNA-binding proteins (Keller et al., 2012). While miRNA biogenesis has been clearly shown to be affected in sALS, it is unclear the consequence of this mass downregulation, and how it may contribute to TDP-43, FUS and RGNEF pathogenesis.

In the current study, we describe two miRNAs, miR-194 and miR-b2122, that are predicted to regulate TDP-43, FUS and RGNEF. The novel miR-b2122 is expressed in human spinal motor neurons, significantly downregulated in sALS patients, and regulates the expression of all three of these RNA-binding proteins. Further, an ALS-associated mutation within the *FUS* 3'UTR located in the miRNA recognition element (MRE) of miR-b2122 disrupts its ability to suppress gene expression. Overall, our results suggest that the downregulation of miR-b2122 in sALS could result in altered levels of all three of these RNA-binding proteins, contributing to the pathological state of TDP-43, FUS and RGNEF observed within motor neurons of sALS patients.

## 4.3 Materials and Methods

### 4.3.1 Tissue samples

Spinal cord tissue was obtained from sALS patients and age-matched, neurologically intact individuals (**Table 4.1**). All ALS cases were both clinically and neuropathologically confirmed using the El Escorial Criteria (World Federation of Neurology Research Group on Neuromuscular Disease, 1994). All research was approved by "The University of Western Ontario Research Ethics Board for Health Sciences Research Involving Human Subjects (HSREB)". Written consent for autopsy was obtained from the next of kin at the time of death or from the patient antemortem in accordance with the London Health Sciences Centre consent for autopsy. Cases were genotyped and confirmed to have no known mutations in *SOD1*, *TARDBP*, *FUS*, *RGNEF* or expanded repeats in *C9orf72*.

**4.3.2 3' RACE**

Total RNA extraction was performed on SH-SY5Y cells and spinal cord tissue from neurologically intact humans using TRIzol reagent (Life Technologies Inc., Ambion, Carlsbad, CA, USA). This was followed by cDNA synthesis and PCR with the SMARTer 5'/3' RACE Kit (Takara Bio. Inc., Clontech, USA) to amplify the *TARDBP*, *FUS* and *RGNEF* 3'UTRs according to the manufactures instructions using the following forward primers: *TARDBP* 5'-TAG ACA GTG GGG TTG TGG TTG GTT GGT A-3', *FUS* 5'- GCA GGG AGA GGC CGT ATT AAT TAG CCT-3' and *RGNEF* 5'-GCC CCG AGG TAA TGG AAC TTA ATC G-3'. 3'UTRs were identified using a 1% agarose gel containing a SYBR Safe dye. 3'UTR bands were excised and extracted from the agarose gel, and then individually cloned into a pGEMT-easy vector according to manufactures instructions (Promega, Madison, WI, USA). All 3'UTRs were confirmed using Sanger sequencing.

**4.3.3 MiRNA selection**

**Table 4.1**. Patient demographics.

| Cases | Gender | Age of symptom onset | Symptom onset | Age of death | Cause of Death |
|---|---|---|---|---|---|
| Control | F | - | - | 62 | Heart Attack |
| | M | - | - | 74 | Stroke |
| | F | - | - | 68 | Unknown |
| | M | - | - | 68 | Brain Tumor |
| | M | - | - | 75 | Unknown |
| | F | - | - | 53 | Pneumonia |
| | F | - | - | 74 | Leukemia |
| | M | - | - | 67 | Unknown |
| ALS | F | 58 | Unknown | 60 | Unknown |
| | M | 69 | Upper/lower limbs | 72 | Unknown |
| | F | 40 | Bulbar | 41 | Systemic Failure |
| | M | 55 | Unknown | 61 | Pneumonia |
| | M | 64 | Upper/lower limbs | 67 | Respiratory Failure |
| | F | 69 | Respiratory Symptoms | 71 | Respiratory Failure |
| | M | 63 | Unknown | 64 | Unknown |
| | F | 47 | Bulbar | 49 | Respiratory Failure |

MiRNAs predicted to target *TARDBP*, *FUS* and *RGNEF* 3'UTRs were selected using miRanda software. Further, the sequence of the miRNA had to be perfectly complementary to the miRNA recognition element (MRE) from +2 to +7. Novel miRNAs currently not found with the miRanda program were manually checked to see if their seed sequence had an MRE within the 3'UTR of *TARDBP*, *FUS* and *RGNEF*. We only considered those miRNAs for which we identified MREs within the 3'UTR isoforms of *TARDBP*, *FUS* and *RGNEF* in the spinal cord tissue.

**4.3.4 Real-time PCR**

Total miRNA extractions were performed on ventral lumbar spinal cord tissue using the mirVana miRNA extraction kit according to manufactures instructions (Life Technologies Inc., Ambion, Carlsbad, CA, USA). Yield and purity of the miRNA extracts were measured using spectrophotometry (Nanodrop, ThermoFisher Scientific, Burlington, ON, Canada), while integrity was measured using Bioanalyzer (Aligent Technologies Canada Inc., Missasauga, ON, Canada) analysis. MiRNA extracts were reversed transcribed and then subjected to real-time PCR using miRCURY LNA$^{TM}$ Universal RT microRNA PCR (Exiqon, Woburn, MA, USA) and ExiLENT SYBR Green master mix (Exiqon, Woburn, MA, USA) kits, respectively, according to manufacturer's instructions. To detect novel miRNAs, miRNAs extracts went under reverse transcription using the Taqman microRNA reverse transcriptase kit (Life Technologies Inc., Applied Biosystems, Forest City, CA, USA), and then were pre-amplified using the Taqman PreAmp Master Mix Kit (Life Technologies Inc., Applied Biosystems, Forest City, CA, USA) followed by real-time PCR with the TaqMan Universal PCR Master Mix (x2) no AmpErase UNG (Life Technologies Inc., Applied Biosystems, Roche, Branchburg, NJ, USA). The 7900 HT Real Time PCR system was used to read PCR outputs. Relative expression of miRNAs was

normalized to an internal control (miR-16-5p), followed by comparison of the relative expression of candidate miRNAs between ALS cases and a control population using the $2^{-\Delta\Delta CT}$ method. Negative values show downregulation and positive values upregulation of the expression. Statistical significance was determined using Student's t-test, and samples were considered significantly different if $p<0.05$.

### 4.3.5 Fluorescent *in situ* hybridization (FISH)

Neuropathologically normal human lumbar spinal cord tissue was formalin-fixed, paraffin-embedded and cut into 7µm sections. Samples were UV treated overnight prior to the experiment to reduce lipofuscin-induced autofluorescent signaling. FISH of miRNAs was performed as described before (de Planell-Saguer et al., 2010). Probes for miRNA detection were designed with double DIG labels (Exiqon, Woburn, MA, USA), and were targeted by a DIG-HRP secondary antibody (1:100; Roche, Indianapolis, IN, USA) and Tyramide Signal Amplification tagged with a Cy3 fluorophore (PerkinElmer, Waltham, MA, USA). Olympus FV1000 confocal microscope was used to observe miRNA expression within spinal motor neurons.

### 4.3.6 Cell culture and plasmid construction

HEK293T and SH-SY5Y cells were cultured in Dulbecco's Modified Eagle's Media (DMEM) containing 10% Fetal Bovine Serum (FBS). Cells were incubated at 37°C with 5% $CO_2$.

3'UTR isoforms of RNA-binding proteins identified in the human spinal cord tissue were individually cloned into the pmirGLO vector in between SalI and NheI restriction enzyme sites and downstream from the firefly luciferase gene (Promega, Madison, WI, USA). Site-directed

mutagenesis assays were done by adding a two-nucleotide mutation within the +2 and +3 positions of each miR-194 or miR-b2122 MRE using the Site-Directed Mutagenesis Kit II (Aligent Technologies Canada Inc., Missasauga, ON, Canada) according to the manufacturer's instructions. Mutations were carefully designed to ensure no changes to mRNA secondary structure using RNAfold WebServer (http://rna.tbi.univie.ac.at/cgi-bin/RNAfold.cgi).

### 4.3.7 Luciferase assay

HEK293T cells were seeded into 96 well plates (9,000 cells per well) 24 hours prior to transfection. Cells were co-transfected with 3.5 fmol of pmirGLO plasmid and 100 nM of miRNA mimics according to the Lipofectamine 2000 protocol (Life Technologies Inc., Invitrogen, Burlington, ON, Canada). Luciferase activity was measured 24 hours post-transfection using the Dual-GLO Luciferase Assay System (Promega, Madison, WI, USA). Firefly activity was normalized to renilla activity. Experimental design and normalization of data was performed as previously described (Campos-Melo et al., 2014). Data was quantified as relative difference from the control and expressed as mean ± SEM. Statistical significance was determined by performing Student's t-test, and was considered significantly different if $p<0.05$.

### 4.3.8 Relative quantitative RT-PCR

To determine the effects of miR-194 and miR-b2122 on the luciferase mRNA expression when it contained the 3'UTR of *TARDBP*, *FUS* or *RGNEF*, HEK293T cells were seeded into 24 well plates (20,000 cells per well) 48 hours prior to transfection. Cells were co-transfected with 20.6 fmol of pmirGLO plasmid and 100 nM of miRNA mimics according to the Lipofectamine 2000 protocol (Life Technologies Inc., Invitrogen, Burlington, ON, Canada). 24 hours after transfection, total RNA extraction was performed using TRIzol reagent (Life Technologies Inc.,

Ambion, Carlsbad, CA, USA) followed by first-strand cDNA synthesis (Life Technologies Inc., Invitrogen, Burlington, ON, Canada) and PCR amplification of firefly and renilla cDNA as previously described (Campos-Melo et al., 2013). Data was quantified as relative difference from the control and expressed as mean ± SEM. Statistical significance was determined by performing Student's t-test and was considered significantly different if $p < 0.05$.

To identify whether miR-194 and miR-b2122 could regulate the endogenous mRNA expression of these three RNA-binding proteins within a neuronal-derived cell line, SH-SY5Y cells were seeded into 6-well plates (500,000 cells per well) 24 hours prior to the transfection. 100 nM of miRNA mimics and anti-miRs were then either transfected individually or co-transfected. 24 hours after transfection total RNA extraction was performed using TRIzol reagent (Life Technologies Inc., Ambion, Carlsbad, CA, USA) followed by cDNA synthesis (Life Technologies Inc., Invitrogen, Burlington, ON, Canada). Quantitative PCR (qPCR) to determine the relative change in endogenous mRNA expression of *TARDBP*, *FUS* and *RGNEF* was performed using following primers: TARDBP *for*: 5'-CAG GGT GGG TTT GGT AAC GT-3' *rev*: 5'-AAA GCC CCC ATT AAA ACC AC-3'; FUS *for*: 5'-TCG GGA CCA AGG ATC ACG TC-3' *rev*: 5'-ATC TGG TTT AGG GGC CTT ACA CTG-3'; RGNEF *for*: 5'-AGG AAC GCA ATA ACT GGA TGA GAC G-3' *rev*: 5'-TTC CAC CTT CTC CCC TGC ATC AG-3'; 18S RNA *for*: 5'-AGT TGG TGG AGC GAT TTG TC-3' *rev*: 5'-TTC CTC GTT CAT GGG GAA TA-3'. All expression profiles were normalized to 18S RNA levels prior to comparison. One-way ANOVA followed by a Tukey's post-hoc was used to determine statistical differences in endogenous mRNA expression, and samples were significantly different if $p < 0.05$.

**4.3.9 Western blot analysis**

SH-SY5Y cells were seeded into 6-well plates (500,000 cells per well) 24 hours prior to the experiment. 100 nM of miRNA mimics and inhibitors were then either transfected individually or co-transfected. 48 hours after transfection total protein extraction was performed using NP40 lysis buffer containing proteinase inhibitors (cOmplete, Roche, Indianapolis, IN, USA), followed by sonication. Samples were suspended in loading buffer and proteins were denatured at 90°C for 5 minutes. Samples ran on a 12% SDS-gel and transferred to a nitrocellulose membrane. To measure endogenous levels of TDP-43, FUS and RGNEF, the membrane was probed with either anti-TDP-43 (1:2500; Proteintech, 10782-2-AP), anti-FUS (1:3000; Proteintech, 11570-1-AP), or anti-RGNEF (1:1000; Abcam, ab157095) rabbit antibodies, respectively. Blots were then probed with an HRP-secondary antibody (goat anti-rabbit; 1:5000; Life Technologies Inc., Invitrogen, Burlington, ON, Canada). Blots were stripped using stripping buffer (2% SDS, 62.5 mM Tris-HCl, 100 mM β-mercaptoethanol, pH 6.8) and re-probed for GAPDH using anti-GAPDH rabbit antibody (1:2500; Abcam, ab9485). Relative protein expression of TDP-43, FUS and RGNEF were normalized to GAPDH expression levels. One-way ANOVA followed by a Tukey's post-hoc was used to determine statistical differences in endogenous protein expression, and samples were significantly different if $p<0.05$.

## 4.4 Results

### 4.4.1 A small group of miRNAs contain MREs within the mRNA 3'UTR of *TARDBP*, *FUS,* and *RGNEF*.

Spinal cord tissue from neurologically intact individuals was used to determine the 3'UTR isoform(s) of *TARDBP*, *FUS* and *RGNEF* being expressed. *TARDBP* consistently showed one 3'UTR isoform across all human samples with a length of 1398bp (BC095435.1) (**Fig. 4.1A**) (Ayala et al., 2011). Subject two appeared to have a higher band, but we were unable

to confirm a longer 3'UTR through sequencing, and for that reason, we focused only on the

transcript that was consistently expressed across all samples.

*FUS* contained one 3'UTR isoform within three different control cases, which was 150bp

in length (**Fig. 4.1A**) (NM_004960). While *RGNEF* appeared to have three 3'UTR isoforms in

each control case, we were only able to confirm the top and bottom bands through sequencing.

The two *RGNEF* 3'UTR isoforms that were confirmed had a length of 177bp and 981bp, which

we termed *RGNEF*-short and *RGNEF*-long, respectively (**Fig. 4.1A**).  Both short and long

3'UTRs of *RGNEF* have been previously described (NM_001244364.1 and NM_0010804079.2,

respectively).

Subsequently, we identified 5 miRNAs which had MREs within the 3'UTR of all three of

these RNA-binding proteins. However, our previous work has indicated that miR-548d-3p was

not dysregulated in sALS cases, and thus was eliminated from further analysis. We also

previously observed that miR-194 is downregulated in sALS patients (Campos-Melo et al.,

2013), while miR-b2122, miR-sb659 and miR-548x have not been analyzed for dysregulation

within sALS patients (**Fig. 4.1B and C**). The latter four miRNAs were thus of interest for further

analysis.

### 4.4.2 MiR-194 and miR-b2122 are downregulated in the spinal cord tissue of sALS patients.

We characterized the relative expression of miR-194, miR-548x, miR-sb659 and miR-

b2122 within the spinal cord tissue of sALS patients compared to control subjects. Using real-

time PCR, we observed that miR-194 and miR-b2122 were significantly downregulated in sALS

patients (**Fig. 4.2**). The downregulation of miR-194 is consistent with what we reported

previously using TaqMan Array (Campos-Melo et al., 2013). Using FISH, we confirmed that

both miR-194 and miR-b2122 were strongly expressed within human spinal motor neurons of control samples with little to no non-motor neuronal expression, suggesting that the downregulation of these two miRNAs is likely motor neuron specific (**Fig. 4.3**).

**4.4.3 MiR-b2122 regulates a reporter linked to either *TARDBP*, *FUS*, or *RGNEF* 3'UTR.**

A reporter gene assay was used to examine the effect of miR-194 and miR-b2122 on the regulation of firefly luciferase protein when it contained the 3'UTR of either *TARDBP*, *FUS*, or *RGNEF* that we identified within the human spinal cord. MiR-b2122 significantly reduced firefly protein activity when it contained either the *TARDBP*, *FUS*, *RGNEF*-short, or *RGNEF*-long 3'UTR, whereas miR-194 downregulated firefly protein activity only when it contained either the *TARDBP* or *FUS* 3'UTR, and had no effect when it contained the *RGNEF*-long 3'UTR (**Fig. 4.4A**). MiR-194 did not contain an MRE within the *RGNEF*-short 3'UTR and thus the interaction between these two components was not examined. Further, to determine if miR-194 and miR-b2122 could also alter luciferase mRNA levels, we performed RT-PCR analysis. The results in the RT-PCR analysis matched the downregulation seen by these two mRNAs in the luciferase reporter gene assay, indicating that the effect of these miRNAs involves regulation of the levels of mRNA species (**Fig. 4.4B**).

To study if miR-194 and miR-b2122 were regulating firefly luciferase by directly interacting with the 3'UTR, we mutated two nucleotides within the MRE sites of miR-194 and miR-b2122. Mutating the miR-b2122 MRE sites within either the *TARDBP*, *FUS*, *RGNEF*-short, or *RGNEF*-long 3'UTR significantly abolished the ability of miR-b2122 to reduce firefly luciferase activity. Similarly, mutating the miR-194 MRE sites within either *TARDBP* or *FUS* ablated miR-194 downregulation of luciferase activity (**Fig. 4.5**). These findings indicate that

**A**

**B**

TARDBP    FUS

Down-regulated in ALS
miR-194

Previously Uncharacterized in ALS
miR-548x
miR-sb659
miR-b2122

Not shown to be dysregulated in ALS
miR-548d-3p

**C**
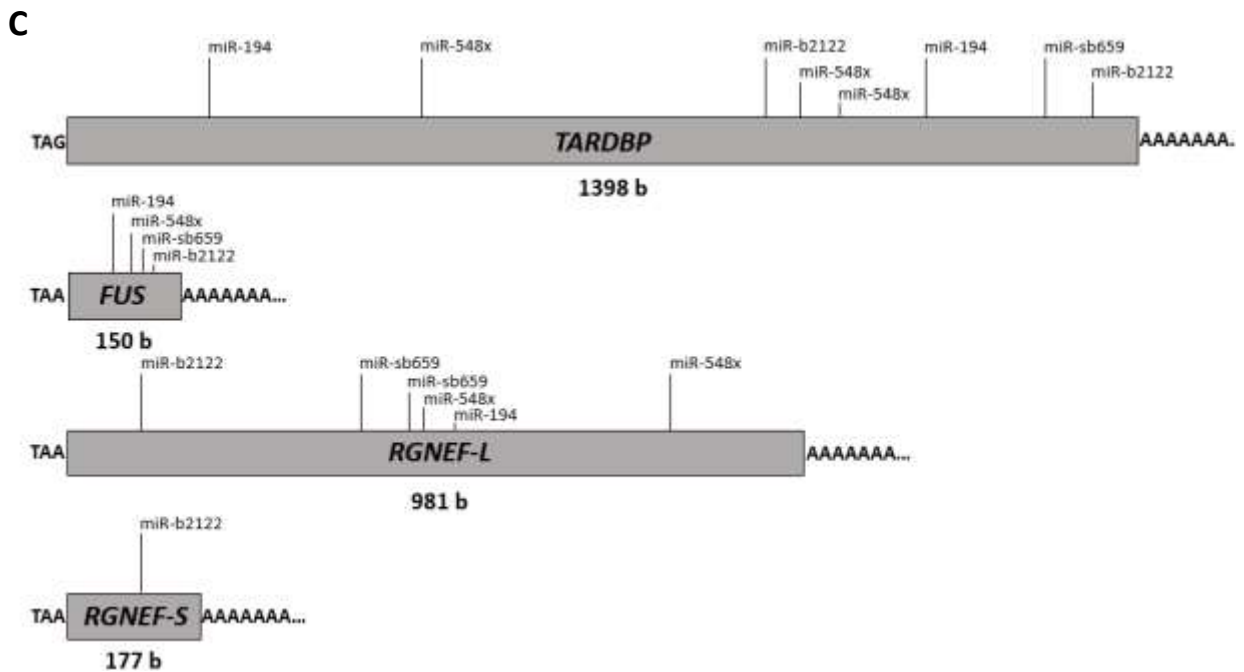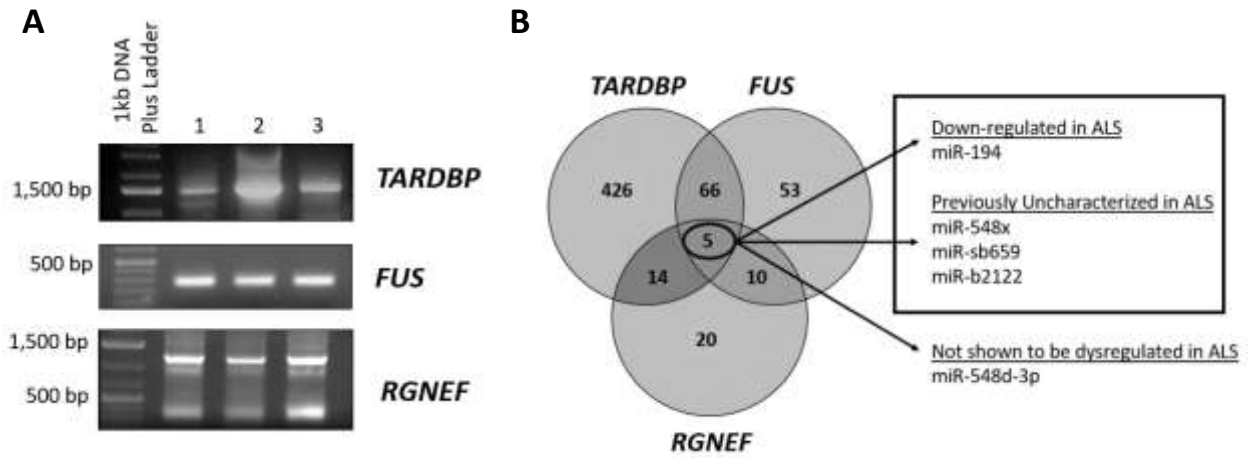
**Figure 4.1. A small group of miRNAs have MREs within the 3'UTRs of *TARDBP*, *FUS*, and *RGNEF*.** (A) 3'RACE PCR identified the 3'UTRs of *TARDBP, FUS* and *RGNEF* that are expressed in the human spinal cord tissue within three different control samples. One isoform of both *TARDBP* and *FUS* were identified with a length of 1,398 and 150 bases, respectively. Two isoforms of *RGNEF,* which we have termed *RGNEF*-short (*RGNEF*-S) and *RGNEF*-long (*RGNEF*-L) 3'UTRs, were identified in all three subjects running at 177 and 981 bases, respectively. Bands in figures appear higher than actual 3'UTR size, as primers were designed upstream from stop codon. (B) Five miRNAs were identified to have binding sites within the *TARDBP*, *FUS* and *RGNEF* mRNA 3'UTRs. MiR-548d-3p in previous work has shown to have no dysregulation in sALS, and thus, four miRNAs (outlined in the black box) went under further study. (C) Schematic of all *TARDBP*, *FUS* and *RGNEF* 3'UTRs identified within human spinal cord, and location of MREs for miRNA candidates.
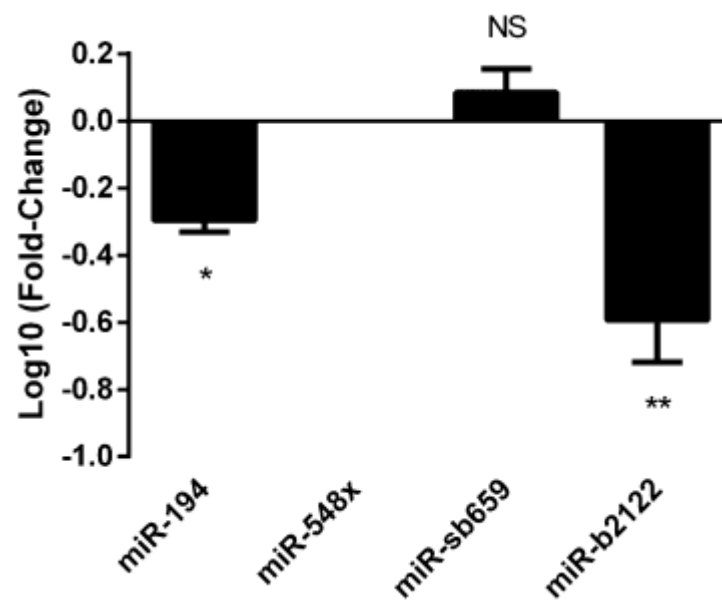
**Figure 4.2. Differential expression of candidate miRNAs within the spinal cord of sALS patients.** Candidate miRNA expression was examined in ventral spinal cord tissue of sALS patients (n=8) and control subjects (n=5). MiR-194 and miR-b2122 were significantly downregulated in sALS patients, while miR-sb659 showed no difference and miR-548x was not expressed in the spinal cord tissue. Data was expressed as log10 (fold-change) $\pm$ SEM, and significance was determined using Students t-test (**=p<0.01, *p<0.05, NS=p>0.05).

miR-b2122

miR-194

Positive Control (miR-124)

Negative Control (miR-548c)
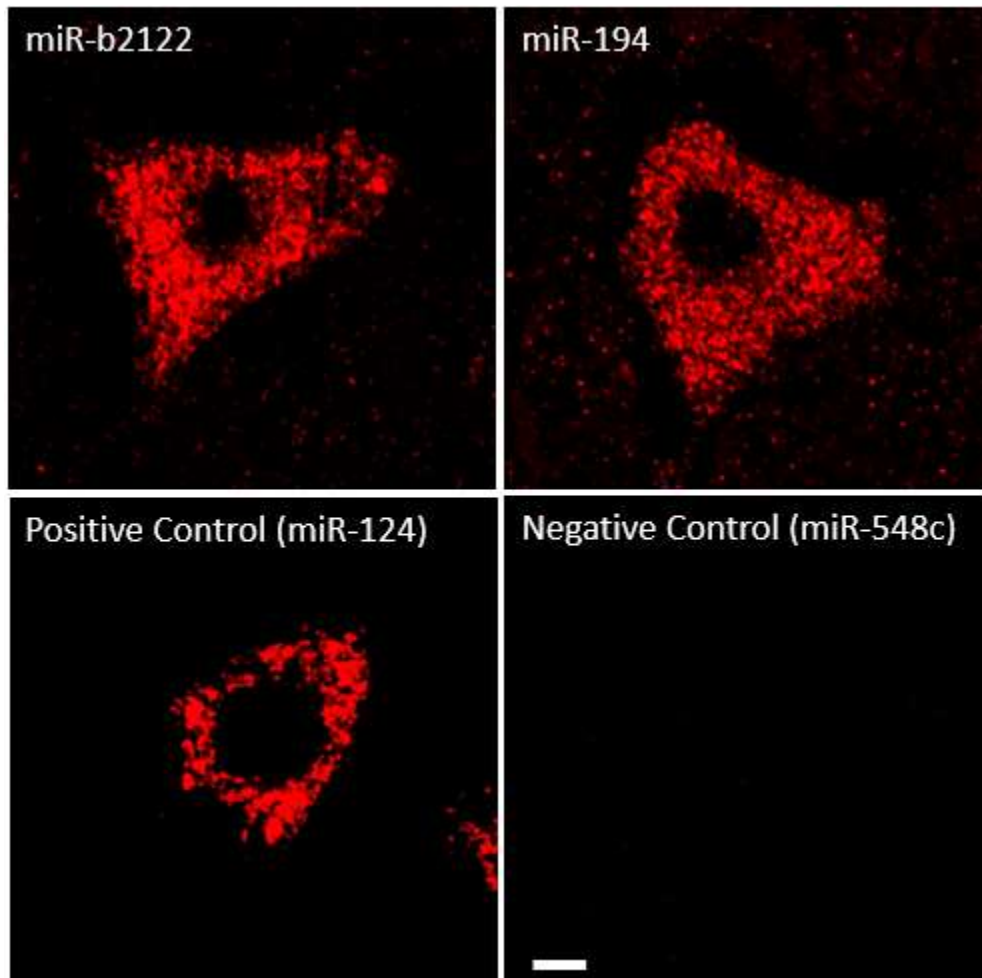
**Figure 4.3. MiR-194 and miR-b2122 are expressed in human spinal motor neurons.** Ventral

lumbar human spinal cord of control tissue (n=1) was analyzed using FISH to determine the

expression of miR-194 and miR-b2122 within motor neurons. Both miRNAs showed strong

positive staining within motor neurons. MiR-124 and miR-548c were used as positive and

negative controls, respectively. Scale bar represents 10µm.

**A**

TARDBP 3'UTR

FUS 3'UTR

RGNEF-short 3'UTR

RGNEF-long 3'UTR

**B**

TARDBP 3'UTR

FUS 3'UTR

RGNEF-short 3'UTR

RGNEF-long 3'UTR
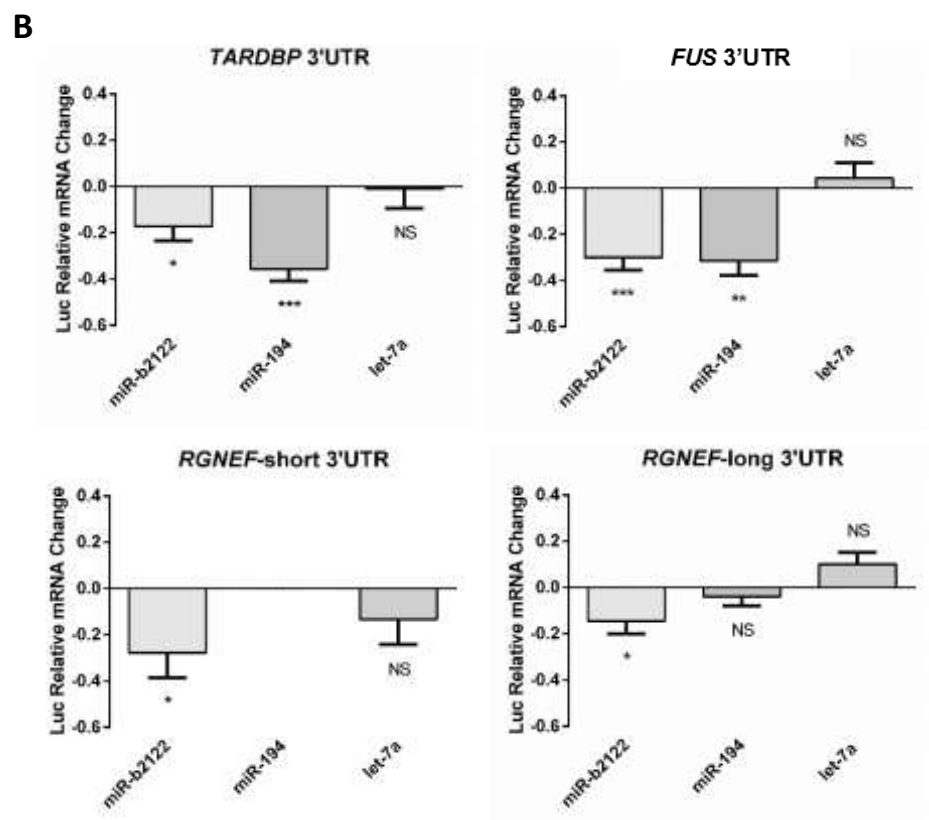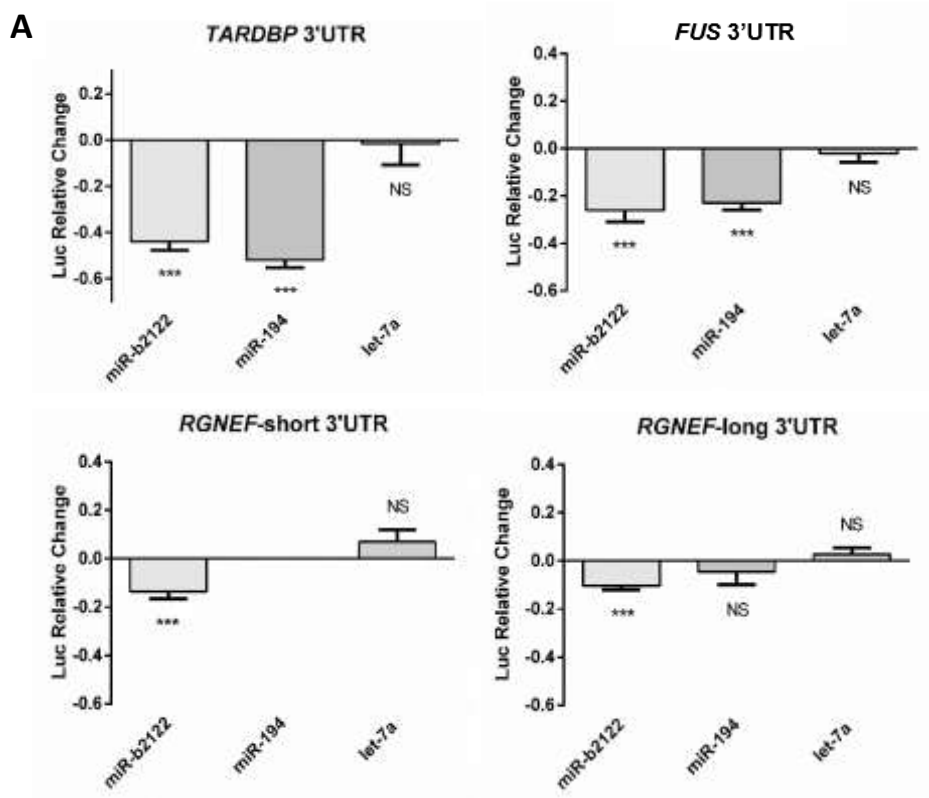
**Figure 4.4. MiR-b2122 reduces firefly luciferase activity when it contains either the**

***TARDBP*, *FUS* or *RGNEF* 3'UTR.** HEK293T cells were transfected with a pmirGLO plasmid

containing the 3'UTR of one of the RNA-binding proteins of interest either with or without miR-

194 or miR-b2122. PmirGLO plasmid without any 3'UTRs were also transfected with or without

miRNAs of interest to determine the miRNAs effect on the plasmid itself. (A) Reporter gene

assay revealed miR-b2122 reduced firefly activity when it contained either the *TARDBP*, *FUS*,

or *RGNEF*-short/long 3'UTR, whereas miR-194 downregulated firefly levels when it contained

either *TARDBP*, *FUS*, but not *RGNEF*-long. MiR-194 has no MRE in RGNEF-short, and thus,

the interaction between the two was not examined. (B) RT-qPCR results showed similar

suppression of mRNA levels as observed in the reporter gene assay. Let-7a was used as a

negative control for these experiments. Firefly was normalized to renilla luciferase, and then

further normalized to account for the effect of each miRNA on the pmirGLO vector to determine

the exact effect that each miRNA has on each 3'UTR. Each miRNA was compared to its own

individual control based on the normalization of the data. Data is expressed as sample mean

(n=3) $\pm$ SEM, and significance was determined using a Student's t-test (\*\*\*=$p<0.001$,

\*\*=$p<0.01$, \*=$p<0.05$, NS=$p>0.05$).
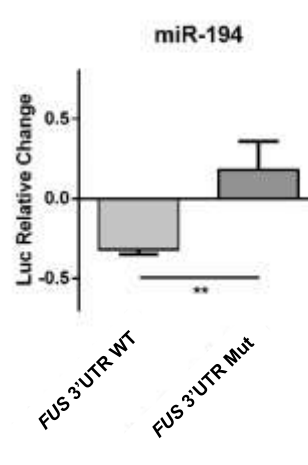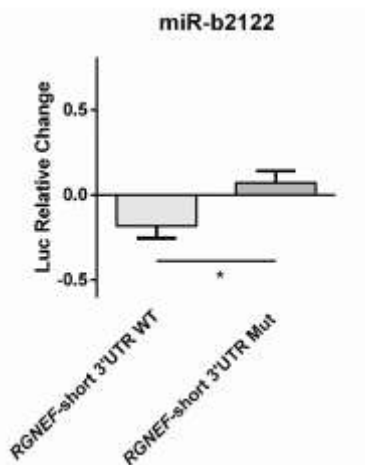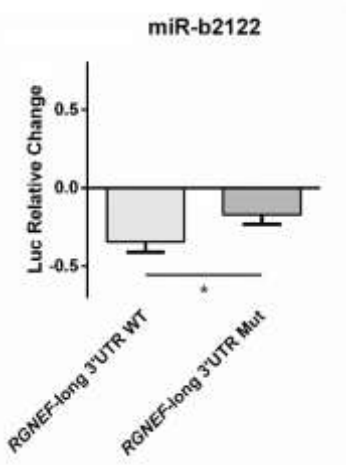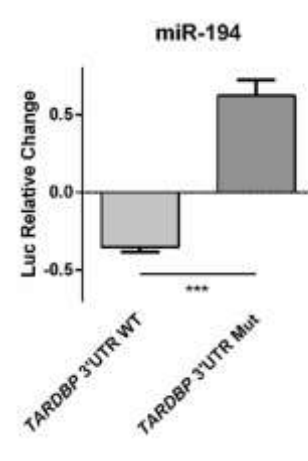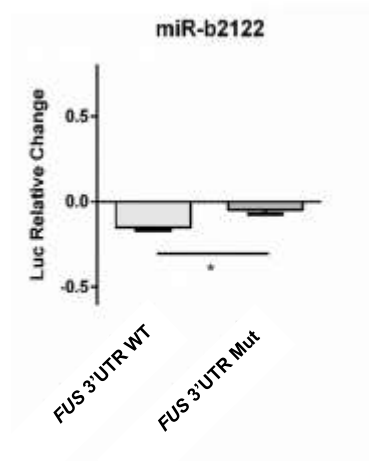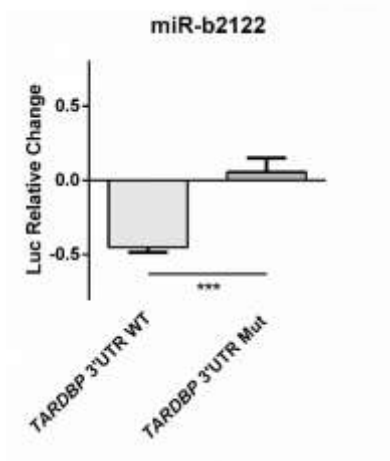
**Figure 4.5. MiR-b2122 and miR-194 directly interact with their 3'UTR targets.** HEK293T

cells were co-transfected with either the pmirGLO plasmid containing the wild-type 3'UTR, or

the 3'UTR mutant, and either with or without the miRNA of interest. Mutations within the MRE

of miR-b2122 in the *TARDBP*, *FUS*, and *RGNEF* 3'UTRs, and the MRE of miR-194 in the

*TARDBP* and *FUS* 3'UTRs abolished each miRNAs ability to reduce firefly activity. Firefly was

normalized to renilla, and then further normalized to the effect of each miRNA on the pmirGLO

vector to determine the miRNAs exact effect on the 3'UTR. Data is expressed as sample mean

(n=3) ± SEM, and significance was determined using a student's t-test (\*\*\*=p<0.001,

\*\*=p<0.01, \*=p<0.05).

both miR-194 and miR-b2122 directly interact with their 3'UTR targets to regulate gene expression.

### 4.4.4 MiR-b2122 regulates endogenous TDP-43, FUS and RGNEF within a human neuronal cell line.

Next, we decided to determine if miR-b2122 and miR-194 regulate the endogenous mRNA expression of *TARDBP, FUS* and *RGNEF* within a human neuronal-derived cell line – SH-SY5Y cells. SH-SY5Y cells express the *TARDBP*, *FUS* and *RGNEF* 3'UTR isoforms we identified with in the spinal cord. SH-SY5Y cells showed multiple bands in the *TARDBP* lane, but we were not able to confirm the top two bands through sequencing, only the 1398 b 3'UTR isoform identified in spinal cord, which also appears to be dominantly expressed in SH-SY5Y cells (**Fig. 4.6A**). Also, endogenous expression of miR-b2122 and miR-194 in SH-SY5Y cells was confirmed through real-time PCR (**Fig. 4.6B**).

Transfection of miR-b2122 lead to a significant downregulation in *TARBDP*, *FUS* and *RGNEF* mRNA levels. Further, co-transfection of miR-b2122 with its anti-miR abrogates the downregulation of these transcripts via miR-b2122. Transfection of the anti-miR of miR-b2122 alone lead to an upregulation in mRNA levels of all three genes (**Fig. 4.7A**). The upregulation observed with the addition of the anti-miR, suggests that miR-b2122 does regulate these RNA-binding proteins endogenously within this neuronal cell line. Let-7a was used as negative control, as we showed it has no effect on the endogenous mRNA levels of these three genes (**Fig. 4.8**).

Further, we also transfected miR-194 and/or its anti-miR into SH-SY5Y cells. Similar to the reporter gene assays, miR-194 only reduced *TARDBP* and *FUS* endogenous mRNA levels

with no effect on *RGNEF* mRNA levels, which was abolished when co-transfecting miR-194

with its anti-miR (**Fig. 4.7B**). Also, only adding the anti-miR of miR-194 caused a strong trend

towards upregulation of *TARDBP* mRNA expression, but no change in the *FUS* transcript levels,

suggesting miR-194 might play a role in regulating *TARDBP* gene expression within SH-SY5Y

cells. Overall, these results suggest that miR-b2122 is the central regulator of *TARDBP*, *FUS* and

*RGNEF* mRNA expression.

To determine whether the alteration in mRNA levels was associated with alterations in

protein expression, we examined protein levels of TDP-43, FUS and RGNEF post-transfection of

miR-b2122 (**Fig. 4.9A**). MiR-b2122 alone had no significant effect on the protein levels of TDP-

43 within the cell, but when the anti-miR alone was added, there was a strong trend towards

upregulation of TDP-43. This upregulation was significantly different from when miR-b2122

was transfected alone, suggesting that endogenous miR-b2122 is likely participating keeping

TDP-43 protein at steady-state levels, but loss of this miRNA leads to an increase in TDP-43

protein output (**Fig. 4.9B**). Transfection of miR-b2122 alone showed a strong trend towards the

downregulation in FUS protein levels, which was abrogated when the anti-miR was co-

transfected with miR-b2122. The transfection of the anti-miR of miR-b2122 alone did lead to a

significant upregulation of FUS protein levels, indicating miR-b2122 regulates protein synthesis

of FUS endogenously (**Fig. 4.9B**).

Interestingly, miR-b2122 had the reverse effect on the protein levels of RGNEF as

compared to the changes observed at the mRNA level (**Fig. 4.9B**). Transfection of miR-b2122

alone lead to increased RGNEF protein levels, which was reduced to the control levels when

**A**
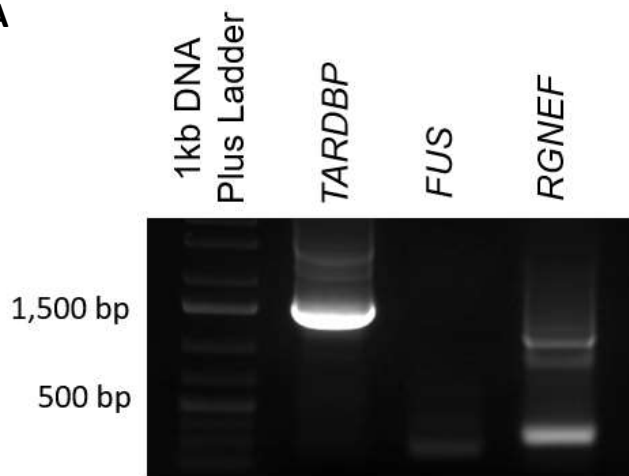


**B**
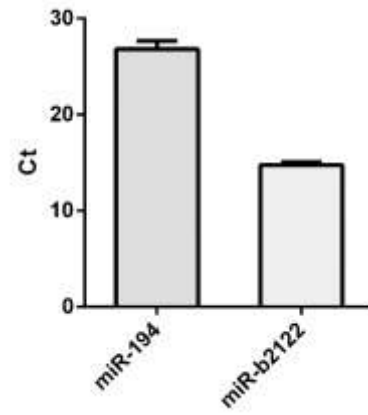
**Figure 4.6. 3'UTR isoforms of RNA-binding proteins, and miR-194 and miR-b2122 are**

**expressed in SH-SY5Y cells.** (A) 3'RACE PCR showing *TARDBP*, *FUS* and *RGNEF* 3'UTR

isoforms expressed in SH-SY5Y cells. *FUS* and *RGNEF* isoforms match those expressed in

human spinal cord. *TARDBP* showed multiple isoforms, but only the 1398bp isoform identified

in spinal cord could be confirmed by sequencing. (B) Real-time PCR indicating the expression of

miR-194 and miR-b2122 in SH-SY5Y cells (n=3).
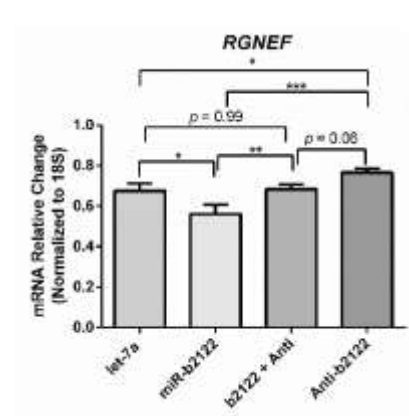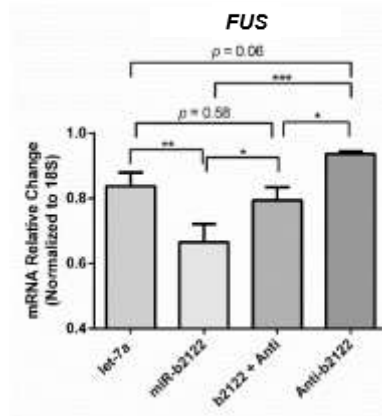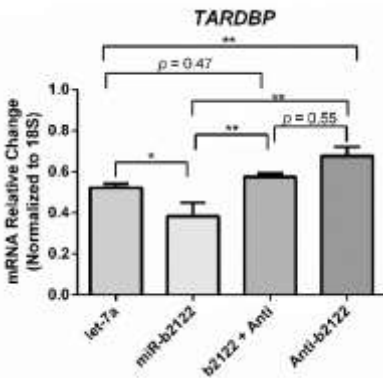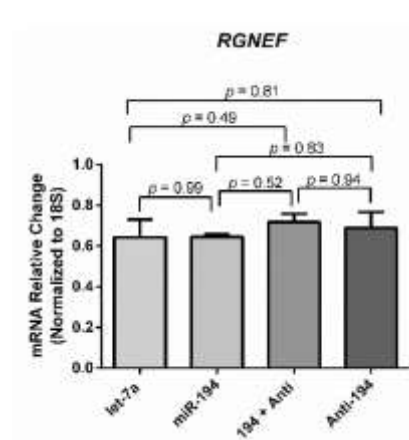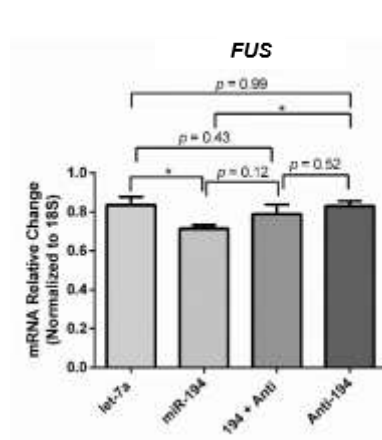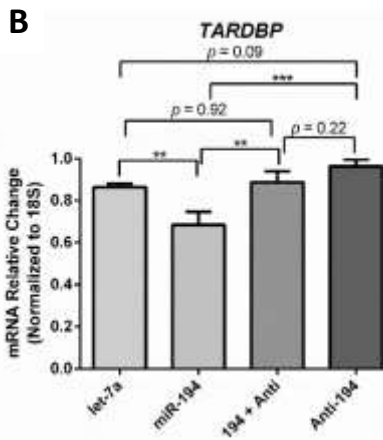
**Figure 4.7. MiR-b2122 regulates mRNA expression of *TARDBP*, *FUS* and *RGNEF* in a human-derived neuronal cell line.** SH-SY5Y cells were transfected individually with miR-194 or miR-b2122, or co-transfected with miR-194 or miR-b2122, and their anti-miRs. Transfection of let-7a was used as a negative control. (A) Transfection of miR-b2122 significantly downregulates the mRNA levels of *TARDBP*, *FUS* and *RGNEF*, while co-transfection of miR-b2122 with its anti-miR led to a recovery in the mRNA levels. Transfection of the anti-miR alone led to increased mRNA expression of all three RNA-binding proteins (B) Transfection of miR-194 alone resulted in reduction of *TARDBP* and *FUS*, which was abolished when it was co-transfected with its anti-miR. No effect was observed on RGNEF when miR-194 and/or its anti-miR were transfected. Data was expressed as the mean $(n=3) \pm$ SEM, and significance was determined using a one-way ANOVA followed by a Tukey's post-hoc. (***=$p<0.001$, **=$p<0.01$ *=$p<0.05$).
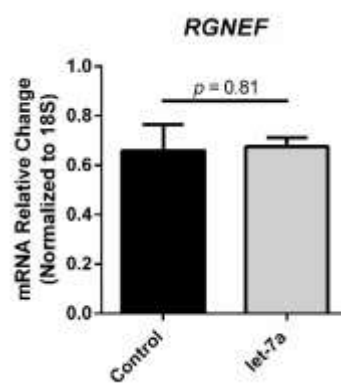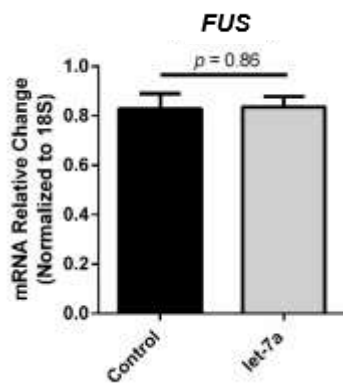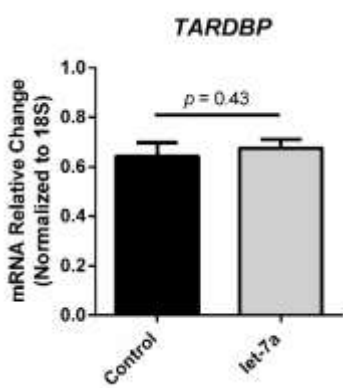
**Figure 4.8. Let-7a has no effect on mRNA levels of *TARDBP*, *FUS*, or *RGNEF* within SH-SY5Y cells.** Let-7a was transfected into SH-SY5Y cells to determine if it changed the basal mRNA levels of *TARDBP*, *FUS* or *RGNEF*, and was compared to a non-transfected control. The data indicated no significant change in the transcript levels of either *TARDBP* (p=0.64), *FUS* (p=0.51), or *RGNEF* (p=0.74) between the two conditions. Data is expressed as sample mean (n=3) ± SEM, and significance was determined using a Student's t-test.
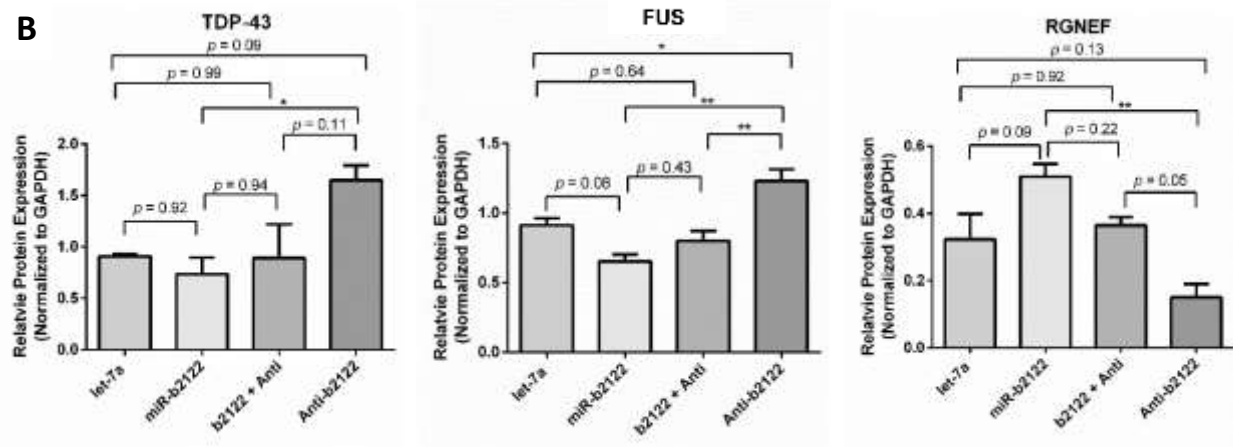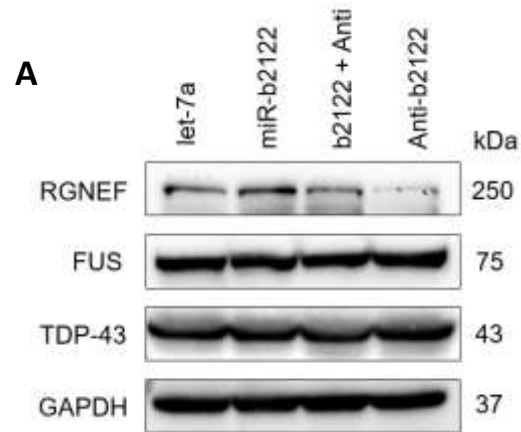
**Figure 4.9. MiR-b2122 alters protein levels of TDP-43, FUS and RGNEF within a human-derived neuronal cell line.** Changes in protein levels of TDP-43, FUS and RGNEF were studied when SH-SY5Y cells were transfected with either miR-b2122, miR-b2122 plus its anti-miR, or the anti-miR alone. Transfection of let-7a was used as a negative control. (A) Western blot showing expression of TDP-43, FUS, RGNEF, and GAPDH (B) Quantification of Western blots for TDP-43, FUS and RGNEF protein levels. TDP-43 and FUS show small reductions in protein levels when transfected with miR-b2122 alone, while their protein levels increased when the anti-miR is added. Differences in protein levels when miR-b2122 or the anti-miR are added alone are significantly different for both TDP-43 and FUS. RGNEF has increased and decreased protein levels when either miR-b2122 or its anti-miR are added alone, respectively, and these differences are significantly different from one another. Protein levels were normalized to GAPDH. Data was expressed as the mean (n=3) ± SEM, and significance was determined using a one-way ANOVA followed by a Tukey's post-hoc (**=$p<0.01$, *=$p<0.05$).

miR-b2122 was co-transfected with its anti-miR. Transfection of the anti-miR alone led to reduced levels of RGNEF compared with let-7a. While these results were not significantly different from the negative control, there was a significant difference in RGNEF protein levels between when either miR-b2122 or the anti-miR were transfected alone. All data was compared to let-7a (negative control), as we showed it, has no effect on the protein levels of these three genes (**Fig. 4.10**). Overall, these results indicate that miR-b2122 can regulate FUS protein expression, while having minor changes on TDP-43 and RGNEF protein levels.

**4.4.5 An ALS-associated mutation in *FUS* 3'UTR is located in miR-b2122 MRE.**

Previously, mutations within the *FUS* 3'UTR were found within ALS patients, all of which lead to the overexpression and increased cytoplasmic mislocalization of FUS protein (Sabatelli et al., 2013). Interestingly, one of these mutations (*c.108C>T) is located in the +2 position of the MRE for miR-b2122 (**Fig. 4.11A**), suggesting this would critically affect the ability of miR-b2122 to bind and reduce *FUS* expression. We sought to investigate whether this mutation would affect the ability to regulate firefly expression when the firefly gene was linked to the *FUS* 3'UTR that contained the *c.108C>T mutation. Indeed, this mutation significantly abolished the ability for miR-b2122 to reduce the firefly expression, compared to when the firefly gene contained the wild-type *FUS* 3'UTR (**Fig. 4.11B**). This result implies that FUS would be overexpressed without proper regulation of miR-b2122 via direct interaction with the 3'UTR.

Based on the previous result, we decided to examine if sALS cases that showed a downregulation in miR-b2122 would have an increase in FUS expression. In sALS cases that showed a downregulation of miR-b2122 there was a 3-fold increase in FUS protein expression

(**Fig. 4.11C and D**), suggesting a relationship between reduced levels of miR-b2122 and increase FUS expression.

**4.5 Discussion**

In this study, we identified miR-b2122 to be a central regulator of ALS-linked RNA-binding proteins TDP-43, FUS and RGNEF. We showed that miR-b2122 was significantly downregulated within the spinal cord tissue of sALS patients, and specifically expressed within motor neurons. MiR-194, which was also found be downregulated in sALS patients, regulates the mRNA expression of *TARDBP* and *FUS*, but not *RGNEF*. Together, our data introduces a novel miRNA (miR-b2122) to sALS pathology and indicates that the downregulation of this miRNA in sALS could affect a regulatory network of RNA-binding proteins within motor neurons, contributing to the disease pathology.

The 3'UTRs for *TARDBP*, *FUS*, and *RGNEF* identified in spinal cord match those that have been previously described; however, for *TARDBP* we were only able to describe one 3'UTR isoform, while previous authors have described multiple. The *TARDBP* 3'UTR isoform we described matches the pA1 transcript isoform (Ayala et al., 2011). Whether this is the only isoform expressed in spinal cord, or a limitation of our technique, the pA1 isoform is known to be the dominant transcript expressed in steady-state conditions, and has been shown to be the main isoform for TDP-43 protein synthesis (Avendano-Vazquez et al., 2012; Bembich et al., 2014; Koyama et al., 2016). Further, it has been hypothesized that the pA1 isoform is the one overexpressed in ALS (Koyama et al., 2016), providing another reason why we decided to focus on the pA1 isoform and its interactions with miR-194 and miR-b2122.  MiR-194 is a well-known tumor suppressor, and reduced levels of miR-194 has been linked to both cancer and diabetes

**A**

**B**
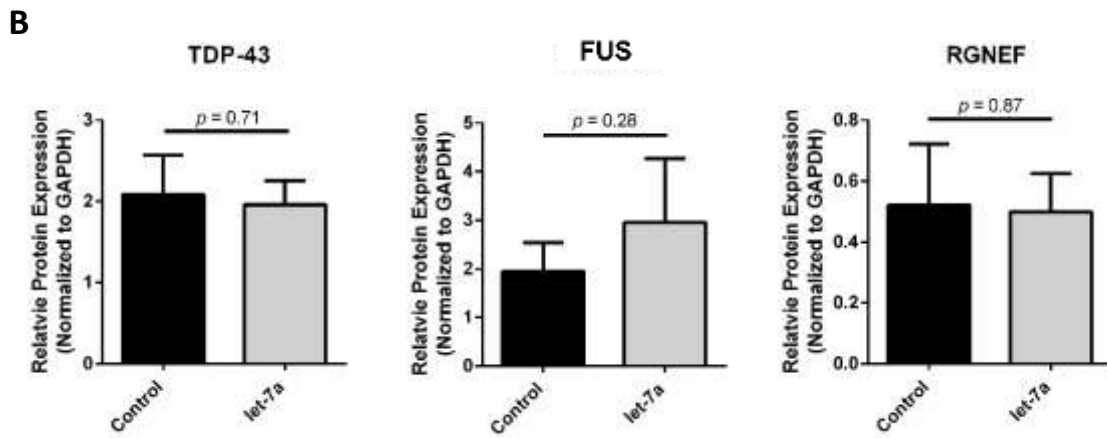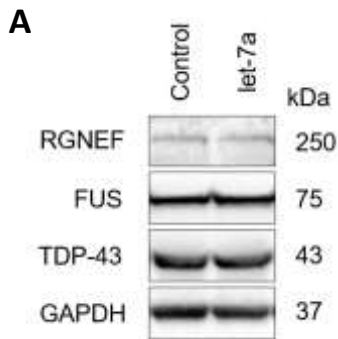
**Figure 4.10. Let-7a has no effect on protein levels of TDP-43, FUS, or RGNEF within SH-SY5Y cells.** Let-7a was transfected into SH-SY5Y cells to determine if it changed the basal protein levels of TDP-43, FUS or RGNEF, and was compared to a non-transfected control. The data indicated no significant change in the protein levels of either TDP-43 ($p=0.71$), FUS ($p=0.28$), or RGNEF ($p=0.87$) between the two conditions. Data is expressed as sample mean ($n=3$) ± SEM, and significance was determined using a Student's t-test.

**A**

FUS 3'UTR WT      5'-CCAAGGGUUUUUUUGUGUCG-3'

miR-b2122      3'-GUCUCACCGGUUGAACACAGA-5'

FUS 3'UTR ALS mut      5'-CCAAGGGUUUUUUUGUGU*T*G-3'

**B**
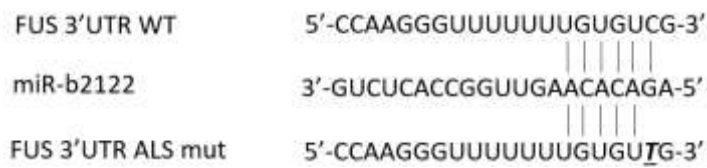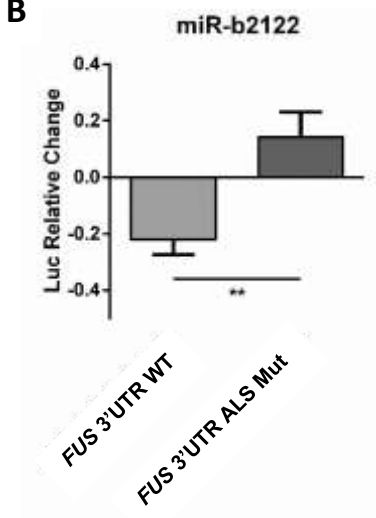
miR-b2122

**C**

**D**
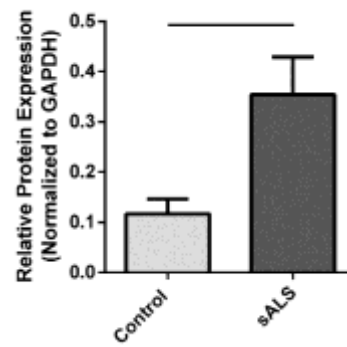
**Figure 4.11. ALS-associated mutation within *FUS* 3'UTR inhibits the ability for miR-b2122 to reduce firefly activity.** HEK293T cells were co-transfected with either the pmirGLO plasmid containing the wild-type *FUS* 3'UTR, or the mutated form, and either with or without miR-b2122. (A) ALS-associated mutation (*c.108 C>T) affects the +2 binding site of the miR-b2122 MRE. (B) ALS-associated mutation within the *FUS* 3'UTR inhibits miR-b2122 from reducing firefly activity. Firefly expression was normalized to renilla expression, and then further normalized to account for the effect miR-b2122 on the pmirGLO vector itself to determine the miRNAs exact effect on the 3'UTR (n=3). (C) Western blot of FUS protein expression in the spinal cord of 7 sALS cases versus 5 control subjects. (D) Quantification of western blot. Data is expressed as sample mean ± SEM, and significance was determined using a Student's t-test (**=p<0.01; *=p<0.05).

(Bao et al., 2015; Dong et al., 2011; Latouche et al., 2016; Song et al., 2012; Zhang et al., 2016; Zhou et al., 2016). Interestingly, the dysfunctional pathways identified within both of these diseases relate to those described in ALS (Bao et al., 2015; Latouche et al., 2016). For example, miR-194 expression has been shown to be switched off by NF-kB - a proinflammatory transcription factor that has been associated with ALS progression via increase activation in astrocytes and microglia (Bao et al., 2015; Frakes et al., 2014; Swarup et al., 2011). Further, overexpression of TDP-43 has been related to an increase in NF-kB activation (Swarup et al., 2011). In this study, reduction of miR-194 leads to increased levels of *TARDBP* mRNA, and thus, through its regulation of TDP-43, miR-194 may be part of an inflammatory regulatory network that contributes to ALS progression.

Since miR-b2122 was a novel miRNA identified by our group previously [Ishtiaq et al., 2014], this is the first pathway in which this miRNA has been implicated. Our data would suggest that the downregulation of miR-b2122 would lead to a significant increase in *TARDBP*, *FUS* and *RGNEF* mRNA levels in sALS patients. This is consistent with the increase of *TARDBP* mRNA and protein levels observed in sALS patients (Swarup et al., 2011). Further, rodent models overexpressing wild-type human FUS and TDP-43 do develop age-related motor deficiencies and cytoplasmic protein aggregation in motor neurons similar to that seen in ALS cases (Janssens et al., 2013; Mitchell et al., 2013; Wils et al., 2010; Xu et al., 2010). However, the latter models look at the overexpression of a single gene, when it is the dysregulation of both expression and localization of multiple RNA-binding proteins which contributes to the disease progression. This makes miR-b2122 an intriguing miRNA, as its downregulation in sALS would contribute to the overexpression and dysregulation of multiple RNA-binding proteins involved in the pathogenesis of ALS.

While TDP-43, FUS and RGNEF protein levels showed discrete changes when compared to the negative control, there were significant changes between when miR-b2122 and its anti-miR were transfected alone, suggesting that either overexpression, or reduced activity of miR-b2122, does in fact alter protein levels. These noticeable changes to the TDP-43, FUS and RGNEF protein levels when miR-b2122 levels are increased or decreased, suggests that chronic changes to miR-b2122 activity might have more drastic effects on protein levels within the cell over-time.

Interestingly, RGNEF protein levels went in the opposite direction of the mRNA levels within our study. While rare to see inverse correlations between mRNA and protein levels of a single gene, it is not unprecedented (Marinova et al., 2015; Xiu et al., 2014). This could imply that when miR-b2122 binds to the *RGNEF* 3'UTR, its role is to maintain low levels of mRNA while keeping the transcript in a translationally stable state, and thus, loss of its binding stabilizes the mRNA molecule, but leaves the transcript in a translationally silent state. The latter phenomenon is a common one seen within stress and transport granules within neurons (Anderson and Kedersha, 2008; Buchan, 2014; Panas et al., 2016). However, this would suggest that there is competition between miR-b2122 and another miRNA, or RNA-binding protein at the *RGNEF* 3'UTR which would need further investigation.

We sought to determine whether an ALS mutation located in the MRE of miR-b2122 within the *FUS* 3'UTR affected the ability of miR-b2122 to reduce gene expression. Clinically, the patient identified with this FUS 3'UTR mutation (*c.108C>T) had limb onset ALS with severe limb weakness and respiratory difficulties. Previously, fibroblast cells cultured from the ALS patient with this mutation showed an overexpression of FUS mRNA and protein and an increase in cytoplasmic localization – two factors believed to contribute to ALS development

(Sabatelli et al., 2013). Despite identifying these phenotypes there was no clear mechanism to why this may happen. In this study, we showed that loss of direct interaction between miR-b2122 and the *FUS* 3'UTR may play a critical role in FUS overexpression. Further, we were able to show that reduce levels of miR-b2122 in sALS spinal cord seems to be related to an increase in FUS protein expression. In addition, reduction of the levels of miR-b2122 in a neuronal cell line (SH-SY5Y) using anti-b2122 hindered the ability for miR-b2122 to reduce endogenous *FUS* leading to an overall increase in both mRNA and protein levels.

In this study, we have not only provided an explanation of the significance for reduced levels of miR-b2122 in sALS, but provide a molecular link showing the importance of the interaction between miR-b2122 and the *FUS* 3'UTR. Thus, dysregulation of miR-b2122 either through reduce levels or mutations within the MRE could be a major contributing factor to FUS dysregulation and pathogenesis in ALS. In a different study, a group examined another ALS-related mutation within the *FUS* 3'UTR, which lead to an overexpression of FUS. This aberrant expression of FUS was attributed to the loss of its interaction with miR-141/200a due to the 3'UTR mutation (Dini Modigliani et al., 2014). These findings emphasize the importance of examining mutations outside of the coding regions, as alterations within the 3'UTR can have drastic effects on both protein expression and localization (Berkovits and Mayr, 2015; Mayr, 2016).

While it is interesting to note the relationship between the dysregulation of RNA-binding proteins and miRNAs, it is still unclear how miRNAs, like miR-b2122 and miR-194, become reduced in sALS. However, there is strong evidence suggesting that the miRNA biogenesis pathway is disrupted in sALS, as both TDP-43 and FUS are crucial parts of miRNA production (Kawahara and Mieda-Sato, 2012; Morlando et al., 2012). More specifically, it appears that the

dysregulation in miRNA biogenesis happens at the level of DICER, as it is the mature miRNA form and not the pre-miRNA form showing a global downregulation in sALS (Emde et al., 2015). Also, ALS-linked mutations in TDP-43 and FUS affects miRNA biogenesis specifically at the level DICER (Emde et al., 2015). Thus, it is plausible that TDP-43 and/or FUS could regulate the biogenesis of miR-b2122 and miR-194, suggesting a negative feedback loop between RNA-binding proteins and miRNAs exists and it is the loss of this negative feedback loop that drives, at least in part, sALS disease progression.

It has been previously shown that the pathogenesis of sALS patients likely does not rely on the dysregulation of a single RNA-binding protein, but a combination of TDP-43, FUS and RGNEF, as they co-aggregate with each other in motor neurons of sALS patients (Keller et al., 2012). In the current study, we have identified a single miRNA that regulates all three of these RNA-binding proteins. The observation that miR-b2122 is downregulated in sALS suggests that this miRNA may play an essential role in the pathogenic mechanism of sALS. As we further look at those miRNAs related to ALS, we start developing an understanding of a miRNA network critical for motor neuron function which we have previously termed MotomiRs (Hawley et al., 2017). Further, it would be intriguing to know whether these miRNAs play a role in closely related neurodegenerative diseases, including primary lateral sclerosis (PLS), spinal muscular atrophy (SMA), or frontotemporal dementia (FTD). Based on the current study, miR-b2122 should be added to the already established list of MotomiRs, as it regulates a network of RNA-binding proteins essential for motor neuron function, and its regulation could potentially contribute to motor neuron degeneration in ALS.

## 4.6 References

Al-Chalabi, A., van den Berg, L.H., and Veldink, J. (2017). Gene discovery in amyotrophic lateral sclerosis: implications for clinical management. Nat Rev Neurol *13*, 96-104.

Anderson, P., and Kedersha, N. (2008). Stress granules: the Tao of RNA triage. Trends Biochem Sci *33*, 141-150.

Avendano-Vazquez, S.E., Dhir, A., Bembich, S., Buratti, E., Proudfoot, N., and Baralle, F.E. (2012). Autoregulation of TDP-43 mRNA levels involves interplay between transcription, splicing, and alternative polyA site selection. Genes Dev *26*, 1679-1684.

Ayala, Y.M., De Conti, L., Avendano-Vazquez, S.E., Dhir, A., Romano, M., D'Ambrogio, A., Tollervey, J., Ule, J., Baralle, M., Buratti, E.*, et al.* (2011). TDP-43 regulates its mRNA levels through a negative feedback loop. EMBO J *30*, 277-288.

Bao, C., Li, Y., Huan, L., Zhang, Y., Zhao, F., Wang, Q., Liang, L., Ding, J., Liu, L., Chen, T.*, et al.* (2015). NF-kappaB signaling relieves negative regulation by miR-194 in hepatocellular carcinoma by suppressing the transcription factor HNF-1alpha. Sci Signal *8*, ra75.

Bembich, S., Herzog, J.S., De Conti, L., Stuani, C., Avendano-Vazquez, S.E., Buratti, E., Baralle, M., and Baralle, F.E. (2014). Predominance of spliceosomal complex formation over polyadenylation site selection in TDP-43 autoregulation. Nucleic Acids Res *42*, 3362-3371.

Berkovits, B.D., and Mayr, C. (2015). Alternative 3' UTRs act as scaffolds to regulate membrane protein localization. Nature *522*, 363-367.

Blokhuis, A.M., Groen, E.J., Koppers, M., van den Berg, L.H., and Pasterkamp, R.J. (2013). Protein aggregation in amyotrophic lateral sclerosis. Acta Neuropathol *125*, 777-794.

Buchan, J.R. (2014). mRNP granules. Assembly, function, and connections with disease. RNA Biol *11*, 1019-1030.

Campos-Melo, D., Droppelmann, C.A., He, Z., Volkening, K., and Strong, M.J. (2013). Altered microRNA expression profile in Amyotrophic Lateral Sclerosis: a role in the regulation of NFL mRNA levels. Mol Brain *6*, 26.

Campos-Melo, D., Droppelmann, C.A., Volkening, K., and Strong, M.J. (2014). Comprehensive luciferase-based reporter gene assay reveals previously masked up-regulatory effects of miRNAs. Int J Mol Sci *15*, 15592-15602.

Cestra, G., Rossi, S., Di Salvio, M., and Cozzolino, M. (2017). Control of mRNA Translation in ALS Proteinopathy. Front Mol Neurosci *10*, 85.

Chen, S., Sayana, P., Zhang, X., and Le, W. (2013). Genetics of amyotrophic lateral sclerosis: an update. Mol Neurodegener *8*, 28.

de Planell-Saguer, M., Rodicio, M.C., and Mourelatos, Z. (2010). Rapid in situ codetection of noncoding RNAs and proteins in cells and formalin-fixed paraffin-embedded tissue sections without protease treatment. Nat Protoc *5*, 1061-1073.

Dini Modigliani, S., Morlando, M., Errichelli, L., Sabatelli, M., and Bozzoni, I. (2014). An ALS-associated mutation in the FUS 3'-UTR disrupts a microRNA-FUS regulatory circuitry. Nat Commun *5*, 4335.

Dong, P., Kaneuchi, M., Watari, H., Hamada, J., Sudo, S., Ju, J., and Sakuragi, N. (2011). MicroRNA-194 inhibits epithelial to mesenchymal transition of endometrial cancer cells by targeting oncogene BMI-1. Mol Cancer *10*, 99.

Droppelmann, C.A., Campos-Melo, D., Ishtiaq, M., Volkening, K., and Strong, M.J. (2014). RNA metabolism in ALS: when normal processes become pathological. Amyotroph Lateral Scler Frontotemporal Degener *15*, 321-336.

Droppelmann, C.A., Keller, B.A., Campos-Melo, D., Volkening, K., and Strong, M.J. (2013a). Rho guanine nucleotide exchange factor is an NFL mRNA destabilizing factor that forms cytoplasmic inclusions in amyotrophic lateral sclerosis. Neurobiol Aging *34*, 248-262.

Droppelmann, C.A., Wang, J., Campos-Melo, D., Keller, B., Volkening, K., Hegele, R.A., and Strong, M.J. (2013b). Detection of a novel frameshift mutation and regions with homozygosis within ARHGEF28 gene in familial amyotrophic lateral sclerosis. Amyotroph Lateral Scler Frontotemporal Degener *14*, 444-451.

Emde, A., Eitan, C., Liou, L.L., Libby, R.T., Rivkin, N., Magen, I., Reichenstein, I., Oppenheim, H., Eilam, R., Silvestroni, A.*, et al.* (2015). Dysregulated miRNA biogenesis downstream of cellular stress and ALS-causing mutations: a new mechanism for ALS. EMBO J *34*, 2633-2651.

Figueroa-Romero, C., Hur, J., Lunn, J.S., Paez-Colasante, X., Bender, D.E., Yung, R., Sakowski, S.A., and Feldman, E.L. (2016). Expression of microRNAs in human post-mortem amyotrophic lateral sclerosis spinal cords provides insight into disease mechanisms. Mol Cell Neurosci *71*, 34-45.

Frakes, A.E., Ferraiuolo, L., Haidet-Phillips, A.M., Schmelzer, L., Braun, L., Miranda, C.J., Ladner, K.J., Bevan, A.K., Foust, K.D., Godbout, J.P.*, et al.* (2014). Microglia induce motor neuron death via the classical NF-kappaB pathway in amyotrophic lateral sclerosis. Neuron *81*, 1009-1023.

Freibaum, B.D., Chitta, R.K., High, A.A., and Taylor, J.P. (2010). Global analysis of TDP-43 interacting proteins reveals strong association with RNA splicing and translation machinery. J Proteome Res *9*, 1104-1120.

Hawley, Z.C.E., Campos-Melo, D., Droppelmann, C.A., and Strong, M.J. (2017). MotomiRs: miRNAs in Motor Neuron Function and Disease. Front Mol Neurosci *10*, 127.

Hideyama, T., Yamashita, T., Aizawa, H., Tsuji, S., Kakita, A., Takahashi, H., and Kwak, S. (2012). Profound downregulation of the RNA editing enzyme ADAR2 in ALS spinal motor neurons. Neurobiol Dis *45*, 1121-1128.

Janssens, J., Wils, H., Kleinberger, G., Joris, G., Cuijt, I., Ceuterick-de Groote, C., Van Broeckhoven, C., and Kumar-Singh, S. (2013). Overexpression of ALS-associated p.M337V human TDP-43 in mice worsens disease features compared to wild-type human TDP-43 mice. Mol Neurobiol *48*, 22-35.

Kawahara, Y., and Mieda-Sato, A. (2012). TDP-43 promotes microRNA biogenesis as a component of the Drosha and Dicer complexes. Proc Natl Acad Sci U S A *109*, 3347-3352.

Keller, B.A., Volkening, K., Droppelmann, C.A., Ang, L.C., Rademakers, R., and Strong, M.J. (2012). Co-aggregation of RNA binding proteins in ALS spinal motor neurons: evidence of a common pathogenic mechanism. Acta Neuropathol *124*, 733-747.

Koyama, A., Sugai, A., Kato, T., Ishihara, T., Shiga, A., Toyoshima, Y., Koyama, M., Konno, T., Hirokawa, S., Yokoseki, A.*, et al.* (2016). Increased cytoplasmic TARDBP mRNA in affected spinal motor neurons in ALS caused by abnormal autoregulation of TDP-43. Nucleic Acids Res *44*, 5820-5836.

Latouche, C., Natoli, A., Reddy-Luthmoodoo, M., Heywood, S.E., Armitage, J.A., and Kingwell, B.A. (2016). MicroRNA-194 Modulates Glucose Metabolism and Its Skeletal Muscle Expression Is Reduced in Diabetes. PLoS One *11*, e0155108.

Ma, Y., Tang, L., Chen, L., Zhang, B., Deng, P., Wang, J., Yang, Y., Liu, R., Yang, Y., Ye, S.*, et al.* (2014). ARHGEF28 gene exon 6/intron 6 junction mutations in Chinese amyotrophic lateral sclerosis cohort. Amyotroph Lateral Scler Frontotemporal Degener *15*, 309-311.

Marinova, Z., Monoranu, C.M., Fetz, S., Walitza, S., and Grunblatt, E. (2015). Region-specific regulation of the serotonin 2A receptor expression in development and ageing in post mortem human brain. Neuropathol Appl Neurobiol *41*, 520-532.

Mayr, C. (2016). Evolution and Biological Roles of Alternative 3'UTRs. Trends Cell Biol *26*, 227-237.

Mitchell, J.C., McGoldrick, P., Vance, C., Hortobagyi, T., Sreedharan, J., Rogelj, B., Tudor, E.L., Smith, B.N., Klasen, C., Miller, C.C.*, et al.* (2013). Overexpression of human wild-type FUS causes progressive motor neuron degeneration in an age- and dose-dependent fashion. Acta Neuropathol *125*, 273-288.

Morlando, M., Dini Modigliani, S., Torrelli, G., Rosa, A., Di Carlo, V., Caffarelli, E., and Bozzoni, I. (2012). FUS stimulates microRNA biogenesis by facilitating co-transcriptional Drosha recruitment. EMBO J *31*, 4502-4510.

Panas, M.D., Ivanov, P., and Anderson, P. (2016). Mechanistic insights into mammalian stress granule dynamics. J Cell Biol *215*, 313-323.

Rinchetti, P., Rizzuti, M., Faravelli, I., and Corti, S. (2017). MicroRNA Metabolism and Dysregulation in Amyotrophic Lateral Sclerosis. Mol Neurobiol.

Sabatelli, M., Moncada, A., Conte, A., Lattante, S., Marangi, G., Luigetti, M., Lucchini, M., Mirabella, M., Romano, A., Del Grande, A.*, et al.* (2013). Mutations in the 3' untranslated region of FUS causing FUS overexpression are associated with amyotrophic lateral sclerosis. Hum Mol Genet *22*, 4748-4755.

Song, Y., Zhao, F., Wang, Z., Liu, Z., Chiang, Y., Xu, Y., Gao, P., and Xu, H. (2012). Inverse association between miR-194 expression and tumor invasion in gastric cancer. Ann Surg Oncol *19 Suppl 3*, S509-517.

Swarup, V., Phaneuf, D., Dupre, N., Petri, S., Strong, M., Kriz, J., and Julien, J.P. (2011). Deregulation of TDP-43 in amyotrophic lateral sclerosis triggers nuclear factor kappaB-mediated pathogenic pathways. J Exp Med *208*, 2429-2447.

Taylor, J.P., Brown, R.H., Jr., and Cleveland, D.W. (2016). Decoding ALS: from genes to mechanism. Nature *539*, 197-206.

Tsuiji, H., Iguchi, Y., Furuya, A., Kataoka, A., Hatsuta, H., Atsuta, N., Tanaka, F., Hashizume, Y., Akatsu, H., Murayama, S.*, et al.* (2013). Spliceosome integrity is defective in the motor neuron diseases ALS and SMA. EMBO Mol Med *5*, 221-234.

Wils, H., Kleinberger, G., Janssens, J., Pereson, S., Joris, G., Cuijt, I., Smits, V., Ceuterick-de Groote, C., Van Broeckhoven, C., and Kumar-Singh, S. (2010). TDP-43 transgenic mice develop spastic paralysis and neuronal inclusions characteristic of ALS and frontotemporal lobar degeneration. Proc Natl Acad Sci U S A *107*, 3858-3863.

Xiao, S., McLean, J., and Robertson, J. (2006). Neuronal intermediate filaments and ALS: a new look at an old question. Biochim Biophys Acta *1762*, 1001-1012.

Xiu, J., Zhang, Q., Zhou, T., Zhou, T.T., Chen, Y., and Hu, H. (2014). Visualizing an emotional valence map in the limbic forebrain by TAI-FISH. Nat Neurosci *17*, 1552-1559.

Xu, Y.F., Gendron, T.F., Zhang, Y.J., Lin, W.L., D'Alton, S., Sheng, H., Casey, M.C., Tong, J., Knight, J., Yu, X.*, et al.* (2010). Wild-type human TDP-43 expression causes TDP-43 phosphorylation, mitochondrial aggregation, motor deficits, and early mortality in transgenic mice. J Neurosci *30*, 10851-10859.

Zarei, S., Carr, K., Reiley, L., Diaz, K., Guerra, O., Altamirano, P.F., Pagani, W., Lodin, D., Orozco, G., and Chinea, A. (2015). A comprehensive review of amyotrophic lateral sclerosis. Surg Neurol Int *6*, 171.

Zhang, M., Zhuang, Q., and Cui, L. (2016). MiR-194 inhibits cell proliferation and invasion via repression of RAP2B in bladder cancer. Biomed Pharmacother *80*, 268-275.

Zhou, L., Di, Q., Sun, B., Wang, X., Li, M., and Shi, J. (2016). MicroRNA-194 restrains the cell progression of non-small cell lung cancer by targeting human nuclear distribution protein C. Oncol Rep *35*, 3435-3444.

# Chapter 5

## Evidence of a negative feedback network between TDP-43 and miRNAs dependent on TDP-43 nuclear localization

Zachary C. E. Hawley, Danae Campos-Melo and Michael J. Strong

A version of this chapter was published in the *Journal of Molecular Biology*

**5.1 Abstract**

TAR DNA-binding protein 43 (TDP-43) and Fused in sarcoma (FUS) are DNA/RNA-binding proteins that are integral to RNA processing. Among these functions, both play a critical role in microRNA (miRNA) biogenesis through interactions with either the DROSHA and/or DICER complexes. It has been previously shown that there is a global reduction in miRNA levels within the spinal cord and spinal motor neurons of amyotrophic lateral sclerosis (ALS) patients. The most common pathological feature of TDP-43 and FUS in ALS is a re-distribution from the nucleus to the cytoplasm in motor neurons where they form cytoplasmic inclusions. Among miRNAs dysregulated in ALS, several are known to regulate TDP-43 and FUS expression. In this study, we demonstrate that TDP-43 is in a regulatory negative feedback network with two miRNAs—miR-27b-3p and miR-181c-5p—that is dependent on its nuclear localization within HEK293T cells; however, we are unable to show FUS is in an similar network with the miRNAs it regulates. Further, we show that cellular stress which induces a redistribution of TDP-43 from the nucleus to the cytoplasm correlates with the reduced production of miR-27b-3p and miR-181c-5p. This suggests that reduced nuclear TDP-43 disrupts a negative feedback network between itself and miRNAs. These findings provide a further understanding of altered miRNA biogenesis as a key pathogenic process in ALS.

**5.2 Introduction**

TAR DNA-binding protein 43 (TDP-43) and Fused in Sarcoma (FUS) are primarily nuclear DNA/RNA-binding proteins that are ubiquitously expressed in every cell, and both share a diverse set of functions which include: mRNA transcription, mRNA splicing, mRNA transport, microRNA (miRNA) and long non-coding RNA (lncRNA) processing, mRNA translation, and stress granule formation (Ratti and Buratti, 2016; Svetoni et al., 2016). Several of these functions have been identified as dysregulated within motor neurons of patients with amyotrophic lateral sclerosis (ALS) where both TDP-43 and FUS have been shown to re-locate from the nucleus to the cytoplasm resulting in the subsequent formation of pathological aggregates. In particular, TDP-43 pathology occurs in 97% of all ALS cases, while FUS pathology is only observed in 1% of cases (Campos-Melo et al., 2013; Fratta et al., 2018; Ling et al., 2013; Weskamp and Barmada, 2018).

Cellular stress can induce the re-localization of TDP-43 and FUS from the nucleus to the cytoplasm, where they can partition into stress granule structures (Baradaran-Heravi et al., 2020; Khalfallah et al., 2018; McDonald et al., 2011; Moisse et al., 2009). Accumulation of proteins with low-complexity domains (LCD's), like TDP-43 and FUS, have been shown to phase separate into liquid droplets. However, if left to accumulate, LCD-containing proteins can form irreversible insoluble fibrils which is believed to cause the pathology of these proteins in ALS motor neurons (Kato et al., 2012; Molliex et al., 2015; Murakami et al., 2015). Evidence that stress granules may act as a seed for pathological cytoplasmic aggregates in ALS is that TIA-1—an essential stress granule component—co-localizes with TDP-43 aggregates in ALS motor neurons (Liu-Yesucevitz et al., 2010; Volkening et al., 2009). Further, increased mRNA and protein levels of TDP-43 have been observed within both the spinal cord and motor neurons of

patients with ALS (Koyama et al., 2016; Swarup et al., 2011), suggesting that TDP-43 levels are being aberrantly regulated which may contribute to its accumulation into cytoplasmic aggregates. Further, overexpression of FUS in *in vitro* or *in vivo* models is associated with cytoplasmic inclusion formation similar to what is observed in ALS motor neurons (Mitchell et al., 2013; Patel et al., 2015). Interestingly, both TDP-43 and FUS have been observed to co-aggregate with each other in ALS motor neurons (Keller et al., 2012).

Our lab, and others, have shown that a large pool of miRNAs—small RNA molecules (20-22 nucleotides) that are generally responsible for post-transcriptional gene suppression (Bartel, 2018)—have reduced levels within ALS spinal cord and motor neurons (Campos-Melo et al., 2013; Emde et al., 2015). Further, we have shown that ALS-linked miRNAs suppress TDP-43 and FUS expression suggesting that loss of miRNA function could result in increased levels of TDP-43 and FUS in ALS motor neurons (Hawley et al., 2017). Given the observation that TDP-43 and FUS are involved in the miRNA biogenesis pathway through interactions with either DROSHA and/or DICER complexes (Kawahara and Mieda-Sato, 2012; Morlando et al., 2012), we postulated that TDP-43 and FUS regulates the production of miRNAs that in turn will suppress their expression. We further hypothesize that TDP-43 and FUS are in a negative feedback loop with a specific group of miRNAs and that this function is dependent on their nuclear localization. FUS has been shown to be in a negative feedback loop with ALS-linked miRNAs (miR-141/200a) previously (Dini Modigliani et al., 2014), and therefore, we sought to determine whether there are other miRNAs involved with this negative feedback loop.

In this chapter, we explore the negative feedback network between TDP-43 and two ALS-related miRNAs, miR-27b-3p and miR-181c-5p, in HEK293T cells, and we show that this regulation is dependent on TDP-43 nuclear localization. Further, we show that TDP-43 regulates

the processing of these two miRNAs at different levels within the miRNA biogenesis pathway. In contrast, while we were able to determine two miRNAs (miR-2110 and miR-6804-5p) with MREs in the *FUS* 3'UTR whose expression was promoted by FUS, we were unable to show these miRNAs were in a negative feedback loop.

## 5.3 Methods and Materials

### 5.3.1 Plasmid Constructs

SiRNA resistant plasmids (siRES) were either pC32-FLAG-TDP-43 wild-type or pC32-FLAG-TDP-43 ΔNLS and were resistant to an siRNA that targets endogenous *TARDBP* (siTDP #2) (Deshaies et al., 2018).

*TARDBP* and *FUS* 3'UTRs that are expressed in human spinal cord were linked to the firefly luciferase gene within the pmirGLO plasmid (Promega Cat. # E1330) as described previously (Hawley et al., 2017). Mutations were put into the +2 and +3 position of the miRNA recognition element (MRE) of either miR-27b-3p or miR-181c-5p of the *TARDBP* 3'UTR using the QuikChange Site-Directed Mutagenesis Kit (Agilent Cat. # 210219). Cloned sequences and mutants were confirmed using Sanger sequencing.

### 5.3.2 Cell culture and transfection

HEK293T cells were maintained in Dulbecco's Modified Eagles Media (DMEM; Gibco Cat. # 11965084) which contained 10% fetal bovine serum (FBS) at 37°C with 5% $CO_2$. Sorbitol was added to cell media at a concentration of 400 mM to induce an osmotic stress. Media with sorbitol was then added to HEK293T cells with an 80% confluency. The osmotic stress was maintained for five hours prior to experimentation.

HEK293T cells were seeded into a 6-well plate (150,000 cells/well) and incubated for 48 hours. Cells were then either transfected with 100 nM of SCR (Sigma-Aldrich Cat. # SIC001) or

a custom siRNA targeting endogenous *TARDBP* (siTDP #2; Dharmacon) but not exogenous

*TARDBP* cloned into siRNA resistant (siRES) plasmids as previously described (Deshaies et al.,

2018). 24 hours post-transfection of siTDP #2, cells were transfected again with 2.5μg of either

pcDNA 3.1 (negative control), pC32-FLAG-TDP-43 wild-type or pC32-FLAG-TDP-43 ΔNLS

siRES plasmids. Mature miRNA levels were examined 24 hours post-transfection of plasmids.

Transfections were done using the Lipofectamine 2000 Reagent (Invitrogen Cat. # 11668019)

protocol following the manufacturer's instructions.

### 5.3.3 Microarray analysis

HEK293T cells were seeded into a 6-well plate (150,000 cells/well) and incubated for 48

hours. Cells were either transfected with an 100nM of siRNA SMARTpool targeting *TARDBP*

(siTDP #1; Dharmacon Cat. # L-012394-00-0005), siRNA SMARTpool targeting FUS (siFUS;

Dharmacon Cat. # L-009497-00-0005), or a scramble negative control (SCR; Sigma-Aldrich Cat.

# SIC001) at a 60% confluency using the Lipofectamine 2000 Reagent (Invitrogen Cat. #

11668019) protocol. Total RNA extraction was then performed 48 hours post-transfection using

the RNeasy Mini Kit (Qiagen Cat. # 74106). RNA samples were tested for integrity using

bioanalyzer analysis. Total RNA extracts were sent to the Center of Applied Genomics – TCAG

Facilities at the University of Toronto for microarray analysis using the GeneChip miRNA 4.0

Array (Applied Biosystems Cat. # 902412). Quality control and experimental data from the

microarray was analyzed using the Transcriptome Analysis Console Software (ThermoFisher

Scientific).

### 5.3.4 Real-time PCR

Samples from HEK293T cells underwent a small RNA extraction using the mirVana miRNA Isolation Kit (Invitrogen Cat. # AM1560) to obtain RNA molecules <200nts which allowed us to separate pri-miRNAs (>200nts) from pre-miRNAs (<200nts). Yield and purity of small RNAs was determined using spectrophotometry. When measuring mature miRNA levels, small RNA extracts went under cDNA synthesis using the TaqMan Advanced cDNA Synthesis Kit (Applied Biosystems Cat. # A28007), but when measuring the levels of pre-miRNAs, small RNA extracts went under cDNA synthesis using the SuperScript IV VILO Master Mix with DNease Enzyme (Invitrogen Cat. # 11766050) protocol. All cDNA synthesis protocols were done according to the manufacturers' instructions. Real-time PCR for mature miRNAs and pre-miRNAs was done either using the TaqMan Advanced miRNA Assay (Applied Biosystems Cat. # A25576) or the TaqMan Pre-miRNA Assay (Applied Biosystems Cat. # 4331182), respectively, and the Fast TaqMan Advanced Master Mix (Applied Biosystems Cat. # 4444965) in accordance to the manufactures protocol. Since microarray was normalized to an exogenous control, confirmation of changes to miRNA levels was done using an endogenous control (miR-1296-5p) which showed no change in expression following TDP-43 knockdown. Candidate miRNA expression for the rest of the experiments was normalized to an RNA spike-in (cel-miR-39b-5p). All real-time PCR data was quantified according to the $2^{-\Delta\Delta CT}$ method.

**5.3.5 Reverse transcriptase relative quantitative PCR (RT-qPCR)**

HEK293T cells were either transfected with a SCR (Sigma-Aldrich Cat. # SIC001), miR-27b-3p, miR-181c-5p, miR-2110 or miR-6804-5p human miRNA mimics (Invitrogen Cat. # 4464066) to measure changes to either endogenous *TARDBP* or *FUS* mRNA levels, or cells were transfected with either SCR (Sigma-Aldrich Cat. # SIC001) or siTDP #1 (Dharmacon Cat. # L-012394-00-0005) to measure changes in pri-miRNA levels using the Lipofectamine 2000

Reagent (Invitrogen Cat. # 11668019) protocol. Total RNA extraction using the RNeasy Mini

Kit (Qiagen Cat. # 74106) was performed 48 hours post-transfection. Yield and purity of RNA

was determined using spectrophotometry. RNA extracts went under cDNA synthesis using the

SuperScript II Reverse Transcriptase (Invitrogen Cat. # 18064014) in accordance with the

manufactures instructions which was followed by quantitative PCR using the Platinum Taq DNA

Polymerase (Invitrogen Cat. # 10966018) protocol for amplification via primers outlined in

Table 5.1. Expression levels were normalized to 18S rRNA levels prior to comparison.

### 5.3.6 Luciferase assay

HEK293T cells were co-transfected with either SCR (Sigma-Aldrich Cat. # SIC001), or

human miRNA mimics (miR-27b-3p or miR-181c-5p; Invitrogen Cat. # 4464066) and either an

empty pmirGLO plasmid or a pmirGLO plasmid containing the 3'UTR of *TARDBP* using the

Lipofectamine 2000 Reagent (Invitrogen Cat. # 11668019) protocol. Luciferase activity was

measured 24 hours post-transfection using the Dual-GLO Luciferase Assay System (Promega

Cat. # E2920). Firefly luciferase levels were normalized to renilla luciferase levels, and data was

further normalized to account for the effect the miRNAs have on the plasmid itself prior to

comparison as previously described (Campos-Melo et al., 2014).

### 5.3.7 Western blot

All protein extractions were done from HEK293T cells using the NP40 lysis buffer with

proteinase inhibitors followed by sonication. Protein lysates were resuspended in loading buffer

containing 5% β-mercaptoethanol and denatured at 90°C for 5 minutes. Samples ran on an 10%

SDS-page gel and then were transferred onto a nitrocellulose membrane. Blots were probed with

either rabbit anti-TDP-43 (1:5000; Proteintech Cat. # 10782-2-AP), rabbit anti-FUS (1:5000;

**Table 5.1. Primer Design for RT-qPCR and site-directed mutagenesis assays.**

| Primer Name | Sequence |
|---|---|
| pri-miR-27b forward | 5' AGGGATTACCACGCAACCACGACCTTG 3' |
| pri-miR-27b reverse | 5' CCTTCTCTTCAGGTGCAGAACTTAG 3' |
| pri-miR-181c forward | 5' GGTTTGGGGGAACATTCAACCTGTCG 3' |
| pri-miR-181c reverse | 5' GAATGTTGATTGTGACCTCGGCTGTGG 3' |
| miR-27b mutant forward | 5' CCCTTTGTCAACTGCTGTGTTTGCTGTATGGTGTGTGTTC 3' |
| miR-27b mutant reverse | 5' GAACACACACCATACAGCAAACACAGCAGTTGACAAAGGG 3' |
| miR-181c mutant forward | 5' GATAACCCACATTAGATGAATCCGTTAAGTGAAATGATACTTG 3' |
| miR-181c mutant reverse | 5'CAAGTATCATTTCACTTAACGGATTCATCTAATGTGGGTTATC 3' |

Proteintech Cat. # 11570-1-AP), mouse anti-FLAG (1:2500; Cedarlane Cat. # CLANT146-2),

rabbit anti-DROSHA (1:1000; abcam Cat. # ab12286), rabbit anti-DCGR8 (1:1000; abcam Cat.

# ab191875), mouse anti-XPO5 (1:1000; abcam Cat. # ab57491), mouse anti-DICER (1:1000;

abcam Cat. # ab14601), mouse anti-AGO2 (1:1000; abcam Cat. # ab57113), rabbit anti-TRBP

(1:1000; Proteintech Cat. # 15753-1-AP), or rabbit anti-GAPDH (1:5000; abcam Cat. # ab9485)

and later with an HRP secondary antibody (goat anti-mouse 1:3000; Biorad Cat. # STAR207P,

or goat anti-rabbit 1:5000; Invitrogen Cat. #  65-6120). Data was quantified using densitometry

measured by ImageJ software. Relative protein levels were normalized to GAPDH expression

prior to comparison.

### 5.3.8 Fluorescent in situ hybridization (FISH)

Neuropathologically intact human spinal cord tissue was used to examine whether

candidate miRNAs were expressed in human spinal motor neurons. Tissue was cut into 7μm

sections. FISH was done as previously described (Hawley et al., 2019). MiRCURY LNA

miRNA Detection Probes that targeted miRNA candidates contained 5' and 3' DIG labels

(Qiagen Cat. # 339111), which were further targeted by an HRP secondary antibody (Sigma-

Aldrich Ca. # 11633716001) and a Tyramide Signal Amplification tagged with a Cy3

fluorophore (PerkinElmer Cat. # NEL744001KT). Spinal cord samples were examined for

positive expression of candidate miRNAs using the Leica TSC SP8 confocal microscope.

### 5.3.9 Immunocytochemistry

Cells were fixed using 4% paraformaldehyde (PFA) and blocked with 8% Bovine Serum

Albumin (BSA). Proteins of interest were targeted by either rabbit anti-TDP-43 (1:250;

Proteintech Cat. # 10782-2-AP), goat anti-TIA-1 (1:100; Santa Cruz Cat. # sc-166247), or rabbit

anti-FLAG (1:100; abcam Cat. # ab49763) primary antibodies, which were targeted by Alexa 488 goat anti-rabbit, Alexa 555 donkey anti-goat, and Alexa 488 goat anti-mouse, respectively, secondary antibodies (1:200; Life Technologies Cat. # A32721, A21432, and A32721, respectively). Samples were imaged using the Leica TSC SP8 confocal microscope.

### 5.3.10 Fractionation

Nuclear and cytosolic protein and RNA fractionations was performed using the PARIS kit (Invitrogen Cat. # AM1921) in accordance to the manufacturer's instructions. 100 U/ml of SUPERase IN RNase Inhibitor (Invitrogen Cat. # AM2694) was added to the cell fractionation buffer and cell disruption buffer within the PARIS kit to prevent RNA degradation.

### 5.3.11 Statistics

Significance was determined either using a Students t-test when comparing two conditions, or one-way ANOVA followed by a Tukey's post-hoc when comparing multiple conditions. Data was considered significant if $p<0.05$.

### 5.4 Results

### 5.4.1 Knockdown of either TDP-43 or FUS alters small RNA profile in HEK293T cells

Knockdown of either TDP-43 or FUS in HEK293T cells was accomplished using siRNA pools targeting either *TARDBP* (siTDP #1) or *FUS* (siFUS) mRNA, respectively (**Fig. 5.1A & 5.1E**). MiRNA expression was then analyzed by microarray. The results showed that more than 370 and 300 small RNAs (scaRNAs, snoRNAs, and miRNAs) were significantly dysregulated following knockdown of either TDP-43 or FUS, respectively, most of which were miRNAs (**Fig. 5.1B & 5.1F**; list of small RNAs can be found in **Appendix A**). Interestingly, several miRNAs that were downregulated following knockdown of TDP-43 also contained a miRNA recognition

element (MRE) within the 3'untranslated region (UTR) of *TARDBP* (**Fig. 5.1C**) according to miRanda software. Further, we confirm reduction of miR-141-3p and miR-200a-3p following knockdown of FUS, but also identified two other miRNAs (miR-2110 and miR-6804-5p) downregulated with MREs in the *FUS* 3'UTR (**Fig. 5.1G**) according to miRanda software. However, we could not identify any upregulated miRNAs that had MREs in the *TARDBP* or *FUS* 3'UTRs. We selected five miRNA candidates with MREs in the *TARDBP* 3'UTR that had the greatest reduced fold-change following knockdown of TDP-43, and confirmed with real-time PCR that four of the five selected miRNAs (miR-27b-3p, miR-30a-5p, miR-181c-5p and miR-425-3p) were significantly downregulated after knockdown of TDP-43, while miR-1260b showed a non-significant reduction (**Fig. 5.1D**).

Since miR-141-3p and miR-200a-3p have already been shown to be in a negative feedback loop with FUS which is dependent on FUS nuclear localization (Dini Modigliani et al., 2014), we decided to look at miR-2110 and miR-6804-5p to see if we could expand on this network. We confirmed reduced levels of miR-2110 and miR-6804-5p following knockdown of FUS via real-time PCR (**Fig. 5.1H**).

In previous work, we had shown that out of the 4 miRNA candidates that we identified for TDP-43, miR-27b-3p, miR-181c-5p and miR-425-3p, but not miR-30a-5p, were significantly reduced in ALS spinal cord (Campos-Melo et al., 2013). Further, TargetScan 7.2 showed that only miR-27b-3p and miR-181c-5p had conserved MREs in the *TARDBP* 3'UTR giving them a high probability that they would affect TDP-43 expression, and therefore, we further examined these two miRNAs. However, miR-2110 and miR-6804-5p are not known to be affected in ALS and they do not have conserved MREs in the *FUS* 3'UTR. Despite this information we decided to further explore miR-2110 and miR-6804-5p to determine if there was a potential negative

feedback loop between these miRNAs and FUS. All four miRNA candidates (miR-27b-3p, miR-181c-5p, miR-2110 and miR-6804-5p) were found to be expressed in human spinal motor neurons according to fluorescent *in situ* hybridization analysis (**Fig. 5.2**), and therefore, we decided to explore these miRNAs and their relation to either TDP-43 or FUS expression.

**5.4.2 MiR-27b-3p and miR-181c-5p reduce TDP-43 expression**

To determine whether miRNA candidates regulated either TDP-43 or FUS expression, miRNA mimics of miR-27b-3p, miR-181c-5p, miR-2110 and miR-6804-5p were individually transfected into HEK293T cells. Transfection of either miR-27b-3p or miR-181c-5p led to a reduction of both endogenous TDP-43 protein and mRNA levels 48 hours after transfection (**Fig. 5.3A-C**). However, transfection of either miR-2110 or miR-6804-5p had no effect on FUS protein/mRNA levels (**Fig. 5.3E-G**), indicating these two miRNAs were not in a negative feedback loop with FUS.

Since miRNAs regulate gene expression generally by interacting with the 3'UTR of mRNA, we wanted to determine whether miR-27b-3p and miR-181c-5p regulated *TARDBP* expression via the 3'UTR. Reporter gene assays indicated that when *TARDBP* 3'UTR is linked to a firefly luciferase gene that this leads to a reduction in luciferase activity when in the presence of either exogenous miR-27b-3p or miR-181c-5p (**Fig. 5.3D**). Using the same assay, we examined whether miR-2110 or miR-6804-5p could regulate luciferase expression in the presence of the *FUS* 3'UTR. They had no effect (**Fig.5.3H**). Therefore, we decided to only continue to explore the relationship between TDP-43 and miR-27b-3p/miR-181c-5p.

Next, we determined whether miR-27b-3p and miR-181c-5p regulated *TARDBP* expression through direct interactions with its 3'UTR. Wild-type *TARDBP* 3'UTR, or *TARDBP* 3'UTR containing mutations in the +2 and +3 position of either the miR-27b-3p or miR-181c-5p

**A**

SCR     siTDP #1

TDP-43

GAPDH

**B**
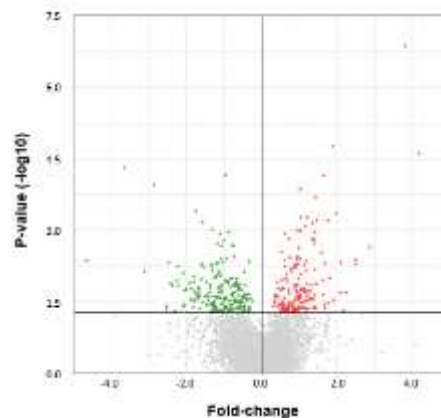


**C**

<u>MiRNAs downregulated and have binding sites in TDP-43 3'UTR</u>

- miR-27b-3p
- miR-23b-3p
- miR-181c-5p
- miR-181b-5p
- miR-107
- miR-373-5p

- miR-26a-5p
- miR-30a-3p
- miR-30a-5p
- miR-361-5p
- miR-425-3p
- miR-1260b

**D**



**E**

SCR     siFUS

FUS

GAPDH
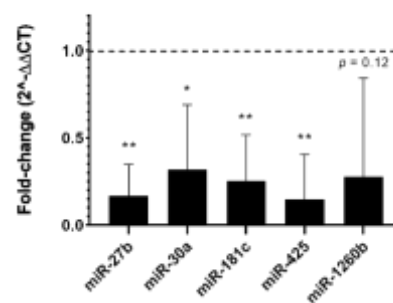
**F**
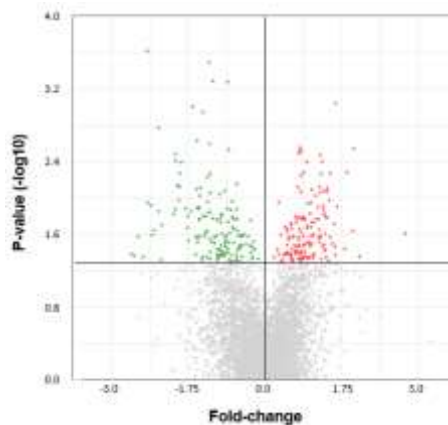


**G**

<u>MiRNAs downregulated and have binding sites in FUS 3'UTR</u>

- miR-141-3p[†]
- miR-200a-3p[†]
- miR-2110
- miR-6804-5p

**H**
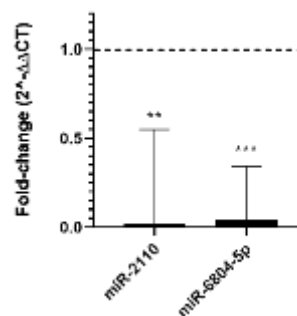
**Figure 5.1. Global change in miRNA expression following knockdown of either TDP-43 or FUS in HEK293T cells using siRNAs.** (A)Western blot showing knockdown of TDP-43 via siRNA (siTDP #1). (B) Volcano plot indicating change in small RNA expression following knockdown of TDP-43 (n=3). Green and red represent downregulated and upregulated RNAs, respectively. (C) List of miRNAs that are downregulated following knockdown of TDP-43 and have binding sites within the *TARDBP* 3'UTR. (D) Real-time PCR was used to confirm the change in candidate miRNA expression following TDP-43 knockdown (n=3). (E) Western blot showing knockdown of FUS via siRNA (siFUS). (F) Volcano plot indicating change in global small RNA expression following knockdown of FUS (n=3). Green and red represent downregulated and upregulated RNAs, respectively. (G) List of miRNAs downregulated following FUS knockdown and have binding sites within the *FUS* 3'UTR. (H) Real-time PCR was used to confirm the change in candidate miRNA expression following FUS knockdown (n=3). Real-time PCR data was normalized to an endogenous control (miR-1296-5p).  Bars represent mean (n=3) fold-change ($2^{-\Delta\Delta CT}$) ± SEM in real-time PCR analyses. Student's t-test was used to determine significance in microarray and real-time analyses (*$p<0.05$, **$p<0.01$, ***$p<0.001$).
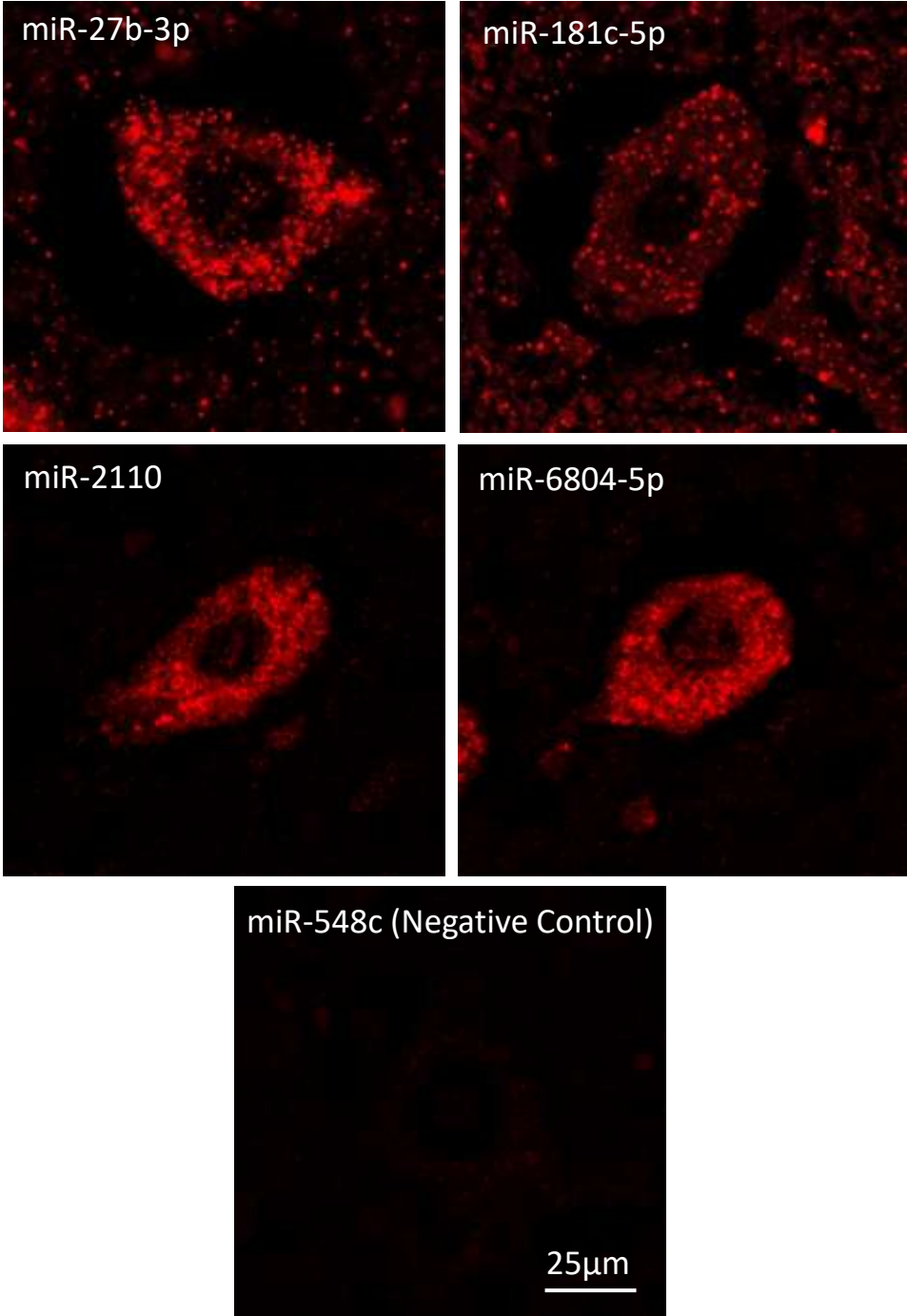
**Figure 5.2. MiR-27b-3p, miR-181c-5p, miR-2110 and miR-6804-5p are expressed in human spinal motor neurons.** A lumbar spinal cord from a neuropathologically intact individual (n=1) was used for fluorescent in situ hybridization (FISH) analysis in order to determine whether miRNA candidates were expressed in human spinal motor neurons. Red puncta indicate positive staining for miRNAs. MiR-548c was used as a negative control. Scale bar represents 25μm.

MREs were linked to a firefly luciferase gene (**Fig. 5.4A**). Reporter gene assays revealed that when the firefly gene contains the *TARDBP* 3'UTR with mutations in either the miR-27b-3p or or miR-181c-5p MREs, miR-27b-3p and miR-181c-5p are no longer able to effect luciferase activity, respectively (**Fig. 5.4B**). This indicates that both miR-27b-3p and miR-181c-5p must interact with the 3'UTR of *TARDBP* in order to reduce gene expression.

### 5.4.3 Nuclear localization of TDP-43 is required to regulate miR-27b-3p and miR-181c-5p expression

Since cellular stress is known to alter TDP-43 localization from the nucleus to the cytoplasm, we wanted to determine whether stress would lead to a reduction in the levels of miR-27b-3p and miR-181c-5p similar to that observed following knockdown of TDP-43. After an induced cellular stress, levels of both miR-27b-3p and miR-181c-5p were significantly reduced concomitant with the expected reduction of nuclear localization of TDP-43 (**Fig. 5.5**).

Based on this information, we next determined if the nuclear localization of TDP-43 is a requirement for the regulation of miR-27b-3p and miR-181c-5p expression. To do this, we used siRNA plasmids (siRES) resistant to a specific siRNA (siTDP #2) which contained either FLAG-tagged wild-type TDP-43 (siRES pC32-FLAG-TDP-43 WT) or FLAG-tagged TDP-43 without its nuclear localization signal (siRES pC32-FLAG-TDP-43 ΔNLS), as previously described (Deshaies et al., 2018). Both plasmids had a transfection efficiency of ~70% (**Fig. 5.6A-B**). SiTDP #2 was able to knockdown endogenous TDP-43 (**Fig. 5.7A**) without affecting the expression of the siRES plasmids (**Fig. 5.6C-E**). The siRES pC32-FLAG-TDP-43 WT plasmid was primarily nuclear, while siRES pC32-FLAG-TDP-43 ΔNLS was primarily cytoplasmic (**Fig. 5.7B**) as expected. 24 hours after transfection of either SCR (negative control) or siTDP #2, either pcDNA 3.1 (negative control), siRES pC32-FLAG-TDP-43 WT, or siRES pC32-FLAG-

TDP-43 ΔNLS were transfected into HEK293T cells. Recovery of both miR-27b-3p and miR-181c-5p to normal levels 48 hours post-knockdown of TDP-43 was seen only when cells were transfected with siRES pC32-FLAG-TDP-43 WT and not when either pcDNA 3.1 or siRES pC32-FLAG-TDP-43 ΔNLS plasmids were transfected (**Fig. 5.7C**), indicating that TDP-43 nuclear localization is necessary for the expression of miR-27b-3p and miR-181c-5p.

**5.4.4 Knockdown of TDP-43 or cellular stress affect primary miRNA processing**

Based on the reduction of mature miRNA levels of miR-27b-3p and miR-181c-5p following knockdown of TDP-43, we wanted to determine at what level in the biogenesis pathway of these two miRNAs TDP-43 was acting. When examining primary miRNA (pri-miRNA) levels following knockdown of TDP-43, we observed that there was a significant increase in the amount of pri-miR-181c, while there was no change pri-miR-27b levels (**Fig. 5.8A**) indicating that TDP-43 only regulates the levels of pri-miR-181c.

We next examined whether cellular stress would have a similar effect on the pri-miRNAs as observed with knockdown of TDP-43. We observed that there was a significant increase in pri-miR-27b and pri-miR-181c following a cellular stress (**Fig. 5.8B**). Taken together, the data suggest that reduced levels of mature miRNA levels either by knockdown of TDP-43 or cellular stress is not due to reduced pri-miRNA levels, but rather, later reduced processing of miRNAs. Given this, we next further investigated precursor structures of miR-27b and miR-181c.

**5.4.5 Knockdown of TDP-43 and cellular stress affects precursor miRNA processing**

Knockdown of TDP-43 showed no change in the overall levels of pre-miR-27b or pre-miR-181c (**Fig. 5.9A**), while cellular stress led to a significant increase in pre-miR-27b but had no effect on pre-miR-181c levels (**Fig. 5.9B**). Since precursor miRNA molecules are present in
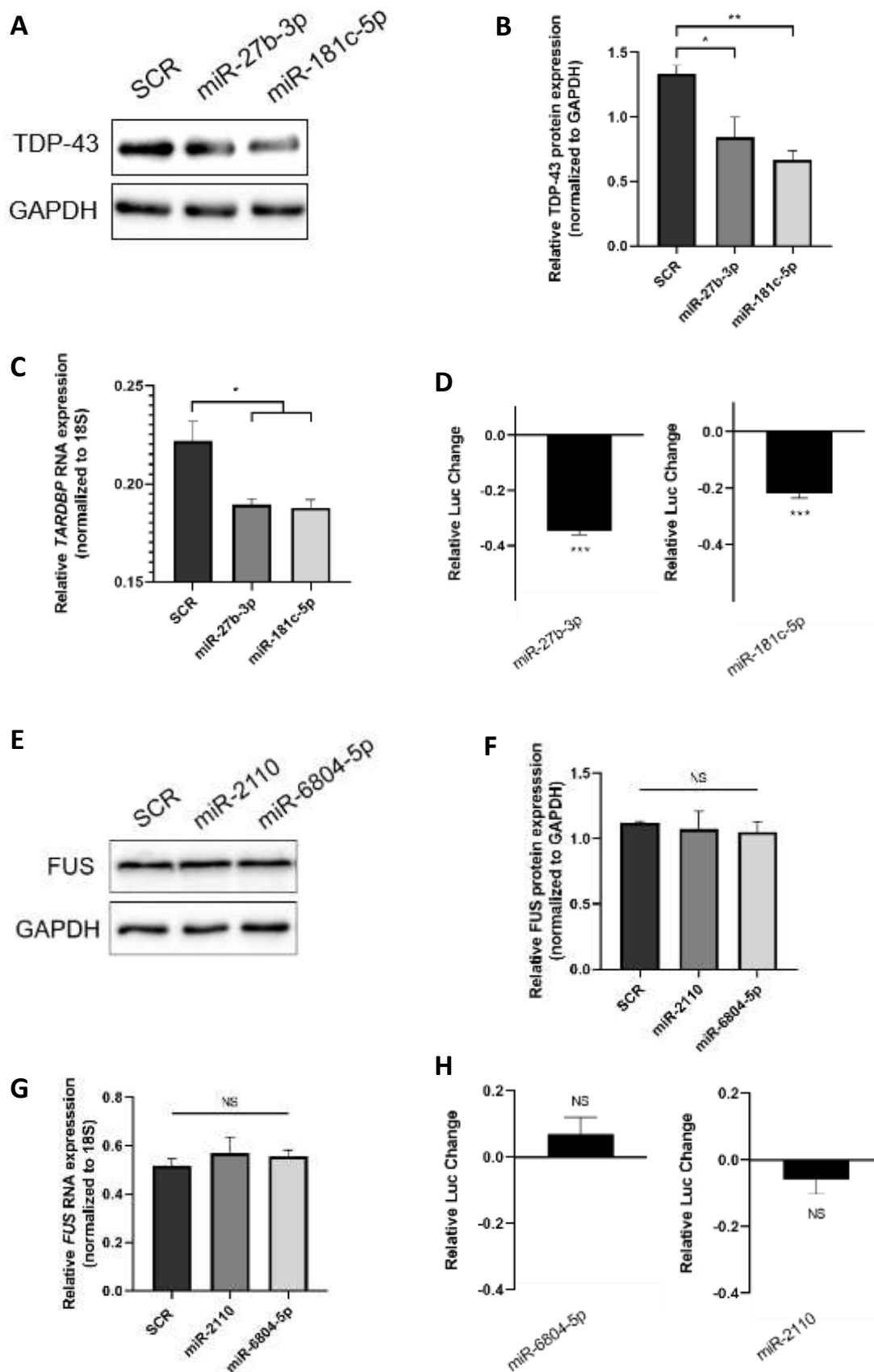
**Figure 5.3. Transfection of miR-27b-3p and miR-181c-5p decreased protein and mRNA expression of TDP-43, while transfection of miR-2110 and miR-6804-5p had no effect on FUS expression within HEK293T cells.** (A) Western blot showing TDP-43 and GAPDH protein levels following transfection of either scramble control (SCR), miR-27b-3p and miR-181c-5p. (B) Quantification of relative TDP-43 protein expression when normalized to GAPDH (n=3). (C) Change in mRNA expression of *TARDBP* when normalized to 18S rRNA following transfection of either SCR, miR-27b-3p, or miR-181c-5p (n=3). (D) Plasmids containing a reporter gene linked to the *TARDBP* 3'UTR were co-transfected in HEK293T cells with either SCR (control), miR-27b-3p, or miR-181c-5p to determine changes in reporter gene expression in the presence of either miR-27b-3p or miR-181c-5p. Data was normalized to renilla expression prior to comparison (n=3). (E) Western blot showing FUS and GAPDH protein levels following transfection of either scramble control (SCR), miR-2110 and miR-6804-5p. (F) Quantification of relative FUS protein expression when normalized to GAPDH (n=3). (G) Change in mRNA expression of *FUS* when normalized to 18S rRNA following transfection of either SCR, miR-2110, or miR-6804-5p (n=3). (H) Plasmids containing a reporter gene linked to the *FUS* 3'UTR were co-transfected in HEK293T cells with either SCR (control), miR-2110, or miR-6804-5p to determine changes in reporter gene expression in the presence of either miR-2110 or miR-6804-5p. Data was normalized to renilla expression prior to comparison (n=3). Bars represent mean ± SEM. Significance was determined using a one-way ANOVA followed by a Tukey's post-hoc for multiple comparisons (B, C, F, and G) and a Student's t-test was used to determine significance between two groups (D and H) ($^{NS}p > 0.05$, $*p < 0.05$, $**p < 0.01$, $***p < 0.001$).

**A**

| | | |
|---|---|---|
| TDP 3'UTR WT | 5' | CCCCUUUGUCAACUGCUGU**GA**A 3' |
| | | | | | | | | |
| miR-27b-3p | 3' | CGUCUUGAAUCGGUGACACUU 5' |
| | | | | | | |
| TDP 3'UTR Mut | 5' | CCCCUUUGUCAACUGCUGU**UU**A 3' |

| | | |
|---|---|---|
| TDP 3'UTR WT | 5' | UAACCCACAUUAGAUGAAU**GU**G 3' |
| | | | | | | | | | |
| miR-181c-5p | 3' | UGAGUGGCUGUCCAACUUACAA 5' |
| | | | | | | |
| TDP 3'UTR Mut | 5' | UAACCCACAUUAGAUGAAU**CC**G 3' |
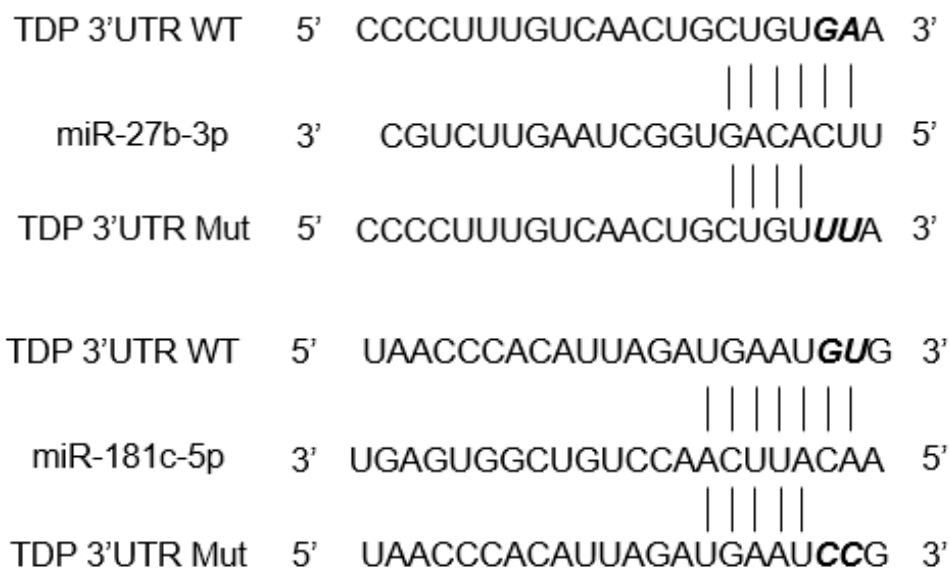
**B**
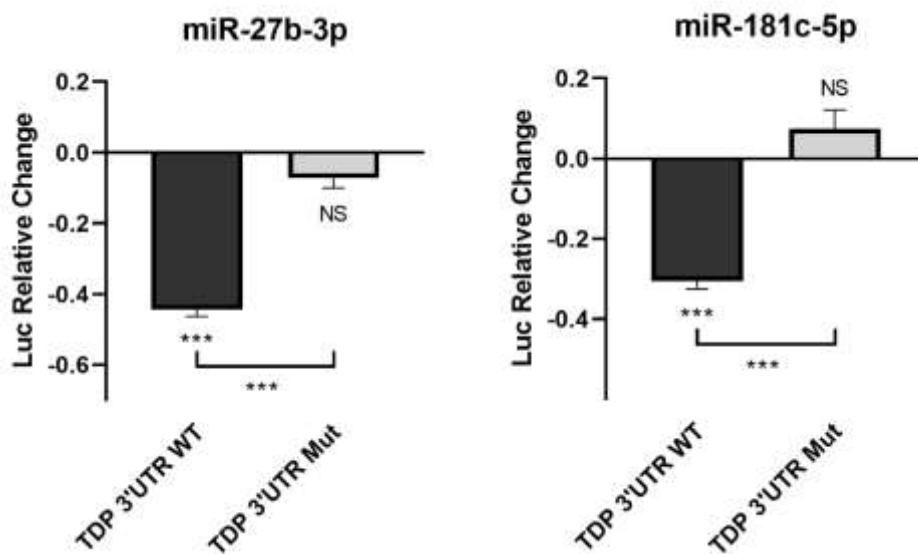
**Figure 5.4 MiR-27b-3p and miR-181c-5p interact with the *TARDBP* 3'UTR to regulate gene expression.** (A) Mutations were put in the +2 and +3 position of the miR-27b-3p or miR-181c-5p MRE within the *TARDBP* 3'UTR. (B) Reporter gene assays showing the change in expression of the reporter gene when its linked to the either the wild-type (TDP WT) or mutated (TDP Mut.) *TARDBP* 3'UTR when in the presence of either miR-27b-3p or miR-181c-5p. Data was normalized to renilla prior to comparison. Bars represent mean (n=3) ± SEM. Significance was determined using a one-way ANOVA followed by a Tukey's post-hoc for multiple comparisons ($^{NS}$p>0.05, ***p<0.001)

**A**



**B**
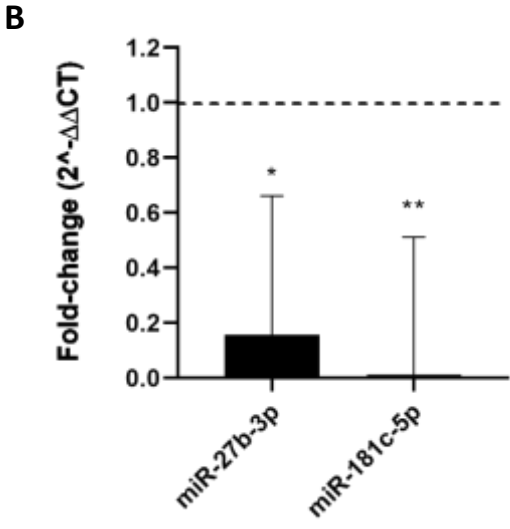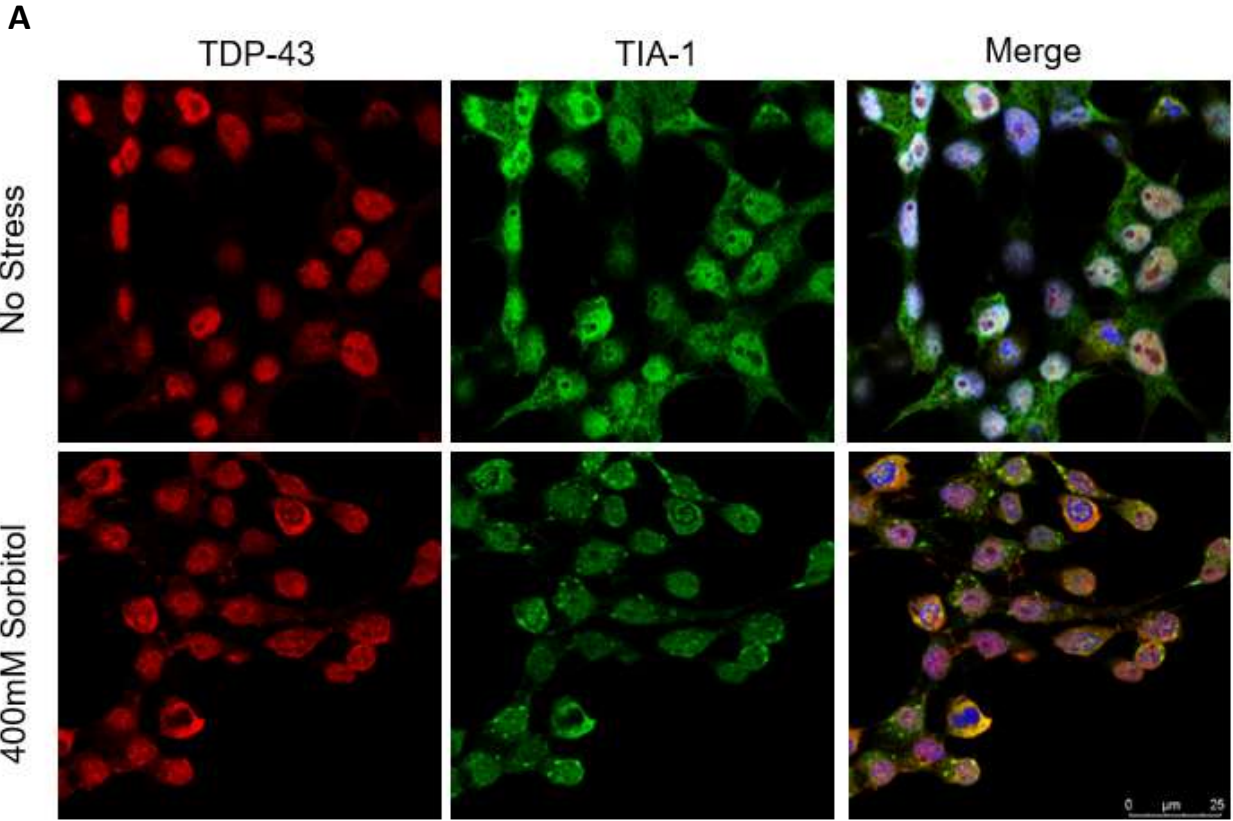
**Figure 5.5. Reduced expression of miR-27b-3p and miR-181c-5p that is concomitant with reduced nuclear TDP-43 levels five hours post osmotic stress.** (A) HEK293T cells were either not treated (control) or treated with 400 mM of sorbitol to induce an osmotic stress. Cells were fixed and stained for TDP-43 (red) and TIA-1 (green) immunofluorescence. (B) MiR-27b-3p and miR-181c-5p expression between non-stressed and stressed cells was measured via real-time PCR. Expression levels were normalized to an exogenous control (cel-miR-39b-5p) prior to comparison. Bar represents mean (n=5) fold-change ($2^{-\Delta\Delta CT}$) ± SEM. Student's t-test was used to determine significance (*p<0.05, **p<0.01).

**A**

| | FLAG | Hoescht | Merge |

siRES TDP-WT

siRES TDPΔNLS

**B**

NS

Transfection Efficiency (Positive Cells/Total Cells)

siRES TDP-WT  siRES TDPΔNLS

**C**

SCR     siTDP #2

FLAG-TDP
endo-TDP

GAPDH

**D**

NS

Relative siRES FLAG-TDP-43 protein expression (normalized to GAPDH)

SCR     siTDP

**E**

***

Relative endogenous TDP-43 protein expression (normalized to GAPDH)

SCR     siTDP
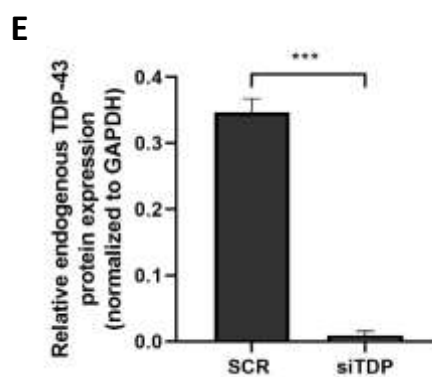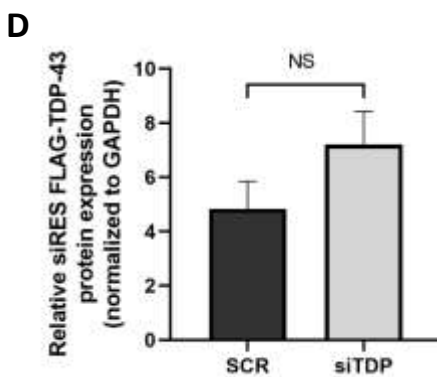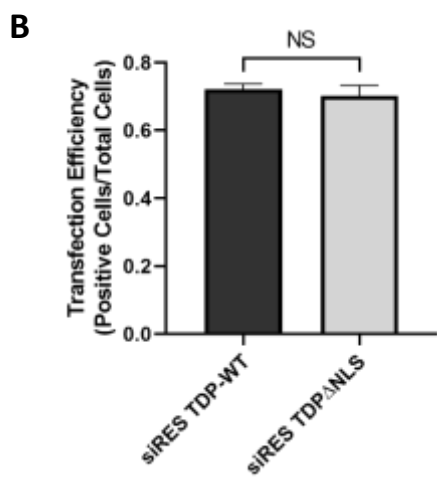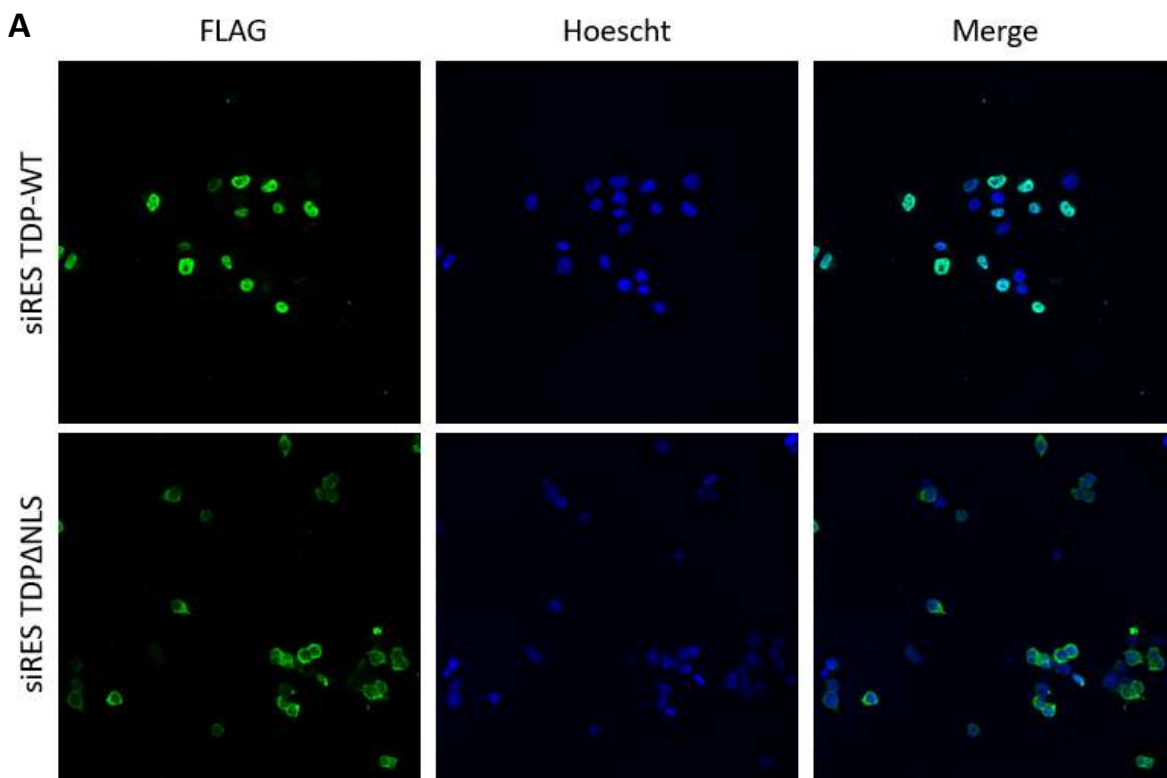
**Figure 5.6. SiRES plasmids have an ~70% transfection efficiency and are resistant to a specific TDP-43 siRNA (siTDP #2).** (A) Immunofluorescence showing the expression of either pC32-FLAG-TDP-43 wild-type (TDP WT) or pC32-FLAG-TDP-43 ΔNLS (TDP ΔNLS) siRES plasmids following transfection within HEK293T cells. (B) Quantification of percentage of cells positive for either siRES TDP WT or TDP ΔNLS plasmids following transfection within HEK293T cells (n=3). (C) Western blot showing expression of endogenous GAPDH, TDP-43 and siRES TDP WT after cells were transfected with either SCR (control) or siTDP #2. (D-E) Quantification of (D) siRES TDP WT or (E) endogenous TDP-43 expression when cells were transfected with either SCR or siTDP #2 (n=3). Expression levels were normalized to GAPDH prior to comparison. Bar represents mean ± SEM. Significance was determined using a Student's t-test ($^{NS}$p>0.05, ***p<0.001).

**A** SCR | siTDP #2 — TDP-43, GAPDH

**B** FLAG | Hoescht | Merge — siRES TDPWT, siRES TDPΔNLS

**C** Fold-change ($2^{-\Delta\Delta CT}$) of miR-27-3p: SCR+pcDNA, siTDP+pcDNA, siTDP+TDPWT, siTDP+TDPΔNLS

**D** Fold-change ($2^{-\Delta\Delta CT}$) of miR-181c-5p: SCR+pcDNA, siTDP+pcDNA, siTDP+TDPWT, siTDP+TDPΔNLS
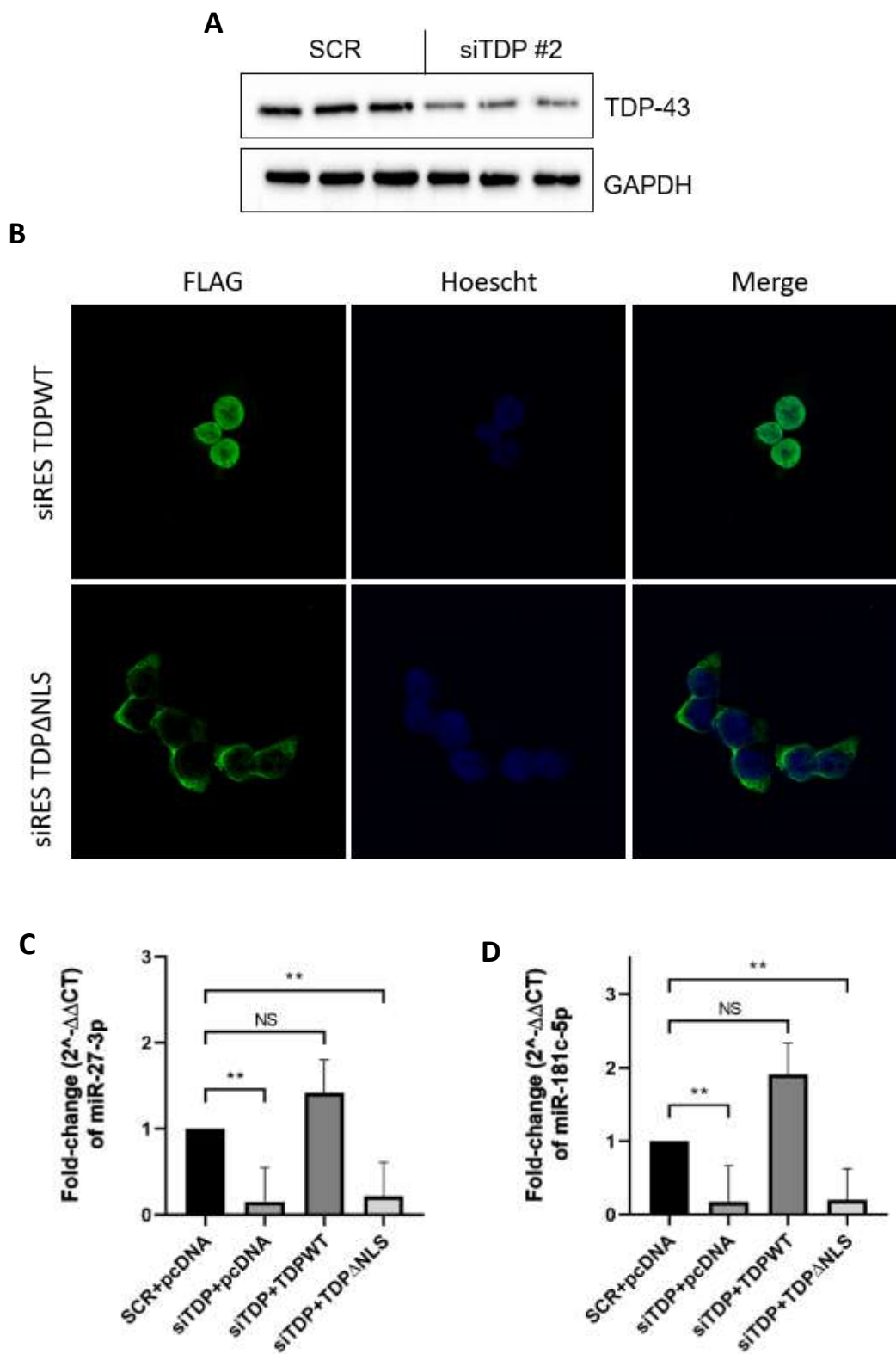
**Figure 5.7. Nuclear localization signal of TDP-43 is required for the regulation of miR-27b-3p and miR-181c-5p expression.** (A) Western blot showing knockdown of TDP-43 following transfection of siRNA (siTDP #2). (B) Immunofluorescence showing localization of either pC32-FLAG-TDP-43 wild-type (TDP WT) or pC32-FLAG-TDP-43 ΔNLS (TDP ΔNLS) siRES plasmids. (C) HEK293T cells were transfected with either SCR (control) or siTDP #2, and then transfected again 24 hours later with either pcDNA (control), TDP WT or TDP ΔNLS plasmids. MiR-27b-3p and miR-181c-5p levels were measured 24 hours after transfection of plasmids. Expression levels were normalized to an exogenous control (cel-miR-39b-5p) prior to comparison. Bar represents mean (n=3) fold-change ($2^{-\Delta\Delta CT}$) ± SEM. SCR+pcDNA samples were negative controls in which the bar representing their expression levels was set at one for comparison purposes. Significance was determined using a one-way ANOVA followed by a Tukey's post-hoc for multiple comparisons ([NS]$p>0.05$, **$p<0.01$).

**A**

pri-miR-27b

Relative pri-miRNA expression (Normalized to 18S)

NS

SCR   siTDP

pri-miR-181c

Relative pri-miRNA expression (Normalized to 18S)

**

SCR   siTDP

**B**

pri-miR-27b

Relative pri-miRNA expression (Normalized to 18S)

*

No Stress   Sorbitol Stress

pri-miR-181c

Relative pri-miRNA expression (Normalized to 18S)

*

No Stress   Sorbitol Stress
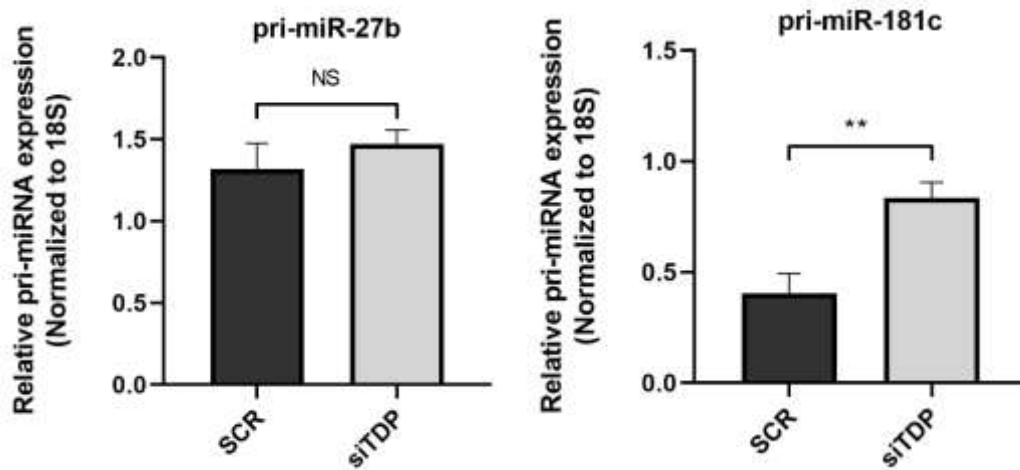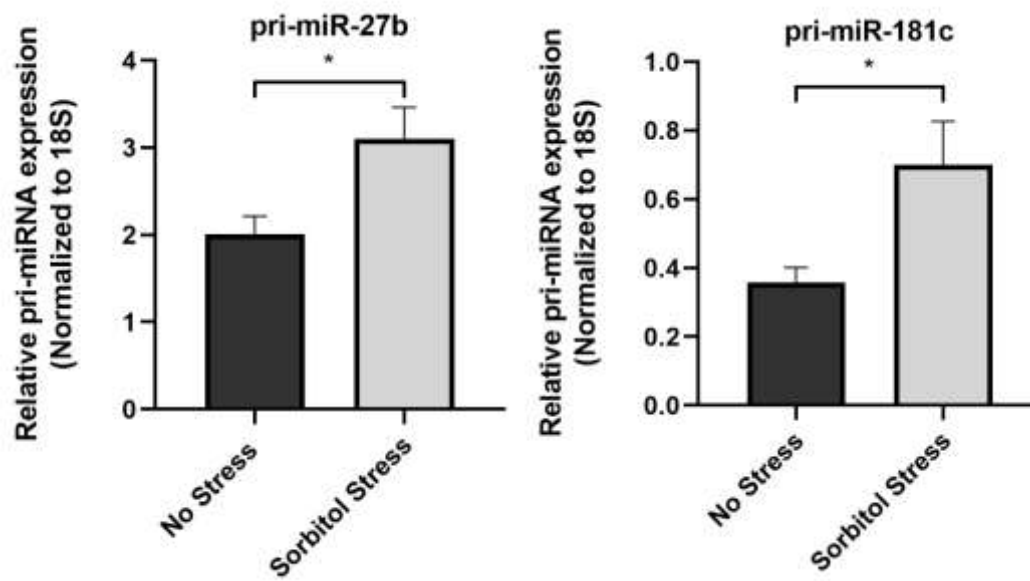
**Figure 5.8. Knockdown of TDP-43 increases levels of pri-miR-181c, while cellular stress increases levels of the pri-miR-27b and pri-miR-181c.** RT-qPCR of pri-miR-27b and pri-miR-181c following (A) knockdown of TDP-43, or (B) an osmotic stress. Expression levels were measured using densitometry and were normalized to 18S rRNA prior to comparison. Bars represent mean (n=4) $\pm$ SEM. Significance was determined using a Student's t-test ($^{NS}$p>0.05, *p<0.05, **p<0.01).

the nucleus and cytoplasm, we wanted to determine the levels of pre-miR-27b and pre-miR-181c within both cellular compartments.

We successfully fractionated samples into nuclear and cytosolic fractions (**Fig. 5.10**). Both knockdown of TDP-43 and an induced cellular stress caused a significant reduction in cytosolic pre-miR-181c, but no significant change in its nuclear levels, whereas there was no significant change in nuclear or cytosolic levels of pre-miR-27b in both conditions (**Fig. 5.11**). This suggests that the knockdown of TDP-43 and cellular stress can affect the levels of certain pre-miRNA molecules within the cytosolic compartment, specifically pre-miR-181c, while having no effect on other pre-miRNA molecules, such as pre-miR-27b.

Despite showing that knocking down TDP-43 causes deficits at several levels of miRNA processing, there was no effect on the expression of the major proteins involved in the miRNA biogenesis pathway at the time we see changes to miRNA levels (**Fig. 5.12**). This suggests that, in this time frame, TDP-43 plays a critical role in the function of proteins within the miRNA biogenesis pathway when processing miR-27b-3p and miR-181c-5p.

## 5.5 Discussion

We have provided evidence of a negative feedback regulatory loop in which TDP-43, miR-27b-3p and miR-181c-5p interact in a manner that is dependent on the nuclear localization of TDP-43. We show that TDP-43 regulates these two miRNAs differently within the miRNA biogenesis pathway, and that cellular stress that reduces TDP-43 nuclear localization had similar, but not the exact same effects on the processing of these two miRNAs as reduced TDP-43 levels.

In our experiments, we were unable to identify miRNAs in a negative feedback network with FUS. Although miR-2110 and miR-6804-5p contained MREs in the *FUS* 3'UTR, there was no evidence to suggest that these two miRNAs regulated FUS expression. Interestingly, two

miRNAs (miR-141-3p and miR-200a-3p) that had been previously shown to be in a negative feedback loop with FUS (Dini Modigliani et al., 2014), were significantly downregulated in our microarray analysis. Thus, while we were unable to expand on the potential miRNAs involved in a negative feedback network with FUS, we still believe that loss of the negative feedback loop between FUS and miR-141/200a could be a major driver of the disease pathogenesis, as both miR-141/200a have been shown to be reduced in ALS spinal cord (Campos-Melo et al., 2013).

TDP-43 has previously been shown to be involved in pri-miRNA and pre-miRNA processing within the DROSHA and DICER complex, respectively (Kawahara and Mieda-Sato, 2012). Interestingly, TDP-43 regulates miRNAs in different ways, including selectively promoting the processing of certain pri-miRNAs, or promoting or preventing the processing of certain pre-miRNAs (Kawahara and Mieda-Sato, 2012; King et al., 2014). However, the molecular reason for this selectivity is still unclear. In line with previous work, our data showed this diverse role of TDP-43 within miRNA biogenesis, where knockdown of TDP-43 led to reduced levels of cytoplasmic pre-miR-181c and mature miR-181c-5p levels but increases in pri-miR-181c levels. Low levels of TDP-43 function likely reduce DROSHA processing, which could explain the accumulation of pri-miR-181c. The reduction of cytoplasmic pre-miR-181c either means that reduced TDP-43 levels impede pre-miR-181c transport or that it promotes the degradation of this pre-miRNA molecule in the cytoplasm. Regardless, it is clear that TDP-43 promotes the production of miR-181c-5p at several levels within the miRNA biogenesis pathway. Further, knockdown of TDP-43 only caused a reduction of mature miR-27b-3p with no effect on the pri and pre-miRNAs, indicating that TDP-43 likely promotes DICER processing of pre-miR-27b. Since TDP-43 interacts with DROSHA and DICER in both an RNA-dependent and independent manner (Kawahara and Mieda-Sato, 2012), it is difficult to know

**A**



**B**
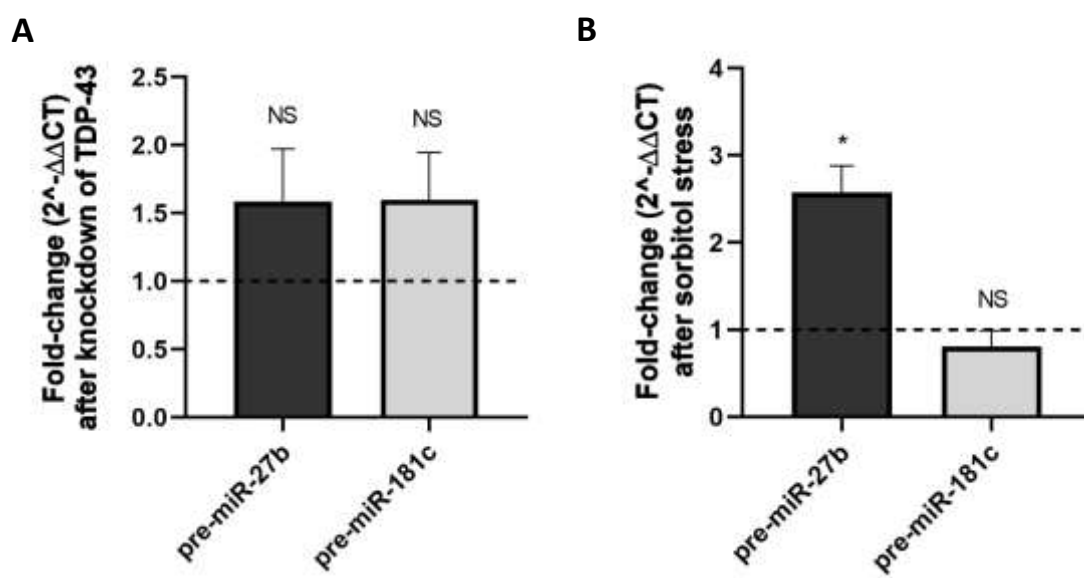
**Figure 5.9. Knockdown of TDP-43 has no effect on overall pre-miR-27b or pre-miR-181c levels, while cellular stress increases levels of pre-miR-27b.** Real time PCR of pre-miR-27b and pre-miR-181c following (A) knockdown of TDP-43, or (B) an osmotic stress. Expression levels were normalized to an exogenous control (cel-miR-39b-5p) prior to comparison. Bar represents mean (n=3) fold-change ($2^{\wedge}$-$\Delta\Delta CT$) $\pm$ SEM. Significance was determined using a Student's t-test ($^{NS}p>0.05$, $^*p<0.05$, $^{**}p<0.01$).

**A**



Cytoplasmic          Nuclear

Lamin A/C

GAPDH

**B**



50bp ladder          Cytoplasmic          Nuclear          Total RNA          Negative Control

250bp
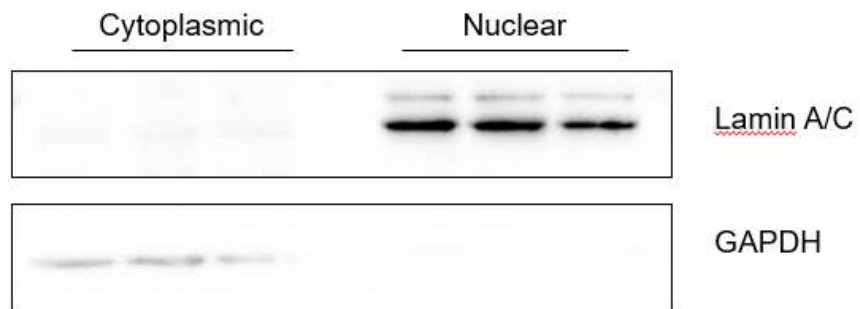
pri-miR-27b
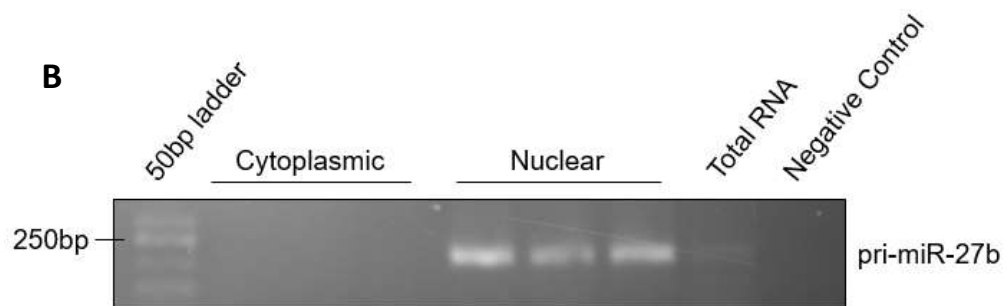
**Figure 5.10. Fractionation protocol successfully separates protein and RNA nuclear and cytosolic fractions.** (A) Western blot showing protein expression of Lamin A/C (nuclear protein) and GAPDH (primarily cytosolic protein) from nuclear and cytosolic protein extracts (n=3). (B) Agarose gel showing PCR amplicons of pri-miR-27b (a nuclear RNA species) expression in nucleus, but not cytosolic RNA extracts (n=3). Total RNA from whole cell extracts was used as a positive control.

**A**

**Nuclear levels**

**Cytoplasmic levels**

**B**

**Nuclear levels**

**Cytoplasmic levels**
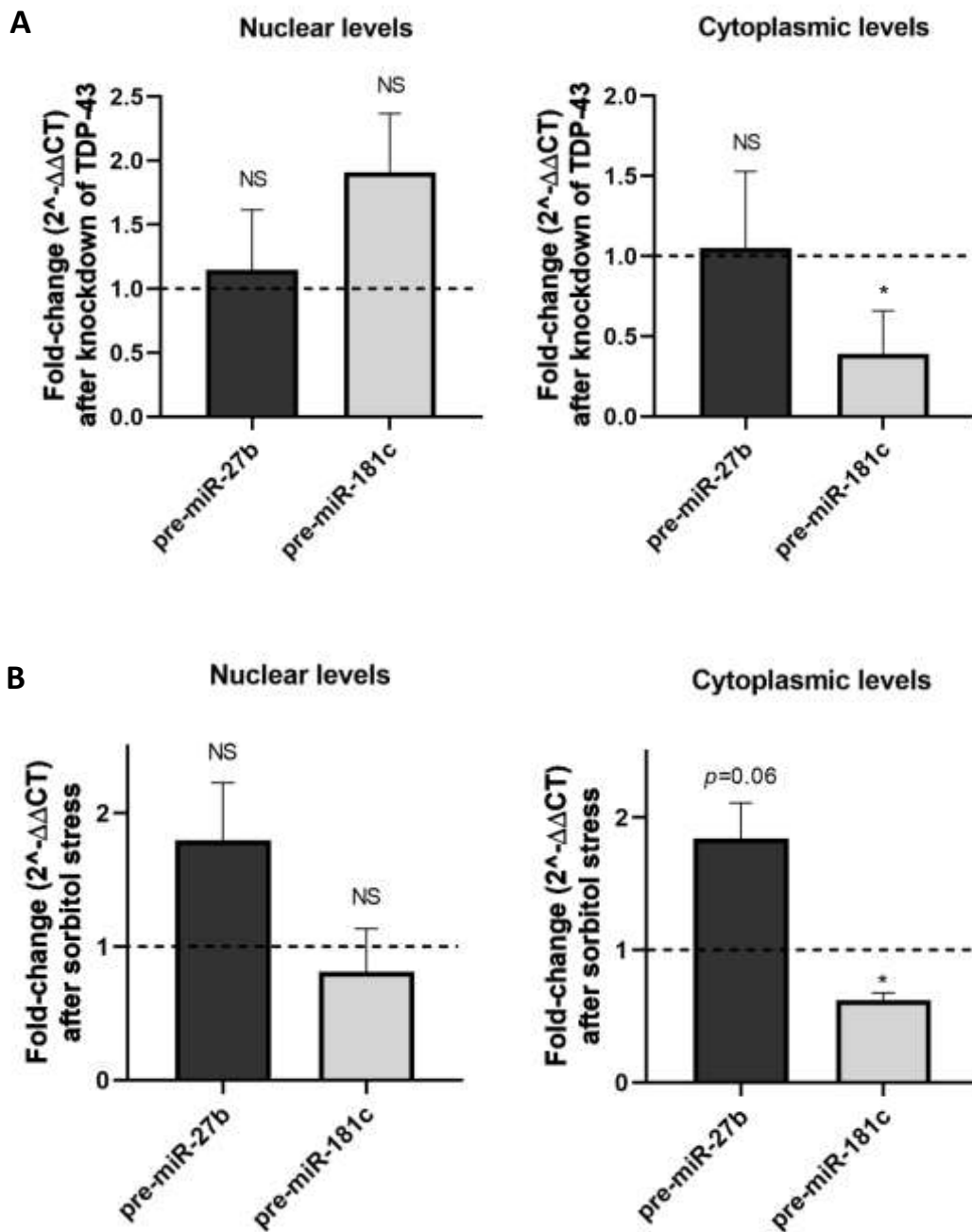
**Figure 5.11. Nuclear/cytosolic fractionation indicated reduced cytoplasmic levels of pre-miR-181c following knockdown of TDP-43 or cellular stress.** Real-time PCR showing levels of nuclear and cytosolic pre-miRNA levels of either miR-27b or miR-181c following (A) knockdown of TDP-43, or (B) osmotic stress. Expression levels were normalized to an exogenous control (cel-miR-39b-5p) prior to comparison. Bar represents mean (n=3) fold-change (2^-ΔΔCT) ± SEM. Significance was determined using a Student's t-test ($^{NS}p>0.05$, $^*p<0.05$).

**Figure 5.12. Knockdown of TDP-43 has no effect on the levels of proteins associated with the miRNA biogenesis pathway.** (A) Western blots showing the protein expression of TDP-43, DROSHA, DCGR8, XPO5, DICER, AGO2, TRBP and GAPDH within HEK293T cells when either transfected with SCR (control) or siTDP #1. (B) Quantification of DROSHA, DCGR8, XPO5, DICER, AGO2 and TRBP protein levels when cells were either transfected with SCR or siTDP #1. Expression levels were normalized to GAPDH prior to comparison. Bar represents mean (n=3) ± SEM. Significance was determined using a Student's t-test (^NSp>0.05).

whether TDP-43 needs to bind directly to either pri- and/or pre-miRNAs, DROSHA and/or

DICER complexes, or both to assist in the processing of these two miRNAs, and therefore,

warrants further investigation.

While TDP-43 has been shown to regulate several different miRNAs in multiple cell

lines, this is the first study, to our knowledge, that shows TDP-43 in a negative feedback network

with miRNAs. Similar networks have been identified between other RNA-binding proteins and

miRNAs, such as FUS and miR-141/200a, and hnRNPA1 and miR-18a (Dini Modigliani et al.,

2014; Fujiya et al., 2014; Guil and Caceres, 2007). These negative feedback networks are likely

critical biological mechanisms that regulate homeostatic levels of RNA-binding proteins and

miRNAs.

Our data suggests that the regulation of miR-27b-3p and miR-181c-5p, and hence the

negative feedback network, are dependent on the nuclear localization of TDP-43 providing

relevance for several neurodegenerative diseases that show accumulation of TDP-43 in neuronal

cytoplasmic inclusions including ALS, FTD and Alzheimer's Disease (Amador-Ortiz et al.,

2007; Arai et al., 2006; Tan et al., 2007). In some cases, TDP-43 has been known to form

intranuclear inclusions in FTD-ALS, FTD and Alzheimer's Disease (Amador-Ortiz et al., 2007;

Neumann et al., 2006), and in this case, it still likely that TDP-43 cannot perform its function in

the miRNA biogenesis pathway due to it being trapped in these inclusions. Thus, both the loss of

nuclear localization and the formation of TDP-43 inclusions likely results in miRNA

dysregulation.

Both miR-27b-3p and miR-181c-5p have been shown to be reduced in the spinal cord of

patients with ALS (Campos-Melo et al., 2013). We show here that these miRNAs are expressed

in motor neurons (**Fig. 5.2**), providing a correlation between TDP-43 cytoplasmic re-localization

and the dysregulation of these two miRNAs within ALS. MiR-181c-5p has been shown to be reduced within the anterior temporal cortex and parietal lobe cortex of patients with Alzheimer's Disease, and in cultures of primary hippocampal neurons from Alzheimer mouse models, indicating that miR-181c-5p may be critical for overall central nervous system and neuronal function (Schonrock et al., 2012; Schonrock et al., 2010). Previous work has already shown that TDP-43 regulates the mature levels of miR-27b-3p and miR-181c-5p, and other members of the miR-181 family (miR-181a-d) in several cell lines (Chen et al., 2018; Di Carlo et al., 2013; Kawahara and Mieda-Sato, 2012). Thus, TDP-43 regulation on the biogenesis of miR-27b-3p and the miR-181a-d family likely represents a broad phenomenon rather than a cell-specific one.

Further, we showed that an induced cellular stress which causes reduced TDP-43 nuclear localization alters miRNA processing leading to a reduction in miR-27b-3p and miR-181c-5p, similar to what was seen after knockdown of TDP-43. This is a critical finding as cellular stress has been shown to drive TDP-43 from the nucleus to the cytoplasm in both *in vitro* and *in vivo* neuronal models (Khalfallah et al., 2018; McDonald et al., 2011; Moisse et al., 2009), indicating that cellular stress, while not the only effect, results in the reduction of nuclear TDP-43 levels to regulate miRNA biogenesis. This may be a major component to the pathogenesis of ALS where an extensive reduction in miRNA levels in spinal cord and motor neurons is observed (Campos-Melo et al., 2013; Emde et al., 2015).

In conclusion, we propose a biological mechanism by which under normal conditions TDP-43 is in a negative feedback network with miRNAs (i.e. miR-27b-3p and miR-181c-5p), and that this is perturbed during cell stress due to reduced TDP-43 nuclear localization. Thus, reduction of nuclear TDP-43 reduces miRNAs levels resulting in a de-repression of the *TARDBP* transcript, and ultimately, increased TDP-43 cytoplasmic levels. This biological mechanism

could have important implications for the pathogenesis of neurodegenerative diseases, such as

ALS, where the reduction of miRNA levels coincides with the upregulation and mis-localization

of TDP-43 (Campos-Melo et al., 2013; Emde et al., 2015; Koyama et al., 2016; Swarup et al.,

2011; Tan et al., 2007). Further, enhancement of miRNA processing at the level of DICER has

been shown to improve motor function of rodent models who carry ALS-related mutations in

TDP-43 (Emde et al., 2015). Since we and others have shown that TDP-43 affects miRNA

processing at multiple levels within the miRNA biogenesis pathway (Kawahara and Mieda-Sato,

2012), an enhancement of both the DROSHA and DICER complexes may be necessary to have

the greatest impact to slow ALS disease progression.

**5.6 References**

Amador-Ortiz, C., Lin, W.L., Ahmed, Z., Personett, D., Davies, P., Duara, R., Graff-Radford, N.R., Hutton, M.L., and Dickson, D.W. (2007). TDP-43 immunoreactivity in hippocampal sclerosis and Alzheimer's disease. Ann Neurol *61*, 435-445.

Arai, T., Hasegawa, M., Akiyama, H., Ikeda, K., Nonaka, T., Mori, H., Mann, D., Tsuchiya, K., Yoshida, M., Hashizume, Y.*, et al.* (2006). TDP-43 is a component of ubiquitin-positive tau-negative inclusions in frontotemporal lobar degeneration and amyotrophic lateral sclerosis. Biochem Biophys Res Commun *351*, 602-611.

Baradaran-Heravi, Y., Van Broeckhoven, C., and van der Zee, J. (2020). Stress granule mediated protein aggregation and underlying gene defects in the FTD-ALS spectrum. Neurobiol Dis *134*, 104639.

Bartel, D.P. (2018). Metazoan MicroRNAs. Cell *173*, 20-51.

Campos-Melo, D., Droppelmann, C.A., He, Z., Volkening, K., and Strong, M.J. (2013). Altered microRNA expression profile in Amyotrophic Lateral Sclerosis: a role in the regulation of NFL mRNA levels. Mol Brain *6*, 26.

Campos-Melo, D., Droppelmann, C.A., Volkening, K., and Strong, M.J. (2014). Comprehensive luciferase-based reporter gene assay reveals previously masked up-regulatory effects of miRNAs. Int J Mol Sci *15*, 15592-15602.

Chen, X., Fan, Z., McGee, W., Chen, M., Kong, R., Wen, P., Xiao, T., Chen, X., Liu, J., Zhu, L.*, et al.* (2018). TDP-43 regulates cancer-associated microRNAs. Protein Cell *9*, 848-866.

Deshaies, J.E., Shkreta, L., Moszczynski, A.J., Sidibe, H., Semmler, S., Fouillen, A., Bennett, E.R., Bekenstein, U., Destroismaisons, L., Toutant, J.*, et al.* (2018). TDP-43 regulates the alternative splicing of hnRNP A1 to yield an aggregation-prone variant in amyotrophic lateral sclerosis. Brain *141*, 1320-1333.

Di Carlo, V., Grossi, E., Laneve, P., Morlando, M., Dini Modigliani, S., Ballarino, M., Bozzoni, I., and Caffarelli, E. (2013). TDP-43 regulates the microprocessor complex activity during in vitro neuronal differentiation. Mol Neurobiol *48*, 952-963.

Dini Modigliani, S., Morlando, M., Errichelli, L., Sabatelli, M., and Bozzoni, I. (2014). An ALS-associated mutation in the FUS 3'-UTR disrupts a microRNA-FUS regulatory circuitry. Nat Commun *5*, 4335.

Emde, A., Eitan, C., Liou, L.L., Libby, R.T., Rivkin, N., Magen, I., Reichenstein, I., Oppenheim, H., Eilam, R., Silvestroni, A.*, et al.* (2015). Dysregulated miRNA biogenesis downstream of cellular stress and ALS-causing mutations: a new mechanism for ALS. EMBO J *34*, 2633-2651.

Fratta, P., Sivakumar, P., Humphrey, J., Lo, K., Ricketts, T., Oliveira, H., Brito-Armas, J.M., Kalmar, B., Ule, A., Yu, Y.*, et al.* (2018). Mice with endogenous TDP-43 mutations

exhibit gain of splicing function and characteristics of amyotrophic lateral sclerosis. EMBO J *37*.

Fujiya, M., Konishi, H., Mohamed Kamel, M.K., Ueno, N., Inaba, Y., Moriichi, K., Tanabe, H., Ikuta, K., Ohtake, T., and Kohgo, Y. (2014). microRNA-18a induces apoptosis in colon cancer cells via the autophagolysosomal degradation of oncogenic heterogeneous nuclear ribonucleoprotein A1. Oncogene *33*, 4847-4856.

Guil, S., and Caceres, J.F. (2007). The multifunctional RNA-binding protein hnRNP A1 is required for processing of miR-18a. Nat Struct Mol Biol *14*, 591-596.

Hawley, Z.C.E., Campos-Melo, D., and Strong, M.J. (2017). Novel miR-b2122 regulates several ALS-related RNA-binding proteins. Mol Brain *10*, 46.

Hawley, Z.C.E., Campos-Melo, D., and Strong, M.J. (2019). MiR-105 and miR-9 regulate the mRNA stability of neuronal intermediate filaments. Implications for the pathogenesis of amyotrophic lateral sclerosis (ALS). Brain Res *1706*, 93-100.

Kato, M., Han, T.W., Xie, S., Shi, K., Du, X., Wu, L.C., Mirzaei, H., Goldsmith, E.J., Longgood, J., Pei, J.*, et al.* (2012). Cell-free formation of RNA granules: low complexity sequence domains form dynamic fibers within hydrogels. Cell *149*, 753-767.

Kawahara, Y., and Mieda-Sato, A. (2012). TDP-43 promotes microRNA biogenesis as a component of the Drosha and Dicer complexes. Proc Natl Acad Sci U S A *109*, 3347-3352.

Keller, B.A., Volkening, K., Droppelmann, C.A., Ang, L.C., Rademakers, R., and Strong, M.J. (2012). Co-aggregation of RNA binding proteins in ALS spinal motor neurons: evidence of a common pathogenic mechanism. Acta Neuropathol *124*, 733-747.

Khalfallah, Y., Kuta, R., Grasmuck, C., Prat, A., Durham, H.D., and Vande Velde, C. (2018). TDP-43 regulation of stress granule dynamics in neurodegenerative disease-relevant cell types. Sci Rep *8*, 7551.

King, I.N., Yartseva, V., Salas, D., Kumar, A., Heidersbach, A., Ando, D.M., Stallings, N.R., Elliott, J.L., Srivastava, D., and Ivey, K.N. (2014). The RNA-binding protein TDP-43 selectively disrupts microRNA-1/206 incorporation into the RNA-induced silencing complex. J Biol Chem *289*, 14263-14271.

Koyama, A., Sugai, A., Kato, T., Ishihara, T., Shiga, A., Toyoshima, Y., Koyama, M., Konno, T., Hirokawa, S., Yokoseki, A.*, et al.* (2016). Increased cytoplasmic TARDBP mRNA in affected spinal motor neurons in ALS caused by abnormal autoregulation of TDP-43. Nucleic Acids Res *44*, 5820-5836.

Ling, S.C., Polymenidou, M., and Cleveland, D.W. (2013). Converging mechanisms in ALS and FTD: disrupted RNA and protein homeostasis. Neuron *79*, 416-438.

Liu-Yesucevitz, L., Bilgutay, A., Zhang, Y.J., Vanderweyde, T., Citro, A., Mehta, T., Zaarur, N., McKee, A., Bowser, R., Sherman, M.*, et al.* (2010). Tar DNA binding protein-43 (TDP-43) associates with stress granules: analysis of cultured cells and pathological brain tissue. PLoS One *5*, e13250.

McDonald, K.K., Aulas, A., Destroismaisons, L., Pickles, S., Beleac, E., Camu, W., Rouleau, G.A., and Vande Velde, C. (2011). TAR DNA-binding protein 43 (TDP-43) regulates stress granule dynamics via differential regulation of G3BP and TIA-1. Hum Mol Genet *20*, 1400-1410.

Mitchell, J.C., McGoldrick, P., Vance, C., Hortobagyi, T., Sreedharan, J., Rogelj, B., Tudor, E.L., Smith, B.N., Klasen, C., Miller, C.C.*, et al.* (2013). Overexpression of human wild-type FUS causes progressive motor neuron degeneration in an age- and dose-dependent fashion. Acta Neuropathol *125*, 273-288.

Moisse, K., Mepham, J., Volkening, K., Welch, I., Hill, T., and Strong, M.J. (2009). Cytosolic TDP-43 expression following axotomy is associated with caspase 3 activation in NFL-/- mice: support for a role for TDP-43 in the physiological response to neuronal injury. Brain Res *1296*, 176-186.

Molliex, A., Temirov, J., Lee, J., Coughlin, M., Kanagaraj, A.P., Kim, H.J., Mittag, T., and Taylor, J.P. (2015). Phase separation by low complexity domains promotes stress granule assembly and drives pathological fibrillization. Cell *163*, 123-133.

Morlando, M., Dini Modigliani, S., Torrelli, G., Rosa, A., Di Carlo, V., Caffarelli, E., and Bozzoni, I. (2012). FUS stimulates microRNA biogenesis by facilitating co-transcriptional Drosha recruitment. EMBO J *31*, 4502-4510.

Murakami, T., Qamar, S., Lin, J.Q., Schierle, G.S., Rees, E., Miyashita, A., Costa, A.R., Dodd, R.B., Chan, F.T., Michel, C.H.*, et al.* (2015). ALS/FTD Mutation-Induced Phase Transition of FUS Liquid Droplets and Reversible Hydrogels into Irreversible Hydrogels Impairs RNP Granule Function. Neuron *88*, 678-690.

Neumann, M., Sampathu, D.M., Kwong, L.K., Truax, A.C., Micsenyi, M.C., Chou, T.T., Bruce, J., Schuck, T., Grossman, M., Clark, C.M.*, et al.* (2006). Ubiquitinated TDP-43 in frontotemporal lobar degeneration and amyotrophic lateral sclerosis. Science *314*, 130-133.

Patel, A., Lee, H.O., Jawerth, L., Maharana, S., Jahnel, M., Hein, M.Y., Stoynov, S., Mahamid, J., Saha, S., Franzmann, T.M.*, et al.* (2015). A Liquid-to-Solid Phase Transition of the ALS Protein FUS Accelerated by Disease Mutation. Cell *162*, 1066-1077.

Ratti, A., and Buratti, E. (2016). Physiological functions and pathobiology of TDP-43 and FUS/TLS proteins. J Neurochem *138 Suppl 1*, 95-111.

Schonrock, N., Humphreys, D.T., Preiss, T., and Gotz, J. (2012). Target gene repression mediated by miRNAs miR-181c and miR-9 both of which are down-regulated by amyloid-beta. J Mol Neurosci *46*, 324-335.

Schonrock, N., Ke, Y.D., Humphreys, D., Staufenbiel, M., Ittner, L.M., Preiss, T., and Gotz, J. (2010). Neuronal microRNA deregulation in response to Alzheimer's disease amyloid-beta. PLoS One *5*, e11070.

Svetoni, F., Frisone, P., and Paronetto, M.P. (2016). Role of FET proteins in neurodegenerative disorders. RNA Biol *13*, 1089-1102.

Swarup, V., Phaneuf, D., Dupre, N., Petri, S., Strong, M., Kriz, J., and Julien, J.P. (2011). Deregulation of TDP-43 in amyotrophic lateral sclerosis triggers nuclear factor kappaB-mediated pathogenic pathways. J Exp Med *208*, 2429-2447.

Tan, C.F., Eguchi, H., Tagawa, A., Onodera, O., Iwasaki, T., Tsujino, A., Nishizawa, M., Kakita, A., and Takahashi, H. (2007). TDP-43 immunoreactivity in neuronal inclusions in familial amyotrophic lateral sclerosis with or without SOD1 gene mutation. Acta Neuropathol *113*, 535-542.

Volkening, K., Leystra-Lantz, C., Yang, W., Jaffee, H., and Strong, M.J. (2009). Tar DNA binding protein of 43 kDa (TDP-43), 14-3-3 proteins and copper/zinc superoxide dismutase (SOD1) interact to modulate NFL mRNA stability. Implications for altered RNA processing in amyotrophic lateral sclerosis (ALS). Brain Res *1305*, 168-182.

Weskamp, K., and Barmada, S.J. (2018). TDP43 and RNA instability in amyotrophic lateral sclerosis. Brain Res *1693*, 67-74.

**Chapter 6**

**Discussion and Conclusion**

**6.1 Summary of Results**

In this dissertation, I aimed to elucidate the potential consequences of reduced miRNA levels as seen in ALS, and to understand the mechanism by which miRNAs may become dysregulated in the first place. Data presented showed that reduced miRNA expression may contribute to both RNA-binding protein and intermediate filament pathogenesis as many ALS-linked miRNAs regulate these two protein groups as shown within *in vitro* cell models. Further, I identified a novel negative feedback network between TDP-43 and miRNAs in HEK293T cells which may provide insight into how miRNA levels become reduced in ALS motor neurons.

Chapters 2-3 highlighted several ALS-associated miRNAs that may contribute to the loss of intermediate filament stoichiometry in ALS. Previous work had shown that ALS-associated miRNAs could contribute to the suppression of *NEFL* mRNA—a common phenomenon observed in motor neurons of patients with ALS (Bergeron et al., 1994; Campos-Melo et al., 2013; Wong et al., 2000). However, in mature motor neurons there are 5 main intermediate filaments expressed (NFL, NFM, NFH, PRPH and INA), and it is the overall loss of stoichiometry between these 5 intermediate filaments that drives intermediate filament pathology (Szaro and Strong, 2010). Therefore, I sought to determine the ALS-linked miRNAs that are involved in regulating overall intermediate filament stoichiometry. I identified two miRNAs (miR-105-5p and miR-9-5p) that showed reduced expression in ALS, that are expressed in motor neurons and that regulate the mRNA levels of *NEFL*, *PRPH* and *INA*. MiR-105-5p enhanced the expression of *NEFL* and *PRPH* but suppressed *INA* expression while miR-9-5p suppressed the expression of all three intermediate filaments of interest in the human neuronal-derived cell line IMR-32 (Hawley et al., 2019).

In chapter 3, a series of motor neuron expressing miRNAs that are reduced in ALS were identified to suppress the levels of a reporter gene when interacting with the 3'UTR of either *NEFM* (miR-92a-3p and miR-125b-5p) or *NEFH* (miR-9-5p, miR-20b-5p, miR-92a-3p, miR-223-3p) providing more examples of miRNAs responsible for regulating intermediate filament stoichiometry (Campos-Melo et al., 2018). All this suggests that several miRNAs are responsible for the tight regulation of intermediate filament stoichiometry, and loss of these miRNAs, as seen in ALS, could contribute to intermediate filament pathogenesis.

Chapter 4 focused on ALS-linked miRNAs that are responsible for the regulation of three RNA-binding proteins—TDP-43, FUS and RGNEF—that are known to co-aggregate together in ALS motor neurons (Keller et al., 2012). I identified miR-b2122 to be a central regulator of TDP-43, FUS and RGNEF expression in SH-SY5Y cells—a human neuronal-derived cell line—and further, provided evidence that miR-194-5p may be responsible for TDP-43 and FUS gene silencing. Further, I described an ALS-associated mutation in the *FUS* 3'UTR that was located in the MRE of miR-b2122. This mutation disrupted the ability of miR-b2122 to bind to the 3'UTR of *FUS* to regulate gene expression, providing a genetic link between miRNA regulation and ALS (Hawley et al., 2017b). Since TDP-43 has been shown to be overexpressed in ALS spinal cord and motor neurons and FUS overexpression has been known to cause ALS-like phenotypes within *in vitro* and *in vivo* models, it is clear that the loss of homeostatic levels of these proteins contributes to the disease pathogenesis (Koyama et al., 2016; Mitchell et al., 2013; Sabatelli et al., 2013; Swarup et al., 2011). Thus, the loss of miR-194-5p and miR-b2122 in ALS motor neurons could be a major contributor to the disease progression.

Finally, in Chapter 5, a negative feedback loop between TDP-43 and two ALS-linked miRNAs (miR-27b-3p and miR-181c-5p) that is dependent on TDP-43 nuclear localization was

identified in HEK293T cells, thus providing a biological mechanism that may be disrupted in

ALS (Hawley et al., 2020). While I looked at both TDP-43 and FUS, I did not identify a negative

feedback loop between FUS and miRNAs. However, previous work has shown that FUS is in a

negative feedback loop with two other ALS-linked miRNAs (miR-141-3p and miR-200a-3p;

Dini Modigliani et al., 2014), indicating that this biological mechanism does exist for FUS.

Further, TDP-43 regulated the expression of miR-27b-3p and miR-181c-5p at different levels in

the miRNA biogenesis pathway, as reduced TDP-43 levels led to increased pri-miR-181c and

reduced cytoplasmic pre-miR-181c, while lowering mature miR-27b-3p levels with no changes

to either miR-27b primary or precursor levels. This suggested that TDP-43 regulates miRNAs at

several levels in the biogenesis pathway, consistent with what has been seen previously

(Kawahara and Mieda-Sato, 2012).

Overall, the data presented in this dissertation demonstrates that reduced miRNA levels

in motor neurons of patients with ALS likely contributes to both intermediate filament and RNA-

binding protein pathogenesis in ALS. Further, I have provided a biological mechanism that

provides evidence that loss of TDP-43 nuclear localization, as seen in ALS, may contribute to

the reduction of miRNAs seen in ALS motor neurons.

**6.2 Implications**

**6.2.1 MiRNA network that regulates intermediate filament stoichiometry**

Proper intermediate filament stoichiometry is considered necessary for the formation and

maintenance of cytoskeleton structures in neuronal cells (Szaro and Strong, 2010). Alterations to

this stoichiometry have been associated with the formation of intermediate filament aggregates

that are observed in ALS motor neurons (Beaulieu and Julien, 2003; Beaulieu et al., 1999; Kriz

et al., 2000; Lee et al., 1994; Wong et al., 2000; Zhu et al., 1997). Previous work has indicated

two ALS-related RNA-binding proteins (TDP-43 and RGNEF) and miRNAs play essential roles in regulating the levels of *NEFL* mRNA (Campos-Melo et al., 2013; Volkening et al., 2010; Volkening et al., 2009). The work presented here identified 8 miRNAs, in addition to the five miRNAs previously shown to regulate *NEFL* (Campos-Melo et al., 2013; Ishtiaq et al., 2014), that are responsible for regulating the transcript levels of the five main intermediate filaments (*NEFL*, *NEFM*, *NEFH*, *PRPH* and *INA*) expressed in mature neurons (Campos-Melo et al., 2018; Hawley et al., 2019).

Identification of these interactions between miRNAs and intermediate filaments highlights the complex network of *trans*-acting regulatory elements that are required to maintain the appropriate spatiotemporal stoichiometry of these proteins. This fact paired with the evidence that these miRNAs are reduced in ALS shows that a highly sophisticated regulatory network between miRNAs and intermediate filaments is likely to be disrupted in ALS, thus contributing to the formation of intermediate filament cytoplasmic aggregates. Beyond miRNAs, we know that RNA-binding proteins play an integral role in post-transcriptionally regulating neurofilament stoichiometry, including TDP-43, RGNEF, hnRNPK, ALDOA, ALDOC, HuB, 14-3-3 and hnRNPE1/E2 (Antic et al., 1999; Canete-Soler et al., 2005; Droppelmann et al., 2013; Ge et al., 2007; Stefanizzi and Canete-Soler, 2007; Thyagarajan and Szaro, 2004, 2008; Volkening et al., 2010; Volkening et al., 2009). Amongst these proteins, TDP-43, RGNEF and 14-3-3 have been associated with ALS pathology, indicating that the dysregulation of these proteins could also contribute to loss of intermediate filament stoichiometry (Keller et al., 2012). It is still unclear how miRNAs and RNA-binding proteins work together to finely regulate intermediate stoichiometry and how their co-dysregulation in ALS contributes to overall intermediate filament pathology.

Further, there is evidence that long non-coding RNAs (lncRNAs), small nucleolar RNAs (snoRNAs), and circular RNAs (circRNAs) are increasingly associated with ALS (Dolinar et al., 2019; Errichelli et al., 2017; Nishimoto et al., 2013; Riva et al., 2016; Salvatori et al., 2020). This provides even further complexity, as miRNAs, lncRNAs, snoRNAs, circRNAs and RNA-binding proteins work together to tightly regulate gene expression both transcriptionally and post-transcriptionally (Salvatori et al., 2020). While it is still unclear how lncRNAs, snoRNAs and circRNAs contribute to ALS pathogenesis, it will be interesting to determine if these non-coding RNA molecules play an essential role in regulating neuronal intermediate stoichiometry and how that may be affected in ALS.  However, the understanding of the role of ALS-linked miRNAs in neuronal intermediate filament post-transcriptional regulation has allowed us to develop a deeper knowledge of the potential pathogenesis of these proteins in ALS. This has provided a foundation to further explore these networks in neuron models to determine how these miRNAs work with RNA-binding proteins, and potentially other non-coding RNA species, to regulate neuronal intermediate filament stoichiometry, and how this system may be manipulated to prevent the loss of intermediate filament stoichiometry in ALS motor neurons (Wong et al., 2000).

### 6.2.2 Potential contributions of miRNAs in RNA-binding protein pathogenesis

An overwhelming amount of evidence has shown that the simple accumulation of LCD-containing proteins, like the RNA-binding proteins observed in ALS, can cause them to phase separate into irreversible insoluble aggregates (Conicella et al., 2016; Kato et al., 2012; Murakami et al., 2015; Murray et al., 2017). Thus, several research groups have searched for ways to prevent the toxic cytoplasmic accumulation of these proteins as potential therapeutics (Barmada et al., 2010; Tamaki et al., 2018; Tradewell et al., 2012). The work presented in this

dissertation provides a unique perspective in the potential use of miRNAs as a therapeutic target to prevent the accumulation of these proteins into cytoplasmic aggregates.

The data provided in this dissertation indicates that reduced miRNA levels, as seen in ALS, could contribute to the overexpression, and potentially the formation of cytoplasmic aggregates by RNA-binding proteins. MiR-b2122 was identified to silence the mRNA expression of three RNA-binding proteins (TDP-43, FUS and RGNEF) that co-aggregate with each other in ALS motor neurons (Hawley et al., 2017b; Keller et al., 2012). Overexpression of TDP-43 and FUS have both been shown to result in the formation of cytoplasmic aggregates in both *in vitro* and *in vivo* models, and further, both have been shown to have increased levels in the spinal cord of ALS patients (Dini Modigliani et al., 2014; Hawley et al., 2017b; Koyama et al., 2016; Mitchell et al., 2013; Swarup et al., 2011; Xu et al., 2010). In our work, we had identified a relationship between reduced levels of miR-b2122 and increased levels of FUS in the spinal cord of sALS patients, and an ALS-associated genetic variant in the *FUS* mRNA 3'UTR that prevents miR-b2122 from binding to the *FUS* 3'UTR to regulate gene expression (Hawley et al., 2017b). All this put together, suggests miR-b2122 may be a potential therapeutic target to reduce the RNA-binding protein expression via gene silencing and prevent the aggregation of all three of these proteins.

### 6.2.3 Identification of novel negative feedback network

A novel negative feedback network between TDP-43 and miRNAs was identified providing further insight biological mechanisms that may be affected in ALS motor neurons. The identification of this network not only has major implications for our understanding ALS disease progression, but as well our understanding of basic biological networks.

Negative feedback networks are classic self-regulating biological systems designed to maintain homeostasis (Tsang et al., 2007). Since miRNAs have been described as the "master regulators", it is not surprising that miRNAs are involved in several negative and positive feedback networks. Further, in a panel of over 70 pre-miRNA baits, researchers were able to pulldown over 180 RNA-binding proteins that preferentially bound to specific miRNA groups which demonstrated the vast network of RNA-binding proteins that participate in the biogenesis of a small subset of miRNAs (Treiber et al., 2017). Several RNA-binding proteins have been shown to be in negative, positive and double negative feedback networks with miRNAs indicating the importance of these two groups to work together to maintain homeostasis (Tsang et al., 2007).

Under physiological stress conditions, several RNA-binding proteins leave the nucleus and enter the cytoplasm to form stress granule structures, including TDP-43 (Protter and Parker, 2016). Further, cellular stress has generally shown to cause a reduction in miRNA processing (Emde et al., 2015), as I showed with miR-27b-3p and miR-181c-5p. Therefore, one hypothesis may be that reduced miRNA processing during stress allows for de-repression of RNA-binding proteins needed for stress granule formation, but overaccumulation of LCD-containing RNA-binding proteins—which are prone to aggregate—either through chronic or repeated stresses may induce the formation of insoluble cytoplasmic aggregates. Thus, while reduced miRNA processing may be beneficial for a rapid stress response, repeated or chronic stresses increase the risk of developing cytoplasmic aggregates that are toxic to the cell.

The identification of a negative feedback network between TDP-43 and miRNAs is the second negative feedback network that has been identified between ALS-related miRNAs and RNA-binding proteins. The first was identified between FUS and two miRNAs—miR-141/200a-

3p (Dini Modigliani et al., 2014). Beyond TDP-43 and FUS, other ALS-related RNA-binding proteins have been implicated in the miRNA biogenesis pathway including TAF15, EWSR1, hnRNPA1, hnRNPA2B1, MATR3, TIA-1 and ATXN2 (Alarcon et al., 2015; Ballarino et al., 2013; Guil and Caceres, 2007; Kapeli et al., 2016; Kooshapur et al., 2018; Ouyang et al., 2017; Sanchez-Jimenez et al., 2013; Weiss et al., 2019). Therefore, several regulatory networks between miRNAs and RNA-binding proteins may be disrupted in ALS. Identification of these regulatory networks, how they are disrupted in ALS, there contribution to ALS pathogenesis, and how to restore these networks will assist in our understanding of ALS development and potential therapeutic targets.

Further, TDP-43 forms cytoplasmic aggregates in 97% of all cases regardless of genetic background (Ling et al., 2013). Therefore, identification for pathways that may explain the accumulation of TDP-43 in the cytoplasm has become critical. Loss of a negative feedback between TDP-43 and miRNA due to loss of nuclear localization, as shown in Chapter 5, may contribute to the formation of TDP-43 cytoplasmic aggregates in ALS. Therefore, if we are able to identify this negative feedback loop in motor neuron models, and further, show it is disrupted in ALS motor neuron models, it will be necessary to target this pathway to see if we can restore homeostatic levels of miR-27b-3p and miR-181c-5p to lower levels of TDP-43 to hopefully alleviate ALS-like phenotypes.

**6.2.4 Development of therapeutics targeting miRNA pathways**

In this dissertation, I have identified 10 ALS-linked miRNAs that could contribute to intermediate filament and RNA-binding protein pathogenesis. This is likely an underrepresentation of the total amount of miRNAs that are involved in in the disease pathogenesis. This data highlights that there is not a single miRNA that will ameliorate the

dysfunctional physiology observed in ALS motor neurons, but rather a whole host of miRNAs, each individually contributing to the disease process. This is critical to understand if we are going to develop therapeutics that target miRNA pathways.

Targeting individual miRNAs in ALS likely will have minimal effects in terms of a therapeutic. Rather we need to focus on developing drugs that are able to reboot the miRNA biogenesis pathway. In chapter 5 of this thesis, I showed that reduced nuclear TDP-43, as seen in 97% of all ALS cases, can inhibit efficient processing of miRNAs at multiple levels in the biogenesis pathway. Thus, rather than targeting specific miRNAs, developing therapeutics that increase the efficiency of DROSHA and DICER to process pri- and pre-miRNAs, respectively, may be a better approach. Enoxacin is a drug that can enhance miRNA biogenesis by interacting with TRBP to enhance DICER pre-miRNA processing (Shan et al., 2008). In ALS transgenic mouse models containing ALS-causing mutations in either SOD1 or TDP-43, enoxacin has been proven to delay motor deficiencies that are developed in these models, thus providing some evidence that enhancement of the miRNA biogenesis pathway could be an effective therapeutic approach (Emde et al., 2015). However, many of the RNA-binding proteins that are involved in ALS also interact with DROSHA to promote miRNA biogenesis. Thus, a better therapeutic may be one that improves the efficiency of both DROSHA and DICER processing.

Two acetylase inhibitors—trichostatin A and nicotinamide—have been shown to increase levels of DROSHA and enhance miRNA processing (Tang et al., 2013). In particular, nicotinamide is derivative form of vitamin B3 which has been implicated as potential therapeutic for several neurodegenerative diseases, including ALS (Fricker et al., 2018; Naia et al., 2017; Schondorf et al., 2018; Xie et al., 2019; Zhou et al., 2020). Nicotinamide is a critical metabolite involved in converting NADH to NAD+, an important process for the production of ATP

(Poddar et al., 2019). Low levels of NAD+ has been seen in animal models of Alzheimer's Disease, Parkinson's Disease, Huntingtion's Disease and ALS, suggesting that oxidation of NADH may be a deficient process in neurodegeneration (Fricker et al., 2018; Zhou et al., 2020). Further, nicotinamide has been shown to prevent DNA damage, apoptosis, maintain cell membrane structure and reduce oxidative stress, all of which has been associated with several neurodegenerative diseases (Surjana et al., 2010; Turunc Bayrakdar et al., 2014). Recent work in ALS SOD1 mouse models has shown that nicotinamide may be a potential for therapeutic for ALS patients who contain SOD1 mutations (Zhou et al., 2020). Therefore, while nicotinamide is already being considered for an ALS therapeutic, understanding whether these beneficial affects occur in part by restoring miRNA homeostasis will be essential to understand its therapeutic effect and whether it can be used for non-mtSOD1 ALS patients.

While further work in iPSC-derived motor neuronal cell lines and *in vivo* models still need to be done, restoring miRNA production may be a potential therapeutic avenue by combining nicotinamide and enoxacin to increase both DROSHA and DICER activity, respectively, and in turn, overall miRNA processing.

**6.3 Caveats**

The data presented in this dissertation has identified critical ALS-linked miRNAs responsible for regulating intermediate filaments and RNA-binding proteins related to the disease, and a negative feedback network, that if lost, may contribute to driving the disease pathogenesis. Despite the significance of this work in developing our understanding of the biological networks that connect ALS-associated miRNAs, intermediate filaments and RNA-binding proteins, there are some caveats that should be taken into consideration.

First, the cell models in which these interactions were characterized limit our ability to determine how significant these interactions are to ALS. As previously mentioned, miRNA expression, regulation and function can be highly dependent on cell type, cell environment, and altered cell physiology (Berezikov, 2011; Hawley et al., 2017a). Therefore, if we really want to understand these networks of miRNAs that are associated with ALS, we need to study these interactions in motor neuron models. Research using human iPSC-derived motor neuron models has proven to be effective in understanding specific aspects of motor neuron biology that would otherwise be missed if looking in other cell models. For example, the regulation of TDP-43 on *STMN2* expression and its significance to ALS was discovered only because researchers used human iPSC-derived motor neuron models. This would have not been identified looking in other non-neuronal models, as *STMN2* has neuronal specific expression, and further, the addition of the cryptic exon, as seen in *STMN2* when TDP-43 expression is suppressed, is a human specific affect (Klim et al., 2019; Melamed et al., 2019). All this indicates using the appropriate models are important when discussing disease. A major experiment in our work was the FISH analyses to ensure that the miRNAs we were studying in our models were also expressed in motor neurons, and hence, provide an increased likelihood that the biological pathways identified in our models also exist in motor neurons. However, while our models allowed us to find several pathways that are likely related to the disease, we need to move into more complex models, and start understanding the specific relationship between miRNAs, intermediate filaments and RNA-binding proteins within motor neurons.

Second, while we have shown several miRNAs that likely contribute to the pathology of the disease, at this point we have no data to support that loss of miRNA expression can induce the formation of cytoplasmic aggregates similar to those seen in ALS motor neurons. Mutations

in the 3'UTR of *FUS* that disrupt miRNA binding and gene silencing can induce cytoplasmic aggregates of FUS protein (Dini Modigliani et al., 2014; Morlando et al., 2012). However, it is still unclear whether the resulting pathology from those mutations is caused from loss of miRNA regulation or other factors. Further, while several lines of work have shown loss of intermediate filament stoichiometry induces the formation of intermediate filament aggregates (Robertson et al., 2002), does loss of miRNA regulators that alter the stoichiometry enough to induce intermediate filament pathology is still in question.

Finally, our assays where miRNA expression was either overexpressed or inhibited could have technical experimental issues. This is because when you transfect a miRNA mimic, the amount of miRNA that is present within the cellular system could easily out compete other *trans*-acting molecules that would normally regulate your gene of interest, even if your miRNA candidate does not regulate it normally. Further, ablating miRNA function in a cell via an inhibitor does not necessarily represent the changes seen in ALS spinal cord where we generally see reduced levels and not complete loss of the miRNA. Thus, we need to determine the threshold in which the change of expression in our miRNA candidates results in a change in the expression of our genes of interest, and determine if that is representative of what is seen in ALS spinal cord and motor neurons.

Studying how reduced expression of specific ALS-related miRNAs using *in vitro* and *in vivo* motor neuron models will be necessary to understand the contribution of miRNAs to disease pathology and whether loss of miRNA regulation alone can drive ALS-like proteinopathies and motor neuron death. These are critical caveats to consider when interpreting the data, and further experiments will need to be done in motor neuron models to more accurately understand MotomiR biology and how loss of these miRNAs may contribute to the pathology of the disease.

**6.4 Future Directions**

As mentioned in the previous section, a major future direction for this work is to determine whether the loss of miRNA function can induce intermediate filament and/or RNA-binding protein ALS-like proteinopathies. For example, does reduction or loss of miR-105-5p or miR-9-5p—two miRNAs know to regulate *NEFL*, *PRPH* and *INA* mRNA expression—result in intermediate filament aggregation? Does loss of miR-b2122 lead to cytoplasmic aggregates of TDP-43, FUS and RGNEF? The answer to these questions will be necessary to understand the contribution these miRNAs have in the progression of the disease. Some evidence has shown that knocking out *Dicer* in mouse motor neurons can recapitulate loss of intermediate filament stoichiometry and induce motor neuron death (Haramati et al., 2010). However, knockout of *Dicer* would cause a global downregulation of miRNAs in motor neurons and does not provide any information on specific miRNAs. Therefore, further analyzing the miRNAs identified in this dissertation and whether loss of these miRNAs via knockdown or knockout models could contribute to both intermediate filament and RNA-binding protein dysregulation, ALS-like pathologies and motor neuron death will help us to understand their contribution to disease pathogenesis.

Another important factor to consider is that miRNAs are promiscuous molecules where one miRNA can have many targets, as seen in the work presented in this dissertation. While I focused on the affect miRNA candidates would have on RNA-binding proteins and intermediate filaments, there could be other pathways affected due to the loss of the miRNAs I studied. For example, miR-105-5p and miR-9-5p, two miRNAs shown to regulate intermediate filament expression in this dissertation (Hawley et al., 2019), have also been shown to suppress the expression of several cell-cycle genes to promote cell-cycle arrest (Zhang et al., 2017; Zhang et

al., 2019). One theory in ALS is that many of these cell-cycle genes that are normally suppressed in post-mitotic motor neurons are activated in ALS motor neurons, putting cells in a S phase rather than a $G_0$ phase (Ranganathan and Bowser, 2003; Ranganathan and Bowser, 2010; Sharma et al., 2017). The re-entry of post-mitotic neurons into the cell-cycle has been shown to lead to activation of apoptotic pathways and subsequent neuron death (Sharma et al., 2017). Thus, reduced levels of miR-105-5p and miR-9-5p, as seen in ALS, may contribute to the re-entry of ALS motor neurons into the cell-cycle, triggering apoptotic pathways, rather than disrupting intermediate filament stoichiometry, or the loss of these miRNAs could be contributing to both. Moving forward it will be necessary to determine all the pathways in which these miRNAs are contributing to in motor neurons to understand the full impact of the loss of these miRNAs in ALS.

In chapters 2 and 4, miRNAs that were predicted to regulate all our intermediate filaments or RNA-binding proteins of interest but were previously shown to have no change in expression in ALS spinal cord were not considered for our study (**Fig. 2.1 & 4.1**). This does not mean these miRNAs are not important. This is because if they are unchanged, they may become the dominant regulators of our genes of interest when the other miRNAs are reduced. Therefore, it will be crucial to not only determine how miRNAs that have altered levels in ALS affect the expression of our genes of interest, but as well as those miRNAs that are unchanging in ALS spinal cord and motor neurons.

Genetic association studies focusing on miRNA encoding regions could have a massive impact on our understanding of the relevance of miRNAs in ALS pathogenesis. As previously mentioned, mutations within the *FUS* 3'UTR located in two MREs—miR-141/200a-3p and miR-b2122—cause overexpression and cytoplasmic aggregates of FUS protein, like the pathology

seen in ALS motor neurons (Dini Modigliani et al., 2014; Hawley et al., 2017b; Morlando et al., 2012). This gives us an indication that loss of miRNA regulation on critical genes could contribute to the disease pathogenesis, giving significance to the mass downregulation of miRNAs seen in the spinal motor neurons of ALS patient groups. More recently, several rare mutations were identified in the miR-218 gene of patients with ALS (Reichenstein et al., 2019). These are the first genetic variants to date that have been identified in miRNA regions of the genome that are associated with ALS. Mutations in miR-218 reduced its processing by DICER, and further, less of this miRNA led to reduce motor neuron activity (Reichenstein et al., 2019). More genetic studies like these could identify miRNAs critical to motor neuron function and disease, better enabling us to find therapeutic targets. Historically, genetic studies have focused on coding regions of the genome with little work done outside those regions. However, now knowing non-coding regions of the genome contain critical genetic information to regulate cell physiology, expanding our efforts to look at miRNA genetic material may further drive our understanding of miRNAs role in disease pathogenesis and which miRNAs are the most critical to disease development.

**6.5 Conclusion**

The research presented in this dissertation provided a foundational understanding of the potential consequence and cause of miRNA dysregulation in ALS. With the use of *in vitro* models, several miRNAs were identified to be critical for the regulation of RNA-binding protein expression and intermediate filament stoichiometry, and thus, loss of these miRNAs, as seen in ALS, may contribute to the pathogenesis of these two protein groups (**Fig. 6.1**). Finally, a novel negative feedback network between TDP-43 and miRNAs was identified in HEK293T cell models which could have major implications in our understanding of not only ALS development,

but other neurodegenerative diseases that have TDP-43 proteinopathies. Knowing that reduced miRNAs may play a major role in ALS pathogenesis, it is now time to move forward into *in vitro* and *in vivo* motor neuron models, which is a critical step if we are to develop potential therapeutics that target these miRNA regulatory networks.

260
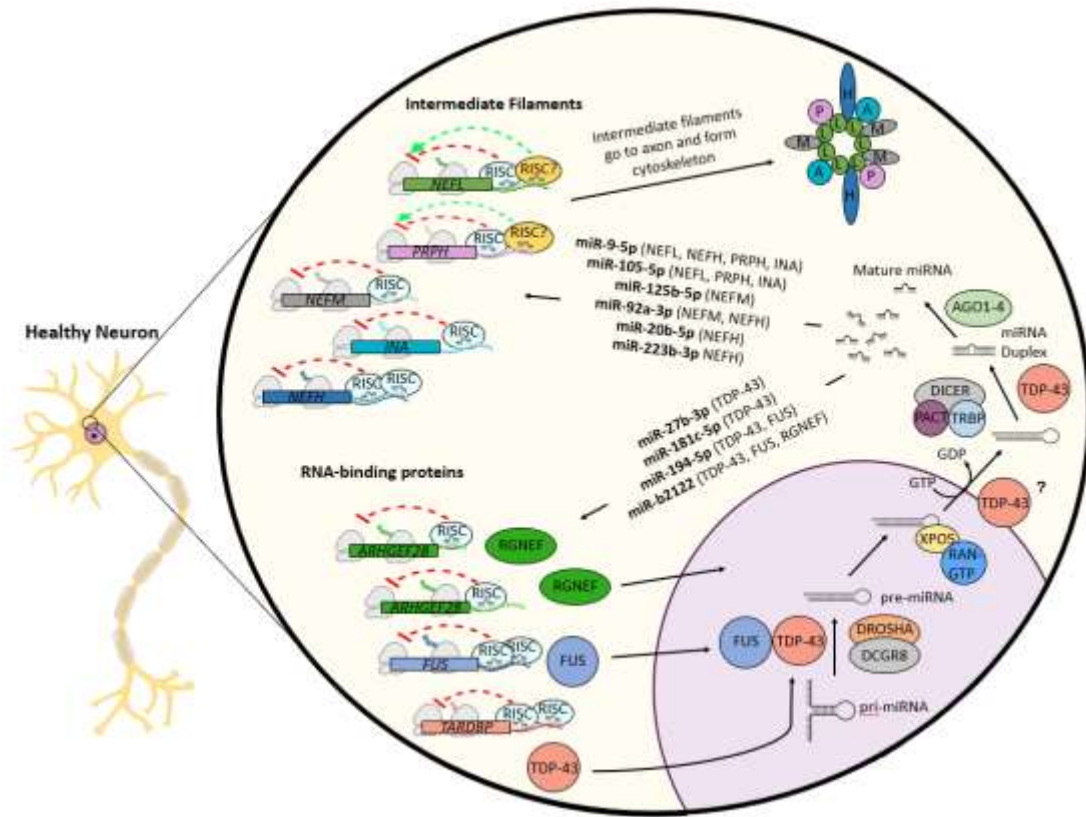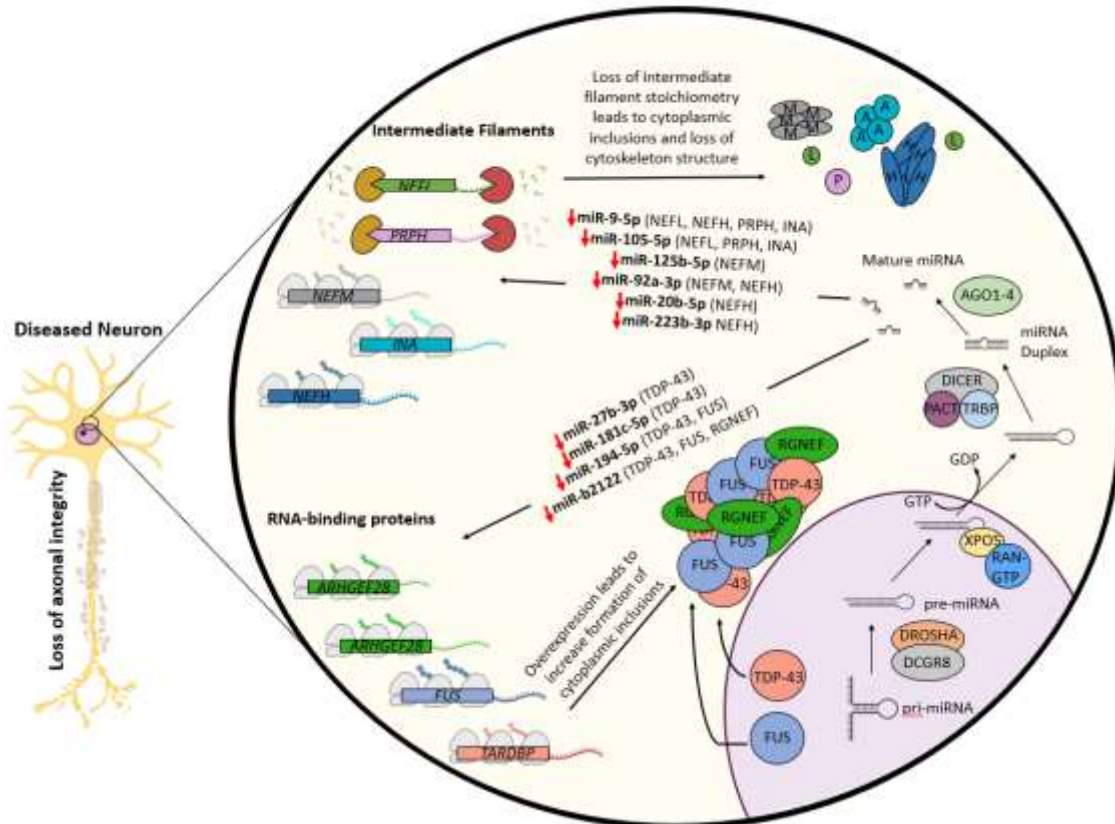
**Figure 6.1. Hypothesis of miRNA contribution to ALS pathogenesis.** (A) Healthy motor

neuron. TDP-43 contributes to miRNA biogenesis by assisting in pri- and pre-miRNA

processing with DROSHA and DICER complexes, respectively. Further, we provided evidence

that TDP-43 potentially assists in pre-miRNA export. FUS also assists in pri-miRNA processing.

Certain miRNAs, as identified in this thesis, target RNA-binding protein transcripts to suppress

and limit their expression. We showed this creates a negative feedback loop between TDP-43

and miR-27b-3p/miR-181c-5p and suggests that these regulatory networks are essential in

maintaining homeostatic levels of RNA-binding proteins and miRNAs. Further, we showed that

certain ALS-linked miRNAs target neuronal intermediate filament transcripts to promote or

suppress their expression, which is essential in maintaining stochiometric levels of intermediate

filament proteins (NFL [L], NFM [M], NFH [H], PRPH [P], or INA [A]) . This allows for proper

cytoskeleton formation, which is necessary to maintain axonal integrity, and in turn, overall

neuronal transport and function. (B) Diseased motor neuron. Due to the loss of TDP-43 and FUS

nuclear (purple) localization and their formation into cytoplasmic (yellow) inclusions, reduced

miRNA processing is observed. Lower miRNA levels result in de-repression of ALS-linked

RNA-binding proteins such as TDP-43, FUS and RGNEF. This rise in production of RNA-

binding proteins results in increased formation of toxic cytoplasmic inclusions through phase

separation. Further, lower miRNA levels will cause loss of intermediate filament stoichiometry

due to either degradation or overexpression of intermediate filament transcripts. This results in

intermediate filament cytoplasmic inclusions and loss of cytoskeleton formation, and

subsequentially, loss of axonal integrity. Overall, I hypothesize that reduced miRNAs levels, as

seen in ALS, results in the increased formation of toxic cytoplasmic inclusions and a loss of

proper cytoskeleton formation leading to motor neuron death.

## 6.6 References

Alarcon, C.R., Goodarzi, H., Lee, H., Liu, X., Tavazoie, S., and Tavazoie, S.F. (2015). HNRNPA2B1 Is a Mediator of m(6)A-Dependent Nuclear RNA Processing Events. Cell *162*, 1299-1308.

Antic, D., Lu, N., and Keene, J.D. (1999). ELAV tumor antigen, Hel-N1, increases translation of neurofilament M mRNA and induces formation of neurites in human teratocarcinoma cells. Genes Dev *13*, 449-461.

Ballarino, M., Jobert, L., Dembele, D., de la Grange, P., Auboeuf, D., and Tora, L. (2013). TAF15 is important for cellular proliferation and regulates the expression of a subset of cell cycle genes through miRNAs. Oncogene *32*, 4646-4655.

Barmada, S.J., Skibinski, G., Korb, E., Rao, E.J., Wu, J.Y., and Finkbeiner, S. (2010). Cytoplasmic mislocalization of TDP-43 is toxic to neurons and enhanced by a mutation associated with familial amyotrophic lateral sclerosis. J Neurosci *30*, 639-649.

Beaulieu, J.M., and Julien, J.P. (2003). Peripherin-mediated death of motor neurons rescued by overexpression of neurofilament NF-H proteins. J Neurochem *85*, 248-256.

Beaulieu, J.M., Nguyen, M.D., and Julien, J.P. (1999). Late onset of motor neurons in mice overexpressing wild-type peripherin. J Cell Biol *147*, 531-544.

Berezikov, E. (2011). Evolution of microRNA diversity and regulation in animals. Nat Rev Genet *12*, 846-860.

Bergeron, C., Beric-Maskarel, K., Muntasser, S., Weyer, L., Somerville, M.J., and Percy, M.E. (1994). Neurofilament light and polyadenylated mRNA levels are decreased in amyotrophic lateral sclerosis motor neurons. J Neuropathol Exp Neurol *53*, 221-230.

Campos-Melo, D., Droppelmann, C.A., He, Z., Volkening, K., and Strong, M.J. (2013). Altered microRNA expression profile in Amyotrophic Lateral Sclerosis: a role in the regulation of NFL mRNA levels. Mol Brain *6*, 26.

Campos-Melo, D., Hawley, Z.C.E., and Strong, M.J. (2018). Dysregulation of human NEFM and NEFH mRNA stability by ALS-linked miRNAs. Mol Brain *11*, 43.

Canete-Soler, R., Reddy, K.S., Tolan, D.R., and Zhai, J. (2005). Aldolases a and C are ribonucleolytic components of a neuronal complex that regulates the stability of the light-neurofilament mRNA. J Neurosci *25*, 4353-4364.

Conicella, A.E., Zerze, G.H., Mittal, J., and Fawzi, N.L. (2016). ALS Mutations Disrupt Phase Separation Mediated by alpha-Helical Structure in the TDP-43 Low-Complexity C-Terminal Domain. Structure *24*, 1537-1549.

Dini Modigliani, S., Morlando, M., Errichelli, L., Sabatelli, M., and Bozzoni, I. (2014). An ALS-associated mutation in the FUS 3'-UTR disrupts a microRNA-FUS regulatory circuitry. Nat Commun *5*, 4335.

Dolinar, A., Koritnik, B., Glavac, D., and Ravnik-Glavac, M. (2019). Circular RNAs as Potential Blood Biomarkers in Amyotrophic Lateral Sclerosis. Mol Neurobiol *56*, 8052-8062.

Droppelmann, C.A., Keller, B.A., Campos-Melo, D., Volkening, K., and Strong, M.J. (2013). Rho guanine nucleotide exchange factor is an NFL mRNA destabilizing factor that forms cytoplasmic inclusions in amyotrophic lateral sclerosis. Neurobiol Aging *34*, 248-262.

Emde, A., Eitan, C., Liou, L.L., Libby, R.T., Rivkin, N., Magen, I., Reichenstein, I., Oppenheim, H., Eilam, R., Silvestroni, A.*, et al.* (2015). Dysregulated miRNA biogenesis downstream of cellular stress and ALS-causing mutations: a new mechanism for ALS. EMBO J *34*, 2633-2651.

Errichelli, L., Dini Modigliani, S., Laneve, P., Colantoni, A., Legnini, I., Capauto, D., Rosa, A., De Santis, R., Scarfo, R., Peruzzi, G.*, et al.* (2017). FUS affects circular RNA expression in murine embryonic stem cell-derived motor neurons. Nat Commun *8*, 14741.

Fricker, R.A., Green, E.L., Jenkins, S.I., and Griffin, S.M. (2018). The Influence of Nicotinamide on Health and Disease in the Central Nervous System. Int J Tryptophan Res *11*, 1178646918776658.

Ge, W.W., Volkening, K., Leystra-Lantz, C., Jaffe, H., and Strong, M.J. (2007). 14-3-3 protein binds to the low molecular weight neurofilament (NFL) mRNA 3' UTR. Mol Cell Neurosci *34*, 80-87.

Guil, S., and Caceres, J.F. (2007). The multifunctional RNA-binding protein hnRNP A1 is required for processing of miR-18a. Nat Struct Mol Biol *14*, 591-596.

Haramati, S., Chapnik, E., Sztainberg, Y., Eilam, R., Zwang, R., Gershoni, N., McGlinn, E., Heiser, P.W., Wills, A.M., Wirguin, I.*, et al.* (2010). miRNA malfunction causes spinal motor neuron disease. Proc Nat Acad Sci U S A *107*, 13111-13116.

Hawley, Z.C.E., Campos-Melo, D., Droppelmann, C.A., and Strong, M.J. (2017a). MotomiRs: miRNAs in Motor Neuron Function and Disease. Front Mol Neurosci *10*, 127.

Hawley, Z.C.E., Campos-Melo, D., and Strong, M.J. (2017b). Novel miR-b2122 regulates several ALS-related RNA-binding proteins. Mol Brain *10*, 46.

Hawley, Z.C.E., Campos-Melo, D., and Strong, M.J. (2019). MiR-105 and miR-9 regulate the mRNA stability of neuronal intermediate filaments. Implications for the pathogenesis of amyotrophic lateral sclerosis (ALS). Brain Res *1706*, 93-100.

Hawley Z.C.E., Campos-Melo, D., and Strong, M.J. (2020). Evidence of a negative feedback network between TDP-43 and miRNAs dependent on TDP-43 nuclear localization. J. Mol. Biol. *Accepted*.

Ishtiaq, M., Campos-Melo, D., Volkening, K., and Strong, M.J. (2014). Analysis of novel NEFL mRNA targeting microRNAs in amyotrophic lateral sclerosis. PLoS One *9*, e85653.

Kapeli, K., Pratt, G.A., Vu, A.Q., Hutt, K.R., Martinez, F.J., Sundararaman, B., Batra, R., Freese, P., Lambert, N.J., Huelga, S.C.*, et al.* (2016). Distinct and shared functions of ALS-associated proteins TDP-43, FUS and TAF15 revealed by multisystem analyses. Nat Commun *7*, 12143.

Kato, M., Han, T.W., Xie, S., Shi, K., Du, X., Wu, L.C., Mirzaei, H., Goldsmith, E.J., Longgood, J., Pei, J.*, et al.* (2012). Cell-free formation of RNA granules: low complexity sequence domains form dynamic fibers within hydrogels. Cell *149*, 753-767.

Kawahara, Y., and Mieda-Sato, A. (2012). TDP-43 promotes microRNA biogenesis as a component of the Drosha and Dicer complexes. Proc Natl Acad Sci U S A *109*, 3347-3352.

Keller, B.A., Volkening, K., Droppelmann, C.A., Ang, L.C., Rademakers, R., and Strong, M.J. (2012). Co-aggregation of RNA binding proteins in ALS spinal motor neurons: evidence of a common pathogenic mechanism. Acta Neuropathol *124*, 733-747.

Klim, J.R., Williams, L.A., Limone, F., Guerra San Juan, I., Davis-Dusenbery, B.N., Mordes, D.A., Burberry, A., Steinbaugh, M.J., Gamage, K.K., Kirchner, R.*, et al.* (2019). ALS-implicated protein TDP-43 sustains levels of STMN2, a mediator of motor neuron growth and repair. Nat Neurosci *22*, 167-179.

Kooshapur, H., Choudhury, N.R., Simon, B., Muhlbauer, M., Jussupow, A., Fernandez, N., Jones, A.N., Dallmann, A., Gabel, F., Camilloni, C.*, et al.* (2018). Structural basis for terminal loop recognition and stimulation of pri-miRNA-18a processing by hnRNP A1. Nat Commun *9*, 2479.

Koyama, A., Sugai, A., Kato, T., Ishihara, T., Shiga, A., Toyoshima, Y., Koyama, M., Konno, T., Hirokawa, S., Yokoseki, A.*, et al.* (2016). Increased cytoplasmic TARDBP mRNA in affected spinal motor neurons in ALS caused by abnormal autoregulation of TDP-43. Nucleic Acids Res *44*, 5820-5836.

Kriz, J., Zhu, Q., Julien, J.P., and Padjen, A.L. (2000). Electrophysiological properties of axons in mice lacking neurofilament subunit genes: disparity between conduction velocity and axon diameter in absence of NF-H. Brain Res *885*, 32-44.

Lee, M.K., Marszalek, J.R., and Cleveland, D.W. (1994). A mutant neurofilament subunit causes massive, selective motor neuron death: implications for the pathogenesis of human motor neuron disease. Neuron *13*, 975-988.

Ling, S.C., Polymenidou, M., and Cleveland, D.W. (2013). Converging mechanisms in ALS and FTD: disrupted RNA and protein homeostasis. Neuron *79*, 416-438.

Melamed, Z., Lopez-Erauskin, J., Baughn, M.W., Zhang, O., Drenner, K., Sun, Y., Freyermuth, F., McMahon, M.A., Beccari, M.S., Artates, J.W.*, et al.* (2019). Premature

polyadenylation-mediated loss of stathmin-2 is a hallmark of TDP-43-dependent neurodegeneration. Nat Neurosci *22*, 180-190.

Mitchell, J.C., McGoldrick, P., Vance, C., Hortobagyi, T., Sreedharan, J., Rogelj, B., Tudor, E.L., Smith, B.N., Klasen, C., Miller, C.C.*, et al.* (2013). Overexpression of human wild-type FUS causes progressive motor neuron degeneration in an age- and dose-dependent fashion. Acta Neuropathol *125*, 273-288.

Morlando, M., Dini Modigliani, S., Torrelli, G., Rosa, A., Di Carlo, V., Caffarelli, E., and Bozzoni, I. (2012). FUS stimulates microRNA biogenesis by facilitating co-transcriptional Drosha recruitment. EMBO J *31*, 4502-4510.

Murakami, T., Qamar, S., Lin, J.Q., Schierle, G.S., Rees, E., Miyashita, A., Costa, A.R., Dodd, R.B., Chan, F.T., Michel, C.H.*, et al.* (2015). ALS/FTD Mutation-Induced Phase Transition of FUS Liquid Droplets and Reversible Hydrogels into Irreversible Hydrogels Impairs RNP Granule Function. Neuron *88*, 678-690.

Murray, D.T., Kato, M., Lin, Y., Thurber, K.R., Hung, I., McKnight, S.L., and Tycko, R. (2017). Structure of FUS Protein Fibrils and Its Relevance to Self-Assembly and Phase Separation of Low-Complexity Domains. Cell *171*, 615-627 e616.

Naia, L., Rosenstock, T.R., Oliveira, A.M., Oliveira-Sousa, S.I., Caldeira, G.L., Carmo, C., Laco, M.N., Hayden, M.R., Oliveira, C.R., and Rego, A.C. (2017). Comparative Mitochondrial-Based Protective Effects of Resveratrol and Nicotinamide in Huntington's Disease Models. Mol Neurobiol *54*, 5385-5399.

Nishimoto, Y., Nakagawa, S., Hirose, T., Okano, H.J., Takao, M., Shibata, S., Suyama, S., Kuwako, K., Imai, T., Murayama, S.*, et al.* (2013). The long non-coding RNA nuclear-enriched abundant transcript 1_2 induces paraspeckle formation in the motor neuron during the early phase of amyotrophic lateral sclerosis. Mol Brain *6*, 31.

Ouyang, H., Zhang, K., Fox-Walsh, K., Yang, Y., Zhang, C., Huang, J., Li, H., Zhou, Y., and Fu, X.D. (2017). The RNA binding protein EWS is broadly involved in the regulation of pri-miRNA processing in mammalian cells. Nucleic Acids Res *45*, 12481-12495.

Poddar, S.K., Sifat, A.E., Haque, S., Nahid, N.A., Chowdhury, S., and Mehedi, I. (2019). Nicotinamide Mononucleotide: Exploration of Diverse Therapeutic Applications of a Potential Molecule. Biomolecules *9*.

Protter, D.S.W., and Parker, R. (2016). Principles and Properties of Stress Granules. Trends Cell Biol *26*, 668-679.

Ranganathan, S., and Bowser, R. (2003). Alterations in G1 to S Phase Cell-Cycle Regulators during Amyotrophic Lateral Sclerosis. Am J Pathol. *162*, 823-835.

Ranganathan, S., and Bowser, R. (2010). p53 and Cell Cycle Proteins Participate in Spinal Motor Neuron Cell Death in ALS. Open Pathol J. *1*, 11-22.

Reichenstein, I., Eitan, C., Diaz-Garcia, S., Haim, G., Magen, I., Siany, A., Hoye, M.L., Rivkin, N., Olender, T., Toth, B.*, et al.* (2019). Human genetics and neuropathology suggest a link between miR-218 and amyotrophic lateral sclerosis pathophysiology. Sci Transl Med *11*.

Riva, N., Clarelli, F., Domi, T., Cerri, F., Gallia, F., Trimarco, A., Brambilla, P., Lunetta, C., Lazzerini, A., Lauria, G.*, et al.* (2016). Unraveling gene expression profiles in peripheral motor nerve from amyotrophic lateral sclerosis patients: insights into pathogenesis. Sci Rep *6*, 39297.

Robertson, J., Kriz, J., Nguyen, M.D., and Julien, J.P. (2002). Pathways to motor neuron degeneration in transgenic mouse models. Biochimie *84*, 1151-1160.

Sabatelli, M., Moncada, A., Conte, A., Lattante, S., Marangi, G., Luigetti, M., Lucchini, M., Mirabella, M., Romano, A., Del Grande, A.*, et al.* (2013). Mutations in the 3' untranslated region of FUS causing FUS overexpression are associated with amyotrophic lateral sclerosis. Hum Mol Genet *22*, 4748-4755.

Salvatori, B., Biscarini, S., and Morlando, M. (2020). Non-coding RNAs in Nervous System Development and Disease. Front Cell Dev Biol *8*, 273.

Sanchez-Jimenez, C., Carrascoso, I., Barrero, J., and Izquierdo, J.M. (2013). Identification of a set of miRNAs differentially expressed in transiently TIA-depleted HeLa cells by genome-wide profiling. BMC Mol Biol *14*, 4.

Schondorf, D.C., Ivanyuk, D., Baden, P., Sanchez-Martinez, A., De Cicco, S., Yu, C., Giunta, I., Schwarz, L.K., Di Napoli, G., Panagiotakopoulou, V.*, et al.* (2018). The NAD+ Precursor Nicotinamide Riboside Rescues Mitochondrial Defects and Neuronal Loss in iPSC and Fly Models of Parkinson's Disease. Cell Rep *23*, 2976-2988.

Shan, G., Li, Y., Zhang, J., Li, W., Szulwach, K.E., Duan, R., Faghihi, M.A., Khalil, A.M., Lu, L., Paroo, Z.*, et al.* (2008). A small molecule enhances RNA interference and promotes microRNA processing. Nat Biotechnol *26*, 933-940.

Sharma, R., Kumar, D., Jha, N.K., Jha, S.K., Ambasta, R.K., and Kumar, P. (2017). Re-expression of cell cycle markers in aged neurons and muscles: Whether cells should divide or die?. Biochim Biophys Acts Mol Basis Dis. *1863*, 324-336.

Stefanizzi, I., and Canete-Soler, R. (2007). Coregulation of light neurofilament mRNA by poly(A)-binding protein and aldolase C: implications for neurodegeneration. Brain Res *1139*, 15-28.

Surjana, D., Halliday, G.M., and Damian, D.L. (2010). Role of nicotinamide in DNA damage, mutagenesis, and DNA repair. J Nucleic Acids *2010*.

Swarup, V., Phaneuf, D., Dupre, N., Petri, S., Strong, M., Kriz, J., and Julien, J.P. (2011). Deregulation of TDP-43 in amyotrophic lateral sclerosis triggers nuclear factor kappaB-mediated pathogenic pathways. J Exp Med *208*, 2429-2447.

Szaro, B.G., and Strong, M.J. (2010). Post-transcriptional control of neurofilaments: New roles in development, regeneration and neurodegenerative disease. Trends Neurosci *33*, 27-37.

Tamaki, Y., Shodai, A., Morimura, T., Hikiami, R., Minamiyama, S., Ayaki, T., Tooyama, I., Furukawa, Y., Takahashi, R., and Urushitani, M. (2018). Elimination of TDP-43 inclusions linked to amyotrophic lateral sclerosis by a misfolding-specific intrabody with dual proteolytic signals. Sci Rep *8*, 6030.

Tang, X., Wen, S., Zheng, D., Tucker, L., Cao, L., Pantazatos, D., Moss, S.F., and Ramratnam, B. (2013). Acetylation of drosha on the N-terminus inhibits its degradation by ubiquitination. PLoS One *8*, e72503.

Thyagarajan, A., and Szaro, B.G. (2004). Phylogenetically conserved binding of specific K homology domain proteins to the 3'-untranslated region of the vertebrate middle neurofilament mRNA. J Biol Chem *279*, 49680-49688.

Thyagarajan, A., and Szaro, B.G. (2008). Dynamic endogenous association of neurofilament mRNAs with K-homology domain ribonucleoproteins in developing cerebral cortex. Brain Res *1189*, 33-42.

Tradewell, M.L., Yu, Z., Tibshirani, M., Boulanger, M.C., Durham, H.D., and Richard, S. (2012). Arginine methylation by PRMT1 regulates nuclear-cytoplasmic localization and toxicity of FUS/TLS harbouring ALS-linked mutations. Hum Mol Genet *21*, 136-149.

Treiber, T., Treiber, N., Plessmann, U., Harlander, S., Daiss, J.L., Eichner, N., Lehmann, G., Schall, K., Urlaub, H., and Meister, G. (2017). A Compendium of RNA-Binding Proteins that Regulate MicroRNA Biogenesis. Mol Cell *66*, 270-284 e213.

Tsang, J., Zhu, J., and van Oudenaarden, A. (2007). MicroRNA-mediated feedback and feedforward loops are recurrent network motifs in mammals. Mol Cell *26*, 753-767.

Turunc Bayrakdar, E., Uyanikgil, Y., Kanit, L., Koylu, E., and Yalcin, A. (2014). Nicotinamide treatment reduces the levels of oxidative stress, apoptosis, and PARP-1 activity in Abeta(1-42)-induced rat model of Alzheimer's disease. Free Radic Res *48*, 146-158.

Volkening, K., Leystra-Lantz, C., and Strong, M.J. (2010). Human low molecular weight neurofilament (NFL) mRNA interacts with a predicted p190RhoGEF homologue (RGNEF) in humans. Amyotroph Lateral Scler *11*, 97-103.

Volkening, K., Leystra-Lantz, C., Yang, W., Jaffee, H., and Strong, M.J. (2009). Tar DNA binding protein of 43 kDa (TDP-43), 14-3-3 proteins and copper/zinc superoxide dismutase (SOD1) interact to modulate NFL mRNA stability. Implications for altered RNA processing in amyotrophic lateral sclerosis (ALS). Brain Res *1305*, 168-182.

Weiss, K., Treiber, T., Meister, G., and Schratt, G. (2019). The nuclear matrix protein Matr3 regulates processing of the synaptic microRNA-138-5p. Neurobiol Learn Mem *159*, 36-45.

Wong, N.K., He, B.P., and Strong, M.J. (2000). Characterization of neuronal intermediate filament protein expression in cervical spinal motor neurons in sporadic amyotrophic lateral sclerosis (ALS). J Neuropathol Exp Neurol *59*, 972-982.

Xie, X., Gao, Y., Zeng, M., Wang, Y., Wei, T.F., Lu, Y.B., and Zhang, W.P. (2019). Nicotinamide ribose ameliorates cognitive impairment of aged and Alzheimer's disease model mice. Metab Brain Dis *34*, 353-366.

Xu, Y.F., Gendron, T.F., Zhang, Y.J., Lin, W.L., D'Alton, S., Sheng, H., Casey, M.C., Tong, J., Knight, J., Yu, X.*, et al.* (2010). Wild-type human TDP-43 expression causes TDP-43 phosphorylation, mitochondrial aggregation, motor deficits, and early mortality in transgenic mice. J Neurosci *30*, 10851-10859.

Zhang, H., Li, Y., Tan, Y., Liu, Q., Jiang, S., Liu, D., Chen, Q., and Zhang, S. (2019). MiR-9-5p Inhibits Glioblastoma Cells Proliferation Through Directly Targeting FOXP2 (Forkhead Box P2). Front Onco *9*, 1176.

Zhang, J., Wu, W., Xu, S., Zhang, J., Zhang, J., Qu, Y, Jiao, Y., Wang, Y., Lu, A., Lou A., *et al.* (2017). MicroRNA-105 inhibits human glioma cell malignancy by directly targeting SUZ12. Tumor Biol *39*, 1-10.

Zhou, Q., Zhu, L., Qiu, W., Liu, Y., Yang, F., Chen, W., and Xu, R. (2020). Nicotinamide Riboside Enhances Mitochondrial Proteostasis and Adult Neurogenesis through Activation of Mitochondrial Unfolded Protein Response Signaling in the Brain of ALS SOD1(G93A) Mice. Int J Biol Sci *16*, 284-297.

Zhu, Q., Couillard-Despres, S., and Julien, J.P. (1997). Delayed maturation of regenerating myelinated axons in mice lacking neurofilaments. Exp Neurol *148*, 299-316.

**Appendix A**

**Tables indicating significant changes to small RNA expression following TDP-43 or FUS knockdown in HEK293T cells**

*Data was collected using a microarray (GeneChip miRNA 4.0 Array) and analyzed using the Transcriptome Analysis Console. See Methods & Materials in Chapter 5 for further details.*

**Table A.1. Small RNAs significantly altered following TDP-43 Knockdown.**

| ID | Transcript ID(Array Design) | P-val | Fold Change | siTDP Avg (log2) | SCR Avg (log2) | FDR P-val | Chromosome |
|---|---|---|---|---|---|---|---|
| 20518879 | hsa-miR-4485 | 0.000000134 | 3.74 | 8.81 | 6.9 | 0.0009 | chr11 |
| 20524036 | hsa-miR-6126 | 0.0000171 | 1.92 | 8.24 | 7.29 | 0.0531 | chr16 |
| 20525395 | hsa-miR-6723-5p | 0.000024 | 4.26 | 5.97 | 3.88 | 0.0531 | chr1 |
| 20518834 | hsa-miR-4454 | 0.0000491 | -3.55 | 6.53 | 8.36 | 0.0795 | chr4 |
| 20535460 | hsa-mir-1298 | 0.0000697 | -1.4 | 1.58 | 2.07 | 0.0795 | chrX |
| 20528733 | hsa-miR-7704 | 0.000072 | 1.77 | 9.78 | 8.96 | 0.0795 | chr2 |
| 20534812 | hsa-mir-29c | 0.0001 | 1.42 | 1.88 | 1.37 | 0.1139 | chr1 |
| 20537518 | hsa-mir-6775 | 0.0001 | -2.69 | 1.4 | 2.83 | 0.107 | chr16 |
| 20509224 | hsa-miR-1908-5p | 0.0002 | 1.64 | 6.74 | 6.03 | 0.1518 | chr11 |
| 20518933 | hsa-miR-4532 | 0.0004 | 1.98 | 7.02 | 6.04 | 0.2686 | chr20 |
| 20536775 | hsa-mir-4500 | 0.0004 | -1.84 | 1.21 | 2.09 | 0.2627 | chr13 |
| 20518892 | hsa-miR-4497 | 0.0005 | 1.52 | 9.21 | 8.61 | 0.2724 | chr12 |
| 20532932 | ENSG00000202449 | 0.0005 | 1.43 | 1.33 | 0.81 | 0.2724 | chr4 |
| 20504413 | hsa-miR-663a | 0.0006 | 1.84 | 6.84 | 5.96 | 0.2741 | chr20 |
| 20518431 | hsa-miR-3910 | 0.0006 | 1.66 | 1.72 | 0.99 | 0.2741 | chr9 |
| 20504433 | hsa-miR-421 | 0.0007 | -1.73 | 5.99 | 6.78 | 0.2805 | chrX |
| 20517942 | hsa-miR-3682-5p | 0.0007 | 1.59 | 1.66 | 0.99 | 0.2805 | chr2 |
| 20533897 | ENSG00000252190 | 0.0008 | 1.5 | 1.89 | 1.31 | 0.2995 | chr1 |
| 20536814 | hsa-mir-4534 | 0.001 | 1.39 | 1.82 | 1.35 | 0.3166 | chr22 |
| 20536889 | hsa-mir-4664 | 0.001 | -1.58 | 1.4 | 2.06 | 0.3166 | chr8 |
| 20537456 | hsa-mir-6715b | 0.001 | 1.43 | 2.23 | 1.72 | 0.3166 | chr10 |
| 20504408 | hsa-miR-652-3p | 0.0011 | -1.35 | 6.84 | 7.27 | 0.3166 | chrX |
| 20507742 | hsa-miR-1469 | 0.0011 | 1.63 | 7.05 | 6.34 | 0.3166 | chr15 |
| 20501197 | hsa-miR-361-5p | 0.0012 | -1.47 | 8.8 | 9.36 | 0.3166 | chrX |
| 20538223 | U68 | 0.0012 | 1.24 | 6.54 | 6.24 | 0.3166 | chr19 |
| 20538181 | U43 | 0.0015 | 1.29 | 10.23 | 9.87 | 0.3694 | chr22 |
| 20536568 | hsa-mir-3664 | 0.0016 | 1.63 | 1.75 | 1.05 | 0.3694 | chr11 |

**Table A.1. Small RNAs significantly altered following TDP-43 Knockdown.**

| ID | Transcript ID(Array Design) | P-val | Fold Change | siTDP Avg (log2) | SCR Avg (log2) | FDR P-val | Chromosome |
|---|---|---|---|---|---|---|---|
| 20537538 | hsa-mir-6795 | 0.0016 | 1.59 | 1.78 | 1.11 | 0.3694 | chr19 |
| 20525526 | hsa-miR-6782-3p | 0.0017 | -1.42 | 1.21 | 1.71 | 0.3779 | chr17 |
| 20533168 | ENSG00000221633 | 0.0019 | 1.63 | 1.91 | 1.21 | 0.4082 | chr3 |
| 20533189 | ENSG00000223027 | 0.0019 | -1.5 | 1.23 | 1.82 | 0.4082 | chr10 |
| 20518816 | hsa-miR-4441 | 0.0021 | -1.3 | 1.08 | 1.46 | 0.4174 | chr2 |
| 20533677 | ENSG00000239033 | 0.0021 | -1.32 | 0.91 | 1.31 | 0.4174 | chr12 |
| 20534818 | hsa-mir-219a-2 | 0.0021 | -1.45 | 1.35 | 1.89 | 0.4174 | chr9 |
| 20500170 | hsa-miR-92a-1-5p | 0.0023 | 2.69 | 3.1 | 1.67 | 0.4247 | chr13 |
| 20536757 | hsa-mir-4485 | 0.0023 | 1.4 | 3.54 | 3.05 | 0.4247 | chr11 |
| 20538180 | U43 | 0.0028 | 1.2 | 10.63 | 10.37 | 0.5084 | chr22 |
| 20536760 | hsa-mir-4487 | 0.0029 | 1.74 | 2.08 | 1.28 | 0.5135 | chr11 |
| 20500489 | hsa-miR-224-5p | 0.0036 | 1.39 | 1.57 | 1.09 | 0.5519 | chrX |
| 20515595 | hsa-miR-3170 | 0.0036 | -1.29 | 1.08 | 1.45 | 0.5519 | chr13 |
| 20500742 | hsa-miR-137 | 0.0037 | 1.3 | 1.08 | 0.7 | 0.5519 | chr1 |
| 20518878 | hsa-miR-4484 | 0.0039 | 1.42 | 8.13 | 7.63 | 0.5519 | chr10 |
| 20533980 | ENSG00000252526 | 0.0039 | -1.38 | 1.34 | 1.81 | 0.5519 | chr16 |
| 20538048 | hsa-mir-8088 | 0.0039 | -1.45 | 1.33 | 1.87 | 0.5519 | chrX |
| 20525416 | hsa-miR-6727-5p | 0.004 | 1.38 | 7.92 | 7.45 | 0.5519 | chr1 |
| 20519441 | hsa-miR-4656 | 0.0041 | 2.37 | 3.53 | 2.29 | 0.5519 | chr7 |
| 20515551 | hsa-miR-3142 | 0.0042 | 1.23 | 1.35 | 1.05 | 0.5519 | chr5 |
| 20500137 | hsa-miR-19b-3p | 0.0044 | -5.02 | 3.6 | 5.93 | 0.5519 | chr13 |
| 20525554 | hsa-miR-6796-3p | 0.0045 | 1.5 | 2.08 | 1.49 | 0.5519 | chr19 |
| 20500721 | hsa-miR-23b-3p | 0.0046 | -1.13 | 9.32 | 9.49 | 0.5519 | chr9 |
| 20504552 | hsa-miR-671-5p | 0.0047 | -1.44 | 5.07 | 5.59 | 0.5519 | chr7 |
| 20500148 | hsa-miR-24-3p | 0.0048 | -1.51 | 7.33 | 7.92 | 0.5519 | chr19 |
| 20500465 | hsa-miR-210-3p | 0.0048 | -2.36 | 3.71 | 4.95 | 0.5519 | chr11 |
| 20536929 | hsa-mir-4698 | 0.0048 | 2.08 | 2.53 | 1.48 | 0.5519 | chr12 |

**Table A.1. Small RNAs significantly altered following TDP-43 Knockdown.**

| ID | Transcript ID(Array Design) | P-val | Fold Change | siTDP Avg (log2) | SCR Avg (log2) | FDR P-val | Chromosome |
|---|---|---|---|---|---|---|---|
| 20506005 | hsa-miR-936 | 0.005 | -1.53 | 1.33 | 1.94 | 0.5519 | chr10 |
| 20519570 | hsa-miR-4728-5p | 0.005 | 2.38 | 4.65 | 3.4 | 0.5519 | chr17 |
| 20525633 | hsa-miR-6780b-5p | 0.005 | 1.79 | 6.13 | 5.29 | 0.5519 | chr6 |
| 20534879 | hsa-mir-151a | 0.005 | -1.75 | 1.47 | 2.27 | 0.5519 | chr8 |
| 20536902 | hsa-mir-4676 | 0.005 | 1.38 | 1.93 | 1.47 | 0.5519 | chr10 |
| 20504342 | hsa-miR-602 | 0.0051 | -1.6 | 2.03 | 2.7 | 0.5519 | chr9 |
| 20525668 | hsa-miR-6853-3p | 0.0051 | 1.39 | 1.63 | 1.15 | 0.5519 | chr9 |
| 20533715 | ENSG00000239084 | 0.0053 | 1.36 | 1.42 | 0.98 | 0.5674 | chr5 |
| 20506878 | hsa-miR-548p | 0.0054 | 1.47 | 1.58 | 1.02 | 0.5674 | chr5 |
| 20501293 | hsa-miR-331-3p | 0.0057 | -2.17 | 3.74 | 4.86 | 0.5674 | chr12 |
| 20536769 | hsa-mir-4495 | 0.0057 | 1.24 | 1.5 | 1.19 | 0.5674 | chr12 |
| 20523019 | hsa-miR-6087 | 0.0058 | 1.37 | 10.47 | 10.02 | 0.5674 | chrX |
| 20532926 | ENSG00000202374 | 0.0059 | -1.59 | 1.44 | 2.1 | 0.5674 | chr4 |
| 20536497 | hsa-mir-4277 | 0.0059 | -1.71 | 1.85 | 2.63 | 0.5674 | chr5 |
| 20536870 | hsa-mir-4650-1 | 0.006 | 1.34 | 1.65 | 1.23 | 0.5674 | chr7 |
| 20536871 | hsa-mir-4650-2 | 0.006 | 1.34 | 1.65 | 1.23 | 0.5674 | chr7 |
| 20533228 | ENSG00000238339 | 0.0065 | 1.31 | 1.98 | 1.59 | 0.6054 | chr2 |
| 20532651 | ACA32 | 0.0066 | 1.63 | 2.66 | 1.95 | 0.6104 | chr11 |
| 20505608 | hsa-miR-675-5p | 0.0069 | 1.51 | 2.05 | 1.46 | 0.6264 | chr11 |
| 20533161 | ENSG00000221398 | 0.007 | -1.58 | 1.39 | 2.05 | 0.6264 | chr21 |
| 20525421 | hsa-miR-6729-3p | 0.0072 | 1.32 | 1.4 | 1 | 0.6264 | chr1 |
| 20532748 | ENSG00000199666 | 0.0072 | -1.48 | 1.24 | 1.8 | 0.6264 | chr1 |
| 20515591 | hsa-miR-1260b | 0.0073 | -2.96 | 3.74 | 5.31 | 0.6264 | chr11 |
| 20501280 | hsa-miR-342-3p | 0.0075 | -1.18 | 8.62 | 8.86 | 0.6379 | chr14 |
| 20536560 | hsa-mir-3656 | 0.008 | -2.07 | 1.66 | 2.71 | 0.6726 | chr11 |
| 20533973 | ENSG00000252495 | 0.0083 | 1.25 | 1.64 | 1.31 | 0.6775 | chr1 |
| 20537204 | hsa-mir-5692c-2 | 0.0083 | 1.43 | 1.79 | 1.27 | 0.6775 | chr7 |

**Table A.1. Small RNAs significantly altered following TDP-43 Knockdown.**

| ID | Transcript ID(Array Design) | P-val | Fold Change | siTDP Avg (log2) | SCR Avg (log2) | FDR P-val | Chromosome |
|---|---|---|---|---|---|---|---|
| 20536728 | hsa-mir-4468 | 0.0084 | -1.5 | 1.34 | 1.92 | 0.6775 | chr7 |
| 20500448 | hsa-miR-181c-5p | 0.0091 | -1.46 | 1.42 | 1.97 | 0.7253 | chr19 |
| 20500456 | hsa-miR-196a-3p | 0.0094 | -1.52 | 1.56 | 2.16 | 0.7344 | chr12 |
| 20522039 | hsa-miR-5703 | 0.0094 | -1.88 | 1.22 | 2.13 | 0.7344 | chr2 |
| 20506898 | hsa-miR-1306-5p | 0.0097 | -1.55 | 1.21 | 1.85 | 0.7474 | chr22 |
| 20537467 | hsa-mir-892c | 0.0099 | 1.86 | 2.22 | 1.33 | 0.7528 | chrX |
| 20500191 | hsa-miR-103a-3p | 0.0102 | -1.31 | 10.45 | 10.83 | 0.7542 | chr20 |
| 20533078 | ENSG00000212391 | 0.0102 | 1.41 | 2.2 | 1.7 | 0.7542 | chr2 |
| 20533463 | ENSG00000238696 | 0.0103 | 1.24 | 1.36 | 1.05 | 0.7542 | chr2 |
| 20533676 | ENSG00000239033 | 0.0105 | -1.26 | 0.94 | 1.28 | 0.7542 | chr12 |
| 20536313 | hsa-mir-3194 | 0.0105 | -1.33 | 1.39 | 1.8 | 0.7542 | chr20 |
| 20504582 | hsa-miR-766-5p | 0.0106 | -1.75 | 1.6 | 2.4 | 0.7576 | chrX |
| 20534302 | HBII-85-11 | 0.0111 | 1.2 | 1.58 | 1.32 | 0.7791 | chr15 |
| 20500791 | hsa-miR-188-5p | 0.0112 | -2.19 | 1.71 | 2.85 | 0.7791 | chrX |
| 20512262 | hsa-miR-2277-3p | 0.0113 | 1.76 | 2.42 | 1.61 | 0.7791 | chr5 |
| 20504583 | hsa-miR-766-3p | 0.0116 | -1.41 | 3.5 | 4 | 0.7791 | chrX |
| 20537158 | hsa-mir-5583-2 | 0.0116 | -1.38 | 1.43 | 1.89 | 0.7791 | chr18 |
| 20534534 | hsa-mir-217 | 0.0118 | 1.27 | 1.59 | 1.25 | 0.7791 | chr2 |
| 20533843 | ENSG00000251974 | 0.012 | 1.15 | 1.07 | 0.87 | 0.7791 | chr2 |
| 20500194 | hsa-miR-106a-5p | 0.0121 | -1.67 | 10.35 | 11.09 | 0.7791 | chrX |
| 20501176 | hsa-miR-99b-5p | 0.0122 | -1.26 | 7.57 | 7.9 | 0.7791 | chr19 |
| 20501312 | hsa-miR-345-5p | 0.0122 | -1.88 | 4.28 | 5.18 | 0.7791 | chr14 |
| 20534858 | hsa-mir-380 | 0.0122 | -1.37 | 1.33 | 1.78 | 0.7791 | chr14 |
| 20537157 | hsa-mir-5583-2 | 0.0128 | -1.36 | 1.44 | 1.89 | 0.7791 | chr18 |
| 20505746 | hsa-miR-874-3p | 0.0129 | -1.95 | 2.62 | 3.59 | 0.7791 | chr5 |
| 20518627 | hsa-miR-548y | 0.0131 | -1.28 | 0.98 | 1.34 | 0.7791 | chr14 |
| 20500144 | hsa-miR-22-3p | 0.0132 | -2.31 | 1.68 | 2.89 | 0.7791 | chr17 |

**Table A.1. Small RNAs significantly altered following TDP-43 Knockdown.**

| ID | Transcript ID(Array Design) | P-val | Fold Change | siTDP Avg (log2) | SCR Avg (log2) | FDR P-val | Chromosome |
|---|---|---|---|---|---|---|---|
| 20518852 | hsa-miR-4467 | 0.0133 | 1.51 | 4.79 | 4.2 | 0.7791 | chr7 |
| 20500196 | hsa-miR-107 | 0.0136 | -1.26 | 10.08 | 10.42 | 0.7791 | chr10 |
| 20517834 | hsa-miR-3620-3p | 0.0136 | 1.65 | 3.04 | 2.32 | 0.7791 | chr1 |
| 20519670 | hsa-miR-4783-3p | 0.0137 | -1.61 | 1.32 | 2.01 | 0.7791 | chr2 |
| 20515607 | hsa-miR-3178 | 0.0138 | 1.37 | 7.99 | 7.53 | 0.7791 | chr16 |
| 20534830 | hsa-mir-361 | 0.0138 | -1.22 | 7.2 | 7.5 | 0.7791 | chrX |
| 20535688 | hsa-mir-937 | 0.014 | -1.61 | 1.57 | 2.26 | 0.7791 | chr8 |
| 20538244 | U73a | 0.0141 | 1.39 | 8.76 | 8.29 | 0.7791 | chr4 |
| 20500419 | hsa-miR-129-1-3p | 0.0142 | 1.36 | 1.31 | 0.87 | 0.7791 | chr7 |
| 20504310 | hsa-miR-582-3p | 0.0142 | -1.17 | 1.09 | 1.32 | 0.7791 | chr5 |
| 20534042 | ENSG00000252787 | 0.0142 | -1.31 | 1.69 | 2.08 | 0.7791 | chr3 |
| 20500162 | hsa-miR-30a-5p | 0.0143 | -2.17 | 1.99 | 3.11 | 0.7791 | chr6 |
| 20504374 | hsa-miR-626 | 0.0143 | -1.44 | 0.79 | 1.31 | 0.7791 | chr15 |
| 20535102 | hsa-mir-450a-1 | 0.0143 | 1.58 | 1.54 | 0.89 | 0.7791 | chrX |
| 20500454 | hsa-miR-187-5p | 0.0145 | -1.46 | 2.03 | 2.57 | 0.7803 | chr18 |
| 20525731 | hsa-miR-6885-5p | 0.0146 | -2.28 | 1.68 | 2.87 | 0.7803 | chr19 |
| 20534315 | HBII-85-22 | 0.0149 | -1.28 | 1.13 | 1.49 | 0.7857 | chr15 |
| 20533699 | ENSG00000239063 | 0.0153 | -1.24 | 1.08 | 1.39 | 0.7857 | chr1 |
| 20500182 | hsa-miR-99a-3p | 0.0154 | 1.36 | 1.52 | 1.08 | 0.7857 | chr21 |
| 20522031 | hsa-miR-5696 | 0.0154 | -1.5 | 1.12 | 1.7 | 0.7857 | chr2 |
| 20506886 | hsa-miR-1288-3p | 0.0156 | -1.81 | 1.3 | 2.15 | 0.7857 | chr17 |
| 20537429 | hsa-mir-548ay | 0.0157 | -1.34 | 1.2 | 1.62 | 0.7857 | chr3 |
| 20525479 | hsa-miR-6759-5p | 0.0158 | -1.24 | 1.24 | 1.56 | 0.7857 | chr12 |
| 20503808 | hsa-miR-193b-3p | 0.016 | -1.48 | 7.5 | 8.07 | 0.7857 | chr16 |
| 20533957 | ENSG00000252433 | 0.0163 | 1.16 | 1.18 | 0.96 | 0.7857 | chr1 |
| 20529782 | hsa-miR-8072 | 0.0165 | 1.47 | 7.11 | 6.56 | 0.7857 | chr12 |
| 20533570 | ENSG00000238863 | 0.0165 | 1.21 | 1.16 | 0.88 | 0.7857 | chr18 |

**Table A.1. Small RNAs significantly altered following TDP-43 Knockdown.**

| ID | Transcript ID(Array Design) | P-val | Fold Change | siTDP Avg (log2) | SCR Avg (log2) | FDR P-val | Chromosome |
|---|---|---|---|---|---|---|---|
| 20519468 | hsa-miR-4670-5p | 0.0168 | 1.22 | 1.75 | 1.46 | 0.7857 | chr9 |
| 20535131 | hsa-mir-376b | 0.0168 | -1.61 | 0.85 | 1.54 | 0.7857 | chr14 |
| 20536884 | hsa-mir-4662a | 0.0168 | 1.46 | 1.66 | 1.12 | 0.7857 | chr8 |
| 20519591 | hsa-miR-4740-3p | 0.0169 | -1.92 | 1.55 | 2.49 | 0.7857 | chr17 |
| 20535101 | hsa-mir-450a-1 | 0.0169 | 1.21 | 1.18 | 0.91 | 0.7857 | chrX |
| 20535879 | hsa-mir-1263 | 0.017 | -1.78 | 2.08 | 2.91 | 0.7857 | chr3 |
| 20532658 | ACA35 | 0.0172 | -1.23 | 1.38 | 1.68 | 0.7857 | chr1 |
| 20500723 | hsa-miR-27b-3p | 0.0173 | -2 | 4.11 | 5.12 | 0.7857 | chr9 |
| 20532645 | ACA2b | 0.0174 | 1.43 | 1.31 | 0.79 | 0.7857 | chr12 |
| 20534091 | ENSG00000253013 | 0.0175 | -1.45 | 1.78 | 2.31 | 0.7857 | chr4 |
| 20537086 | hsa-mir-5094 | 0.0176 | 1.47 | 2.5 | 1.94 | 0.7857 | chr15 |
| 20533733 | ENSG00000239123 | 0.0177 | -1.45 | 1.57 | 2.11 | 0.7857 | chr7 |
| 20506844 | hsa-miR-1251-5p | 0.0178 | 1.37 | 1.52 | 1.07 | 0.7857 | chr12 |
| 20519459 | hsa-miR-4666a-5p | 0.0178 | -1.21 | 1.56 | 1.83 | 0.7857 | chr1 |
| 20534234 | HBII-240 | 0.0178 | 1.28 | 1.31 | 0.96 | 0.7857 | chr5 |
| 20533793 | ENSG00000251775 | 0.018 | 1.19 | 1.53 | 1.27 | 0.7863 | chr2 |
| 20536614 | hsa-mir-3915 | 0.0182 | -1.25 | 1.09 | 1.41 | 0.7863 | chrX |
| 20501772 | hsa-miR-196b-3p | 0.0183 | -2.06 | 2.98 | 4.02 | 0.7863 | chr7 |
| 20535671 | hsa-mir-873 | 0.0183 | 1.53 | 1.65 | 1.04 | 0.7863 | chr9 |
| 20522537 | hsa-miR-5787 | 0.0184 | 1.38 | 7.77 | 7.3 | 0.7863 | chr3 |
| 20518782 | hsa-miR-1268b | 0.0186 | 1.44 | 5.82 | 5.3 | 0.7921 | chr17 |
| 20533113 | ENSG00000212558 | 0.0189 | 1.57 | 1.86 | 1.21 | 0.7967 | chr2 |
| 20500163 | hsa-miR-30a-3p | 0.0191 | -1.86 | 2.64 | 3.53 | 0.8027 | chr6 |
| 20537639 | hsa-mir-6893 | 0.0196 | -1.49 | 1.63 | 2.21 | 0.8148 | chr8 |
| 20520195 | hsa-miR-4999-3p | 0.0199 | -1.45 | 1 | 1.54 | 0.8148 | chr19 |
| 20533553 | ENSG00000238841 | 0.0199 | 1.48 | 1.76 | 1.2 | 0.8148 | chr7 |
| 20536792 | hsa-mir-4514 | 0.02 | -1.28 | 1.29 | 1.65 | 0.8148 | chr15 |

**Table A.1. Small RNAs significantly altered following TDP-43 Knockdown.**

| ID | Transcript ID(Array Design) | P-val | Fold Change | siTDP Avg (log2) | SCR Avg (log2) | FDR P-val | Chromosome |
|---|---|---|---|---|---|---|---|
| 20500130 | hsa-miR-17-5p | 0.0202 | -1.62 | 10.53 | 11.23 | 0.8148 | chr13 |
| 20509227 | hsa-miR-1909-3p | 0.0204 | 2.06 | 3.17 | 2.12 | 0.8148 | chr19 |
| 20533041 | ENSG00000212211 | 0.0204 | 1.39 | 1.67 | 1.2 | 0.8148 | chr3 |
| 20534125 | ENSG00000262620 | 0.0204 | 1.39 | 1.67 | 1.2 | 0.8148 | chrHG1091_PATCH |
| 20506837 | hsa-miR-1246 | 0.0205 | 2.18 | 7.14 | 6.01 | 0.8157 | chr2 |
| 20500132 | hsa-miR-18a-5p | 0.0207 | -1.81 | 7.22 | 8.07 | 0.8181 | chr13 |
| 20500779 | hsa-miR-146a-3p | 0.021 | -1.3 | 1.44 | 1.82 | 0.8181 | chr5 |
| 20535199 | hsa-mir-516a-1 | 0.0211 | 1.29 | 1.36 | 1 | 0.8181 | chr19 |
| 20535200 | hsa-mir-516a-2 | 0.0211 | 1.29 | 1.36 | 1 | 0.8181 | chr19 |
| 20525423 | hsa-miR-6730-3p | 0.0215 | -1.17 | 1.59 | 1.81 | 0.8235 | chr1 |
| 20535457 | hsa-mir-762 | 0.0217 | 1.52 | 2.08 | 1.47 | 0.8235 | chr16 |
| 20538108 | SNORA84 | 0.0218 | -1.13 | 1.76 | 1.94 | 0.8235 | chr9 |
| 20537161 | hsa-mir-5586 | 0.0219 | -1.15 | 1.05 | 1.26 | 0.8235 | chr14 |
| 20536218 | hsa-mir-3132 | 0.022 | -1.33 | 1.48 | 1.88 | 0.8235 | chr2 |
| 20536616 | hsa-mir-3914-2 | 0.022 | 1.42 | 1.47 | 0.96 | 0.8235 | chr7 |
| 20538300 | mgh28S-2411 | 0.0221 | 1.13 | 8.7 | 8.52 | 0.8235 | chr11 |
| 20533286 | ENSG00000238436 | 0.023 | 1.75 | 2.13 | 1.32 | 0.8278 | chr12 |
| 20500787 | hsa-miR-185-5p | 0.0233 | -1.78 | 6.52 | 7.36 | 0.8278 | chr22 |
| 20537253 | hsa-mir-6080 | 0.0234 | -1.67 | 1.68 | 2.42 | 0.8278 | chr17 |
| 20535146 | hsa-mir-493 | 0.0235 | -1.84 | 1.57 | 2.45 | 0.8278 | chr14 |
| 20525515 | hsa-miR-6777-5p | 0.0236 | 1.62 | 3.26 | 2.56 | 0.8278 | chr17 |
| 20500142 | hsa-miR-21-3p | 0.0237 | -1.19 | 1.5 | 1.75 | 0.8278 | chr17 |
| 20500446 | hsa-miR-181b-5p | 0.0239 | -1.31 | 5.88 | 6.27 | 0.8278 | chr1 |
| 20515644 | hsa-miR-3200-5p | 0.0239 | -1.57 | 1.17 | 1.82 | 0.8278 | chr22 |
| 20532737 | ENSG00000199411 | 0.0239 | -1.24 | 1.52 | 1.83 | 0.8278 | chr9 |
| 20517917 | hsa-miR-3664-5p | 0.024 | 1.13 | 1.35 | 1.17 | 0.8278 | chr11 |
| 20506787 | hsa-miR-1237-5p | 0.0243 | 1.4 | 7.38 | 6.89 | 0.8278 | chr11 |

**Table A.1. Small RNAs significantly altered following TDP-43 Knockdown.**

| ID | Transcript ID(Array Design) | P-val | Fold Change | siTDP Avg (log2) | SCR Avg (log2) | FDR P-val | Chromosome |
|---|---|---|---|---|---|---|---|
| 20533253 | ENSG00000238375 | 0.0243 | -1.18 | 1.4 | 1.63 | 0.8278 | chr6 |
| 20538319 | hsa-mir-4466 | 0.0243 | 1.38 | 2.67 | 2.2 | 0.8278 | chr6 |
| 20517909 | hsa-miR-3658 | 0.0244 | 1.16 | 0.96 | 0.75 | 0.8278 | chr1 |
| 20533389 | ENSG00000238581 | 0.0244 | -1.69 | 2.48 | 3.23 | 0.8278 | chr21 |
| 20536546 | hsa-mir-3620 | 0.0244 | -1.79 | 1.37 | 2.21 | 0.8278 | chr1 |
| 20538019 | hsa-mir-8061 | 0.0248 | -1.53 | 1.16 | 1.77 | 0.8278 | chr19 |
| 20529568 | hsa-miR-7977 | 0.0249 | 1.44 | 5.78 | 5.25 | 0.8278 | chr3 |
| 20536885 | hsa-mir-4659b | 0.0249 | 1.53 | 1.6 | 0.99 | 0.8278 | chr8 |
| 20534270 | HBII-52-26 | 0.025 | 1.13 | 1.32 | 1.13 | 0.8278 | chr15 |
| 20535432 | hsa-mir-758 | 0.0251 | -1.52 | 1.71 | 2.31 | 0.8278 | chr14 |
| 20536865 | hsa-mir-4645 | 0.0251 | -1.51 | 1.5 | 2.09 | 0.8278 | chr6 |
| 20517955 | hsa-miR-3691-3p | 0.0252 | -1.62 | 1.66 | 2.36 | 0.8278 | chr6 |
| 20519604 | hsa-miR-4747-5p | 0.0255 | -1.4 | 1.24 | 1.73 | 0.8278 | chr19 |
| 20532859 | ENSG00000201410 | 0.0255 | -1.51 | 1.09 | 1.68 | 0.8278 | chr3 |
| 20536493 | hsa-mir-4276 | 0.0256 | -1.49 | 1.28 | 1.85 | 0.8278 | chr4 |
| 20518897 | hsa-miR-4501 | 0.0257 | -1.52 | 1.02 | 1.63 | 0.8278 | chr13 |
| 20515523 | hsa-miR-3125 | 0.0262 | -1.15 | 0.98 | 1.18 | 0.8278 | chr2 |
| 20537984 | hsa-mir-4433b | 0.0262 | -1.11 | 1.14 | 1.29 | 0.8278 | chr2 |
| 20533462 | ENSG00000238696 | 0.0265 | 1.37 | 1.45 | 0.99 | 0.8278 | chr2 |
| 20535899 | hsa-mir-1277 | 0.0265 | -1.19 | 0.93 | 1.17 | 0.8278 | chrX |
| 20533115 | ENSG00000212565 | 0.0266 | 1.23 | 1.25 | 0.95 | 0.8278 | chr17 |
| 20536766 | hsa-mir-4492 | 0.0266 | -1.46 | 1.67 | 2.22 | 0.8278 | chr11 |
| 20533756 | ENSG00000239153 | 0.0268 | 1.42 | 1.92 | 1.42 | 0.8278 | chr11 |
| 20533606 | ENSG00000238922 | 0.027 | -1.8 | 1.09 | 1.94 | 0.8278 | chr7 |
| 20505747 | hsa-miR-890 | 0.0272 | -1.42 | 0.98 | 1.49 | 0.8278 | chrX |
| 20517821 | hsa-miR-3613-3p | 0.0273 | 1.56 | 6.92 | 6.27 | 0.8278 | chr13 |
| 20518843 | hsa-miR-3135b | 0.0273 | 1.57 | 5.43 | 4.79 | 0.8278 | chr6 |

**Table A.1. Small RNAs significantly altered following TDP-43 Knockdown.**

| ID | Transcript ID(Array Design) | P-val | Fold Change | siTDP Avg (log2) | SCR Avg (log2) | FDR P-val | Chromosome |
|---|---|---|---|---|---|---|---|
| 20534622 | hsa-mir-138-1 | 0.0274 | -1.19 | 1.59 | 1.84 | 0.8278 | chr3 |
| 20533190 | ENSG00000223111 | 0.0275 | -1.4 | 1.33 | 1.82 | 0.8278 | chr10 |
| 20533191 | ENSG00000223182 | 0.0275 | -1.4 | 1.33 | 1.82 | 0.8278 | chr10 |
| 20534172 | ENSG00000265733 | 0.0275 | -1.4 | 1.33 | 1.82 | 0.8278 | chrHG1211_PATCH |
| 20535888 | hsa-mir-1272 | 0.0276 | 1.61 | 1.68 | 1 | 0.8278 | chr15 |
| 20519517 | hsa-miR-4701-5p | 0.0279 | 1.56 | 2.26 | 1.62 | 0.8284 | chr12 |
| 20534238 | HBII-295 | 0.0281 | -1.39 | 1.52 | 1.99 | 0.8284 | chr9 |
| 20538489 | gi:555853 | 0.0281 | -1.14 | 13.45 | 13.63 | 0.8284 | |
| 20525026 | hsa-miR-6512-3p | 0.0283 | -1.29 | 1.2 | 1.57 | 0.8284 | chr2 |
| 20538262 | U85 | 0.0284 | -1.92 | 1.38 | 2.32 | 0.8284 | chr12 |
| 20536900 | hsa-mir-4674 | 0.0286 | 1.58 | 2.37 | 1.71 | 0.8284 | chr9 |
| 20533047 | ENSG00000212229 | 0.0289 | -1.15 | 1.41 | 1.62 | 0.8284 | chr6 |
| 20536970 | hsa-mir-4734 | 0.0289 | 1.4 | 2.43 | 1.94 | 0.8284 | chr17 |
| 20521782 | hsa-miR-4524b-3p | 0.029 | -1.27 | 1.22 | 1.56 | 0.8284 | chr17 |
| 20525453 | hsa-miR-6746-5p | 0.029 | 1.94 | 3.47 | 2.51 | 0.8284 | chr11 |
| 20525706 | hsa-miR-6872-3p | 0.029 | -1.87 | 1.82 | 2.72 | 0.8284 | chr3 |
| 20501233 | hsa-miR-373-5p | 0.0291 | -1.22 | 1.06 | 1.34 | 0.8284 | chr19 |
| 20535918 | hsa-mir-1255b-2 | 0.0294 | -1.41 | 1 | 1.5 | 0.8324 | chr1 |
| 20506788 | hsa-miR-1237-3p | 0.0297 | -1.64 | 1.51 | 2.23 | 0.8331 | chr11 |
| 20535387 | hsa-mir-638 | 0.0297 | 1.12 | 1.86 | 1.69 | 0.8331 | chr19 |
| 20536635 | hsa-mir-676 | 0.0298 | -1.35 | 1.28 | 1.71 | 0.8331 | chrX |
| 20519611 | hsa-miR-4751 | 0.0299 | 1.35 | 1.76 | 1.33 | 0.8331 | chr19 |
| 20521839 | hsa-miR-5590-3p | 0.0301 | -1.22 | 0.89 | 1.18 | 0.8338 | chr2 |
| 20533114 | ENSG00000212558 | 0.0302 | 1.52 | 1.87 | 1.27 | 0.8353 | chr2 |
| 20536437 | hsa-mir-4293 | 0.0306 | -1.86 | 1.49 | 2.39 | 0.8415 | chr10 |
| 20533384 | ENSG00000238575 | 0.0307 | -1.09 | 1.19 | 1.32 | 0.8415 | chr18 |
| 20538016 | hsa-mir-8058 | 0.0309 | 1.49 | 1.9 | 1.32 | 0.8427 | chr16 |

**Table A.1. Small RNAs significantly altered following TDP-43 Knockdown.**

| ID | Transcript ID(Array Design) | P-val | Fold Change | siTDP Avg (log2) | SCR Avg (log2) | FDR P-val | Chromosome |
|---|---|---|---|---|---|---|---|
| 20500751 | hsa-miR-143-5p | 0.0314 | -1.55 | 1.83 | 2.46 | 0.8492 | chr5 |
| 20535453 | hsa-mir-766 | 0.0315 | 1.33 | 1.7 | 1.28 | 0.8492 | chrX |
| 20518803 | hsa-miR-548ad | 0.0316 | -1.29 | 0.89 | 1.26 | 0.8492 | chr2 |
| 20533729 | ENSG00000239111 | 0.0316 | -1.26 | 1.42 | 1.75 | 0.8492 | chr1 |
| 20537586 | hsa-mir-6841 | 0.0318 | 1.21 | 1.43 | 1.15 | 0.85 | chr8 |
| 20536796 | hsa-mir-4518 | 0.0321 | -1.29 | 1.68 | 2.05 | 0.8541 | chr16 |
| 20506869 | hsa-miR-1273a | 0.0324 | -1.56 | 1.33 | 1.98 | 0.855 | chr8 |
| 20519679 | hsa-miR-4787-5p | 0.0324 | 1.29 | 9.22 | 8.85 | 0.855 | chr3 |
| 20502122 | hsa-miR-422a | 0.0326 | -1.22 | 6.64 | 6.93 | 0.855 | chr15 |
| 20536615 | hsa-mir-3914-2 | 0.0326 | 1.46 | 1.52 | 0.97 | 0.855 | chr7 |
| 20533707 | ENSG00000239072 | 0.0332 | 1.43 | 1.95 | 1.44 | 0.8557 | chr2 |
| 20534829 | hsa-mir-26a-2 | 0.0333 | -1.25 | 1.38 | 1.7 | 0.8557 | chr12 |
| 20532669 | ACA40 | 0.0334 | -1.72 | 2.02 | 2.8 | 0.8557 | chr11 |
| 20532862 | ENSG00000201465 | 0.0334 | -1.19 | 1.17 | 1.42 | 0.8557 | chr7 |
| 20500469 | hsa-miR-212-3p | 0.0335 | 1.84 | 3.6 | 2.72 | 0.8557 | chr17 |
| 20535218 | hsa-mir-509-1 | 0.0337 | -1.43 | 1.15 | 1.67 | 0.8557 | chrX |
| 20535638 | hsa-mir-509-2 | 0.0337 | -1.43 | 1.15 | 1.67 | 0.8557 | chrX |
| 20535683 | hsa-mir-509-3 | 0.0337 | -1.43 | 1.15 | 1.67 | 0.8557 | chrX |
| 20533559 | ENSG00000238852 | 0.0339 | -1.22 | 1.45 | 1.74 | 0.8573 | chr2 |
| 20536652 | hsa-mir-374c | 0.0343 | 1.13 | 1.74 | 1.56 | 0.8636 | chrX |
| 20538460 | spike_in-control-17 | 0.035 | 1.2 | 1.68 | 1.42 | 0.8659 | |
| 20533092 | ENSG00000212445 | 0.0354 | -1.56 | 1.59 | 2.23 | 0.8659 | chr16 |
| 20515564 | hsa-miR-3150a-5p | 0.0356 | -1.45 | 1.58 | 2.12 | 0.8659 | chr8 |
| 20532765 | ENSG00000199934 | 0.0358 | -1.34 | 0.94 | 1.36 | 0.8659 | chr1 |
| 20534526 | hsa-mir-210 | 0.0359 | -1.59 | 1.82 | 2.5 | 0.8659 | chr11 |
| 20518882 | hsa-miR-4488 | 0.0364 | 1.27 | 7.51 | 7.16 | 0.8659 | chr11 |
| 20506012 | hsa-miR-941 | 0.0365 | -1.61 | 4.5 | 5.2 | 0.8659 | chr20 |

**Table A.1. Small RNAs significantly altered following TDP-43 Knockdown.**

| ID | Transcript ID(Array Design) | P-val | Fold Change | siTDP Avg (log2) | SCR Avg (log2) | FDR P-val | Chromosome |
|---|---|---|---|---|---|---|---|
| 20518628 | hsa-miR-3939 | 0.0367 | -1.31 | 1.42 | 1.81 | 0.8659 | chr6 |
| 20538044 | hsa-mir-8084 | 0.0367 | 1.23 | 1.28 | 0.98 | 0.8659 | chr8 |
| 20517712 | hsa-miR-4254 | 0.0369 | 1.79 | 2.44 | 1.6 | 0.8659 | chr1 |
| 20536805 | hsa-mir-4525 | 0.037 | -2.04 | 1.46 | 2.49 | 0.8659 | chr17 |
| 20536907 | hsa-mir-4679-1 | 0.037 | 1.17 | 1.1 | 0.87 | 0.8659 | chr10 |
| 20532994 | ENSG00000207130 | 0.0371 | 1.21 | 1.7 | 1.42 | 0.8659 | chr3 |
| 20536318 | hsa-mir-3198-1 | 0.0374 | -1.66 | 1.58 | 2.31 | 0.8659 | chr22 |
| 20536933 | hsa-mir-3198-2 | 0.0374 | -1.66 | 1.58 | 2.31 | 0.8659 | chr12 |
| 20500450 | hsa-miR-182-5p | 0.0375 | -1.55 | 7.51 | 8.14 | 0.8659 | chr7 |
| 20500728 | hsa-miR-124-5p | 0.0375 | 1.33 | 2.22 | 1.81 | 0.8659 | chr20 |
| 20525690 | hsa-miR-6864-3p | 0.0376 | 1.22 | 1.48 | 1.2 | 0.8659 | chr17 |
| 20529133 | hsa-miR-1273h-3p | 0.0377 | 1.23 | 1.88 | 1.59 | 0.8659 | chr16 |
| 20538303 | snR38C | 0.0379 | 1.3 | 8.43 | 8.05 | 0.8659 | chr17 |
| 20533280 | ENSG00000238428 | 0.0383 | -2.4 | 1.17 | 2.43 | 0.8659 | chr2 |
| 20535144 | hsa-mir-202 | 0.0383 | 1.33 | 1.61 | 1.2 | 0.8659 | chr10 |
| 20535822 | hsa-mir-1285-2 | 0.0384 | -1.18 | 1.14 | 1.37 | 0.8659 | chr2 |
| 20537608 | hsa-mir-6862-1 | 0.0385 | -1.53 | 1.27 | 1.89 | 0.8659 | chr16 |
| 20538092 | hsa-mir-6862-2 | 0.0385 | -1.53 | 1.27 | 1.89 | 0.8659 | chr16 |
| 20525466 | hsa-miR-6752-3p | 0.039 | -1.4 | 0.86 | 1.35 | 0.8659 | chr11 |
| 20533988 | ENSG00000252557 | 0.0394 | 1.11 | 1.17 | 1.02 | 0.8659 | chr7 |
| 20537594 | hsa-mir-6849 | 0.0398 | 1.63 | 2.18 | 1.48 | 0.8659 | chr8 |
| 20535143 | hsa-mir-146b | 0.0399 | -1.4 | 1.38 | 1.86 | 0.8659 | chr10 |
| 20504553 | hsa-miR-671-3p | 0.04 | -1.57 | 2.19 | 2.84 | 0.8659 | chr7 |
| 20518856 | hsa-miR-4471 | 0.04 | 1.21 | 1.46 | 1.18 | 0.8659 | chr8 |
| 20534845 | hsa-mir-376c | 0.0403 | 1.32 | 1.52 | 1.11 | 0.8659 | chr14 |
| 20533749 | ENSG00000239141 | 0.0404 | 1.22 | 1.42 | 1.14 | 0.8659 | chr3 |
| 20536576 | hsa-mir-3672 | 0.0404 | -1.19 | 1.21 | 1.46 | 0.8659 | chrX |

**Table A.1. Small RNAs significantly altered following TDP-43 Knockdown.**

| ID | Transcript ID(Array Design) | P-val | Fold Change | siTDP Avg (log2) | SCR Avg (log2) | FDR P-val | Chromosome |
|---|---|---|---|---|---|---|---|
| 20536718 | hsa-mir-4461 | 0.0404 | 1.41 | 1.96 | 1.47 | 0.8659 | chr5 |
| 20537236 | hsa-mir-5739 | 0.0404 | -1.13 | 1.14 | 1.31 | 0.8659 | chr22 |
| 20504328 | hsa-miR-591 | 0.0405 | -1.19 | 0.98 | 1.23 | 0.8659 | chr7 |
| 20518000 | hsa-miR-3714 | 0.0407 | -2.06 | 1.26 | 2.31 | 0.8659 | chr3 |
| 20536641 | hsa-mir-3936 | 0.0408 | 1.47 | 1.89 | 1.34 | 0.8659 | chr5 |
| 20532585 | 14qII-17 | 0.0409 | 1.16 | 1.3 | 1.09 | 0.8659 | chr14 |
| 20533179 | ENSG00000222185 | 0.0409 | 1.28 | 1.23 | 0.87 | 0.8659 | chr14 |
| 20536873 | hsa-mir-4652 | 0.041 | -1.34 | 1.16 | 1.59 | 0.8659 | chr7 |
| 20536028 | hsa-mir-2116 | 0.0411 | -1.25 | 1.39 | 1.71 | 0.8659 | chr15 |
| 20534577 | hsa-mir-124-1 | 0.0414 | 1.27 | 1.31 | 0.97 | 0.8659 | chr8 |
| 20501155 | hsa-miR-194-3p | 0.0418 | -1.89 | 1.32 | 2.23 | 0.8659 | chr11 |
| 20538236 | U71a | 0.0418 | -1.22 | 2.21 | 2.5 | 0.8659 | chr20 |
| 20533593 | ENSG00000238899 | 0.042 | -1.53 | 1.15 | 1.76 | 0.8659 | chr5 |
| 20537563 | hsa-mir-6819 | 0.042 | 1.43 | 2.46 | 1.95 | 0.8659 | chr22 |
| 20536695 | hsa-mir-4441 | 0.0421 | -1.37 | 1.3 | 1.75 | 0.8659 | chr2 |
| 20506004 | hsa-miR-935 | 0.0422 | -1.37 | 6.38 | 6.84 | 0.8659 | chr19 |
| 20515638 | hsa-miR-3196 | 0.0422 | 1.79 | 9.31 | 8.47 | 0.8659 | chr20 |
| 20536509 | hsa-mir-4289 | 0.0424 | -1.24 | 1.61 | 1.92 | 0.8659 | chr9 |
| 20534362 | hsa-mir-22 | 0.0426 | -1.17 | 1.5 | 1.73 | 0.8659 | chr17 |
| 20519409 | hsa-miR-4634 | 0.043 | 1.61 | 1.98 | 1.3 | 0.8659 | chr5 |
| 20533323 | ENSG00000238494 | 0.0431 | 1.27 | 1.68 | 1.33 | 0.8659 | chr15 |
| 20533349 | ENSG00000238535 | 0.0431 | 1.27 | 1.68 | 1.33 | 0.8659 | chr15 |
| 20500486 | hsa-miR-222-3p | 0.0432 | -1.26 | 11.72 | 12.04 | 0.8659 | chrX |
| 20533061 | ENSG00000212309 | 0.0433 | 1.24 | 1.47 | 1.16 | 0.8659 | chr2 |
| 20519473 | hsa-miR-4673 | 0.0434 | -1.56 | 1.91 | 2.55 | 0.8659 | chr9 |
| 20500780 | hsa-miR-149-5p | 0.0435 | -1.23 | 5.69 | 5.98 | 0.8659 | chr2 |
| 20506873 | hsa-miR-1276 | 0.0435 | 1.39 | 1.3 | 0.82 | 0.8659 | chr15 |

**Table A.1. Small RNAs significantly altered following TDP-43 Knockdown.**

| ID | Transcript ID(Array Design) | P-val | Fold Change | siTDP Avg (log2) | SCR Avg (log2) | FDR P-val | Chromosome |
|---|---|---|---|---|---|---|---|
| 20537227 | hsa-mir-5704 | 0.0437 | 1.23 | 1.53 | 1.23 | 0.8659 | chr3 |
| 20525544 | hsa-miR-6791-3p | 0.0441 | 1.35 | 1.75 | 1.31 | 0.8659 | chr19 |
| 20532879 | ENSG00000201701 | 0.0441 | 1.47 | 1.51 | 0.96 | 0.8659 | chr3 |
| 20533390 | ENSG00000238582 | 0.0441 | -1.4 | 1.14 | 1.63 | 0.8659 | chr2 |
| 20517938 | hsa-miR-3680-5p | 0.0442 | 1.51 | 1.79 | 1.19 | 0.8659 | chr16 |
| 20538307 | ENSG00000199552 | 0.0443 | -1.4 | 1.35 | 1.84 | 0.8659 | chr5 |
| 20536557 | hsa-mir-3653 | 0.0444 | -1.41 | 1.96 | 2.46 | 0.8659 | chr22 |
| 20538115 | SNORD125 | 0.0444 | -1.41 | 1.96 | 2.46 | 0.8659 | chr22 |
| 20537439 | hsa-mir-6508 | 0.0445 | 1.49 | 1.77 | 1.19 | 0.8659 | chr21 |
| 20500399 | hsa-miR-199a-5p | 0.0447 | -1.3 | 1.59 | 1.97 | 0.8659 | chr1 |
| 20532847 | ENSG00000201316 | 0.0449 | 1.2 | 1.69 | 1.43 | 0.8659 | chr8 |
| 20534374 | hsa-mir-28 | 0.0449 | -1.12 | 1.6 | 1.77 | 0.8659 | chr3 |
| 20536552 | hsa-mir-3648 | 0.0449 | 1.64 | 3 | 2.29 | 0.8659 | chr21 |
| 20507744 | hsa-miR-1471 | 0.045 | -1.52 | 1.37 | 1.97 | 0.8659 | chr2 |
| 20501157 | hsa-miR-106b-5p | 0.0451 | -1.77 | 7.43 | 8.25 | 0.8659 | chr7 |
| 20536555 | hsa-mir-3651 | 0.0451 | 1.24 | 3.15 | 2.84 | 0.8659 | chr9 |
| 20538106 | SNORA84 | 0.0451 | 1.24 | 3.15 | 2.84 | 0.8659 | chr9 |
| 20537597 | hsa-mir-6852 | 0.0452 | 1.53 | 2.05 | 1.44 | 0.8659 | chr9 |
| 20502452 | hsa-miR-452-3p | 0.0453 | 1.37 | 1.54 | 1.08 | 0.8659 | chrX |
| 20519587 | hsa-miR-4738-5p | 0.046 | 1.22 | 1.55 | 1.26 | 0.8659 | chr17 |
| 20501201 | hsa-miR-362-5p | 0.0461 | -2.41 | 3.84 | 5.11 | 0.8659 | chrX |
| 20536268 | hsa-mir-3161 | 0.0462 | 1.33 | 1.4 | 0.98 | 0.8659 | chr11 |
| 20536464 | hsa-mir-4323 | 0.0464 | -1.32 | 2.4 | 2.8 | 0.8659 | chr19 |
| 20533219 | ENSG00000238328 | 0.0466 | 1.2 | 1.31 | 1.05 | 0.8659 | chr2 |
| 20535414 | hsa-mir-656 | 0.0467 | -1.12 | 1.34 | 1.51 | 0.8659 | chr14 |
| 20520197 | hsa-miR-5000-3p | 0.0469 | 1.4 | 1.43 | 0.95 | 0.8659 | chr2 |
| 20535306 | hsa-mir-568 | 0.0469 | 1.24 | 1.37 | 1.06 | 0.8659 | chr3 |

**Table A.1. Small RNAs significantly altered following TDP-43 Knockdown.**

| ID | Transcript ID(Array Design) | P-val | Fold Change | siTDP Avg (log2) | SCR Avg (log2) | FDR P-val | Chromosome |
|---|---|---|---|---|---|---|---|
| 20538000 | hsa-mir-548ba | 0.047 | 1.25 | 1.21 | 0.89 | 0.8659 | chr2 |
| 20536435 | hsa-mir-4297 | 0.0473 | -1.47 | 2.57 | 3.13 | 0.8659 | chr10 |
| 20533067 | ENSG00000212347 | 0.0474 | 1.35 | 1.2 | 0.77 | 0.8659 | chrX |
| 20534199 | ENSG00000268513 | 0.0474 | 1.35 | 1.2 | 0.77 | 0.8659 | chrHG1435_PATCH |
| 20525420 | hsa-miR-6729-5p | 0.0475 | 1.23 | 8.67 | 8.38 | 0.8659 | chr1 |
| 20535180 | hsa-mir-517a | 0.0479 | -1.18 | 1.13 | 1.37 | 0.8659 | chr19 |
| 20506811 | hsa-miR-548j-3p | 0.048 | -1.54 | 1.16 | 1.78 | 0.8659 | chr22 |
| 20525525 | hsa-miR-6782-5p | 0.048 | 2.12 | 3.13 | 2.05 | 0.8659 | chr17 |
| 20533794 | ENSG00000251778 | 0.048 | -1.51 | 1.25 | 1.85 | 0.8659 | chr21 |
| 20533967 | ENSG00000252458 | 0.048 | -1.14 | 1.36 | 1.55 | 0.8659 | chr5 |
| 20537632 | hsa-mir-6886 | 0.0481 | -1.43 | 2.8 | 3.32 | 0.8659 | chr19 |
| 20538270 | U90 | 0.0482 | -1.35 | 1.85 | 2.28 | 0.8659 | chr3 |
| 20519410 | hsa-miR-4635 | 0.0485 | -1.44 | 3.96 | 4.48 | 0.8659 | chr5 |
| 20502130 | hsa-miR-425-3p | 0.0488 | -2.24 | 2.64 | 3.8 | 0.8659 | chr3 |
| 20518790 | hsa-miR-4421 | 0.0488 | 1.36 | 1.55 | 1.11 | 0.8659 | chr1 |
| 20536504 | hsa-mir-4284 | 0.0488 | 1.27 | 1.91 | 1.56 | 0.8659 | chr7 |
| 20536541 | hsa-mir-3616 | 0.0488 | 1.32 | 2.1 | 1.69 | 0.8659 | chr20 |
| 20538045 | hsa-mir-8085 | 0.0492 | -1.49 | 1.54 | 2.12 | 0.8659 | chr19 |
| 20533700 | ENSG00000239063 | 0.0496 | -1.35 | 1.21 | 1.65 | 0.8659 | chr1 |
| 20500152 | hsa-miR-26a-5p | 0.0497 | -1.43 | 8.25 | 8.77 | 0.8659 | chr12 |
| 20502237 | hsa-miR-20b-5p | 0.0498 | -1.59 | 6.18 | 6.85 | 0.8659 | chrX |
| 20504550 | hsa-miR-758-3p | 0.0498 | -1.59 | 1.18 | 1.84 | 0.8659 | chr14 |
| 20500139 | hsa-miR-20a-5p | 0.0499 | -1.55 | 9.45 | 10.08 | 0.8659 | chr13 |
| 20536578 | hsa-mir-3674 | 0.05 | -1.19 | 1.07 | 1.32 | 0.8659 | chr8 |

**Table A.2. Small RNAs significantly altered following FUS Knockdown.**

| ID | Transcript ID(Array Design) | P-val | Fold Change | siFUS Avg (log2) | SCR Avg (log2) | FDR P-val | Chromosome |
|---|---|---|---|---|---|---|---|
| 20537518 | hsa-mir-6775 | 0.0002 | -2.34 | 1.61 | 2.83 | 0.8811 | chr16 |
| 20534818 | hsa-mir-219a-2 | 0.0003 | -1.49 | 1.31 | 1.89 | 0.8811 | chr9 |
| 20518818 | hsa-miR-4443 | 0.0005 | -1.46 | 6.5 | 7.04 | 0.8811 | chr3 |
| 20535460 | hsa-mir-1298 | 0.0005 | -1.3 | 1.68 | 2.07 | 0.8811 | chrX |
| 20537592 | hsa-mir-6847 | 0.0009 | 1.66 | 2.24 | 1.51 | 0.9953 | chr8 |
| 20536775 | hsa-mir-4500 | 0.001 | -1.69 | 1.33 | 2.09 | 0.9953 | chr13 |
| 20506005 | hsa-miR-936 | 0.0011 | -1.56 | 1.29 | 1.94 | 0.9953 | chr10 |
| 20535879 | hsa-mir-1263 | 0.0017 | -2.15 | 1.81 | 2.91 | 0.9953 | chr3 |
| 20522017 | hsa-miR-548ax | 0.0023 | -1.63 | 0.95 | 1.66 | 0.9953 | chrX |
| 20520348 | hsa-miR-5095 | 0.0025 | -1.49 | 1.31 | 1.88 | 0.9953 | chr1 |
| 20517909 | hsa-miR-3658 | 0.0028 | 1.29 | 1.11 | 0.75 | 0.9953 | chr1 |
| 20529568 | hsa-miR-7977 | 0.0029 | 1.9 | 6.18 | 5.25 | 0.9953 | chr3 |
| 20536752 | hsa-mir-4480 | 0.003 | -1.3 | 1.23 | 1.6 | 0.9953 | chr10 |
| 20533957 | ENSG00000252433 | 0.003 | 1.29 | 1.33 | 0.96 | 0.9953 | chr1 |
| 20537586 | hsa-mir-6841 | 0.0031 | 1.3 | 1.53 | 1.15 | 0.9953 | chr8 |
| 20532591 | 14qII-20 | 0.0032 | 1.28 | 1.53 | 1.18 | 0.9953 | chr14 |
| 20525669 | hsa-miR-6854-5p | 0.0033 | 1.5 | 1.58 | 1 | 0.9953 | chr9 |
| 20504582 | hsa-miR-766-5p | 0.0033 | -1.91 | 1.47 | 2.4 | 0.9953 | chrX |
| 20525546 | hsa-miR-6792-3p | 0.0039 | 1.51 | 1.59 | 0.99 | 0.9953 | chr19 |
| 20536018 | hsa-mir-1976 | 0.0039 | -1.9 | 1.51 | 2.44 | 0.9953 | chr1 |
| 20534091 | ENSG00000253013 | 0.004 | -1.82 | 1.44 | 2.31 | 0.9953 | chr4 |
| 20537456 | hsa-mir-6715b | 0.0041 | 1.36 | 2.16 | 1.72 | 0.9953 | chr10 |
| 20517821 | hsa-miR-3613-3p | 0.0052 | 1.81 | 7.13 | 6.27 | 0.9953 | chr13 |
| 20532932 | ENSG00000202449 | 0.0053 | 1.32 | 1.22 | 0.81 | 0.9953 | chr4 |
| 20525569 | hsa-miR-6804-5p | 0.0054 | -1.85 | 1.25 | 2.14 | 0.9953 | chr19 |
| 20518879 | hsa-miR-4485 | 0.0054 | 1.5 | 7.49 | 6.9 | 0.9953 | chr11 |
| 20536268 | hsa-mir-3161 | 0.0054 | 1.6 | 1.66 | 0.98 | 0.9953 | chr11 |
| 20535402 | hsa-mir-652 | 0.0055 | -1.48 | 1.49 | 2.06 | 0.9953 | chrX |

**Table A.2. Small RNAs significantly altered following FUS Knockdown.**

| ID | Transcript ID(Array Design) | P-val | Fold Change | siFUS Avg (log2) | SCR Avg (log2) | FDR P-val | Chromosome |
|---|---|---|---|---|---|---|---|
| 20533069 | ENSG00000212363 | 0.0057 | 1.3 | 1.3 | 0.91 | 0.9953 | chr5 |
| 20536889 | hsa-mir-4664 | 0.0059 | -1.51 | 1.47 | 2.06 | 0.9953 | chr8 |
| 20518816 | hsa-miR-4441 | 0.0071 | -1.23 | 1.17 | 1.46 | 0.9953 | chr2 |
| 20537988 | hsa-mir-7845 | 0.0073 | -1.88 | 1.54 | 2.45 | 0.9953 | chr2 |
| 20536920 | hsa-mir-4689 | 0.0075 | -1.85 | 1.68 | 2.57 | 0.9953 | chr1 |
| 20536297 | hsa-mir-3181 | 0.0076 | 1.48 | 1.88 | 1.31 | 0.9953 | chr16 |
| 20536025 | hsa-mir-2110 | 0.0076 | 1.27 | 1.93 | 1.58 | 0.9953 | chr10 |
| 20525027 | hsa-miR-6513-5p | 0.0078 | -1.59 | 1.41 | 2.08 | 0.9953 | chr2 |
| 20536800 | hsa-mir-4521 | 0.0078 | 1.57 | 2.25 | 1.6 | 0.9953 | chr17 |
| 20500741 | hsa-miR-135a-3p | 0.008 | -1.64 | 1.15 | 1.86 | 0.9953 | chr3 |
| 20532570 | 14ql-5 | 0.0082 | 1.4 | 1.46 | 0.97 | 0.9953 | chr14 |
| 20520197 | hsa-miR-5000-3p | 0.0083 | 1.53 | 1.56 | 0.95 | 0.9953 | chr2 |
| 20533763 | ENSG00000239159 | 0.0084 | -1.33 | 0.99 | 1.41 | 0.9953 | chr5 |
| 20537563 | hsa-mir-6819 | 0.0085 | 1.57 | 2.6 | 1.95 | 0.9953 | chr22 |
| 20519451 | hsa-miR-4659b-5p | 0.0086 | 1.3 | 1.18 | 0.8 | 0.9953 | chr8 |
| 20518929 | hsa-miR-4529-5p | 0.0087 | 1.5 | 1.78 | 1.2 | 0.9953 | chr18 |
| 20534238 | HBII-295 | 0.0088 | -1.48 | 1.42 | 1.99 | 0.9953 | chr9 |
| 20535842 | hsa-mir-1302-5 | 0.0092 | -1.38 | 0.91 | 1.38 | 0.9953 | chr20 |
| 20500462 | hsa-miR-205-5p | 0.0094 | 1.44 | 1.57 | 1.04 | 0.9953 | chr1 |
| 20535432 | hsa-mir-758 | 0.0094 | -1.6 | 1.63 | 2.31 | 0.9953 | chr14 |
| 20536497 | hsa-mir-4277 | 0.0106 | -1.86 | 1.73 | 2.63 | 0.9953 | chr5 |
| 20537026 | hsa-mir-4776-1 | 0.0107 | 1.59 | 2.13 | 1.46 | 0.9953 | chr2 |
| 20533253 | ENSG00000238375 | 0.011 | -1.27 | 1.29 | 1.63 | 0.9953 | chr6 |
| 20518834 | hsa-miR-4454 | 0.0111 | -1.51 | 7.76 | 8.36 | 0.9953 | chr4 |
| 20533431 | ENSG00000238656 | 0.0112 | 1.11 | 1.02 | 0.87 | 0.9953 | chr8 |
| 20525731 | hsa-miR-6885-5p | 0.0114 | -2.33 | 1.65 | 2.87 | 0.9953 | chr19 |
| 20535446 | hsa-mir-1271 | 0.0114 | 1.4 | 2.05 | 1.57 | 0.9953 | chr5 |
| 20521804 | hsa-miR-548ar-5p | 0.0116 | 1.37 | 1.55 | 1.1 | 0.9953 | chr13 |

**Table A.2. Small RNAs significantly altered following FUS Knockdown.**

| ID | Transcript ID(Array Design) | P-val | Fold Change | siFUS Avg (log2) | SCR Avg (log2) | FDR P-val | Chromosome |
|---|---|---|---|---|---|---|---|
| 20510800 | hsa-miR-1973 | 0.0121 | -2.27 | 1.89 | 3.07 | 0.9953 | chr4 |
| 20536628 | hsa-mir-3910-2 | 0.0122 | 1.52 | 1.99 | 1.39 | 0.9953 | chr9 |
| 20532626 | ACA16 | 0.0125 | 1.68 | 2.58 | 1.83 | 0.9953 | chr1 |
| 20537565 | hsa-mir-6821 | 0.0126 | 1.47 | 1.83 | 1.27 | 0.9953 | chr22 |
| 20533128 | ENSG00000212604 | 0.0126 | -1.61 | 1.17 | 1.86 | 0.9953 | chr15 |
| 20520565 | hsa-miR-5187-5p | 0.013 | -1.63 | 0.92 | 1.62 | 0.9953 | chr1 |
| 20506771 | hsa-miR-1227-5p | 0.013 | -1.77 | 2.91 | 3.74 | 0.9953 | chr19 |
| 20518893 | hsa-miR-4498 | 0.0131 | -1.31 | 2.24 | 2.63 | 0.9953 | chr12 |
| 20532926 | ENSG00000202374 | 0.0132 | -1.61 | 1.42 | 2.1 | 0.9953 | chr4 |
| 20522039 | hsa-miR-5703 | 0.0133 | -1.91 | 1.2 | 2.13 | 0.9953 | chr2 |
| 20537868 | hsa-mir-7152 | 0.0133 | 1.53 | 2.13 | 1.52 | 0.9953 | chr10 |
| 20533760 | ENSG00000239157 | 0.0134 | -1.23 | 1.38 | 1.68 | 0.9953 | chr20 |
| 20519075 | hsa-miR-3973 | 0.0137 | -1.27 | 1.64 | 1.99 | 0.9953 | chr11 |
| 20533280 | ENSG00000238428 | 0.014 | -2.15 | 1.33 | 2.43 | 0.9953 | chr2 |
| 20538115 | SNORD125 | 0.0142 | -1.49 | 1.88 | 2.46 | 0.9953 | chr22 |
| 20536560 | hsa-mir-3656 | 0.0142 | -1.7 | 1.94 | 2.71 | 0.9953 | chr11 |
| 20536557 | hsa-mir-3653 | 0.0142 | -1.49 | 1.88 | 2.46 | 0.9953 | chr22 |
| 20536963 | hsa-mir-4727 | 0.0145 | -1.5 | 1.42 | 2.01 | 0.9953 | chr17 |
| 20537143 | hsa-mir-3680-2 | 0.0148 | 1.53 | 1.83 | 1.21 | 0.9953 | chr16 |
| 20536583 | hsa-mir-3680-1 | 0.0148 | 1.53 | 1.83 | 1.21 | 0.9953 | chr16 |
| 20533583 | ENSG00000238888 | 0.0149 | 1.39 | 1.39 | 0.92 | 0.9953 | chr2 |
| 20520568 | hsa-miR-5189-5p | 0.015 | -1.93 | 2.32 | 3.27 | 0.9953 | chr16 |
| 20500448 | hsa-miR-181c-5p | 0.0152 | -1.37 | 1.51 | 1.97 | 0.9953 | chr19 |
| 20533980 | ENSG00000252526 | 0.0153 | -1.36 | 1.36 | 1.81 | 0.9953 | chr16 |
| 20519408 | hsa-miR-4633-3p | 0.0157 | -1.56 | 1.26 | 1.9 | 0.9953 | chr5 |
| 20504553 | hsa-miR-671-3p | 0.0158 | -1.74 | 2.04 | 2.84 | 0.9953 | chr7 |
| 20533810 | ENSG00000251836 | 0.0158 | 1.55 | 1.92 | 1.29 | 0.9953 | chr10 |
| 20501274 | hsa-miR-340-3p | 0.0159 | 1.25 | 2.03 | 1.71 | 0.9953 | chr5 |

**Table A.2. Small RNAs significantly altered following FUS Knockdown.**

| ID | Transcript ID(Array Design) | P-val | Fold Change | siFUS Avg (log2) | SCR Avg (log2) | FDR P-val | Chromosome |
|---|---|---|---|---|---|---|---|
| 20500454 | hsa-miR-187-5p | 0.016 | -1.53 | 1.96 | 2.57 | 0.9953 | chr18 |
| 20518943 | hsa-miR-548an | 0.0161 | 1.32 | 1.48 | 1.08 | 0.9953 | chrX |
| 20506708 | hsa-miR-1178-5p | 0.0163 | -1.26 | 1.06 | 1.39 | 0.9953 | chr12 |
| 20538215 | U61 | 0.0165 | 1.28 | 3.24 | 2.88 | 0.9953 | chrX |
| 20536605 | hsa-mir-3909 | 0.0165 | 1.57 | 1.97 | 1.31 | 0.9953 | chr22 |
| 20537011 | hsa-mir-4769 | 0.0166 | -1.38 | 1 | 1.46 | 0.9953 | chrX |
| 20538270 | U90 | 0.0168 | -1.45 | 1.74 | 2.28 | 0.9953 | chr3 |
| 20533654 | ENSG00000238996 | 0.0168 | 1.46 | 1.65 | 1.1 | 0.9953 | chr9 |
| 20533156 | ENSG00000221300 | 0.0169 | 1.31 | 1.36 | 0.97 | 0.9953 | chr2 |
| 20537517 | hsa-mir-6774 | 0.017 | -1.6 | 1.67 | 2.35 | 0.9953 | chr16 |
| 20537221 | hsa-mir-5699 | 0.017 | 1.33 | 2.01 | 1.6 | 0.9953 | chr10 |
| 20533047 | ENSG00000212229 | 0.017 | -1.22 | 1.33 | 1.62 | 0.9953 | chr6 |
| 20537519 | hsa-mir-6776 | 0.0171 | 1.47 | 4.53 | 3.97 | 0.9953 | chr17 |
| 20533594 | ENSG00000238900 | 0.0171 | 1.26 | 1.31 | 0.98 | 0.9953 | chr10 |
| 20517819 | hsa-miR-3612 | 0.0173 | -1.25 | 0.89 | 1.21 | 0.9953 | chr12 |
| 20515608 | hsa-miR-3179 | 0.0174 | -1.41 | 1.15 | 1.65 | 0.9953 | chr16 |
| 20506789 | hsa-miR-1238-5p | 0.0175 | -1.6 | 1.33 | 2.01 | 0.9953 | chr19 |
| 20535246 | hsa-mir-545 | 0.0175 | 1.34 | 1.72 | 1.3 | 0.9953 | chrX |
| 20524051 | hsa-miR-6130 | 0.0177 | -1.11 | 0.98 | 1.13 | 0.9953 | chr21 |
| 20521782 | hsa-miR-4524b-3p | 0.0184 | -1.3 | 1.18 | 1.56 | 0.9953 | chr17 |
| 20534194 | ENSG00000268145 | 0.0185 | 1.41 | 1.78 | 1.29 | 0.9953 | chrHG1462_PATCH |
| 20533963 | ENSG00000252441 | 0.0185 | 1.41 | 1.78 | 1.29 | 0.9953 | chrX |
| 20519695 | hsa-miR-4797-5p | 0.0187 | 1.42 | 2 | 1.49 | 0.9953 | chr3 |
| 20533808 | ENSG00000251830 | 0.0187 | -1.38 | 1.42 | 1.89 | 0.9953 | chr6 |
| 20536580 | hsa-mir-3677 | 0.0189 | 1.21 | 2.16 | 1.89 | 0.9953 | chr16 |
| 20533952 | ENSG00000252405 | 0.0189 | 1.26 | 1.32 | 0.99 | 0.9953 | chr16 |
| 20525732 | hsa-miR-6885-3p | 0.0193 | 1.66 | 1.74 | 1.01 | 0.9953 | chr19 |
| 20518785 | hsa-miR-4417 | 0.02 | -2.11 | 1.94 | 3.01 | 0.9953 | chr1 |

**Table A.2. Small RNAs significantly altered following FUS Knockdown.**

| ID | Transcript ID(Array Design) | P-val | Fold Change | siFUS Avg (log2) | SCR Avg (log2) | FDR P-val | Chromosome |
|---|---|---|---|---|---|---|---|
| 20534360 | hsa-mir-20a | 0.02 | 1.21 | 1.47 | 1.2 | 0.9953 | chr13 |
| 20537226 | hsa-mir-5692b | 0.0204 | 1.36 | 1.4 | 0.95 | 0.9953 | chr21 |
| 20504374 | hsa-miR-626 | 0.0209 | -1.26 | 0.98 | 1.31 | 0.9953 | chr15 |
| 20505755 | hsa-miR-889-3p | 0.0211 | 1.16 | 1.18 | 0.97 | 0.9953 | chr14 |
| 20537538 | hsa-mir-6795 | 0.0211 | 1.4 | 1.59 | 1.11 | 0.9953 | chr19 |
| 20536759 | hsa-mir-4487 | 0.0212 | -1.74 | 1.29 | 2.09 | 0.9953 | chr11 |
| 20532571 | 14ql-6 | 0.0214 | 1.17 | 1.53 | 1.3 | 0.9953 | chr14 |
| 20506008 | hsa-miR-938 | 0.0216 | 1.35 | 1.41 | 0.97 | 0.9953 | chr10 |
| 20520217 | hsa-miR-5009-3p | 0.0218 | 1.29 | 1.26 | 0.89 | 0.9953 | chr15 |
| 20535360 | hsa-mir-613 | 0.0218 | 1.21 | 1.76 | 1.48 | 0.9953 | chr12 |
| 20534083 | ENSG00000252985 | 0.022 | -1.25 | 1.46 | 1.78 | 0.9953 | chr9 |
| 20535393 | hsa-mir-643 | 0.0225 | 1.48 | 1.49 | 0.93 | 0.9953 | chr19 |
| 20511549 | hsa-miR-2110 | 0.0228 | -2.23 | 3.11 | 4.26 | 0.9953 | chr10 |
| 20519564 | hsa-miR-4725-5p | 0.023 | -1.52 | 1.35 | 1.96 | 0.9953 | chr17 |
| 20536853 | hsa-mir-4633 | 0.023 | 1.89 | 2.45 | 1.53 | 0.9953 | chr5 |
| 20519432 | hsa-miR-4650-3p | 0.0231 | -1.22 | 1.17 | 1.46 | 0.9953 | chr7 |
| 20535838 | hsa-mir-1302-1 | 0.0232 | 1.18 | 1.21 | 0.98 | 0.9953 | chr12 |
| 20518928 | hsa-miR-4528 | 0.0237 | 1.29 | 1.24 | 0.87 | 0.9953 | chr18 |
| 20535673 | hsa-mir-374b | 0.0242 | -1.53 | 1.49 | 2.11 | 0.9953 | chrX |
| 20538236 | U71a | 0.0244 | -1.29 | 2.13 | 2.5 | 0.9953 | chr20 |
| 20536966 | hsa-mir-4730 | 0.0247 | -1.36 | 2.09 | 2.54 | 0.9953 | chr17 |
| 20518919 | hsa-miR-4521 | 0.0248 | 2.76 | 5.28 | 3.81 | 0.9953 | chr17 |
| 20537229 | hsa-mir-5706 | 0.0248 | -1.36 | 1.18 | 1.62 | 0.9953 | chr5 |
| 20504421 | hsa-miR-654-3p | 0.0249 | 1.55 | 2.01 | 1.38 | 0.9953 | chr14 |
| 20506710 | hsa-miR-1179 | 0.0251 | 1.42 | 1.18 | 0.67 | 0.9953 | chr15 |
| 20532880 | ENSG00000201710 | 0.0251 | -1.16 | 1.08 | 1.29 | 0.9953 | chr14 |
| 20517721 | hsa-miR-4267 | 0.0257 | 1.12 | 1.51 | 1.34 | 0.9953 | chr2 |
| 20519587 | hsa-miR-4738-5p | 0.0258 | 1.42 | 1.77 | 1.26 | 0.9953 | chr17 |

**Table A.2. Small RNAs significantly altered following FUS Knockdown.**

| ID | Transcript ID(Array Design) | P-val | Fold Change | siFUS Avg (log2) | SCR Avg (log2) | FDR P-val | Chromosome |
|---|---|---|---|---|---|---|---|
| 20536602 | hsa-mir-3689b | 0.0258 | -2.26 | 1.55 | 2.72 | 0.9953 | chr9 |
| 20532737 | ENSG00000199411 | 0.026 | -1.32 | 1.43 | 1.83 | 0.9953 | chr9 |
| 20536873 | hsa-mir-4652 | 0.0261 | -1.41 | 1.09 | 1.59 | 0.9953 | chr7 |
| 20535353 | hsa-mir-606 | 0.0261 | 1.49 | 1.74 | 1.16 | 0.9953 | chr10 |
| 20533768 | ENSG00000239172 | 0.0261 | -1.19 | 1.32 | 1.57 | 0.9953 | chr16 |
| 20533626 | ENSG00000238954 | 0.0261 | -1.19 | 1.32 | 1.57 | 0.9953 | chr16 |
| 20533471 | ENSG00000238712 | 0.0261 | -1.19 | 1.32 | 1.57 | 0.9953 | chr16 |
| 20525747 | hsa-miR-6893-5p | 0.0262 | -1.6 | 1.94 | 2.62 | 0.9953 | chr8 |
| 20535926 | hsa-mir-1322 | 0.0262 | 1.39 | 1.44 | 0.97 | 0.9953 | chr8 |
| 20536327 | hsa-mir-3201 | 0.0263 | 1.24 | 1.36 | 1.05 | 0.9953 | chr22 |
| 20537167 | hsa-mir-5590 | 0.0264 | -1.18 | 0.82 | 1.05 | 0.9953 | chr2 |
| 20505746 | hsa-miR-874-3p | 0.0265 | -1.54 | 2.96 | 3.59 | 0.9953 | chr5 |
| 20501178 | hsa-miR-296-5p | 0.0265 | -1.21 | 1 | 1.27 | 0.9953 | chr20 |
| 20534006 | ENSG00000252646 | 0.0265 | 1.32 | 1.71 | 1.31 | 0.9953 | chr1 |
| 20501278 | hsa-miR-328-3p | 0.0266 | -2.5 | 2.34 | 3.66 | 0.9953 | chr16 |
| 20501163 | hsa-miR-200a-3p | 0.0268 | -1.13 | 1.17 | 1.35 | 0.9953 | chr1 |
| 20534534 | hsa-mir-217 | 0.0268 | 1.19 | 1.5 | 1.25 | 0.9953 | chr2 |
| 20533092 | ENSG00000212445 | 0.0268 | -1.64 | 1.51 | 2.23 | 0.9953 | chr16 |
| 20504283 | hsa-miR-562 | 0.0269 | 1.22 | 1.25 | 0.96 | 0.9953 | chr2 |
| 20538016 | hsa-mir-8058 | 0.0269 | 1.6 | 2.01 | 1.32 | 0.9953 | chr16 |
| 20533869 | ENSG00000252083 | 0.0269 | 1.49 | 1.9 | 1.32 | 0.9953 | chr5 |
| 20533068 | ENSG00000212363 | 0.0269 | 1.28 | 1.24 | 0.89 | 0.9953 | chr5 |
| 20502446 | hsa-miR-451a | 0.027 | -1.44 | 1.49 | 2.02 | 0.9953 | chr17 |
| 20519694 | hsa-miR-4796-3p | 0.0273 | 1.47 | 1.55 | 0.99 | 0.9953 | chr3 |
| 20506886 | hsa-miR-1288-3p | 0.0277 | -1.62 | 1.46 | 2.15 | 0.9953 | chr17 |
| 20534829 | hsa-mir-26a-2 | 0.0278 | -1.33 | 1.28 | 1.7 | 0.9953 | chr12 |
| 20500794 | hsa-miR-190a-3p | 0.0282 | -1.49 | 1.03 | 1.6 | 0.9953 | chr15 |
| 20533596 | ENSG00000238902 | 0.0284 | 1.28 | 1.45 | 1.09 | 0.9953 | chr3 |

**Table A.2. Small RNAs significantly altered following FUS Knockdown.**

| ID | Transcript ID(Array Design) | P-val | Fold Change | siFUS Avg (log2) | SCR Avg (log2) | FDR P-val | Chromosome |
|---|---|---|---|---|---|---|---|
| 20525421 | hsa-miR-6729-3p | 0.0286 | 1.19 | 1.25 | 1 | 0.9953 | chr1 |
| 20525706 | hsa-miR-6872-3p | 0.0297 | -1.73 | 1.93 | 2.72 | 0.9953 | chr3 |
| 20537984 | hsa-mir-4433b | 0.0302 | -1.09 | 1.18 | 1.29 | 0.9953 | chr2 |
| 20532729 | ENSG00000199282 | 0.0302 | -1.32 | 1.17 | 1.57 | 0.9953 | chr13 |
| 20533761 | ENSG00000239157 | 0.0306 | -1.46 | 1.16 | 1.71 | 0.9953 | chr20 |
| 20504313 | hsa-miR-584-3p | 0.0307 | 1.48 | 2.05 | 1.48 | 0.9953 | chr5 |
| 20535198 | hsa-mir-527 | 0.0308 | -1.25 | 1.28 | 1.6 | 0.9953 | chr19 |
| 20504429 | hsa-miR-659-5p | 0.031 | -1.62 | 0.96 | 1.65 | 0.9953 | chr22 |
| 20535071 | hsa-mir-196b | 0.031 | 1.36 | 1.91 | 1.47 | 0.9953 | chr7 |
| 20532625 | ACA16 | 0.031 | 1.37 | 2.68 | 2.22 | 0.9953 | chr1 |
| 20525605 | hsa-miR-6822-5p | 0.0311 | -1.29 | 1.31 | 1.68 | 0.9953 | chr3 |
| 20529565 | hsa-miR-7974 | 0.0312 | -1.43 | 1.35 | 1.87 | 0.9953 | chr19 |
| 20506873 | hsa-miR-1276 | 0.0316 | 1.41 | 1.31 | 0.82 | 0.9953 | chr15 |
| 20500779 | hsa-miR-146a-3p | 0.0317 | -1.33 | 1.4 | 1.82 | 0.9953 | chr5 |
| 20536648 | hsa-mir-3942 | 0.0319 | 1.63 | 1.97 | 1.26 | 0.9953 | chr15 |
| 20537228 | hsa-mir-5705 | 0.0321 | 1.38 | 1.77 | 1.3 | 0.9953 | chr4 |
| 20519707 | hsa-miR-4804-5p | 0.0324 | -1.15 | 1.15 | 1.34 | 0.9953 | chr5 |
| 20537444 | hsa-mir-6513 | 0.0326 | 1.53 | 2.03 | 1.42 | 0.9953 | chr2 |
| 20536480 | hsa-mir-4265 | 0.0326 | 1.29 | 1.64 | 1.28 | 0.9953 | chr2 |
| 20532963 | ENSG00000206901 | 0.0328 | 1.33 | 1.82 | 1.41 | 0.9953 | chr2 |
| 20537464 | hsa-mir-6722 | 0.033 | 1.17 | 5.32 | 5.08 | 0.9953 | chr9 |
| 20537446 | hsa-mir-6515 | 0.033 | 1.34 | 1.81 | 1.39 | 0.9953 | chr19 |
| 20535324 | hsa-mir-584 | 0.0332 | -1.18 | 1.46 | 1.7 | 0.9953 | chr5 |
| 20501233 | hsa-miR-373-5p | 0.0334 | 1.24 | 1.65 | 1.34 | 0.9953 | chr19 |
| 20537219 | hsa-mir-5697 | 0.0336 | 1.33 | 1.68 | 1.27 | 0.9953 | chr1 |
| 20536865 | hsa-mir-4645 | 0.0336 | -1.37 | 1.64 | 2.09 | 0.9953 | chr6 |
| 20524053 | hsa-miR-6132 | 0.0337 | -1.11 | 2.22 | 2.37 | 0.9953 | chr7 |
| 20537030 | hsa-mir-4777 | 0.0337 | -1.2 | 1 | 1.26 | 0.9953 | chr2 |

**Table A.2. Small RNAs significantly altered following FUS Knockdown.**

| ID | Transcript ID(Array Design) | P-val | Fold Change | siFUS Avg (log2) | SCR Avg (log2) | FDR P-val | Chromosome |
|---|---|---|---|---|---|---|---|
| 20534582 | hsa-mir-125b-1 | 0.0339 | 1.28 | 1.81 | 1.45 | 0.9953 | chr11 |
| 20537575 | hsa-mir-6831 | 0.034 | 1.26 | 1.85 | 1.52 | 0.9953 | chr5 |
| 20537524 | hsa-mir-6781 | 0.034 | 1.39 | 2.06 | 1.59 | 0.9953 | chr17 |
| 20525685 | hsa-miR-6861-3p | 0.0341 | 1.52 | 1.84 | 1.24 | 0.9953 | chr12 |
| 20519602 | hsa-miR-4746-5p | 0.0344 | 1.66 | 2.26 | 1.53 | 0.9953 | chr19 |
| 20533477 | ENSG00000238722 | 0.0345 | -1.32 | 1.38 | 1.79 | 0.9953 | chr2 |
| 20537213 | hsa-mir-5692a-2 | 0.0347 | -1.09 | 1.42 | 1.55 | 0.9953 | chr8 |
| 20537212 | hsa-mir-5692a-1 | 0.0347 | -1.09 | 1.42 | 1.55 | 0.9953 | chr7 |
| 20533729 | ENSG00000239111 | 0.0359 | -1.2 | 1.49 | 1.75 | 0.9953 | chr1 |
| 20500748 | hsa-miR-141-3p | 0.036 | -1.21 | 1.1 | 1.37 | 0.9953 | chr12 |
| 20505788 | hsa-miR-744-3p | 0.0364 | 1.79 | 2.25 | 1.41 | 0.9953 | chr17 |
| 20533412 | ENSG00000238620 | 0.0365 | -1.41 | 1.15 | 1.64 | 0.9953 | chr10 |
| 20535310 | hsa-mir-570 | 0.0369 | 1.55 | 1.56 | 0.93 | 0.9953 | chr3 |
| 20533821 | ENSG00000251866 | 0.0369 | -1.31 | 1.7 | 2.09 | 0.9953 | chr1 |
| 20500764 | hsa-miR-9-3p | 0.037 | 1.09 | 1.13 | 1.01 | 0.9953 | chr1 |
| 20535101 | hsa-mir-450a-1 | 0.037 | 1.21 | 1.19 | 0.91 | 0.9953 | chrX |
| 20533677 | ENSG00000239033 | 0.037 | -1.07 | 1.2 | 1.31 | 0.9953 | chr12 |
| 20533330 | ENSG00000238506 | 0.0371 | -1.39 | 1.23 | 1.7 | 0.9953 | chr7 |
| 20536506 | hsa-mir-4287 | 0.038 | 1.31 | 1.74 | 1.36 | 0.9953 | chr8 |
| 20533179 | ENSG00000222185 | 0.0381 | 1.27 | 1.22 | 0.87 | 0.9953 | chr14 |
| 20532897 | ENSG00000201853 | 0.0381 | 1.24 | 1.53 | 1.21 | 0.9953 | chr2 |
| 20537083 | hsa-mir-5091 | 0.0383 | 1.54 | 2.09 | 1.47 | 0.9953 | chr4 |
| 20521817 | hsa-miR-548at-3p | 0.0386 | -1.23 | 1.27 | 1.57 | 0.9953 | chr17 |
| 20532798 | ENSG00000200422 | 0.0387 | -1.36 | 1.04 | 1.49 | 0.9953 | chrX |
| 20504190 | hsa-miR-544a | 0.0391 | 1.17 | 1.11 | 0.88 | 0.9953 | chr14 |
| 20535684 | hsa-mir-933 | 0.0392 | -1.48 | 1.72 | 2.29 | 0.9953 | chr2 |
| 20536616 | hsa-mir-3914-2 | 0.0393 | 1.34 | 1.39 | 0.96 | 0.9953 | chr7 |
| 20532598 | 14qII-26 | 0.0397 | -1.11 | 1.24 | 1.39 | 0.9953 | chr14 |

**Table A.2. Small RNAs significantly altered following FUS Knockdown.**

| ID | Transcript ID(Array Design) | P-val | Fold Change | siFUS Avg (log2) | SCR Avg (log2) | FDR P-val | Chromosome |
|---|---|---|---|---|---|---|---|
| 20515610 | hsa-miR-3180-3p | 0.0398 | -1.35 | 2.67 | 3.1 | 0.9953 | chr16 |
| 20535453 | hsa-mir-766 | 0.0404 | 1.27 | 1.63 | 1.28 | 0.9953 | chrX |
| 20532748 | ENSG00000199666 | 0.0406 | -1.31 | 1.42 | 1.8 | 0.9953 | chr1 |
| 20505798 | hsa-miR-543 | 0.0407 | 1.3 | 1.52 | 1.14 | 0.9953 | chr14 |
| 20519481 | hsa-miR-4679 | 0.0409 | 1.25 | 1.41 | 1.09 | 0.9953 | chr10 |
| 20533532 | ENSG00000238806 | 0.041 | 1.19 | 1.36 | 1.11 | 0.9953 | chr17 |
| 20535826 | hsa-mir-1289-2 | 0.0411 | -1.34 | 1.24 | 1.66 | 0.9953 | chr5 |
| 20529147 | hsa-miR-7855-5p | 0.0413 | 1.17 | 1.65 | 1.43 | 0.9953 | chr14 |
| 20500489 | hsa-miR-224-5p | 0.0413 | 1.29 | 1.46 | 1.09 | 0.9953 | chrX |
| 20538460 | spike_in-control-17 | 0.0414 | 1.21 | 1.7 | 1.42 | 0.9953 | |
| 20502455 | hsa-miR-409-5p | 0.0415 | 1.43 | 1.86 | 1.34 | 0.9953 | chr14 |
| 20534617 | hsa-mir-126 | 0.0415 | 1.11 | 2.2 | 2.06 | 0.9953 | chr9 |
| 20518872 | hsa-miR-548ak | 0.0417 | 1.16 | 1.15 | 0.93 | 0.9953 | chr10 |
| 20501294 | hsa-miR-324-5p | 0.0417 | -2.62 | 2.55 | 3.94 | 0.9953 | chr17 |
| 20535873 | hsa-mir-1260a | 0.0418 | -1.4 | 1.54 | 2.02 | 0.9953 | chr14 |
| 20533695 | ENSG00000239058 | 0.0418 | 1.19 | 1.29 | 1.05 | 0.9953 | chrX |
| 20536748 | hsa-mir-4479 | 0.0419 | -1.65 | 1.18 | 1.9 | 0.9953 | chr9 |
| 20534005 | ENSG00000252646 | 0.0419 | 1.42 | 1.64 | 1.14 | 0.9953 | chr1 |
| 20537591 | hsa-mir-6846 | 0.0424 | -1.41 | 1.37 | 1.86 | 0.9953 | chr8 |
| 20536702 | hsa-mir-4449 | 0.0424 | -1.36 | 4.46 | 4.91 | 0.9953 | chr4 |
| 20520580 | hsa-miR-5197-3p | 0.0425 | 1.14 | 1.08 | 0.89 | 0.9953 | chr5 |
| 20520219 | hsa-miR-5010-3p | 0.0426 | -1.27 | 1.51 | 1.86 | 0.9953 | chr17 |
| 20537580 | hsa-mir-6780b | 0.0428 | 1.67 | 2.15 | 1.42 | 0.9953 | chr6 |
| 20506857 | hsa-miR-1263 | 0.043 | -2.57 | 2.45 | 3.81 | 0.9953 | chr3 |
| 20532771 | ENSG00000200026 | 0.0431 | -1.34 | 2.23 | 2.66 | 0.9953 | chr9 |
| 20535683 | hsa-mir-509-3 | 0.0433 | -1.37 | 1.22 | 1.67 | 0.9953 | chrX |
| 20535638 | hsa-mir-509-2 | 0.0433 | -1.37 | 1.22 | 1.67 | 0.9953 | chrX |
| 20535218 | hsa-mir-509-1 | 0.0433 | -1.37 | 1.22 | 1.67 | 0.9953 | chrX |

**Table A.2. Small RNAs significantly altered following FUS Knockdown.**

| ID | Transcript ID(Array Design) | P-val | Fold Change | siFUS Avg (log2) | SCR Avg (log2) | FDR P-val | Chromosome |
|---|---|---|---|---|---|---|---|
| 20536576 | hsa-mir-3672 | 0.0435 | -1.23 | 1.17 | 1.46 | 0.9953 | chrX |
| 20538233 | U70G | 0.0438 | 1.33 | 1.55 | 1.14 | 0.9953 | chr12 |
| 20533088 | ENSG00000212428 | 0.044 | 1.21 | 1.36 | 1.08 | 0.9953 | chr15 |
| 20533022 | ENSG00000212144 | 0.0443 | -1.18 | 1.12 | 1.35 | 0.9953 | chr1 |
| 20504296 | hsa-miR-573 | 0.0444 | 1.39 | 1.57 | 1.1 | 0.9953 | chr4 |
| 20536893 | hsa-mir-4668 | 0.0444 | 1.38 | 1.32 | 0.85 | 0.9953 | chr9 |
| 20519441 | hsa-miR-4656 | 0.0446 | 1.98 | 3.27 | 2.29 | 0.9953 | chr7 |
| 20525673 | hsa-miR-6856-5p | 0.0447 | -1.57 | 1 | 1.65 | 0.9953 | chr9 |
| 20504310 | hsa-miR-582-3p | 0.0447 | -1.1 | 1.18 | 1.32 | 0.9953 | chr5 |
| 20520215 | hsa-miR-5008-3p | 0.0448 | -2.41 | 2.29 | 3.55 | 0.9953 | chr1 |
| 20501240 | hsa-miR-377-5p | 0.0448 | -1.52 | 1.22 | 1.83 | 0.9953 | chr14 |
| 20536757 | hsa-mir-4485 | 0.0448 | 1.07 | 3.14 | 3.05 | 0.9953 | chr11 |
| 20537488 | hsa-mir-6745 | 0.0452 | 1.56 | 1.99 | 1.35 | 0.9953 | chr11 |
| 20533534 | ENSG00000238807 | 0.0452 | 1.33 | 2.01 | 1.6 | 0.9953 | chr17 |
| 20533007 | ENSG00000207299 | 0.0452 | 1.33 | 1.61 | 1.19 | 0.9953 | chr11 |
| 20535131 | hsa-mir-376b | 0.0454 | -1.4 | 1.05 | 1.54 | 0.9953 | chr14 |
| 20535350 | hsa-mir-603 | 0.0455 | -1.4 | 1.04 | 1.52 | 0.9953 | chr10 |
| 20533849 | ENSG00000252000 | 0.0457 | 1.42 | 1.94 | 1.44 | 0.9953 | chr2 |
| 20536615 | hsa-mir-3914-2 | 0.0459 | 1.3 | 1.35 | 0.97 | 0.9953 | chr7 |
| 20533958 | ENSG00000252433 | 0.0459 | 1.36 | 1.41 | 0.96 | 0.9953 | chr1 |
| 20525492 | hsa-miR-6765-3p | 0.046 | 1.32 | 1.86 | 1.46 | 0.9953 | chr14 |
| 20520564 | hsa-miR-5186 | 0.046 | 1.27 | 1.11 | 0.77 | 0.9953 | chr3 |
| 20515515 | hsa-miR-3120-3p | 0.0466 | 1.3 | 1.47 | 1.09 | 0.9953 | chr1 |
| 20515645 | hsa-miR-3200-3p | 0.0467 | -1.48 | 2.23 | 2.8 | 0.9953 | chr22 |
| 20506833 | hsa-miR-548f-5p | 0.0467 | 1.21 | 1.44 | 1.16 | 0.9953 | chr10 |
| 20538031 | hsa-mir-8072 | 0.0467 | -1.05 | 1.94 | 2.01 | 0.9953 | chr12 |
| 20532576 | 14qII-10 | 0.0467 | 1.37 | 1.25 | 0.8 | 0.9953 | chr14 |
| 20533384 | ENSG00000238575 | 0.0468 | -1.09 | 1.19 | 1.32 | 0.9953 | chr18 |

**Table A.2. Small RNAs significantly altered following FUS Knockdown.**

| ID | Transcript ID(Array Design) | P-val | Fold Change | siFUS Avg (log2) | SCR Avg (log2) | FDR P-val | Chromosome |
|---|---|---|---|---|---|---|---|
| 20532731 | ENSG00000199321 | 0.0468 | 1.32 | 1.39 | 0.99 | 0.9953 | chr10 |
| 20533853 | ENSG00000252016 | 0.0474 | 1.5 | 1.97 | 1.38 | 0.9953 | chrX |
| 20536982 | hsa-mir-4744 | 0.0478 | -1.23 | 1.17 | 1.46 | 0.9953 | chr18 |
| 20537064 | hsa-mir-5000 | 0.0479 | -1.29 | 1.33 | 1.7 | 0.9953 | chr2 |
| 20532819 | ENSG00000200891 | 0.0479 | -1.41 | 1.39 | 1.89 | 0.9953 | chr10 |
| 20524999 | hsa-miR-6500-5p | 0.048 | 1.14 | 1.78 | 1.6 | 0.9953 | chr1 |
| 20535810 | hsa-mir-1204 | 0.0481 | 1.23 | 1.93 | 1.63 | 0.9953 | chr8 |
| 20504551 | hsa-miR-1264 | 0.0483 | 1.22 | 1.41 | 1.13 | 0.9953 | chrX |
| 20536287 | hsa-mir-3176 | 0.0483 | -1.57 | 1.78 | 2.44 | 0.9953 | chr16 |
| 20500445 | hsa-miR-181a-2-3p | 0.0484 | -2.11 | 1.72 | 2.8 | 0.9953 | chr9 |
| 20538234 | U70G | 0.0487 | 1.29 | 1.54 | 1.17 | 0.9953 | chr12 |
| 20500135 | hsa-miR-19a-3p | 0.0488 | 1.29 | 1.25 | 0.88 | 0.9953 | chr13 |
| 20532744 | ENSG00000199566 | 0.0494 | 1.22 | 1.98 | 1.69 | 0.9953 | chr12 |
| 20537597 | hsa-mir-6852 | 0.0495 | 1.58 | 2.1 | 1.44 | 0.9953 | chr9 |
| 20504356 | hsa-miR-615-5p | 0.0496 | -1.28 | 2 | 2.35 | 0.9953 | chr12 |
| 20533762 | ENSG00000239159 | 0.0498 | -1.24 | 1.06 | 1.37 | 0.9953 | chr5 |
| 20533966 | ENSG00000252448 | 0.0499 | 1.13 | 1.38 | 1.21 | 0.9953 | chr1 |
| 20533892 | ENSG00000252170 | 0.0499 | -1.2 | 1.53 | 1.79 | 0.9953 | chr3 |

# Appendix B

# Other scientific contributions

# MiR-129-5p: a novel therapeutic target for amyotrophic lateral sclerosis?

**Zachary C. E. Hawley[1,2], Danae Campos-Melo[1], Michael J. Strong[1,2,3,4]^**

[1]Molecular Medicine Group, Robarts Research Institute, [2]Neuroscience Program, [3]Department of Pathology, [4]Department of Clinical Neurological Sciences, Schulich School of Medicine and Dentistry, Western University, London, ON, Canada

*Correspondence to:* Michael J. Strong. Schulich School of Medicine and Dentistry, Western University, London, ON, Canada. Email: mstrong@uwo.ca. *Provenance and Peer Review:* This article was commissioned and reviewed by the Section Editor Mengli Chen, PhD (Jiangsu Province Hospital, Nanjing Medical University, Nanjing, China).

*Comment on:* Loffreda A, Nizzardo M, Arosio A, *et al*. miR-129-5p: A key factor and therapeutic target in amyotrophic lateral sclerosis. Prog Neurobiol 2020;190:101803.

Amyotrophic lateral sclerosis (ALS) is a debilitating neurodegenerative disease that is defined by the progressive loss of motor function due to degeneration of upper and lower motor neurons in the brain and spinal cord tissue, respectively, with an average life-expectancy of 2–5 years post-diagnosis (1). Riluzole and edaravone are currently the only two FDA approved drugs for patients with ALS, but these drugs have minimal effect, extending life only for a matter of months (2).

In 1993, the first causative mutations of ALS were identified in the *SOD1* gene (3). Today, mutations in SOD1 is the second most common cause of genetic ALS (~5–6% of all ALS cases), only falling behind the hexanucleotide repeat expansions observed in *C9ORF72* (~12–14% of all ALS cases). However, the vast majority of ALS cases (~80%) have no known genetic background giving no clear indication on the causative factor that results in the disease development (1). In the last decade, miRNAs have been increasingly implicated in the pathogenesis of ALS due to the mass dysregulation of these molecules observed in ALS spinal cord and motor neurons (4-8).

MiRNAs are small RNA molecules (~22–25 nucleotides) that are primarily responsible for post-transcriptional gene-silencing generally through interactions with the 3'

^Michael J. Strong ORCID: 0000-0003-1988-6262.

untranslated region (UTR) of messenger RNA (mRNA) (9). Their interactions are highly dependent on environmental cues. Therefore, cell development, cell type, cell stress, and aging all have an impact on mRNA post-transcriptional regulation via miRNAs. This is an especially true for neurons which have spatiotemporal needs within the cell where post-transcriptional regulation via miRNAs differs depending on soma, dendritic and axonal needs (9,10). Further, miRNAs are also regulated by other non-coding RNAs (i.e., long non-coding RNAs, circular RNAs, etc.) which work together to control the degree of expression of a gene (11), highlighting the sophistication of these noncoding RNA networks (*Figure 1*). Not surprisingly, because of miRNAs dynamic nature in these RNA networks, it has become increasingly of interest to determine the contribution of miRNAs in disease.

As mentioned, miRNAs have become increasingly implicated in ALS pathogenesis. This has mainly stemmed from observations that in sporadic ALS (sALS) spinal cord and motor neurons there are pools of miRNAs that are reduced (4-6). In contrast, mutant SOD1 (mtSOD1) ALS cases and rodent models have observed that miRNAs are generally upregulated, suggesting inhibition of these miRNAs may have therapeutic effects (7,12,13). In particular, high levels of miR-155 in mtSOD1 rodent models has been reported to promote neuroinflammation. Interestingly, inhibition of this miRNA via antisense oligonucleotides (ASOs) has been shown to decrease
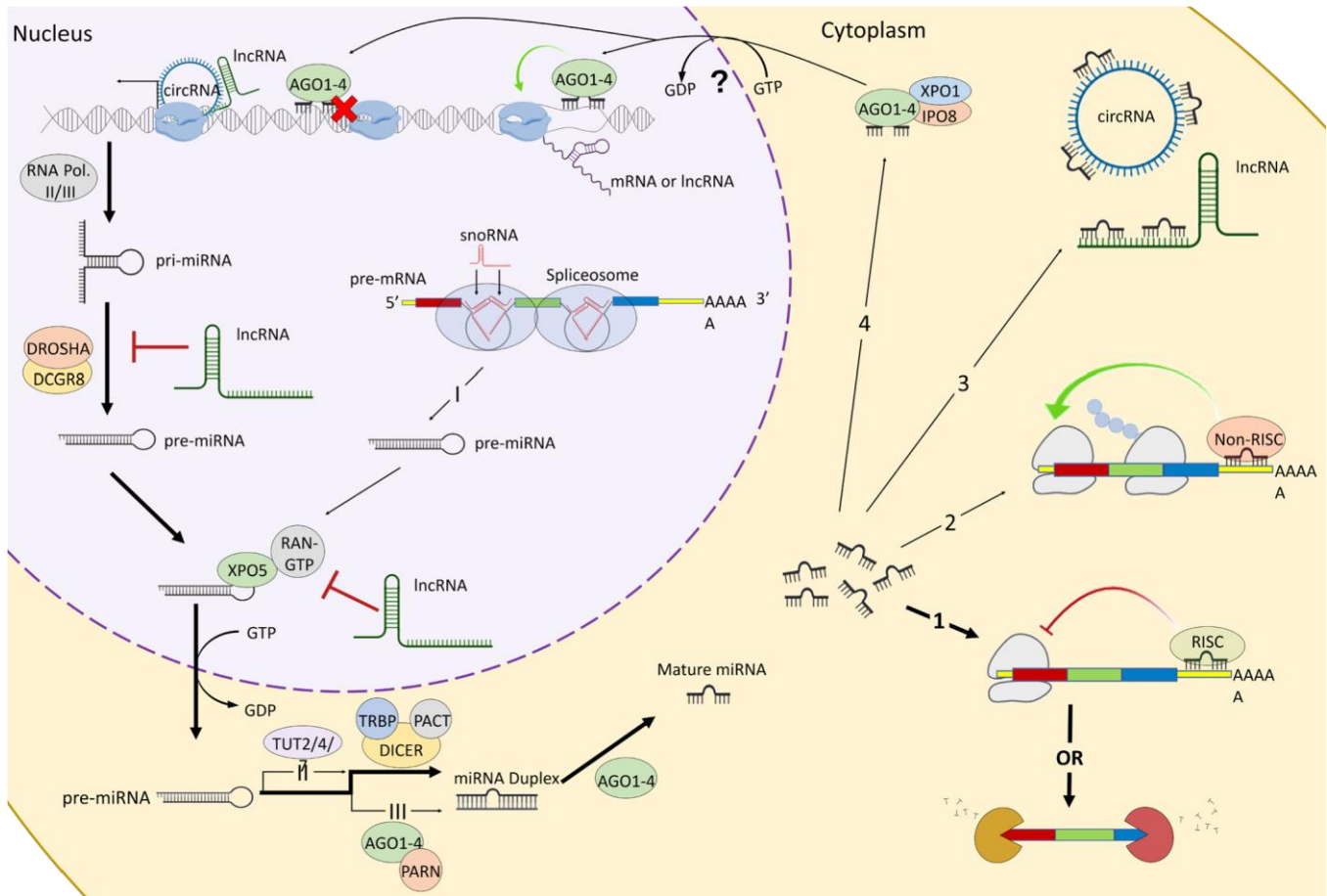
**Figure 1 MiRNA biogenesis and regulation. The** *canonical biogenesis pathway* **(represented by bold arrows): MiRNAs are transcribed from the genome via RNA polymerase (RNA pol.) II/III producing a primary miRNA (pri-miRNA). Interestingly, both circular and long non-coding RNAs (circRNAs and lncRNAs, respectively) are known to assist in RNA pol. II transcription indicating these class of non-coding RNAs may assist in miRNA transcription. Further, these pri-miRNAs can be transcribed into small nucleolar RNA (snoRNA) and transfer RNA (tRNA) transcripts. Once produced, pri-miRNAs are processed by the DROSHA/DCGR8 complex into a pre-miRNA which is shuttled from the nucleus to the cytoplasm via XPO5 and RAN-GTP. Both DROSHA processing and pre-miRNA nuclear export have been shown to be inhibited by lncRNAs. Cytoplasmic pre-miRNAs are then processed by DICER/TRBP/PACT complex to produce a miRNA duplex which is unwound via AGO1-4 creating a mature miRNA.** *Non-canonical biogenesis pathway*: **There are 3 major non-canonical pathways – I) pre-miRNAs are produced directly from the spliceosome after pre-mRNA processing skipping DROSHA/DCGR8 processing; II) cytoplasmic pre-miRNAs need to get mono-uridylated by TUT2/4/7 proteins before being processed by DICER/TRBP/PACT; or III) cytoplasmic pre-miRNAs get processed by AGO1-4/PARN rather than DICER/TRBP/PACT to produce the miRNA duplex.** *MiRNA regulation*: **Once produced miRNA are: (I) incorporated into the RNA-induced silencing complex (RISC) and generally target the 3'UTR of mRNA to suppress translation OR induce mRNA degradation. This represents the primary function of miRNAs; (II) bind to the 3'UTR of mRNA to promote translation and mRNA stability usually with proteins not associated with the RISC complex (non-RISC). However, this is far less common than gene silencing; (III) targeted by circRNAs and lncRNAs that act as sponges to prevent miRNAs from reaching their mRNA targets; (IV) MiRNAs can be incorporated into the AGO complex and transported back into the nucleus via IPO8 and XPO1 to either promote or suppress transcription by binding to promoter/enhancer regions of the genome. While presumed that GTP converts to GDP via IPO8 to allow entry of the miRNA in the nucleus, this has yet to be shown in the literature. This figure highlights this highly sophisticated RNA network between circRNAs/lncRNAs/snoRNAs/ mRNAs that are responsible for regulating miRNA biogenesis and function ensuring gene expression is tightly controlled.**

neuroinflammation and alleviate ALS-like phenotypes in rodent models (7). Others have used miRNAs to reduce SOD1 expression, and in turn reduce mtSOD1s toxic effects, by intrathecally delivering artificial miRNAs that were cloned into an Adeno-associated virus (AAV) and target the

*SOD1* transcript. Use of SOD1 targeting artificial miRNAs has been shown to have therapeutic effects in both rodent and macaque models (14,15). However, the effectiveness of theses therapeutics in humans is still unknown. This previous research provides evidence of the utility of

miRNAs as potential therapeutic targets, and further, highlights the use of either ASOs or AAV-miRNAs as ways to develop therapeutics that will potentially treat neurodegeneration.

Recent work published by Loffreda *et al.*, 2020 in *Progress in Neurobiology* highlights miR-129-5p as another upregulated miRNA in rodent models of mtSOD1 ALS which, if inhibited using an ASO, could have therapeutic effects for patients with ALS (16). The research group looked at mtSOD1 (SOD1 G93A) *in vitro* neuronal cell models in addition to *in vivo* mouse models and determined that mtSOD1 causes an increase in miR-129-5p levels. Further, they observed increased levels of miR-129-5p in peripheral blood mononuclear cell (PMBC) samples of sALS patients, suggesting that this phenomenon may be related to ALS more broadly rather than just those who contain mutations in SOD1. These researchers reported that increased levels of miR-129-5p in both their *in vitro* and *in vivo* models correlates with decreased levels of *ELAVL4*, otherwise known as HuD—a protein critical for neuronal cell identity, maturation, axogenesis, dendrite growth, plasticity and survival (17). Through robust experimental analyses, the authors were able to show that increased levels of miR-129-5p were directly responsible for the reduced levels of HuD, identifying the biological mechanism by which high levels of miR-129-5p may contribute to neurodegeneration. Having made this observation, the authors then examined the ability of an ASO targeting miR129-5p to reduce its levels in mtSOD1 rodent models. Administration of the ASO via intracerebroventricular injection at an early symptomatic stage (post-natal 80 days) led to increased survival, improved motor capabilities, and increased neuromuscular junction connections. However, it only had a mild effect on preventing motor neuron degeneration which was not statistically significant. The authors concluded that while reducing levels of miR-1295p may have some therapeutic effects, the most optimal approach may be to pair their ASO with another miRNAbased therapeutic currently in development—an ASO targeting miR-155 (7,18).

ASO-based therapeutics have become popular as an approach to treat neurodegenerative diseases due to the success in treating Spinal Muscular Atrophy (SMA)—a juvenile neurodegenerative disease caused by loss of lower motor neurons —using an ASO targeting *SMN2* (19). Several modifications to the nucleotide backbone of an ASO can be done to increase its affinity to its target and make it resistant to nucleases. For example, morpholino modifications were used to develop the *SMN2* ASO and the

miR-129-5p ASO (16,19). Morpholino modifications alter the sugar-phosphate backbone by changing the sugar ring from a five-membered to a six-membered ring and the sugar rings are linked to phosphoramidates groups rather than phosphate groups. These modifications have been proven to be beneficial to develop ASOs that either knockdown expression of a specific gene, as seen in Loffreda *et al.*, 2020, or alter mRNA splicing as seen for the ASO that targets *SMN2* (16,19). Moreover, the ASO produced in Loffreda *et al.*, 2020 is called an antagomir—an ASO that targets a miRNA—and they have been increasingly shown to be effective therapeutics. For example, the drug miravirsen, which has completed phase II clinical trials, is an antagomir targeting miR-122 and has been shown to prevent propagation of hepatitis C virus (HCV) RNA in the liver highlighting the potential use of antagomirs in clinical practice (20). Despite these developments, ASOs still have their limitations which include their potential off-target affects, their expense to develop, and their inability to cross the blood-brain barrier; making them difficult to administer for neurological diseases (21). However, the current success of ASO treatments thus far has sparked more innovative research to determine whether further modifications to these oligos will allow us to overcome these limitations, offering new opportunities for therapeutic development.

Loffreda *et al.*, 2020 provides clear evidence that increased levels of miR-129-5p is caused by mtSOD1 and that lowering its levels in mtSOD1 mice has some therapeutic effects; however, it is unclear whether reduction of miR-129-5p would be a good ALS therapeutic more broadly (16). The authors identified increased levels of miR-129-5p in sALS patient PBMCs, but not in human spinal cord or motor neurons (16). As mentioned previously, the environmental context matters when discussing miRNA regulation (9). Further, in the several studies that have examined miRNA expression in the spinal cord and motor neurons of sALS cases, upregulation of miR-129-5p has not been observed (4-6). Thus, it is unclear whether this observation of increased levels of miR-129-5p in PBMCs is relevant to the dysfunction of motor neurons, or more broadly, the central nervous system of the sALS patient group within their study.

Further, the use of an ASO to suppress miR-129-5p expression should be approached with caution. In the central nervous system, miR-129-5p has been shown to suppress apoptosis and alleviate neuroinflammation (22). Low levels of miR-129-5p have been reported in the degenerating brain of patients with Alzheimer's Disease, and lack of this miRNA creates an inflammatory response

that can be neurotoxic (23). Thus, too much or too little of miR129-5p could be damaging to the central nervous system. This is likely because miRNAs can target several transcripts to regulate a network of genes, which can make cells sensitive to fluctuations in miRNA expression. In this case, the authors showed that miR-129-5p regulates HuD levels, but miR-129-5p has also been shown to regulate critical neuronal genes involved in synaptic plasticity (FMR1) and neuroinflammation (HMGB1) (22,24). All this suggests that further work needs to be done to ensure reduction of this miRNA will not have long-term effects that may be more damaging than therapeutic.

Loffreda *et al.*, 2020 proposed that while their ASO had some beneficial effects in their mtSOD1 models, matching it with an ASO that inhibits miR-155 may have the greatest overall therapeutic effect (16). This points to the idea that simply targeting one miRNA may not be enough to ameliorate ALS. In fact, as mentioned previously, several miRNAs have been shown to be upregulated in mtSOD1 models (7,12,13). Further, the article provides data indicating that mtSOD1 increased the levels of DICER, a critical protein in miRNA biogenesis, which may explain why miRNAs are upregulated in mtSOD1 models (16). Therefore, there seems to be a systemic issue with miRNA production in the presence mtSOD1. Thus, lowering levels of DICER might seem to be a better target to slow the production and reduce the toxicity of these upregulated miRNAs in mtSOD1 ALS cases. However, knockout of DICER in mouse motor neurons has been shown to lead to motor neuron degeneration, and thus, reducing levels of DICER should be approached with caution as well (25).

Overall, while this latest work by Loffreda *et al.*, 2020 provides another interesting avenue for miRNAbased therapeutics for ALS, this work still has far to go before we can think about administering it to patients. Large-scale preclinical studies still need to be done to determine if inhibition of miR-129-5p prevents motor neurodegeneration, helps alleviate ALS-like phenotypes in several models of ALS or just SOD1-related models, and finally, determine whether downregulation of this miRNA has any potential negative long-term outcomes (i.e., chronic neuroinflammation). Further, we still do not know whether miR-129-5p is upregulated within the spinal cord or motor neurons of mtSOD1 ALS cases, which will be necessary to address to ensure development of this ASO as a therapeutic is not in vain. All this taken together, miR129-5p could be a potential therapeutic for ALS, but in agreeance with the authors, it is unlikely that targeting this miRNA alone will be enough to completely halt the disease progression (16).

However, the mere identification of this miRNA, its biological network and its potential relevance to disease will be incredibly important to our understanding of mechanisms associated with ALS progression, opening more avenues for potential therapeutics.

## Footnote

## References

1. Taylor JP, Brown RH, Jr., Cleveland DW. Decoding ALS: from genes to mechanism. Nature 2016;539:197-206.
2. Chiò A, Mazzini L, Mora G. Disease-modifying therapies in amyotrophic lateral sclerosis. Neuropharmacology 2020;167:107986.
3. Rosen DR, Siddique T, Patterson D, et al. Mutations in Cu/Zn superoxide dismutase gene are associated with familial amyotrophic lateral sclerosis. Nature 1993;362:59-62.
4. Emde A, Eitan C, Liou LL, et al. Dysregulated miRNA biogenesis downstream of cellular stress and ALS-causing mutations: a new mechanism for ALS. The EMBO journal 2015;34:2633-51.

5. Reichenstein I, Eitan C, Diaz-Garcia S, et al. Human genetics and neuropathology suggest a link between miR218 and amyotrophic lateral sclerosis pathophysiology. Sci Transl Med 2019;11:eaav5264.

6. Campos-Melo D, Droppelmann CA, He Z, et al. Altered microRNA expression profile in Amyotrophic Lateral Sclerosis: a role in the regulation of NFL mRNA levels. Molecular brain 2013;6:26.

7. Butovsky O, Jedrychowski MP, Cialic R, et al. Targeting miR-155 restores abnormal microglia and attenuates disease in SOD1 mice. Ann Neurol 2015;77:75-99.

8. Williams AH, Valdez G, Moresi V, et al. MicroRNA-206 delays ALS progression and promotes regeneration of neuromuscular synapses in mice. Science 2009;326:1549-54.

9. Hawley ZCE, Campos-Melo D, Droppelmann CA, et al. MotomiRs: miRNAs in Motor Neuron Function and Disease. Front Mol Neurosci 2017;10:127.

10. Rotem N, Magen I, Ionescu A, et al. ALS Along the Axons - Expression of Coding and Noncoding RNA Differs in Axons of ALS models. Sci Rep 2017;7:44500.

11. Salvatori B, Biscarini S, Morlando M. Non-coding RNAs in Nervous System Development and Disease. Front Cell Dev Biol 2020;8:273.

12. Zhou F, Guan Y, Chen Y, et al. miRNA-9 expression is upregulated in the spinal cord of G93A-SOD1 transgenic mice. Int J Clin Exp Pathol 2013;6:1826-38.

13. Marcuzzo S, Kapetis D, Mantegazza R, et al. Altered miRNA expression is associated with neuronal fate in G93A-SOD1 ependymal stem progenitor cells. Exp Neurol 2014;253:91-101. Stoica L, Todeasa SH, Cabrera GT, et al. Adeno-associated virus-delivered artificial microRNA extends survival and delays paralysis in an amyotrophic lateral sclerosis mouse model. Ann Neurol 2016;79:687-700.

14. Borel F, Gernoux G, Sun H, et al. Safe and effective superoxide dismutase 1 silencing using artificial microRNA in macaques. Sci Transl Med 2018;10:eaau6414.

15. Loffreda A, Nizzardo M, Arosio A, et al. miR-129-5p: A key factor and therapeutic target in amyotrophic lateral sclerosis. Prog Neurobiol 2020;190:101803.

16. Bronicki LM, Jasmin BJ. Emerging complexity of the HuD/ELAVl4 gene; implications for neuronal development, function, and dysfunction. RNA 2013;19:1019-37.

17. Koval ED, Shaner C, Zhang P, et al. Method for widespread microRNA-155 inhibition prolongs survival in ALS-model mice. Hum Mol Genet 2013;22:4127-35.

18. Finkel RS, Mercuri E, Darras BT, et al. Nusinersen versus Sham Control in Infantile-Onset Spinal Muscular Atrophy. N Engl J Med 2017;377:1723-32.

19. Janssen HL, Reesink HW, Lawitz EJ, et al. Treatment of HCV infection by targeting microRNA. N Engl J Med 2013;368:1685-94.

20. Schoch KM, Miller TM. Antisense Oligonucleotides: Translation from Mouse Models to Human Neurodegenerative Diseases. Neuron 2017;94:1056-70.

21. Wan G, An Y, Tao J, et al. MicroRNA-129-5p alleviates spinal cord injury in mice via suppressing the apoptosis and inflammatory response through HMGB1/TLR4/NFkappaB pathway. Biosci Rep 2020;40:BSR20193315.

22. Zeng Z, Liu Y, Zheng W, et al. MicroRNA-129-5p alleviates nerve injury and inflammatory response of Alzheimer's disease via downregulating SOX6. Cell Cycle 2019;18:3095-110.

23. Zongaro S, Hukema R, D'Antoni S, et al. The 3' UTR of FMR1 mRNA is a target of miR-101, miR-129-5p and miR-221: implications for the molecular pathology of FXTAS at the synapse. Hum Mol Genet 2013;22:1971-82.

24. Haramati S, Chapnik E, Sztainberg Y, et al. miRNA malfunction causes spinal motor neuron disease. Proc Natl Acad Sci U S A 2010;107:13111-6.

# ZACHARY C. E. HAWLEY, H. BSc.
## Curriculum Vitae

## Education

**Western University, London, ON, Canada**
- Doctor of Philosophy (Ph.D.)            Sept. 2015 – Nov. 2020
  *Neuroscience*

- Bachelor of Science Honours (H. BSc.)      Sept. 2010 – Apr. 2015
  *Honours Specialization in Genetics with a Major in Medical Sciences*

## Research Experience

**Ph.D. Candidate**                  Sept. 2015 – Oct. 2020
*Department of Neuroscience, Western University*
- Supervisor: Michael J. Strong

**Visiting Scholar**                   Jan. 2020 – Jul. 2020
*Department of Stem Cell and Regenerative Biology, Harvard University*
- Supervisor: Kevin Eggan

**Dean's Undergraduate Research Opportunities Program**    May 2015 – Aug. 2015
*Schulich School of Medicine and Dentistry, Western University*
- Supervisor: Michael J. Strong

**Honors Research Thesis**               Sept. 2014 – Apr. 2015
*Department of Biology, Western University*
- Supervisor: Kathleen A. Hill

**Student Research Volunteer**            May 2014 – Aug. 2014
*Department of Biology, Western University*
- Supervisor: Kathleen A. Hill

## Awards, Honors & Achievements

**Michael Smith Foreign Student Supplement Scholarship ($6,000 CAD)**
- Awarded: December 10th, 2019 | From: Canadian Institute of Health Research

**Nellie Farthing Fellowship in Medical Sciences valued ($3,000 CAD)**
- Awarded: July 24th, 2019 | From: Schulich School of Medicine and Dentistry

**Best Presentation at mRNA Turnover conference**
- Awarded: June 22nd, 2019 | From: The RNA Society

**CIHR Travel Award ($1,000 CAD)**
- Awarded: June 3rd, 2019 | From: Canadian Institute of Health Research

**Canadian Student Health Research Forum Presenter – top 5% of PhD's selected across Canada**
- Awarded: May 26th, 2019 | From: Western University

**mRNA Turnover Travel Award ($506.17 CAD)**
- o  Awarded: May 24th, 2019 | From: The RNA Society

**Drs. Madge and Charles Macklin Fellowship for Teaching & Research in Medical Sciences ($4,250 CAD)**
- o  Awarded: June 29th, 2018 | From: Schulich School of Medicine and Dentistry

**London Health Research Day Platform Presentation Award ($650 CAD)**
- o  Awarded: May 10th, 2018 | From: London Health Research Academic Committee

**The Lucille & Norton Wolf Trainee Publication Award ($1,000 CAD)**
- o  Awarded: May 10th, 2018 | From: London Health Research Academic Committee

**Poster Award Finalist**
- o  Awarded: April 30th, 2018 | From: ALS Canada

**Queen Elizabeth II Graduate Scholarship in Science and Technology ($15,000 CAD)**
- o  Awarded: April 30th, 2018 | From: The School of Graduate and Postdoctoral Studies

**CIHR Doctoral Award – Fredrick Banting and Charles Best Canada Graduate Scholarship ($105,000 CAD)**
- o  Awarded: April 17th, 2018 | From: Canadian Institute of Health Research

**Neuroscience Travel Award ($500 CAD)**
- o  Awarded: October 2nd, 2017 | From: Neuroscience Program, Western University

**Robarts Research Institute Trainee Award ($100 CAD)**
- o  Awarded: May 26th, 2017 | From: Robarts Research Institute Award

**Ontario Graduate Scholarship (OGS) valued at $15,000 CAD (Sept. 2017)**
- o  Awarded: May 26th, 2017 | From: The School of Graduate and Postdoctoral Studies

**Neuroscience Travel Award ($500 CAD)**
- o  Awarded: February 1st, 2017 | From: Neuroscience Program, Western University

**Poster Award Finalist**
- o  Awarded: April 28th, 2016 | From: ALS Canada

**Deans Undergraduate Research Opportunities Program award valued at $6,000 CAD (May 2015)**
- o  Awarded: April 15th, 2015 | From: Schulich School of Medicine and Dentistry

## Publications (h-index - 4)

1) Campos-Melo, D., **Hawely, ZCE.** & Strong, MJ. RNA species are active players in stress granules dynamic and function. *Under revision in Front. Cell Devel. Biol.* (2020).
2) **Hawely, ZCE.,** Campos-Melo, D. & Strong, MJ. Negative feedback network between TDP-43 and multiple microRNAs is dependent on TDP-43 nuclear localization. *Accepted in J. Mol. Biol.* (2020).
3) **Hawely, ZCE.,** Campos-Melo, D. & Strong, MJ. MiR-129-5p: A novel therapeutic for ALS?. *Non-coding RNA Investigation.* Accepted (2020).
4) **Hawely, ZCE.,** Campos-Melo, D. & Strong, MJ. MiR-105 and miR-9 regulate the mRNA stability of neuronal intermediate filaments. Implications for the pathogenesis of amyotrophic lateral sclerosis (ALS). *Brain Res.* (2019). doi.org/10.1016/j.brainres.2018.10.032.
5) Campos-Melo, D*., **Hawley, ZCE*.** & Strong, MJ. Dysregulation of human NEFM and NEFH mRNA stability by ALS-linked miRNAs. *Mol. Brain* (2018). doi.org/10.1186/s13041-018-0386-3. (*shared first author).
6) **Hawely, ZCE.,** Campos-Melo, D. & Strong, MJ. Novel miR-b2122 regulates several ALS-related RNA-binding proteins. *Mol. Brain* (2017). doi.org/10.1186/s13041-017-0326-7.
7) **Hawely, ZCE*.,** Campos-Melo, D*., Droppelmann CA. & Strong, MJ. MotomiRs: miRNAs in motor neuron function and disease. *Front. Mol. Neurosci*. (2017). doi:10.3389/fnmol.2017.00127. (*shared first author).

## Platform Presentations

1) **†mRNA Turnover: Mechanisms, Regulation, and Implications in Age-Related Diseases** – Montreal, QC, Canada (Jun. 2019).
2) **†London Health Research Day** – London, ON, Canada (May 2018).
3) **Eukaryotic RNA Turnover** – Oxford, England (May 2017).
4) **†Robarts Research Retreat** – London, ON, Canada. (May 2017).
5) **Society for Neuroscience (SfN)** – San Diego, CA, USA. (Nov. 2016).
6) **Regulatory & Non-Coding RNA Meeting** – Cold Spring Harbor Laboratories, NY, USA. (Aug. 2016)
7) **Robarts Research Retreat** – London, ON, Canada. (May 2016).
8) **Western's Neuroscience Research Day** – London, ON, Canada (Apr. 2016).

*All presentations were selected through as competitive selection process based on abstract
†Award-winning presentations

## Poster Presentations

1) **15th Andre-Delambre Annual Symposium** – Montreal, QC, Canada. (Sept. 2019).
2) **Canadian Student Health Research Forum** – Winnipeg, MAN, Canada. (Jun. 2019).
3) **Cell Symposium: Regulatory RNAs** – Berlin, Germany. (May 2019).
4) **London Health Research Day** – London, ON, Canada. (May 2019).
5) **International Symposium on ALS/MND** – Glasgow, Scotland. (Dec. 2018).
6) **Toronto RNA Enthusiasts Day (TREnDs)** – Toronto, ON, Canada. (Aug. 2018).
7) **RNA Society** – Berkeley, CA, USA. (May 2018).
8) **ALS Canada Research Forum** – Toronto, ON, Canada. (Apr. 2018).
9) **Toronto RNA Enthusiasts Day (TREnDs)** – Toronto, ON, Canada. (Aug. 2017).
10) **London Health Research Day** – London, ON, Canada. (May 2017).
11) **RNA Metabolism in Neurological Diseases** – San Diego, CA, USA. (Nov. 2016).
12) **Robarts Research Retreat** – London, ON, Canada. (May 2016).
13) **ALS Canada Research Forum** – Toronto, ON, Canada. (Apr. 2016).

## Teaching Experiences

| | | |
|---|---|---|
| o | **Elementary Student Activity Leader** \| Canadian Medical Hall of Fame | Sept. 2015 – Jan. 2020 |
| o | **Teaching Assistant** \| Principles of Neuroscience Graduate Course | Jan. 2016 – Apr. 2017 |
| o | **Teaching Assistant** \| Neuroscience Undergraduate Thesis Course | Sept. 2015 – Apr. 2016 |

## Reviewing Experience

| | | |
|---|---|---|
| o | **Neuroscience Research Blog Reviewing Editor** | Jun. 2019 - present |
| o | **Manuscript Reviewer – Annals of Neurology** | April 2020 |
| o | **Manuscript Reviewer – Brain Communications** | October 2019 |
| o | **Scholarship Q&A Session Volunteer** | September 2018/2019 |
| o | **Manuscript Reviewer – Journal of Neuroscience** | July 2018 |
| o | **Manuscript Reviewer – Journal of Neurochemistry** | October 2017 |

## Leadership Experience

- o **Robarts Association for Trainees Chair** | Robarts Research Institute    Jan. 2016 – Apr. 2017
- o **Leadership & Academic Mentorship Program Leader** | Success Center    Jan. 2016 – Apr. 2016
- o **Associate Vice President of Orientation** | University Student Council    Arp. 2014 – May 2015
- o **Residence Orientation Coordinator** | Housing, Western University    Jan. 2013 – Apr. 2014
- o **Head Orientation Leader** | Housing, Western University    Feb. 2012 – Apr. 2013
- o **Orientation Leader** | Housing, Western University    Mar. 2011 – Apr. 2012

## Interviews and Media Relations

- o **Radio Interview:** *Current research in Amyotrophic Lateral Sclerosis (ALS).* Gradcast, CHRW 94.9 FM (February 2016)
- o **Radio Interview:** *Genes, ALS, and that new Grad Student Smell with Zach Hawley***.** Gradcast, CHRW 94.9 FM (July 2015)
- o **News Article:** *Why is it important to vote in the federal election.* Schulich School of Medicine and Dentistry Newsletter (October 2015)